DEGRADABLE CELLULOSE WET ADHESIVES

ADHESIVES WITH CONTROLLABLE DEGRADABILITY FOR WET CELLULOSIC MATERIALS

By

DONG YANG, B.Eng. M.Eng.

A Thesis Submitted to the School of Graduate Studies

in Partial Fulfilment of the Requirements

for the Degree of Doctor of Philosophy

McMaster University

DOCTOR OF PHILOSOPHY (2018) McMaster University

(Chemical Engineering) Hamilton, Ontario

TITLE: Adhesives with Controllable Degradability for Wet Cellulosic Materials

AUTHOR: Dong Yang

B.Eng. (Nanjing Forestry University, China)

M.Eng. (South China University of Technology, China)

SUPERVISOR: Dr. Robert H. Pelton

NUMBER OF PAGES: ix, 189

Lay Abstract

Wet strength is important for paper products such as paper towels and paper packaging. In paper manufacturing, cellulose wet adhesives are applied to enhance the strength of wet papers by “gluing” together individual cellulose fibers. However, the recycling of wet strength papers is a challenge because the current adhesives prevent the easy disintegration of waste paper back to a suspension of discrete cellulose fibers. As an important part of the bio-based economy, the next generation of paper products are required to be both strong in water and easy to recycle. This thesis explores new designs for wet-strength adhesives that will facilitate recycling.

Both nanoparticles and linear polymers were synthesized in this study as cellulose wet adhesives. Many important properties of wet adhesives were probed, including the size of nanoparticles, the pre-treatment of cellulose surfaces, the dosage of adhesives and the choice of adhesive chemistries. A few types of novel cellulose wet adhesives with controllable degradability were synthesized and evaluated. I demonstrated that the cellulose wet adhesion can be “switched off” in response to subtle pH changes, reducing agents or sugars, showing a promising start for the recycling of wet strength papers.

Abstract

Cellulose wet adhesives are applied to enhance the wet strength of paper products by binding individual cellulose fibers together. However, the recycling of the wet strength paper is a challenge as the fibers are hard to re-disperse in water. This project demonstrates new strategies for developing cellulose wet adhesives with controllable degradability, facilitating the recycling of wet strength papers.

In this project, regenerated cellulose membranes were used to simulate cellulose fibers. In adhesion measurements, two wet cellulose membranes were laminated with a thin layer of adhesive (1–30 mg/m^2), and the 90-degree wet-peel was used as a measure of cellulose wet adhesion. It was shown that the wet-peel was a simple and reliable method to evaluate the wet adhesives for paper products.

Cellulose wet adhesives, in the form of microgels or linear polymers, were synthesized by incorporation of hydrazide, amine or azetidinium functional groups that can form covalent bonds to cellulose surfaces. Two strategies to design degradable adhesives were demonstrated in this project. 1) Reductant-responsive microgel adhesives were created by introducing cleavable disulfide linkages, either in the polymer chains tethering adhesive groups or as the microgel crosslinks. More than 70% reduction in wet adhesion was achieved after exposure to a reductant. 2) Degradable polymer cohesive bonds were used to “switch off” the cellulose wet adhesion. This adhesive was created by introducing labile boronate-dextran complexes to the PVAm adhesive layer between cellulose surfaces. The introduction of this new interaction between PVAm chains enhanced the cellulose wet adhesion. In response to subtle pH changes or the presence of monosaccharides, the wet adhesion decreased by 60%.

Acknowledgements

First and foremost, I would like to express my deepest thanks to my research supervisor, Dr. Robert Pelton, for his guidance throughout my studies. His dedication and passion in research show me the path to be a better scientist. His generosity and kindness in life showed me the way to be a better person. I really enjoyed the freedom in my projects and the opportunities to meet the brightest minds in many conferences. I am very fortunate to have this privilege to work with him over the last four years.

I would like to thank my supervisory committee members, Prof. Todd Hoare and Prof. Kari Dalnoki-Veress, for their valuable advice in this project. I enjoyed the experience of working with them very much. I would like to thank our laboratory manager Mr. Doug Keller and administrative secretary Ms. Sally Watson for their great help in the past years. Also, I would like to acknowledge the Natural Sciences and Engineering Research Council of Canada and BASF for their financial support.

I would like to extend a great deal of appreciation to all my colleagues in the McMaster Interfacial Technologies Group for their support and friendship. Many thanks to Dr. Emil Gustafsson, Dr. Carla Abarca, and Dr. Qiang Fu for their training and advice. To Dr. Songtao Yang, Dr. Zhen Hu, Dr. Xiaofei Dong, Yuanhua Li, Fengyan Wang, and Hongfeng Zhang for their very helpful discussion. To Taylor Stimpson, Yang Chen and Alexander Sotra for their important contributions to this project.

I cannot express enough thanks to my parents and my sister for all their love and support. Although I am studying an ocean away, they remind me where I come from, who I am, and who I want to become.

Above all else I would like to express my deepest love and appreciation to my wife Tingting Zhu. Over the last decade, we moved together across the country (China) and then came to another continent (Canada). Through all the happiness, excitement, hardship and confusion, we have grown and evolved together. No one knows where our future will take us, but I know whether it is over the mountains or across the ocean, I cannot wait to write our next chapter together.

Table of Contents

List of Abbreviations and Symbols

AA	Acrylic acid
AAPH	2,2'-Azobis(2-amidinopropane) dihydrochloride
ADH	Adipic acid dihydrazide
AFM	Atomic force microscopy
BAC	*N*,*N*′-Bis(acryloyl)cystamine
CMC	Carboxymethyl cellulose
CPAM	Cationic polyacrylamide
CTAB	Cetyltrimethylammonium bromide
DADMAC	Diallyldimethylammonium chloride
DLS	Dynamic light scattering
DMAEMA	2-(Dimethylamino)ethyl methacrylate
DMAP	4-Dimethylaminopyridine
DMSO	Dimethyl sulfoxide
DP	Degree of polymerization
DS	Degree of substitution
DTDH	Dithiodipropionic acid dihydrazide
DTT	Dithiothreitol
EDC	1-Ethyl-3-(3-dimethylaminopropyl)carbodiimide
GC-PAM	Glyoxylated cationic polyacrylamide
HBA	4-Hydroxybenzoic acid
MBA	*N*,*N*′-Methylenebisacrylamide
MWCO	Molecular weight cut-off
NHS	*N*-Hydroxysuccinimide
NMR	Nuclear magnetic resonance
NIPAM	*N*-isopropylacrylamide
NIPMAm	*N*-isopropylmethacrylamide

PAE	Polyamide-epichlorohydrin
PDI	Polydispersity index
PVAm	Polyvinylamine
PVSK	Poly(vinyl sulfate) potassium salt
QCM-D	Quartz crystal microbalance with dissipation
SCD	Streaming current detector
SDS	Sodium dodecyl sulfate
TEMED	Tetramethylethylenediamine
TEMPO	2,2,6,6-Tetramethylpiperidine-1-yl)oxyl

Chapter 1

Introduction and Objectives

As the most abundant renewable material on the planet, cellulose is the cornerstone of the ongoing transformation to a bio-based economy.[1, 2] Cellulose has a hydrophilic surface, reflecting the high density of hydroxyl groups. Because of this hydrophilicity, there is no tendency for wet cellulose surfaces to adhere to one another. Cellulose wet adhesion is a long-standing issue in paper manufacturing and now has significance in many new areas, such as building materials, surgical implants, nanocellulose composites, bioactive sensors, and agricultural materials.[2-7]

Paper is one of the most widely used materials in the world. We are surrounded by paper products from the early morning to the late night. Decades ago, the pulp and paper industry was regarded as a big source of water pollution.[8] With the implementation of pollution control legislation and the development of cleaner manufacturing technology, the pollution problem in paper manufacturing is now a lesser concern. Instead, paper is now regarded as one of the most promising candidates to replace non-renewable materials such as plastics and non-recyclable materials such as textiles. In the current market, there would be high demand for paper products with high wet strength and good recyclability. However, there is no available technology to manufacture papers with such properties so far. For example, it was estimated that between 2.5 and 10 billion paper coffee cups were used every year in the UK, but less than 1 in 400 cups was recycled due to technological limitations.[9] In this chapter, I will first introduce the background of paper manufacturing and paper products. Then the relationship between the paper wet strength and cellulose adhesion will be explained. Lastly, I will introduce the goal of this project followed by my major approaches.

1.1 Paper — a Composite Material

Paper is a composite material that consists of layers of deposited cellulose fibers and additives. The cellulose fibers are typically 20–30 μm in diameter and 1–3 mm in length, with hollow tube-like structures and wall thicknesses that typically range from 3–5 μm.[10] In paper manufacturing, the tube-like fibers are dried and collapsed into ribbon-like structures with a thickness twice of the fiber wall.[10] In paper, the ribbon-like fibers are stacking on top of each other (Figure 1-1). The overlapping areas between two fibers are called "fiber-fiber joints."

Additives are laminated together with cellulose fibers in paper products. Some additives, such as retention aids and defoamers, are applied to improve the efficiency of manufacturing process, while others, such as strengthening resins, fillers, and softeners, are applied to improve the performance of paper products.[11] The size of paper additives varies significantly. The fillers can be as large as a few micrometers, while the small molecular additives, such as rosins and surfactants, are smaller than 1 nm. Common polymeric additives are water soluble with a hydrodynamic diameter in the range of 10–100 nm in water.

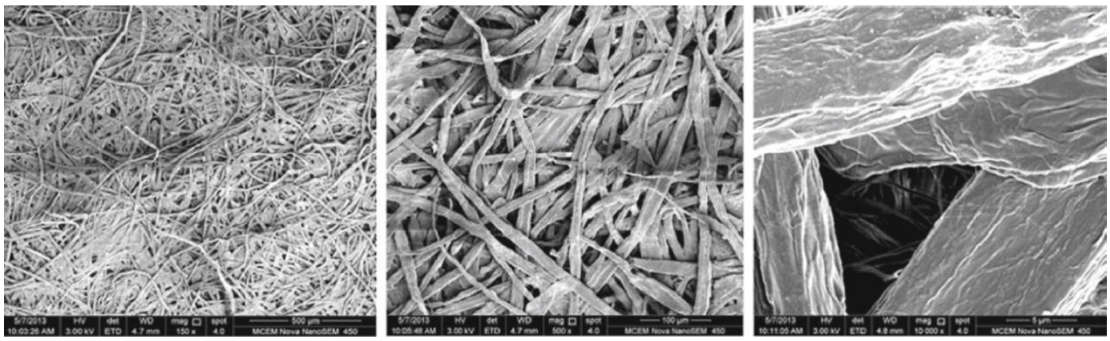

Figure 1-1 Morphologies of paper made of hardwood fibers examined by scanning electron microscope. From left to right, the scale bar represents a length of 500, 100 and 5 μm. Pictures from Garnier *et al.*[12]

Cellulose fibers from wood are most commonly used in paper manufacturing, while other fibers from waste paper, crops and bamboo are also used.[13] A typical structure of wood cell wall is shown in Figure 1-2. Cellulose fibers are bound together with two other major components, lignin and hemicellulose, along with other minor components, such as pectins, phenols, and fats.[14] Take softwood as an example: it consists of 45–50% cellulose, 25–35% lignin, and 25–35% hemicellulose.[15, 16]

Pulping is the process that releases the cellulose fibers from the lignocellulose matrix, yielding water-dispersible cellulose fibers. In chemical pulp, which accounts for 74% of global pulp production in 2013, cellulose fibers are dispersed by removing the "adhesives" between cellulose fibers, i.e. lignin and hemicellulose.[17, 18] For example,

bleached softwood kraft pulp, a typical chemical pulp, consists of ~ 80% cellulose, < 1% lignin, and ~ 20% hemicellulose.[19]

Cellulose fibers are good water-absorbing materials. The water saturation point of cellulose fibers is approximately 35% solids content.[10] Below this point, free water appears and forms a continuous water network spanning many fibers; above this point, the fiber is not saturated with associated water. The saturation point of cellulose fibers is closely related to the porosity of the fiber, the charge on fiber surface, and the components of the fiber.

The porous structure of cellulose fibers is created when some components, such as lignin and hemicellulose, are removed during pulping and bleaching processes.[20] In Andreasson *et al.*, the NMR spectrum of wet, unbleached kraft pulp showed an average pore radius of 15 nm, and inverse size exclusion chromatography showed an average surface pore radius of 3 nm.[20] The pore size is affected by many factors, such as the environmental pH, ionic strength and fiber cross-linking density.

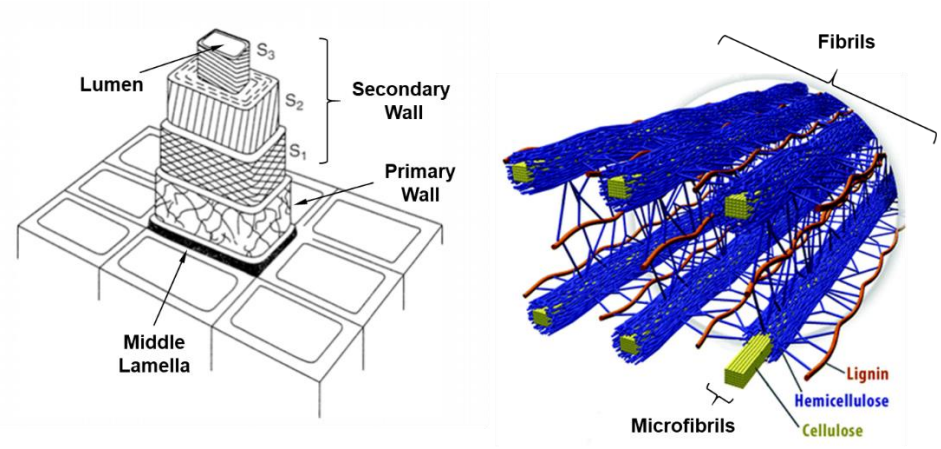

Figure 1-2 Diagram of the cell wall of wood fibers (left) and the spatial arrangement of cellulose, hemicellulose, and lignin in the cell wall (right). Picture adapted from Welton *et al.* and Booker *et al.*[21, 22]

Cellulose fibers have rough surfaces. Cellulose constitutes the fiber structure through elementary fibrils, microfibrils and fibrils. Elementary fibrils have diameters of 2–5 nm, which consists of 30–40 cellulose chains connecting through hydrogen bonds. Microfibrils are agglomerates of elementary fibrils with diameters of 5–50 nm. Fibrils are a bundle of microfibrils with diameters of 0.1–1 μm.[23, 24] Elementary fibrils, microfibrils, and fibrils extending from the fiber surfaces provide the roughness in a range of nanometers to micrometers.

Cellulose fibers are typically negatively charged in water. The charge density depends on the fiber type and the treatment conditions, such as pulping and bleaching. Generally, the

charge is derived from the carboxyls, sulfonic acids, and phenolics.[15] The total charge of the bleached kraft pulp is typically in the range of 30–80 μeq/g and the surface charge is in the range 10–40 μeq/g.[25]

1.2 Wet Chemistry of Cellulose Fibers

Cellulose is the major component in most cellulose fibers, especially in chemical pulps. Cellulose is a polysaccharide consisting of β-1,4 bonded glucose rings (Figure 1-3).[26] Cellulose has a high density of hydroxyl groups (19 mmol/g), similar to that of polyvinyl alcohol (23 mmol/g), which makes it a highly hydrophilic material. Take wood fiber as an example. The DP of cellulose is typically in a range of 300–1,700.[2] At one end of the cellulose chain, the reducing end, there is a glucose unit with a hemiacetal form, which can convert to an aldehyde form.[27]

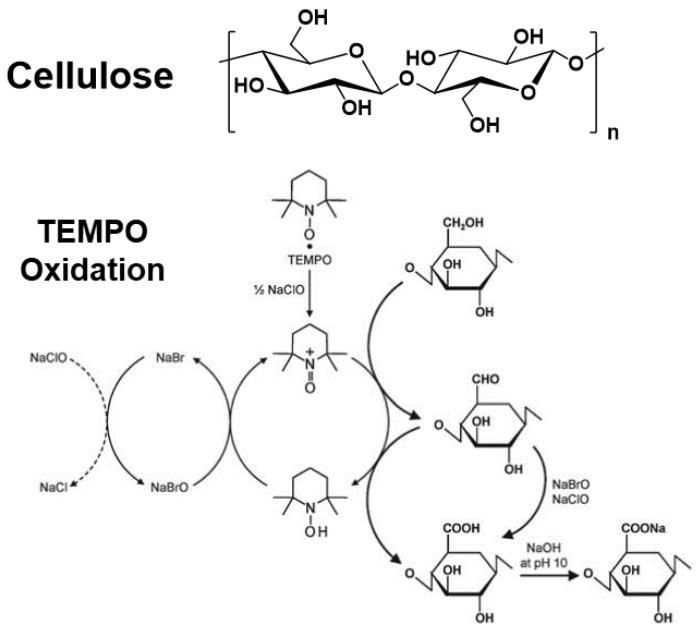

Figure 1-3 The structure of cellulose and the selective oxidation of C6 primary hydroxyls on cellulose to C6 aldehyde/carboxylate groups by TEMPO oxidation in water at pH 10. Picture adapted from Isogai *et al.*[28]

Cellulose is hydrophilic but not water soluble. The semi-crystalline structure of cellulose leads to its water insolubility, because the crystalline regions are not accessible to water molecules.[27, 29] Crystalline regions in cellulose are highly ordered, contributing to paper strength, while amorphous regions lack a regular arrangement, providing paper flexibility.[27] The reaction of cellulose in the water phase is commonly heterogeneous. As the hydroxyls on the surface of cellulose are weak nucleophiles, grafting on cellulose

hydroxyls often involves the catalysis of acid and base, or heating. Thus, many pre-treatments have been developed to surface activate cellulose materials.

Oxidation. Oxidation is a common method to modify the surface of cellulose materials. Sodium periodate can be used to cleave the glucose ring at C2 and C3 and generate aldehyde groups on cellulose. After a 4-hour oxidation, the content of aldehyde can reach 4.7 mmol/g on cellulose fibers, and the degrees of crystallinity and DP of cellulose decrease.[30]

2,2,6,6-Tetramethylpiperidine-1-yl)oxyl (TEMPO) oxidation is a very useful tool in cellulose research.[31] It is a mild oxidation that selectively oxidizes the hydroxyls on cellulose C6 to aldehydes and carboxyls (Figure 1-3). The functional groups introduced in oxidation provide new potential binding sites on the cellulose surface and increase the adsorption of cationic polymers.[32] In Isogai *et al.*, after a mild TEMPO oxidation, carboxylate and aldehyde groups were introduced to cotton linters up to 0.7 and 0.3 mmol/g, respectively.[33] Most of these groups were present on cellulose crystal surfaces and in amorphous regions.[33]

Cellulose primers. Cellulose surfaces can be "primed" by grafting polymers or small molecules to provide functionalities.[1] Carboxymethyl cellulose (CMC) modification is a popular method to functionalize the surface of cellulose with carboxyl groups. CMC is attached to the cellulose surface by irreversible physical adsorption.[34] Unlike chemical modification, this process does not change the structure of cellulose materials. The adsorption of CMC can be promoted by a low DS, a higher adsorption temperature, or a higher ionic strength.[34] CMC modification is a great method to increase paper dry and wet strength with wet-strength resins and reduce the friction and flocculation of fibers.[24, 35, 36] The major drawbacks of the CMC treatment are the long pre-treatment time and the requirement of high temperatures.[37]

Polyvinylamine (PVAm) "primed" cellulose can be prepared by covalently grafting PVAm on oxidized cellulose.[1] Cationic amines on PVAm first adsorb on the cellulose surface and then graft on it by reacting with aldehydes. PVAm overcompensates the anionic charge on oxidized cellulose surface due to its high charge density, making it positively charged.[1] Most polymers with a cationic charge, such as cationic polyacrylamide, can be "primed" on cellulose via electrostatic attraction. However, the lack of covalent bonding will compromise the reliability of the primer and provide little improvement to paper wet strength.[32]

The cellulose surface can be modified by small molecules. In paper manufacturing, sizing agents are covalently coupled to cellulose to hydrophobically modify the paper product.[38] Alkyl ketene dimer is a popular sizing agent with a propiolactone ring and an extended hydrophobic alkyl chain.[39] It reacts with hydroxyls on cellulose via esterification. The reaction takes place most efficiently in neutral or slightly basic conditions at 90–110 ºC. Epichlorohydrin and chloroacetic acid are also small molecule additives that are used to modify the surface of cellulose fibers in paper manufacturing.[40, 41] In the textile industry, reactive dyes are used to graft chromophores to cellulose by reacting with the hydroxyls of cellulose, where triazine rings bearing one or two chlorine atoms are used to introduce

amines, thiols, glycine, or even lignin model compounds on fiber surfaces (Figure 1-4).[42, 43] Organofunctional silane coupling agents can also be used to modify the surface of cellulose fibers. Silanes anchor on cellulose via silanol groups, which can condense with hydroxyls of cellulose and also self-condense.[44, 45] The surface property of the modified fiber is dominant by the silane structure.

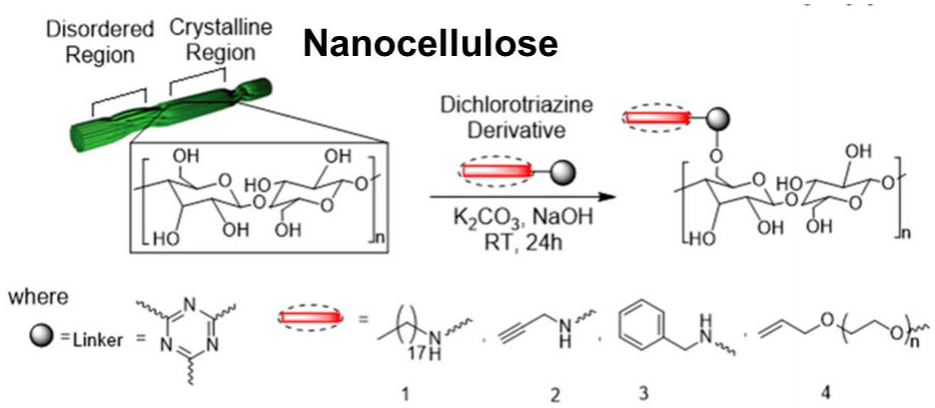

Figure 1-4 Chemical grafting of 4,6-dichloro-1,3,5-triazine derivatives onto nanocellulose in water phase. Picture adapted from Fatona *et al.*[43]

Pre-treatments. The reactivity and accessibility of cellulose fibers can be enhanced by various pre-treatments without introducing new functional groups, such as mercerization and ethylamine treatment.[46] Mercerization changes the cellulose structure in fibers from the native form of cellulose I to the more stable cellulose II, which provides more inter-fiber hydrogen bonding and better adhesion between fiber and resins.[47] In Kim *et al.*, mercerized fibers showed a higher Young's modulus and tensile strength, due to the removal of hemicellulose and lignin in fibers under the alkaline treatment.[47] Native cellulose cannot be totally dissolved by TEMPO oxidation under regular conditions due to the limited accessibility of cellulose materials. However, after regeneration or mercerization, most C6 hydroxyls on cellulose can be TEMPO oxidized. With a high TEMPO dosage, long oxidation time, or high temperature, regenerated or mercerized cellulose can be oxidized to water-soluble polyglucuronic acids.[48]

Others. There are many more methods and processes that modify cellulose surfaces. For example, cellulose can be non-selectively oxidized by enzymes and strong oxidants, such as ozone and sodium hypochlorite.[49] The hydrolysis of cellulose fibers is catalyzed under acid conditions in water.[50] A loss of paper strength happens after acid hydrolysis due to the cellulose chain scission.[27] As another example, atom transfer radical polymerization was used to modify the surface of cellulose via a "grafting from" strategy. In Deng *et al.*, fluorescent poly(*N*-isopropylacrylamide) brushes were grafted from cellulose surfaces, providing a thermo-enhanced fluorescent property.[51]

1.3 Paper Wet Strength

Paper products are manufactured on paper machines and dried on steam-heated cylinders at high temperatures. The Page equation below is a widely recognized empirical model for paper tensile strength.[52] Many assumptions are made in the equation, including that the paper sheets are uniformly formed and that the fibers are straight, have no crimps or kinks, and have a uniform elastic modulus. According to the equation, paper strength is determined by many factors, such as fiber morphology, fiber strength, and fiber-fiber joint strength.[52]

$$\frac{1}{T} = \frac{9}{8 \cdot Z} + \frac{12 \cdot A \cdot \rho \cdot g}{b \cdot P \cdot L \cdot RBA}$$

in which T is the tensile strength expressed as breaking length; Z is the zero-span tensile strength expressed as breaking length; A, P and L are the average fiber cross-sectional area, perimeter and length, respectively; b is the bond strength per unit area between fibers; RBA is the relative bonded area of the paper sheet; ρ is the fiber density and g is the acceleration due to gravity.

In dry papers, the fiber-fiber joint strength mainly derives from hydrogen bonding and polymer inter-diffusion between cellulose surfaces.[31] Although the bonding energies of van der Waals forces and hydrogen bonds are low, the high density of these interactions gives fiber-fiber joints a decent dry adhesion. Due to the relatively high fiber-fiber joint strength, when dry paper breaks, both single fibers and fiber-fiber joint break.[10]

The wet strength of paper is one of the most important properties of paper products, especially for applications such as packaging and filtration. Unlike dry strength, wet fibers show weak fiber-fiber joints and slide over each other very easily.[53] Typically, no fibers break when wet paper ruptures.[10] Thus, the best strategy to enhance the strength of wet papers is to introduce fiber-fiber bonds that are stable in water.[54] In paper manufacturing, two different types of paper wet strength are most commonly measured and monitored: wet-web strength and wet strength.

Wet-web strength. Wet-web strength is the strength of the "never-dried" paper sheet on paper machine. Specifically, paper engineers and chemists are interested in the wet-web strength of paper sheets during the "open draw", when the sheets are transferred between the press section and the drying section. At this point, the paper sheet is running through a gap (a few centimeters) under stress without any support.[10] Typically, the never-dried paper sheet at the open draw has a solids content of 30–50%, which is very weak and prone to break.[10, 55, 56] In practice, wet-web breaks at high production speed result in great losses in paper manufacturing.[57]

There is no TAPPI standard method for evaluating wet-web strength yet, but we find many useful methods designed and validated in different labs. For example, in van de Ven's lab, paper handsheets were prepared with a metal template mold placed on the metal screen of a handsheet machine.[58] The never-dried paper strips were "pre-cut" during the handsheet preparation using the metal template. The wet-web strength of these strips was measured by a tensile machine after a wet pressing. Stuman *et al.* reported another method for the wet-web strength measurement.[59] In this method, handsheets were prepared and pressed to a solids content of 49 ± 2%. The never-dried sheets were then sandwiched between two stiff plastic sheets and cut for testing purposes. The strength of the wet sample was tested using TAPPI Method T494. As another example, VTT Process and Metso Paper developed an IMPACT-fast tensile test rig to measure wet-web strength with an average strain rate of 1 m/s.[15, 56]

The never-dried paper sheets show a low strength due to the lack of fiber-fiber bonding in the presence of water. Typically, fiber-fiber joint strength increases with a higher solids content (Figure 1-5).[58, 60] When paper is very wet (solids content < 30%), it is generally believed that fiber-fiber joints are held together by water bridges.[10] The attractive capillary force, which is called the "Campbell effect", arises from the curvature of the meniscus of the free water at fiber-fiber joints.[61] With the removal of water associated with fibers (solids content > 50%), hydrogen bonding at fiber-fiber joints starts to form with the contact of the two cellulose surfaces.[55] It is still under debate what dominates the wet-web strength at a solids content of 30–50%, which is the typical solids content of the wet-web at the open draw. Van de Ven *et al.* proposed that wet fibers are held together by fiber entanglements and friction at the transitional point.[10, 62]

The introduction of polymer bridges between cellulose fibers can enhance the wet strength of paper, but the efficiency only maximizes after water removal.[63] In fact, it is found that the addition of polyelectrolytes at the paper-making process is always detrimental to the wet-web strength.[55, 58] First, the strong electrostatic attraction between polyelectrolytes may aggregate fibers, which compromises the paper formation. Second, the adsorbed polyelectrolytes at the fiber surfaces create a repulsive electrosteric stabilization effect between fibers, preventing the approach of two fiber surfaces in water. In Salminen *et al.*, instead of adding additives at the wet end, polymer additives were sprayed on the wet-web to improve the wet-web strength.[56]

Another possible method to prevent wet-web breaks is to increase the solids content at the open draw by adding retention aids.[56] The addition of flexible and thin cellulose microfibrils can also improve the wet-web strength. The microfibrils provide extra fiber entanglements in the wet-web.[55] As another example of wet-web enhancement, Tejado *et al.* used 1-ethyl-3-(3-dimethylaminopropyl)carbodiimide (EDC) to conjugate the dihydrazide crosslinkers between CMC-modified fibers, where a 500% increase in wet-web strength was achieved.[63]

In the Pelton lab, we showed two ideas that improved the wet-web strength significantly: 1) phenylboronate-derivatized PVAm, which can covalently bond with the reducing end

of cellulose in water,[64] and 2) the application of PVAm with CMC-modified cellulose, where electrostatic attractions will hold the wet-web together.[36]

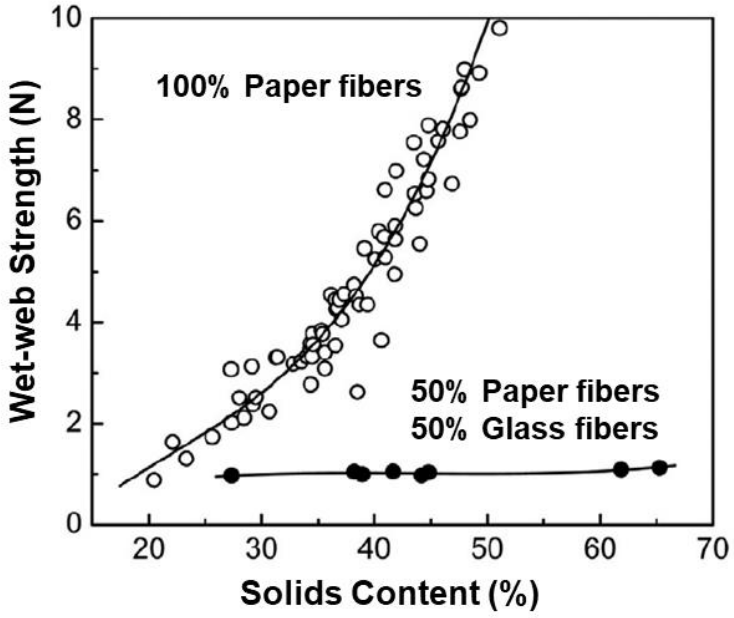

Figure 1-5 Wet-web strength of sheets made from 100% cellulose fibers and from 50:50 mixtures of glass and cellulose fibers. Picture adapted from Tejado and van de Ven.[60]

Wet strength. Wet strength is an important property for many paper products, such as agricultural papers, filter papers, and tissue papers. These paper products will be exposed to moist or wet environment during their application. Wet strength is different from wet-web strength of a never-dried paper sheet. Paper samples in wet strength measurements have been "once-dried" on a paper machine. Wet-web strength requires the strength of fiber-fiber joints to form underwater, whereas wet strength requires the strength of fiber-fiber joints to form after drying and stay stable when rewetted in water.

As described in TAPPI method T456 for paper wet strength measurement, paper samples are first dried and cut into standard samples. The samples are rewetted in an aqueous solution before the tensile measurement. The most meaningful measurement is to measure the paper wet strength under the application condition, where the pH, temperature, the duration of rewetting and other parameters should be considered.

Wet-strength papers are papers that retain > 15% of their dry tensile strength in water.[65] Wet-strength resins are paper additives used to increase the paper wet strength — the strength of a rewetted paper.[66] These wet-strength resins are water soluble cationic polymers that can adsorb on negatively charged cellulose fiber surfaces. The

development of wet-strength resins was initiated during World War II. Since then, one major change happened in the 1960s, when a shift was made from acidic-curing resins to alkaline-curing resins.[65]

Conventional wet-strength resin mechanisms have been described in a few review papers.[65, 66] Two mechanisms have been used to explain the paper wet strength, including the protection mechanism and the reinforcement mechanism.[66] The protection mechanism explains that the resins can self-crosslink on fibers. The crosslinked network curbs the the swelling of the fiber-fiber joints in water and protects inter-fiber hydrogen bonds from being destroyed completely.[54] The reinforcement mechanism explains that the wet strength of paper derives from the covalently bonded fiber-fiber joints. Wet-strength resins crosslink two fibers covalently when hydrogen bonds between fibers are disrupted in water. It is believed that the real mechanism for most wet-strength resins is a combination of these two effects. However, from a mechanical perspective, the mechanism of the paper wet strength is still not clear.[54]

Wet-strength resins are divided into two groups: "temporary resins" and "permanent resins."[54] From a chemistry perspective, temporary resins are usually based on reactive aldehydes that form hydrolyzable linkages with cellulose fibers, whereas the permanent resins are able to form covalent bonds with fibers that are stable in water.

Temporary wet-strength resins are used exclusively for tissue papers, which need an "immediate" wet strength and a great dispersion after immersing in water.[63, 67] In a work Georgia-Pacific published in *TAPPI Journal*,[67] the wet strength of tissue papers after rewetting for 5 seconds was measured as the immediate wet strength, and the wet strength after 5 minutes' rewetting was measured to evaluate the decay rate of wet strength.

The first commercial temporary wet-strength resin is acid-curing, cationic dialdehyde starch. The dialdehyde starch resin provides paper wet strength under a manufacturing environment of pH < 4.5, as the formation of hemiacetals is catalyzed by acidic conditions.[66] More recently, glyoxylated cationic polyacrylamide (GC-PAM) resins were introduced, which contain aldehyde groups, non-reactive amides, and cationic groups, such as diallyldimethylammonium chloride (DADMAC).[65, 68] GC-PAM shows a stable effectiveness up to pH 6. In tissue manufacturing, GC-PAM is often employed in neutral to alkaline conditions.[65] Both dialdehyde starch and GC-PAM contain aldehydes that form hemiacetal and acetal bonds with cellulose fibers after drying. The formation of these labile covalent bonds provides paper a high immediate wet strength and an excellent degradability after rewetting for a short time.

The most commonly used permanent wet-strength resins in paper manufacturing include urea-formaldehyde, melamine-formaldehyde, amine-epichlorohydrin and polyamine. Acidic-curing resin urea-formaldehydes are the earliest cationic wet-strength resins. They are the condensation products of urea, formaldehyde, and a small amount of polyamine.[66] Urea-formaldehydes enhance paper wet strength mainly via the protection mechanism. After dewatering under acidic conditions (optimum pH 4.5), the resin crosslinks by covalent linkages and generates a three-dimensional structure on fiber, although it is not

able to covalently crosslink between fiber surfaces. Melamine-formaldehydes share many similarities with urea-formaldehydes. However, melamine-formaldehydes are able to react with hydroxyls on cellulose, enhancing wet fiber-fiber joints via both the protection mechanism and the reinforcement mechanism.[66]

Alkaline-curing amine-epichlorohydrin resins are the most important commercial resins in the paper industry, accounting for over 90% of the market.[65, 69] The chemistry of these resins has been thoroughly reviewed.[65, 66, 70] Polyamide-epichlorohydrin (PAE) is a crosslinked three-dimensional polyamide with active azetidinium groups (Figure 1-6).[71] In a typical PAE, there are azetidiniums and a small amount of secondary and tertiary amines on the backbone, and one primary amine and one carboxyl at the end of the chain.[66] Commercial PAE shows a high polydispersity with a molecular weight of 7–1000 kDa, as reported by Obokata *et al*.[71] The final structure of the resin is highly dependent on its synthetic process and the storage condition.

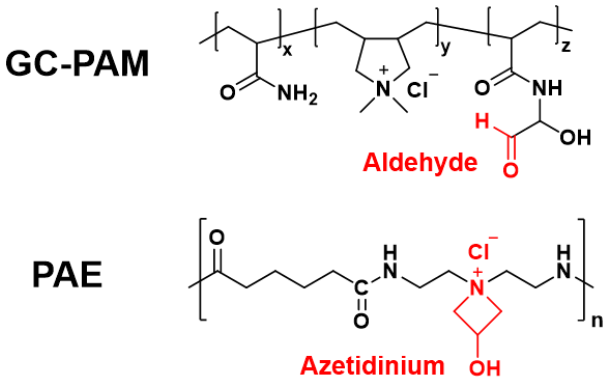

Figure 1-6 Chemical structures of GC-PAM and PAE.

PAE grafts on fibers covalently to form ester bonds by reacting with the carboxylate groups of cellulose fiber, but not with hydroxyls. The formation of ester bonds happens after the drying and is proposed to be the major reason for the strengthening effect of PAE.[72] The self-crosslinking of PAE happens between azetidinium groups and the carboxylate group at the end of the chain.[66] However, it is still under discussion whether the self-crosslinking enhances the paper wet strength.[72, 73] Obokata and Isogai showed the deterioration of PAE was very limited within a year at pH 4.2–4.5 at 4 ºC. However, after 8.9 years under the same condition, 50% of the azetidinium groups present in the fresh PAE were lost via the ring-opening reaction.[70] The reactivity of azetidiniums can be enhanced at a high temperature.

Another group of commercial wet-strength resins are polymers with amine groups, such as polyethyleneimine and chitosan.[32, 65, 74] A number of explanations have been proposed for their strengthening effect: 1) the electrostatic attraction between cationic amines and anionic cellulose; 2) the formation of hydrogen bonds; 3) the formation of a sterically

favoured complex with cellulose; and 4) covalent bonding with cellulose, such as amide (with carboxyls) and imine (with aldehydes).[66, 75] However, none of these explanations is widely accepted in academia or industry.

Although wet chemistry is the most important factor to enhance paper wet strength, other factors need to be considered in manufacturing of wet-strength paper, such as the formation of flocs and the porosity of fibers. Weak spots between the fiber flocs lead to a non-uniform paper sheet which gives a weak strength.[58] The degree of the wet-strength resin penetration into the fiber wall is also important.[20] If the resins are limited to only the external parts of fiber walls, a delamination of the fiber wall may happen under stress due to its multilamellar structure. The resins with smaller molecular weights can crosslink the fiber wall and thus less intra-fiber delamination may happen. However, papers with highly crosslinked single fibers are typically stiffer and more brittle.

In this thesis, I mainly focus on paper wet strength. This is the strength of wet-strength papers, such as filter papers and premium paper towels, when we use them in a moist or wet environment. This is also the strength we need to overcome when the wet strength paper is recycled. If readers are interested, paper dry strength has been addressed in a few excellent review papers.[11, 65] Wet-web strength is discussed as a part of this thesis in Chapters 2 and 3, and Appendix B. It is worth mentioning that dry strength, wet-web strength and wet strength are not independent properties.

1.4 Cellulose Wet Adhesion

Adhesion is a broad topic that involves a lot of research areas, including coating, adhesive, bio-material, pulp and paper, and food. In some applications, such as glues and medical tapes, we design the chemistry to increase the adhesion between surfaces, while in other applications, such as anti-fouling coatings and stabilizing nanoparticles, the adhesion at the interface should be minimized.

From a thermodynamics point of view,[76] adhesion can be described as the work of adhesion W:

$$W = \gamma_1 + \gamma_2 - \gamma_{12}$$

where γ_1 and γ_2 are the surface energies of materials 1 and 2 and where γ_{12} is the interfacial energy at the interface of materials 1 and 2. Thus, W is the energy change in the process of eliminating two surfaces and the creating of a new interface.

At the molecular level, adhesion is derived from intermolecular attractive interactions.[77] As two smooth surfaces approach each other within a distance of a few nanometers, they jump into contact due to intermolecular interactions, such as van der Waals forces and

hydrogen bonding. For example, pressure-sensitive adhesives are very common adhesives in daily life. They enhance the adhesion between two surfaces by 1) increasing the contact area, and 2) dissipating energy thanks to the viscoelastic property of the adhesive polymer. Typically, a thick layer of pressure-sensitive adhesive with a thickness > 100 micrometers is used in real application.

Wet adhesion is the adhesion between two surfaces in a solvent, mostly water. In nature, we find many examples of wet adhesion. In human body, cells are bound together in aqueous environment.[78] Many proteins are naturally sticky and resistant to water and have been used as wood adhesives for indoor and outdoor applications.[78] With the booming of the bio-economy, cellulose wet adhesion becomes important not only to traditional paper products but also to new cellulosic materials, such as nanocellulose composites.[5]

In this thesis, I use paper products as an example for the introduction of cellulose wet adhesion. When wet-web is running on a paper machine, the adhesion at never-dried fiber-fiber joints is called cellulose "never-dried wet adhesion" in this thesis (Figure 1-7). When paper is dry, a high density of crosslinks forms between cellulose surfaces at fiber-fiber joints, including covalent and noncovalent bonding. This interfacial adhesion is called cellulose "dry adhesion". The dried adhesive layer is very thin (< 10 nm) and rigid. Adhesives between dry cellulose surfaces behave more similarly to highly crosslinked resins in thermoset adhesives rather than viscoelastic polymers in pressure-sensitive adhesives.

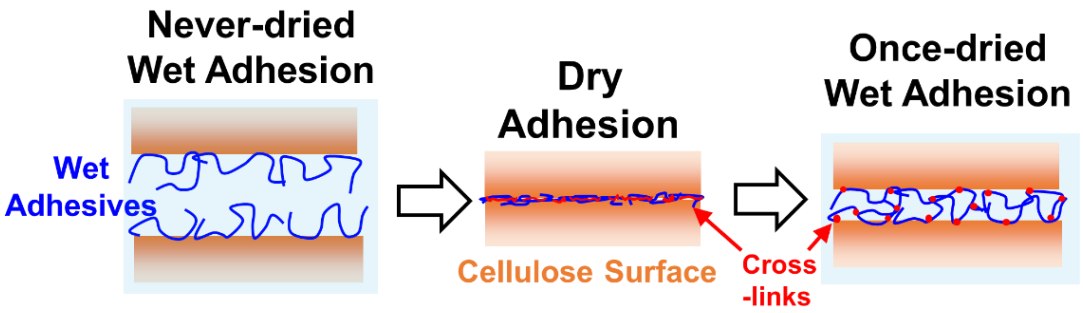

Figure 1-7 Schematic diagram of cellulose adhesion.

When once-dried paper is rewetted, many of the crosslinks that formed between cellulose surfaces after curing now dissociate, due to the presence of water. These include hydrogen bonds and hydrolyzable covalent linkages. After rewetting, the crosslinked adhesive layer is swollen with water, leading to a lower elastic modulus and a higher thickness. The swollen adhesive layer behaves like a hydrogel, and water works as the plasticizer and gives polymers high mobility.[79] The adhesion at this interface is called cellulose "once-dried wet adhesion" in this thesis (Figure 1-7).

A strong cellulose wet adhesion is the key to manufacturing wet strength papers. The wet adhesives at cellulose-cellulose interfaces are different from traditional adhesives for the following reasons:

1) During the formation of wet adhesion, the major driving force for the approaching of the two cellulose surfaces is water removal, instead of external pressure.
2) The thickness of adhesive layer (typically < 100 nanometers) at the interface is a few orders of magnitude lower compared to traditional adhesives (> 100 micrometers).
3) The adhesive layer has a high water content.

So far, there is no single theory to explain cellulose adhesion in a satisfactory manner.[80] Investigators continue to debate the relative contribution of van der Waals forces, hydrogen bonds, electrostatic forces and covalent bonds at the cellulose interface in various situations.[65]

Capillary force. Capillary force is one of the major sources of never-dried wet adhesion. There are two types of water between wet cellulose surfaces: free water and water associated with the swollen cellulose.[58] Take cellulose fibers as an example. At a low solids content (< 30%), the free water at fiber-fiber joint will form a water bridge connecting the two cellulose surfaces.[55] Due to the hydrophilic nature of cellulose, the water bridges form concave menisci and lead to a capillary attraction between two surfaces, which is called the Campbell effect (Figure 1-8).[61] The pressure inside the water bridge is lower than the pressure outside, and the pressure difference over the curved water can be calculated from the Laplace equation.[55] In addition to the Laplace pressure, surface tension and wetting forces are also important components of the capillary force.[62]

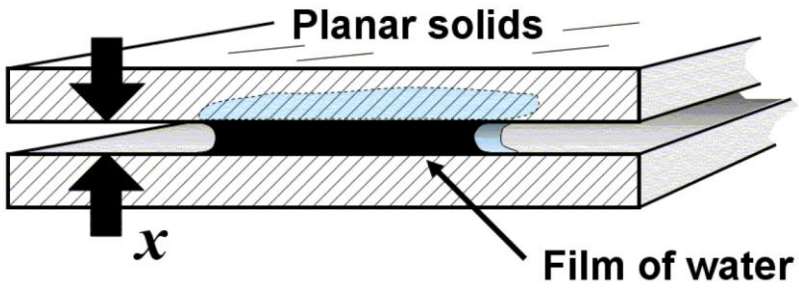

Figure 1-8 Illustration of a film of water between two flat, smooth, wetted surfaces. The negatively curved meniscus results in an attraction force. Picture from Hubbe.[24]

When the solids content of cellulose fibers increases above a critical point (typically 30%, depending on fiber sources), the majority of free water at fiber-fiber joints is

removed, followed by the removal of water associated with fibers.[55] The capillary attraction will decrease significantly due to the absence of free water.

Capillary forces show different effects on cellulose surfaces with different surface roughness. The attractive capillary force may change significantly in value on a rough surface and even switch to repulsion in extreme cases when the meniscus curvature changes from negative to positive.[58] For cellulose materials with rough surfaces, the capillary force deforms the soft cellulose surface during drying and increases the area of intimate contact.[81]

Hydrogen bonding. Hydrogen bonding is a short-range interaction that occurs over distances of 0.1–0.3 nm.[80, 82] It is generally accepted that the hydrogen bonding is the major reason for cellulose dry adhesion. During drying, a high density of hydrogen bonds forms between hydroxyls of adjacent cellulose surfaces.[80] In water, however, hydrogen bonding between cellulose surfaces is very vulnerable. Water breaks the hydrogen bonds between cellulose and binds to cellulose by hydrogen bonding to form associated water. Currently, there is no quantitative study on the relationship between the solids content of cellulose and the formation of hydrogen bonding between cellulose surfaces.[65]

Van der Waals forces. Van der Waals forces are non-specific and long-range interactions for cellulosic materials. The bonding energy of van der Waals forces is 0.5–2.0 kcal/mol.[42] The van der Waals interaction between two crossed cylinders is described in the equation below:

$$W_{vd} = \frac{-A \cdot \sqrt{R_1 \cdot R_2}}{6 \cdot D}$$

where W_{vd} is the interaction energy derived from van der Waals forces, A is the Hamaker constant of the material, R_1 and R_2 are the radii of the cylinders, and D is the distance between the surfaces.[65] In electrolyte aqueous solution, van der Waals interactions between cellulose surfaces are significant with a distance up to 40 nm.[83] The Hamaker constant for cellulose in water is measured to be 9×10^{-21} J.[83] Although the Hamaker constant of cellulose in water is one order of magnitude lower than that in air (8×10^{-20} J), it stays positive, which means the van der Waals force is attractive between wet cellulose surfaces.

Interdiffusion. Some of the most important molecular interactions for cellulose adhesion, such as hydrogen bonding and covalent bonding, only form within a distance of a few angstroms. It is important to have a molecular-level contact between two surfaces to obtain a high degree of cellulose adhesion, in either dry or wet state. Interdiffusion is a mechanism that increases the area available for intermolecular adhesion forces.[81, 82] The

key concept in this mechanism is that the polymer chains on cellulose surfaces must be mobile and able to mix during drying.[84]

Much of the cellulose within cellulosic materials is present as immobile crystals. Other parts consist of amorphous cellulose, which exhibits limited mobility in water. Thus, the introduction of water soluble polymers is necessary to enhance the interdiffusion between cellulose surfaces. From a kinetic point of view, since the adhesive bonds between cellulose fibers are formed during drying in paper manufacturing, the diffusion of neighboring polymers must occur within this timescale. From a thermodynamic point of view, a negative free energy of mixing facilitates a better polymer interdiffusion. In our previous work, we found that the adhesion between two polymer-modified cellulose surfaces is low when the polymers are not compatible with each other, preventing mixing. The low adhesion is due to the lack of interdiffusion between cellulose surfaces.[82] Further study is needed to quantitatively evaluate the contribution of interdiffusion to cellulose adhesion.[81]

Electrostatic interaction. Cellulose surfaces with the same charge show strong electrostatic repulsion in water as the result of osmotic pressure (Figure 1-9). Cellulose surfaces with the opposite charge show electrostatic attraction due to the formation of electrostatic bonding. Electrostatic bonds show a higher bonding energy (10–30 kcal/mol) than hydrogen bonds (4–6 kcal/mol).[42, 85] An advantage of electrostatic attraction is its instantaneous formation in water, which makes it a great candidate for never-dried wet adhesion. Electrostatic attraction also facilitates the formation of hydrogen bonding and covalent bonding by shortening the distance between the two surfaces. However, the electrostatic interaction alone is still too weak to provide a strong cellulose adhesion. For example, PolyDADMAC is a cationic polymer that can adsorb on cellulose via electrostatic attraction. When cellulose is laminated with polyDADMAC, it shows a weak wet adhesion.[65] The influence of electrostatic interaction on wet adhesion is very dependent on the conditions of the medium, such as the pH, the electrolyte concentration and the valence of the counterions.[80]

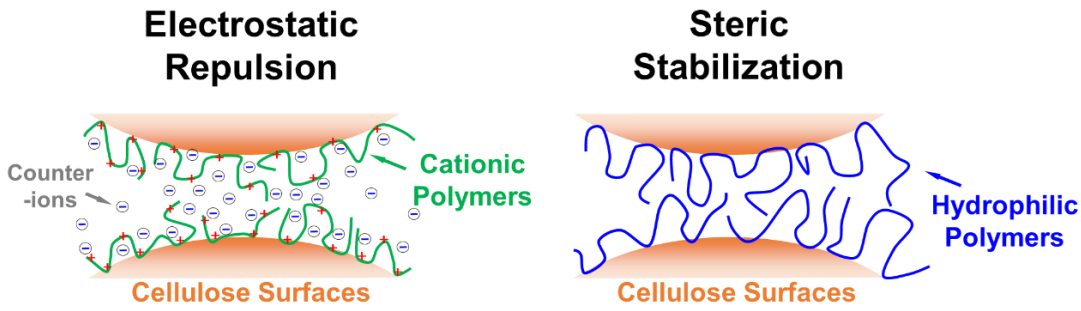

Figure 1-9 Schematic diagrams of electrostatic repulsion and steric stabilization in aqueous dispersions.

Steric stabilization. Steric stabilization is another potential factor that influences the formation of cellulose wet adhesion.[11, 86] Wet cellulose surfaces behave similarly to swollen hydrogels. Due to the steric stabilization effect, hydrated surfaces with mobile cellulose/polymer chains repel each other in water (Figure 1-9).[58, 87] In the case of cellulose coated by hemicellulose or adsorbed with water-soluble polymers, the effect of steric stabilization will be stronger due to higher polymer mobility on the surface. The hydrated hemicellulose or polymer layer can extend as far as 10–100 nm.[58] With further drying, capillary forces would bring these gel-like layers together. The polymer chains would start to interdiffuse at the interface, providing more entanglements and potential crosslinks.[88] Bastidas *et al.* used AFM to observe long-range repulsive interactions between extended microfibrils on cellulose cell walls.[89] The repulsion were believed to arise from the surface electrostatic repulsion and the steric stabilization. Also, Claesson *et al.* reported that the steric barrier between two cellulose surfaces prevents a polymer chain from crossing over from one surface and binding to the other.[87]

Covalent bonding. The covalent bond (50–100 kcal/mol) is the strongest individual bond possible between cellulose surfaces.[42] There is only one functional group on cellulose surface - hydroxyls, and three types of functional groups on oxidized cellulose, hydroxyls, aldehydes and carboxyls. Most adhesives that covalently crosslink cellulose surfaces are designed to target these three groups. Many covalent bonds are able to resist hydrolysis, making them great candidates to enhance both dry and wet adhesion. For example, azetidinium groups in PAE react with carboxylates on oxidized cellulose, providing ester bonding between cellulose surfaces. However, there are three disadvantages of covalent bonding: 1) the formation of covalent bonds often requires drying, the use of expensive catalyst, long curing time or high temperature; 2) cellulose modification is always required; and 3) the bonding density is much lower than hydrogen bonds or van der Waals interactions.

Collision of two functional groups is necessary for the formation of covalent bonds in water. Unlike small molecules, the collision between polyelectrolytes is dominated by their colloidal properties. With two surfaces exhibiting attractive forces in water, the mobile polymer chains attached on one surface are more likely to collide with the other surface. If two surfaces exhibit a high degree of repulsion in water due to electrosteric stabilization, as is the case with most cellulose surfaces, drying is necessary to reduce the distance between surfaces. For amphoteric cellulose surfaces, the situation is more complicated. With the right conditions, two amphoteric polymers can form polyelectrolyte complexes in water due to patching effects or bridging effects, facilitating the formation of covalent bonds in water.

1.5 Recent Studies on Cellulose Wet Adhesives

Cellulose wet adhesion is critical for paper wet strength. The strategies used to enhance cellulose wet adhesion are reviewed in this section. Many methods have been used to evaluate wet adhesion between cellulose surfaces, including tensile tests, peel tests,[53] surface force apparatus,[90] colloidal probe microscopes,[86] and AFM.[91] Different forms of

cellulose surfaces have been prepared for adhesion measurements, such as cellulose fibers, regenerated fibers/membranes,[92] spin-coated films,[86] cellulose colloids,[86] and Langmuir–Blodgett cellulose films.[90] The appearance of cellulose surfaces with nanoscale smoothness makes the measurement of cellulose adhesion at the molecular level possible. The force-distance relationship of specific interactions between cellulose surfaces, such as van der Waals forces, electrostatic interaction, and steric stabilization, have been observed.[76]

It is widely accepted that polymer adsorption is necessary for cellulose wet adhesives, but the adsorption does not guarantee strong adhesion. For example, cationic polyacrylamides and polyDADMAC can adsorb onto cellulose but do not result in significant wet adhesion.[57] Crosslinks between cellulose surfaces are required. The crosslinks can be either covalent linkages or non-covalent ones, as long as they are stable in water.

PVAm is an interesting cellulose wet adhesive that has been studied in the Pelton lab for many years.[75, 93] PVAm adsorbs spontaneously and irreversibly on cellulose surfaces in water, generating cationic interfaces. The primary amines on PVAm react with the aldehydes on oxidized cellulose to give imine (Schiff base) and aminal covalent linkages between cellulose surfaces.[75] Saito and Isogai showed that the addition of 0.6 wt % PVAm in TEMPO-oxidized cellulose fibers led to a 300% increase in paper wet strength.[32] Chen *et al.* reported phenylboronate-derivatized PVAm gave instantaneous adhesion between wet cellulose without a drying or heating step.[64, 94] More details of PVAm chemistry can be found in a review paper Pelton published in 2014, including their properties in water, derivatizations, interfacial interactions, and applications.[75]

Polypeptides are renewable cellulose wet adhesives that share a similar mechanism with PVAm. In the Pelton lab, polylysine, a polypeptide, was applied between oxidized cellulose surfaces. A high degree of wet adhesion was observed due to the covalent bonding between the polylysine and oxidized cellulose after drying.[53] Based on this preliminary work, twenty proteins were compared as potential paper wet adhesives on oxidized cellulose.[78, 95] We found a strong wet adhesion could be achieved with proteins containing a high content of primary amine moieties and a curing with moderate heating.

Hydroxyls of cellulose are weak nucleophiles. A lot of interesting studies show that electrophiles, such as carboxyls, isocyanates, and aldehydes can be used as adhesive groups to crosslink hydroxyls on the cellulose surfaces directly.[65]

Polycarboxylic acids are applied to crosslink cotton cellulose in the textile industry, producing wrinkle-resistant cotton fabrics.[65] Carboxylates crosslink with hydroxyls of cellulose by esterification. Yang *et al.* reported that kraft paper sheets treated with polymaleic acid showed an enhanced wet strength after curing at high temperature (> 150 ºC) with sodium hypophosphite as catalyst.[96] However, paper embrittlement was found in polycarboxylic acid enhancement. In Tanaka's lab, polymers containing isocyanate groups were investigated as paper wet-strength additives.[97] Isocyanates are crosslinkers that react with hydroxyls of cellulose, but they show a low stability in water.[98]

In addition to polyelectrolytes, nanocellulose is another potential carrier of electrophilic adhesive groups. In Ni *et al.*, periodate-oxidized cellulose nanocrystals showed a similar wet strength enhancing performance with polyethyleneimine on bleached kraft fibers.[99] The aldehydes on the nanocellulose crosslinked with cellulose, providing wet strength. Small molecule electrophiles, such as dialdehydes[100] and dicarboxyls,[96] have also been used as paper-strengthening agents. However, the retention of small molecule additives in paper manufacturing is a challenge.

Covalent crosslinks can bind two cellulose surfaces, enhancing cellulose wet adhesion. However, they show disadvantages in some applications. Take nanocellulose materials as an example. Permanent covalent crosslinks hamper the post-processing of these materials and lead to a loss of toughness. In Toivonen *et al.*, chitosan was used to introduce non-covalent, multivalent physical interactions to crosslink nanocellulose.[101] Comparing to covalent crosslinks, non-covalent crosslinks are more tunable and more responsive to the surrounding environment. Moreover, they show great potential to be sacrificial bonds for energy dissipation during physical deformation.[101]

A 2016 publication reported that an excellent wet adhesion was obtained by applying PVAm on CMC-modified cellulose surfaces with or without drying (Figure 1-10).[36] It is believed that the wet adhesion was due to the formation of polyelectrolyte complexes between PVAm and CMC. Laine *et al.* also showed that the combination of cationic polybrene and anionic CMC-modified cellulose fiber led to a high paper wet strength due to the electrostatic interaction and hydrophobic effect.[102]

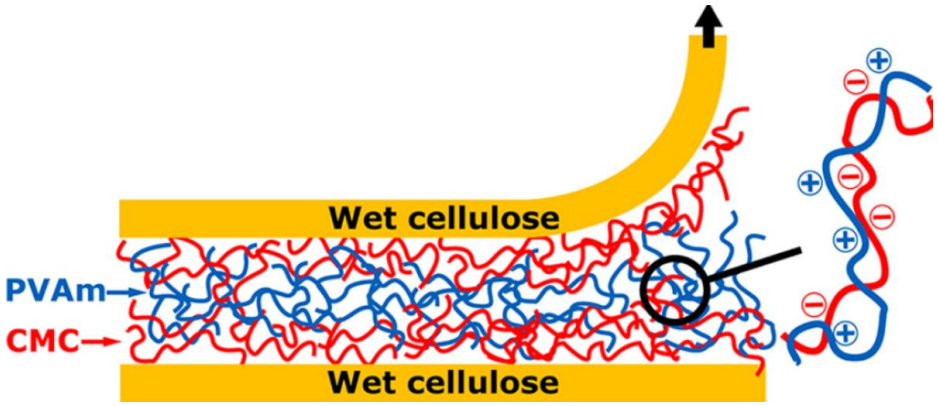

Figure 1-10 Schematic diagram of CMC-modified cellulose materials laminated with PVAm. Picture from Gustafsson *et al.*[36]

Delgado *et al.* prepared zwitterionic cellulose fibers by grafting cellulose with amino acids, including L-lysine and L-tyrosine.[85] The zwitterionic fibers provided a high wet-web strength at solids content above 40%. In Wagberg *et al.*, dopamine moieties were grafted on carboxymethylated cellulose nanofibrils.[103] The wet stability of the nanocellulose film was enhanced in the presence Fe^{3+} ions due to the complexes formed

between grafted dopamine moieties. It was also reported that multivalent metal ions, such as Al^{3+} and Fe^{3+}, were used to enhance cellulose wet adhesion in TEMPO-oxidized nanocellulose films.[104]

Cellulose-binding domains bind specifically to the cellulose surface. With cellulose-binding domains grafted on polymers, the adsorption of this derivatized polymer on cellulose is improved significantly.[5] Galembeck *et al.* proposed an interesting idea to increase cellulose wet adhesion without introducing covalent bonding.[105] Cellulose alkaline aqueous solutions were applied between paper sheets as wet adhesives. After drying, the regenerated cellulose formed an amorphous matrix interpenetrating with the paper matrix, providing joint wet adhesion that was resistant to water.

The normal adsorption limit of wet adhesives on cellulose surface is about 1 mg/m^2.[11] Between laminated cellulose surfaces, there will be two adsorbed polymer layers, which have a thickness of ~ 2 nm after drying.[11] Compared to the roughness on dry cellulose fibers (1 nm – 1 μm), this nanoscale adhesive layer is unlikely to significantly increase the contact area at fiber-fiber joints. Thus, the increase of polymer adsorption on cellulose would lead to a higher wet adhesion due to 1) higher energy dissipation when the joint breaks, 2) a higher contact area between cellulose surfaces, especially rough surfaces, and 3) a possible higher density of crosslinks between cellulose surfaces. Many interesting strategies have been proposed to increase the adsorption coverage of adhesives at cellulose surfaces, enhancing the cellulose wet adhesion.

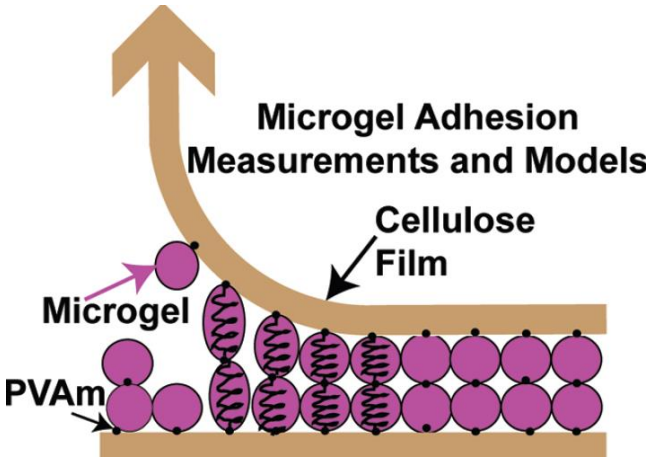

Figure 1-11 Microgel wet adhesives between cellulose surfaces. Picture from Wen *et al.*[106]

Polyelectrolyte complexes were used to increase the adhesive coverage at cellulose surfaces.[107] These complexes are prepared by simply mixing oppositely charged PVAm and CMC. Once adsorbed on cellulose, the adsorption limit of polyelectrolyte complexes is much higher than linear polymers. The complexes are able to dissipate energy under

tensile and shear stress.[108] In Gärdlund *et al.*, PAE and CMC complexes were used as the paper wet-strength resin.[109] The paper wet strength increased 100% compared to the paper enhanced by PAE only. Polyampholytes give the similar performance as polyelectrolyte complexes.[24] On bleached kraft fibers, polyampholytes achieve a higher adsorption and a more effective strength enhancement compared to cationic polyelectrolytes.

Microgel is another option to increase the adhesive coverage at cellulose surfaces (Figure 1-11). In the Pelton lab, PVAm microgels showed a much higher adsorption on regenerated cellulose compared to linear PVAm, and the cellulose wet adhesion exhibited by the microgel adhesives was one order of magnitude higher.[110] In follow-up studies, a mechanistic model was developed to analyze the wet-peel energy between cellulose surfaces.[106, 111] In the model, microgel adhesives were regarded as springs that bound two cellulose surfaces and were stretched during the wet-peel. The wet-peel energy was a function of both adhesive covalent bonding and the energy consumed by microgel stretching.

A polyelectrolyte multilayer can be created by consecutive, repeated adsorption of cationic and anionic polymers (Figure 1-12).[11, 112] The adsorption coverage of this layer-by-layer film is much higher than a single layer of polymers and can be measured by a quartz crystal microbalance technique. Feng *et al.* showed a high cellulose wet adhesion was achieved with PVAm and CMC multilayers.[113] In Laine *et al.*, PAE and nanocellulose were adsorbed on cellulose fiber in sequence.[37] This strategy did not put more PAE at fiber-fiber joints, but it provided a more uniform distribution of substances in the paper matrix, leading to higher paper dry and wet strength.

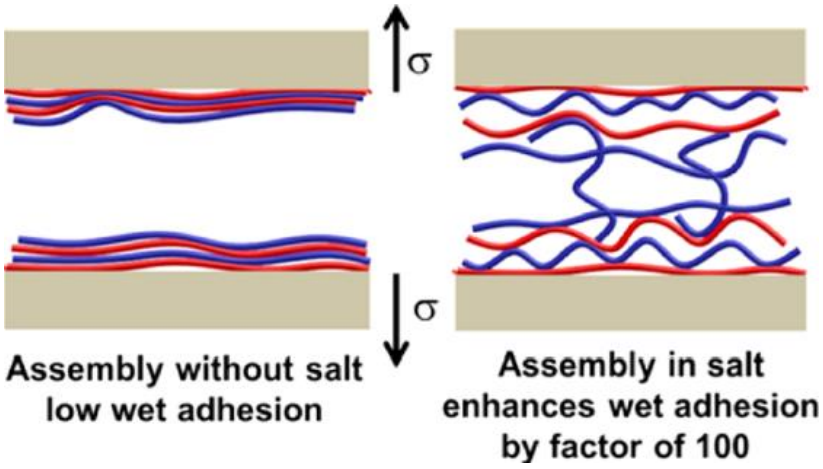

Figure 1-12 Layer-by-layer adhesive film in the absence and presence of salt during the film formation. Poly(allylamine hydrochloride) and hyaluronic acid were used in this study. Picture from Wagberg *et al.*[112]

Wet stability and wet strength are major challenges for nanocellulose materials as well.[101] Most nanocellulose films are not stable in water due to the high hydrophilicity of cellulose. As in paper products, the strength at wet fiber-fiber joints is the key to the wet strength of nanocellulose materials. Studies showed that inter-fiber cross-linking and surface hydrophobization are viable solutions to increase the wet strength.[104] In Hakalahti *et al.*, nanocellulose films with high water stability were prepared using TEMPO-oxidized nanocellulose and polyvinylalcohol additives, where the film was enhanced due to the formation of hemiacetal bonds.[114]

As described in this chapter, currently we have a deep understanding of cellulose chemistry and traditional cellulose wet adhesives. However, no systematic study has been done yet to design cellulose wet adhesives with controllable degradability, which requires much new knowledge, including the design of appropriate measurements, the selection of degradable chemistry, and the synthesis of cellulose adhesives.

1.6 Objectives

I believe that we are at the beginning of a long-term transformation whereby renewable materials based on wood pulp fibers and new nanocellulose composites will replace non-renewable plastics.[7] Strong paper wet strength while maintaining recyclability is one of the major challenges and the target of my work.

In this thesis, I propose to design the next generation of wet adhesives that provide both strong cellulose wet adhesion and controllable degradability to enhance the recycling of wet strength papers. There are four specific objectives in this work:

1. To understand the role of adhesive organization at cellulose interfaces in the formation of wet adhesion.
2. To explore how to further enhance the wet adhesion between cellulose surfaces, using either linear polymer adhesives or microgel adhesives.
3. To develop best strategies of incorporating degradable linkages in wet adhesives to improve their degradability.
4. To develop proofs of concept that demonstrate routes to design cellulose wet adhesives that provide high wet adhesion, while show excellent degradability in response of specific stimuli, such as subtle pH changes, the presence of sugars or reductants.

1.7 Thesis Outline

The thesis consists of three parts (Figure 1-13).

The first part is Chapter 2. A testing procedure called “wet-peel measurement” is introduced in this part. The wet-peel measurement is designed to augment conventional wet paper testing when evaluating wet adhesives and cellulose surface treatments. In the

measurement, a thin layer of wet adhesives is pressed between two wet regenerated cellulose membranes to form a laminate, acting as the physical model for fiber-fiber joints in paper products. The 90-degree wet-peel force is a direct measure of the adhesion at the wet cellulose interface. The wet-peel measurement offers: 1) a comparison of wet adhesive performance at the same polymer content at the wet cellulose interface; 2) a measurement of both once-dried wet adhesion and never-dried wet adhesion; and 3) a demonstration of the influence of cellulose surface modifications on wet adhesion.

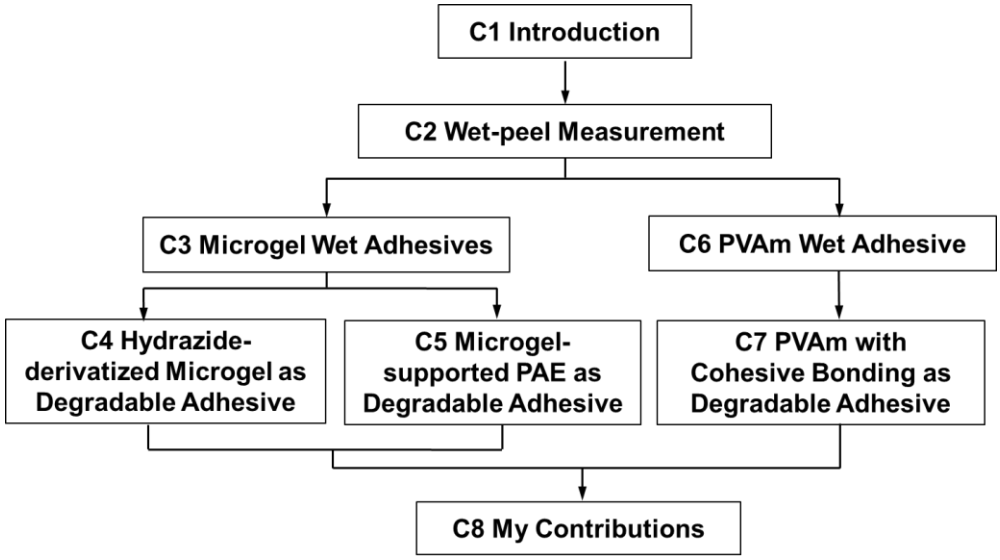

Figure 1-13 Illustration of the thesis outline.

The second part includes Chapter 3, 4 and 5. In this part, microgels are synthesized, characterized and evaluated as cellulose wet adhesives. In Chapter 3, hydrazide-derivatized microgels are synthesized to give strong adhesion to wet, TEMPO-oxidized, regenerated cellulose membranes. The design rules for the microgel adhesives are discussed including the charge, the crosslinking density and the hydrazide grafting on microgels. In Chapter 4, a labile, hydrazide-derivatized microgel is designed to provide a strong yet degradable wet adhesion after exposure to a weak reducing agent. The reductant responsivity is obtained by introducing cleavable disulfide linkages, either in the chains tethering the adhesive hydrazide groups, or as degradable cross-links in the microgels. In Chapter 5, the design of degradable microgel adhesives for wet cellulose is further developed. Microgels with labile disulfide crosslinks are used to load the commercial wet strength resin PAE. The microgel-supported PAE is a promising start as a degradable cellulose wet adhesive due to the cationic surface charge, good degradability, reactive azetidiniums near surfaces and no involvement of chemical conjugation nor organic solvent.

The third part includes Chapter 6 and 7. In this part, I explore the possibilities to convert a linear polymer PVAm to a degradable wet adhesive. In Chapter 6, the conditions are elucidated whereby strong adhesive joints between two wet cellulose surfaces can be achieved with PVAm adhesives. The influence of many factors on cellulose wet adhesion has been studied, such as polymer solution pHs, application methods, cellulose modification and dosages at the interface. In Chapter 7, boronate-derivatized PVAm and dextran-derivatized PVAm are synthesized to promote the cohesion of polymers at the laminate joint. The grafting facilitates the formation of boronic ester bonding between the polymer layers and increases the adsorption of the polymer on cellulose surfaces. I demonstrate that a subtle pH change or a monosaccharide exposure can be used to degrade the cellulose wet adhesion by "switching off" the cohesion between the polymer layers.

References

(1) Shi, S.; Pelton, R.; Fu, Q.; Yang, S. Comparing Polymer-Supported Tempo Mediators for Cellulose Oxidation and Subsequent Polyvinylamine Grafting. *Industrial & Engineering Chemistry Research* **2014,** *53*, 4748-4754.

(2) Klemm, D.; Heublein, B.; Fink, H. P.; Bohn, A. Cellulose: Fascinating Biopolymer and Sustainable Raw Material. *Angewandte Chemie International Edition* **2005,** *44*, 3358-3393.

(3) Wang, J.; Yiu, B.; Obermeyer, J.; Filipe, C. D. M.; Brennan, J. D.; Pelton, R. Effects of Temperature and Relative Humidity on the Stability of Paper-Immobilized Antibodies. *Biomacromolecules* **2012,** *13*, 559-564.

(4) Pelton, R. Bioactive Paper Provides a Low-Cost Platform for Diagnostics. *TrAC Trends in Analytical Chemistry* **2009,** *28*, 925-942.

(5) Sato, T.; Ali, M. M.; Pelton, R.; Cranston, E. D. DNA Stickers Promote Polymer Adsorption onto Cellulose. *Biomacromolecules* **2012,** *13*, 3173-3180.

(6) Pahimanolis, N.; Salminen, A.; Penttilä, P. A.; Korhonen, J. T.; Johansson, L.-S.; Ruokolainen, J.; Serimaa, R.; Seppälä, J. Nanofibrillated Cellulose/Carboxymethyl Cellulose Composite with Improved Wet Strength. *Cellulose* **2013,** *20*, 1459-1468.

(7) Kanie, O.; Tanaka, H.; Mayumi, A.; Kitaoka, T.; Wariishi, H. Composite Sheets with Biodegradable Polymers and Paper, the Effect of Paper Strengthening Agents on Strength Enhancement, and an Evaluation of Biodegradability. *Journal of Applied Polymer Science* **2005,** *96*, 861-866.

(8) Pokhrel, D.; Viraraghavan, T. Treatment of Pulp and Paper Mill Wastewater—a Review. *Science of The Total Environment* **2004,** *333*, 37-58.

(9) Poortinga, W.; Whitaker, L. Promoting the Use of Reusable Coffee Cups through Environmental Messaging, the Provision of Alternatives and Financial Incentives. *Sustainability* **2018,** *10*, 873.

(10) Tejado, A.; Van De Ven, T. G. M. Why Does Paper Get Stronger as It Dries? *Materials Today* **2010,** *13*, 42-49.

(11) Pelton, R. On the Design of Polymers for Increased Paper Dry Strength-a Review. *Appita journal* **2004,** *57*, 181.

(12) Su, J.; Zhang, L.; Batchelor, W.; Garnier, G. Paper Engineered with Cellulosic Additives: Effect of Length Scale. *Cellulose* **2014,** *21*, 2901-2911.

(13) Mazhari Mousavi, S. M.; Hosseini, S. Z.; Resalati, H.; Mahdavi, S.; Rasooly Garmaroody, E. Papermaking Potential of Rapeseed Straw, a New Agricultural-Based Fiber Source. *Journal of Cleaner Production* **2013,** *52*, 420-424.

(14) Nordell, P. Wet-Strength Development of Paper. 2006.

(15) Nikolaeva, M. Measurement and Improvement of Wet Paper Wet Strength. Lappeenranta University of Technology, 2010.

(16) Sun, Y.; Cheng, J. Hydrolysis of Lignocellulosic Materials for Ethanol Production: A Review. *Bioresource Technology* **2002,** *83*, 1-11.

(17) Saavedra Salas, I. Model-Based Optimization of a Compactcooking G2 Digesting Process Stage. **2016**.

(18) Santos, A. J.; Anjos, O.; Simoes, R. Influence of Kraft Cooking Conditions on the Pulp Quality of Eucalyptus Globulus. *Appita Journal* **2008,** *61*, 148.

(19) Spence, K. L.; Venditti, R. A.; Habibi, Y.; Rojas, O. J.; Pawlak, J. J. The Effect of Chemical Composition on Microfibrillar Cellulose Films from Wood Pulps: Mechanical Processing and Physical Properties. *Bioresource Technology* **2010,** *101*, 5961-5968.

(20) Andreasson, B.; Forsström, J.; Wågberg, L. Determination of Fibre Pore Structure: Influence of Salt, Ph and Conventional Wet Strength Resins. *Cellulose* **2005,** *12*, 253-265.

(21) Booker, R. E.; Sell, J. The Nanostructure of the Cell Wall of Softwoods and Its Functions in a Living Tree. *Holz als Roh- und Werkstoff* **1998,** *56*, 1.

(22) Brandt, A.; Grasvik, J.; Hallett, J. P.; Welton, T. Deconstruction of Lignocellulosic Biomass with Ionic Liquids. *Green Chemistry* **2013,** *15*, 550-583.

(23) Chinga-Carrasco, G. Cellulose Fibres, Nanofibrils and Microfibrils: The Morphological Sequence of Mfc Components from a Plant Physiology and Fibre Technology Point of View. *Nanoscale Research Letters* **2011,** *6*, 417-417.

(24) Hubbe, M. A. Bonding between Cellulosic Fibers in the Absence and Presence of Dry-Strength Agents–a Review. *BioResources* **2007,** *1*, 281-318.

(25) Gärdlund, L.; Norgren, M.; Wågberg, L.; Marklund, A. The Use of Polyelectrolyte Complexes (Pec) as Strength Additives for Different Pulps Used for Production of Fine Paper. *Nordic Pulp & Paper Research Journal* **2007,** *22*, 210-216.

(26) Yang, D.; Zhong, L.-X.; Yuan, T.-Q.; Peng, X.-W.; Sun, R.-C. Studies on the Structural Characterization of Lignin, Hemicelluloses and Cellulose Fractionated by Ionic Liquid Followed by Alkaline Extraction from Bamboo. *Industrial Crops and Products* **2013,** *43*, 141-149.

(27) Whitmore, P. M.; Bogaard, J. Determination of the Cellulose Scission Route in the Hydrolytic and Oxidative Degradation of Paper. *Restaurator* **1994,** *15*, 26-45.

(28) Isogai, A.; Saito, T.; Fukuzumi, H. Tempo-Oxidized Cellulose Nanofibers. *Nanoscale* **2011,** *3*, 71-85.

(29) Yang, D.; Peng, X.-W.; Zhong, L.-X.; Cao, X.-F.; Chen, W.; Sun, R.-C. Effects of Pretreatments on Crystalline Properties and Morphology of Cellulose Nanocrystals. *Cellulose* **2013,** *20*, 2427-2437.

(30) Hou, Q.; Liu, W.; Liu, Z.; Bai, L. Characteristics of Wood Cellulose Fibers Treated with Periodate and Bisulfite. *Industrial & Engineering Chemistry Research* **2007,** *46*, 7830-7837.

(31) Diflavio, J.-L.; Pelton, R.; Leduc, M.; Champ, S.; Essig, M.; Frechen, T. The Role of Mild Tempo–Nabr–Naclo Oxidation on the Wet Adhesion of Regenerated Cellulose Membranes with Polyvinylamine. *Cellulose* **2007,** *14*, 257-268.

(32) Saito, T.; Isogai, A. Wet Strength Improvement of Tempo-Oxidized Cellulose Sheets Prepared with Cationic Polymers. *Industrial & engineering chemistry research* **2007,** *46*, 773-780.

(33) Saito, T.; Isogai, A. Tempo-Mediated Oxidation of Native Cellulose. The Effect of Oxidation Conditions on Chemical and Crystal Structures of the Water-Insoluble Fractions. *Biomacromolecules* **2004,** *5*, 1983-1989.

(34) Laine, J.; Lindstrom, T.; Nordmark, G. G.; Risinger, G. Studies on Topochemical Modification of Cellulosic Fibres Part 1. Chemical Conditions for the Attachment of Carboxymethyl Cellulose onto Fibres. *Nordic Pulp & Paper Research Journal* **2000,** *15*, 520-526.

(35) Laine, J.; Lindstrom, T.; Nordmark, G.; Risinger, G. Studies on Topochemical Modification of Cellulosic Fibres-Part 3. The Effect of Carboxymethyl Cellulose Attachment on Wet-Strength Development by Alkaline-Curing Polyamide-Amine Epichlorohydrin Resins. *Nordic Pulp & Paper Research Journal* **2002,** *17*, 57-60.

(36) Gustafsson, E.; Pelton, R.; Wågberg, L. Rapid Development of Wet Adhesion between Carboxymethylcellulose Modified Cellulose Surfaces Laminated with Polyvinylamine Adhesive. *ACS Applied Materials & Interfaces* **2016,** *8*, 24161-24167.

(37) Ahola, S.; Österberg, M.; Laine, J. Cellulose Nanofibrils—Adsorption with Poly(Amideamine) Epichlorohydrin Studied by Qcm-D and Application as a Paper Strength Additive. *Cellulose* **2007,** *15*, 303-314.

(38) Wang, J.; Monton, M. R. N.; Zhang, X.; Filipe, C. D. M.; Pelton, R.; Brennan, J. D. Hydrophobic Sol-Gel Channel Patterning Strategies for Paper-Based Microfluidics. *Lab on a Chip* **2014,** *14*, 691-695.

(39) Lindström, T.; Larsson, P. T. Alkyl Ketene Dimer (Akd) Sizing: A Review. *Nordic Pulp & Paper Research Journal* **2008,** *23*, 202-209.

(40) Guo, M.; Her, S.; Keunen, R.; Zhang, S.; Allen, C.; Winnik, M. A. Functionalization of Cellulose Nanocrystals with Peg-Metal-Chelating Block

Copolymers Via Controlled Conjugation in Aqueous Media. *ACS Omega* **2016,** *1*, 93-107.

(41) Barai, B. K.; Singhal, R. S.; Kulkarni, P. R. Optimization of a Process for Preparing Carboxymethyl Cellulose from Water Hyacinth (Eichornia Crassipes). *Carbohydrate Polymers* **1997,** *32*, 229-231.

(42) Delgado-Fornué, E.; Contreras, H. J.; Toriz, G.; Allan, G. G. Adhesion between Cellulosic Fibers in Paper. *Journal of Adhesion Science and Technology* **2011,** *25*, 597-614.

(43) Fatona, A.; Berry, R. M.; Brook, M. A.; Moran-Mirabal, J. M. Versatile Surface Modification of Cellulose Fibers and Cellulose Nanocrystals through Modular Triazinyl Chemistry. *Chemistry of Materials* **2018,** *30*, 2424-2435.

(44) Bel-Hassen, R.; Boufi, S.; Salon, M. C. B.; Abdelmouleh, M.; Belgacem, M. N. Adsorption of Silane onto Cellulose Fibers. Ii. The Effect of Ph on Silane Hydrolysis, Condensation, and Adsorption Behavior. *Journal of applied polymer science* **2008,** *108*, 1958-1968.

(45) Koga, H.; Kitaoka, T.; Isogai, A. In Situ Modification of Cellulose Paper with Amino Groups for Catalytic Applications. *Journal of Materials Chemistry* **2011,** *21*, 9356-9361.

(46) Buschle-Diller, G.; Zeronian, S. H. Enhancing the Reactivity and Strength of Cotton Fibers. *Journal of Applied Polymer Science* **1992,** *45*, 967-979.

(47) Kim, J. T.; Netravali, A. N. Mercerization of Sisal Fibers: Effect of Tension on Mechanical Properties of Sisal Fiber and Fiber-Reinforced Composites. *Composites Part A: Applied Science and Manufacturing* **2010,** *41*, 1245-1252.

(48) Isogai, A.; Kato, Y. Preparation of Polyuronic Acid from Cellulose by Tempo-Mediated Oxidation. *Cellulose* **1998,** *5*, 153-164.

(49) Beeson, W. T.; Phillips, C. M.; Cate, J. H. D.; Marletta, M. A. Oxidative Cleavage of Cellulose by Fungal Copper-Dependent Polysaccharide Monooxygenases. *Journal of the American Chemical Society* **2012,** *134*, 890-892.

(50) Stephens, C. H.; Whitmore, P. M.; Morris, H. R.; Bier, M. E. Hydrolysis of the Amorphous Cellulose in Cotton-Based Paper. *Biomacromolecules* **2008,** *9*, 1093-1099.

(51) Wu, W.; Huang, F.; Pan, S.; Mu, W.; Meng, X.; Yang, H.; Xu, Z.; Ragauskas, A. J.; Deng, Y. Thermo-Responsive and Fluorescent Cellulose Nanocrystals Grafted with Polymer Brushes. *Journal of Materials Chemistry A* **2015**.

(52) Page, D. A Theory for Tensile Strength of Paper. *Tappi* **1969,** *52*, 674-&.

(53) Kurosu, K.; Pelton, R. Simple Lysine-Containing Polypeptide and Polyvinylamine Adhesives for Wet Cellulose. *Journal of pulp and paper science* **2004,** *30*, 228-232.

(54) Chen, N.; Hu, S.; Pelton, R. Mechanisms of Aldehyde-Containing Paper Wet-Strength Resins. *Industrial & engineering chemistry research* **2002,** *41*, 5366-5371.

(55) De Oliveira, M. H. Wet Web Strength Development of Paper. McGill University, 2007.

(56) Salminen, K.; Kataja-Aho, J.; Lindqvist, H.; Retulainen, E.; Rantanen, T.; Sundberg, A. In *The Effects of Certain Polymers on Tensile Strength and Tension Relaxation of Wet Web*, PaperCon. TAPPI PaperCon Conference, Covington, KY USA, 2011; pp 825-832.

(57) Chen, W.; Leung, V.; Kroener, H.; Pelton, R. Polyvinylamine− Phenylboronic Acid Adhesion to Cellulose Hydrogel. *Langmuir* **2009,** *25*, 6863-6868.

(58) Alince, B.; Vanerek, A.; De Oliveira, M. H.; Van De Ven, T. G. The Effect of Polyelectrolytes on the Wet-Web Strength of Paper. *Nordic Pulp & Paper Research Journal* **2006,** *21*, 653-658.

(59) Stuman, F., The Influence of Filler Content and Process Additives on Wet Web Strength and Runnability. PaperCon: 2011.

(60) Tejado, A.; Van De Ven, T. In *The Strength of Wet Paper: Capillary Forces or Entanglement Friction?*, International Paper and Coating Chemistry Symposium Hamilton, Canada. 7th, 2009.

(61) Campbell, W. B. The Cellulose-Water Relationship in Paper-Making. **1933**.

(62) Van De Ven, T. G. M. Capillary Forces in Wet Paper. *Industrial & Engineering Chemistry Research* **2008,** *47*, 7250-7256.

(63) Tejado, A.; Antal, M.; Liu, X.; Van De Ven, T. G. M. Wet Cross-Linking of Cellulose Fibers Via a Bioconjugation Reaction. *Industrial & Engineering Chemistry Research* **2011,** *50*, 5907-5913.

(64) Chen, W.; Cui, Y.; Pelton, R. The Remarkable Adhesion of Cellulose Hydrogel to Polyvinylamine Bearing Pendent Phenylboronic Acid. *Journal of Adhesion Science and Technology* **2011,** *25*, 543-555.

(65) Lindström, T.; Wågberg, L.; Larsson, T. In *On the Nature of Joint Strength in Paper—a Review of Dry and Wet Strength Resins Used in Paper Manufacturing*, 13th Fundamental research symposium, The Pulp and Paper Fundamental Research Society Cambridge, UK: 2005; pp 457-562.

(66) Espy, H. H. The Mechanism of Wet-Strength Development in Paper: A Review. *Tappi Journal* **1995,** *78*, 90-100.

(67) Potter, F. S.; Johnson, J. W.; Wright, T. L.; Hagiopol, C. A New Perspective on Tissue Wet Strength Decay: The Real Values. *Tappi* **2013,** *12*, 9-15.

(68) Proverb, R. J.; Pawlowska, L. M. Temporary Wet Strength Resin for Paper Applications. Pat. 2011.

(69) Obokata, T.; Isogai, A. 1h- and 13c-Nmr Analyses of Aqueous Polyamideamine–Epichlorohydrin Resin Solutions. *Journal of Applied Polymer Science* **2004,** *92*, 1847-1854.

(70) Obokata, T.; Isogai, A. Deterioration of Polyamideamine–Epichlorohydrin (Pae) in Aqueous Solutions During Storage: Structural Changes of Pae. *Journal of Polymers and the Environment* **2004,** *13*, 1-6.

(71) Obokata, T.; Yanagisawa, M.; Isogai, A. Characterization of Polyamideamine-Epichlorohydrin (Pae) Resin: Roles of Azetidinium Groups and Molecular Mass of Pae in

Wet Strength Development of Paper Prepared with Pae. *Journal of Applied Polymer Science* **2005,** *97*, 2249-2255.

(72) Obokata, T.; Isogai, A. The Mechanism of Wet-Strength Development of Cellulose Sheets Prepared with Polyamideamine-Epichlorohydrin (Pae) Resin. *Colloids and Surfaces A: Physicochemical and Engineering Aspects* **2007,** *302*, 525-531.

(73) Siqueira, E. J.; Salon, M.-C. B.; Belgacem, M. N.; Mauret, E. Carboxymethylcellulose (Cmc) as a Model Compound of Cellulose Fibers and Polyamideamine Epichlorohydrin (Pae)–Cmc Interactions as a Model of Pae–Fibers Interactions of Pae-Based Wet Strength Papers. *Journal of Applied Polymer Science* **2015,** *132*, n/a-n/a.

(74) Chen, Z.; Zhang, H.; Song, Z.; Qian, X. Preparation and Application of Maleic Anhydride-Acylated Chitosan for Wet Strength Improvement of Paper. *BioResources* **2013,** *8*, 3901-3911.

(75) Pelton, R. Polyvinylamine: A Tool for Engineering Interfaces. *Langmuir* **2014**.

(76) Zhao, B.; Kwon, H. J. Adhesion of Polymers in Paper Products from the Macroscopic to Molecular Level — an Overview. *Journal of Adhesion Science and Technology* **2011,** *25*, 557-579.

(77) Kendall, K., *Molecular Adhesion and Its Applications: The Sticky Universe*. Springer Science & Business Media: 2007.

(78) Li, X.; Pelton, R. Enhancing Wet Cellulose Adhesion with Proteins. *Industrial & Engineering Chemistry Research* **2005,** *44*, 7398-7404.

(79) Merindol, R.; Diabang, S.; Felix, O.; Roland, T.; Gauthier, C.; Decher, G. Bio-Inspired Multiproperty Materials: Strong, Self-Healing, and Transparent Artificial Wood Nanostructures. *ACS nano* **2015,** *9*, 1127-1136.

(80) Fornué, E. D.; Allan, G. G.; Quiñones, H. J. C.; González, G. T.; Saucedo, J. T. Fundamental Aspects of Adhesion between Cellulosic Surfaces in Contact—a Review. *O Papel* **2011,** *72*, 85-90.

(81) Hirn, U.; Schennach, R. In *Fiber-Fiber Bond Formation and Failure: Mechanisms and Analytical Techniques*, Advances in pulp and paper research, Oxford 2017: 16th Fundamental Research Symposium, Oxford, September 2017, The Pulp and Paper Fundamental Research Society: 2017.

(82) Pelton, R.; Zhang, J.; Wågberg, L.; Rundlöf, M. In *The Role of Surface Polymer Compatibility in the Formation of Fiber/Fiber Bonds in Paper*, Nordic Pulp & Paper Research Journal, 2000; pp 400-406.

(83) Notley, S. M.; Pettersson, B.; Wågberg, L. Direct Measurement of Attractive Van Der Waals' Forces between Regenerated Cellulose Surfaces in an Aqueous Environment. *Journal of the American Chemical Society* **2004,** *126*, 13930-13931.

(84) Zhao, B.; Bursztyn, L.; Pelton, R. Simple Approach for Quantifying the Thermodynamic Potential of Polymer–Polymer Adhesion. *The Journal of Adhesion* **2006,** *82*, 121-133.

(85) Delgado, E.; López-Dellamary, F.; Allan, G.; Andrade, A.; Contreras, H.; Regla, H.; Cresson, T. Zwitterion Modification of Fibres: Effect of Fibre Flexibility on Wet Strength of Paper. *Journal of pulp and paper science* **2004,** *30*, 141-144.

(86) Leporatti, S.; Sczech, R.; Riegler, H.; Bruzzano, S.; Storsberg, J.; Loth, F.; Jaeger, W.; Laschewsky, A.; Eichhorn, S.; Donath, E. Interaction Forces between Cellulose Microspheres and Ultrathin Cellulose Films Monitored by Colloidal Probe Microscopy—Effect of Wet Strength Agents. *Journal of colloid and interface science* **2005,** *281*, 101-111.

(87) Claesson, P. M.; Dedinaite, A.; Rojas, O. J. Polyelectrolytes as Adhesion Modifiers. *Advances in colloid and interface science* **2003,** *104*, 53-74.

(88) Pelton, R. A Model of the External Surface of Wood Pulp Fibers. *Nordic Pulp and Paper Research Journal (Sweden)* **1993**.

(89) Bastidas, J. C.; Venditti, R.; Pawlak, J.; Gilbert, R.; Zauscher, S.; Kadla, J. F. Chemical Force Microscopy of Cellulosic Fibers. *Carbohydrate Polymers* **2005,** *62*, 369-378.

(90) Österberg, M. The Effect of a Cationic Polyelectrolyte on the Forces between Two Cellulose Surfaces and between One Cellulose and One Mineral Surface. *Journal of colloid and interface science* **2000,** *229*, 620-627.

(91) Notley, S. M.; Chen, W.; Pelton, R. Extraordinary Adhesion of Phenylboronic Acid Derivatives of Polyvinylamine to Wet Cellulose: A Colloidal Probe Microscopy Investigation. *Langmuir* **2009,** *25*, 6898-6904.

(92) Wen, Q.; Pelton, R. Design Rules for Microgel-Supported Adhesives. *Industrial & Engineering Chemistry Research* **2012,** *51*, 9564-9570.

(93) Pelton, R.; Hong, J. Some Properties of Newsprint Impregnated with Polyvinylamine. *Tappi journal* **2002,** *1*, 21-25.

(94) Chen, W.; Lu, C.; Pelton, R. Polyvinylamine Boronate Adhesion to Cellulose Hydrogel. *Biomacromolecules* **2006,** *7*, 701-702.

(95) Su, S.; Pelton, R. Bovine Serum Albumin (Bsa) as an Adhesive for Wet Cellulose. *Cellulose* **2006,** *13*, 537-545.

(96) Yang, C. Q.; Xu, Y.; Wang, D. Ft-Ir Spectroscopy Study of the Polycarboxylic Acids Used for Paper Wet Strength Improvement. *Industrial & Engineering Chemistry Research* **1996,** *35*, 4037-4042.

(97) Zhang, X.; Tanaka, H. Synthesis of Polymers Containing Isocyanate Groups and Use of Polymers as Paper Dry and Wet Strength Additives. *J Wood Sci* **1999,** *45*, 425.

(98) Siqueira, G.; Bras, J.; Dufresne, A. New Process of Chemical Grafting of Cellulose Nanoparticles with a Long Chain Isocyanate. *Langmuir* **2010,** *26*, 402-411.

(99) Sun, B.; Hou, Q.; Liu, Z.; Ni, Y. Sodium Periodate Oxidation of Cellulose Nanocrystal and Its Application as a Paper Wet Strength Additive. *Cellulose* **2015,** *22*, 1135-1146.

(100) Xu, G. G.; Yang, C. Q.; Deng, Y. Applications of Bifunctional Aldehydes to Improve Paper Wet Strength. *Journal of Applied Polymer Science* **2002,** *83*, 2539-2547.

(101) Toivonen, M. S.; Kurki-Suonio, S.; Schacher, F. H.; Hietala, S.; Rojas, O. J.; Ikkala, O. Water-Resistant, Transparent Hybrid Nanopaper by Physical Cross-Linking with Chitosan. *Biomacromolecules* **2015,** *16*, 1062-1071.

(102) Aarne, N.; Vesterinen, A.-H.; Kontturi, E.; Seppälä, J.; Laine, J. A Systematic Study of Noncross-Linking Wet Strength Agents. *Industrial & Engineering Chemistry Research* **2013,** *52*, 12010-12017.

(103) Karabulut, E.; Pettersson, T.; Ankerfors, M.; Wågberg, L. Adhesive Layer-by-Layer Films of Carboxymethylated Cellulose Nanofibril–Dopamine Covalent Bioconjugates Inspired by Marine Mussel Threads. *ACS Nano* **2012,** *6*, 4731-4739.

(104) Shimizu, M.; Saito, T.; Isogai, A. Water-Resistant and High Oxygen-Barrier Nanocellulose Films with Interfibrillar Cross-Linkages Formed through Multivalent Metal Ions. *Journal of Membrane Science* **2016,** *500*, 1-7.

(105) Ferreira, E. S.; Lanzoni, E. M.; Costa, C. a. R.; Deneke, C.; Bernardes, J. S.; Galembeck, F. Adhesive and Reinforcing Properties of Soluble Cellulose: A Repulpable Adhesive for Wet and Dry Cellulosic Substrates. *ACS Applied Materials & Interfaces* **2015,** *7*, 18750-18758.

(106) Wen, Q.; Pelton, R. Microgel Adhesives for Wet Cellulose: Measurements and Modeling. *Langmuir* **2012,** *28*, 5450-5457.

(107) Feng, X.; Pelton, R.; Leduc, M. Mechanical Properties of Polyelectrolyte Complex Films Based on Polyvinylamine and Carboxymethyl Cellulose. *Industrial & Engineering Chemistry Research* **2006,** *45*, 6665-6671.

(108) Feng, X.; Pelton, R.; Leduc, M.; Champ, S. Colloidal Complexes from Poly(Vinyl Amine) and Carboxymethyl Cellulose Mixtures. *Langmuir* **2007,** *23*, 2970-2976.

(109) Gärdlund, L.; Wågberg, L.; Gernandt, R. Polyelectrolyte Complexes for Surface Modification of Wood Fibres: Ii. Influence of Complexes on Wet and Dry Strength of Paper. *Colloids and Surfaces A: Physicochemical and Engineering Aspects* **2003,** *218*, 137-149.

(110) Miao, C.; Chen, X.; Pelton, R. Adhesion of Poly(Vinylamine) Microgels to Wet Cellulose. *Industrial & Engineering Chemistry Research* **2007,** *46*, 6486-6493.

(111) Wen, Q. Microgel Based Adhesive for Wet Paper Strength. McMaster University, 2012.

(112) Pettersson, T.; Pendergraph, S. A.; Utsel, S.; Marais, A.; Gustafsson, E.; Wågberg, L. Robust and Tailored Wet Adhesion in Biopolymer Thin Films. *Biomacromolecules* **2014,** *15*, 4420-4428.

(113) Feng, X.; Zhang, D.; Pelton, R. Adhesion to Wet Cellulose–Comparing Adhesive Layer-by-Layer Assembly to Coating Polyelectrolyte Complex Suspensions 2nd Icc 2007, Tokyo, Japan, October 25–29, 2007. *Holzforschung* **2009,** *63*, 28-32.

(114) Hakalahti, M.; Salminen, A.; Seppälä, J.; Tammelin, T.; Hänninen, T. Effect of Interfibrillar Pva Bridging on Water Stability and Mechanical Properties of Tempo/Naclo 2 Oxidized Cellulosic Nanofibril Films. *Carbohydrate polymers* **2015,** *126*, 78-82.

Chapter 2

Wet-peel — a Tool for Evaluating Cellulose Wet Adhesives

This chapter describes the wet-peel measurement in detail. Instead of using paper samples, regenerated cellulose membranes were used to simulate cellulose fibers. The 90-degree wet-peel was used to measure the wet adhesion between cellulose surfaces. This easy and reliable measurement provide me a deep understanding of the adhesion forces between cellulose surfaces. In this thesis, I have used wet-peel measurements to evaluate the performance of various cellulose wet adhesives, such as microgel adhesives (Chapters 3–5), polymer adhesives (Chapters 6, 7 and Appendix A), and layer-by-layer adhesives (Appendix B).

The data within this chapter have been collected by me with the assistance of Dr. John-Louis DiFlavio and Dr. Emil Gustafsson. Dr. DiFlavio conducted a part of the wet-peel measurements, and Dr. Gustafsson conducted the experiment involving paper handsheets. I summarized the data and wrote the draft myself. Dr. Robert Pelton helped me analyze the results and re-write parts of the draft as necessary.

This chapter and the supporting information are reprinted as they appear in *Nordic Pulp & Paper Research Journal* with permission from the Walter de Gruyter GmbH.

Wet-peel: a Tool for Comparing Wet-strength Resins

Dong Yang, John-Louis DiFlavio, Emil Gustafsson, and Robert Pelton

Nordic Pulp & Paper Research Journal, 2018

https://doi.org/10.1515/npprj-2018-001

Paper chemistry

Dong Yang, John-Louis DiFlavio, Emil Gustafsson and Robert Pelton*

Wet-peel: a tool for comparing wet-strength resins

https://doi.org/10.1515/npprj-2018-0013
Received June 7, 2018; accepted July 27, 2018

Abstract: We propose that a testing procedure we call wet-peel significantly augments conventional wet paper testing when comparing wet-strength resin efficacy or the influence wood pulp fiber surface treatments on wet paper strength. A thin layer of wet-strength resin is sandwiched between a pair of thin, wet regenerated cellulose membranes to form a laminate, which is a physical model for fiber-fiber joints in paper. In the wet-peel method, the ninety-degree wet-delamination force gives a direct measure of adhesion in the wet cellulose-cellulose joint. Wet-peel measurements offer: 1) comparisons of wet-strength polymers at the same content of polymer in the laminate joint without the influences of varying fines contents, formation or paper density; 2) measurements of both the wet-strength of cured, dried joints, and the strength of never-dried joints (i. e. analogous to wet-web strength); 3) demonstrations of the influence of fiber surface chemistry modifications including oxidation and the presence of firmly bound polymers; and, 4) the evaluation of more exotic joint structures including layer-by-layer assemblies, microgels and colloidal polyelectrolyte complexes.

Keywords: peel delamination; resin testing; wet-strength; wet-web strength.

Introduction

Wet strength is one the most difficult paper properties to improve. Whereas polyethylene films have the same strength wet or dry, paper products undergo a catastrophic loss of strength when exposed to water. Individual wood pulp fibers are somewhat weaker wet than dry; unbleached pulp fibers have about the same strength wet or dry, whereas bleached fibers can be up to 30 % weaker (Gurnagul and Page 1989). However, fiber weakening does not explain the low strength of wet paper. Instead, water swelling of fiber-fiber joints severs hydrogen bonds and both weakens the joints and renders the fiber wall more susceptible to delamination. The current solution is the use of wet-strength resins that strengthen wet fiber-fiber joints. The chemical companies supplying the paper industry continue to evolve wet-strength resin technologies. The gold standard for evaluating new wet-strength resins is a papermachine trial. However, much of the early development work typically employs wet tensile measurements of laboratory made paper. We started working on wet strength chemistries in 2002 and have developed a new laboratory wet strength measurement that augments handsheet wet tensile measurements, giving much additional information. The goal of this paper is to describe the technique which we call "Wet-peeling", illustrating the utility of wet-peel measurements with data collected over the last 15 years.

Wet-peeling is a variation of an approach first described by McLaren in 1948 (McLaren 1948). Two wet, regenerated cellulose membranes are stacked with a thin layer of wet-strength resin between them. The stack is pressed (laminated), dried, and then rewetted. The resulting laminate is a physical model for wet fiber-fiber joints in paper. Wet laminate strength is measured as the 90-degree peel delamination force required to separate the two membranes.

Most of the results presented below employed examples from three types of commercial wet-strength resins; polyamideamine-epichlorohydrin (PAE), polyvinylamine (PVAm), and glyoxalated cationic polyacrylamide (GC-PAM). PAE, a modified condensation polymer, is arguably the most common type of wet-strength resin used today. The literature reports a very broad range of weight-average molecular weights (7 to 1,100 kDa) and very broad molecular weight distribution (Obokata et al. 2005). PAE has a moderate cationic charge; our sample gave 2 meq/g, based on polyelectrolyte titration. With drying and heating, azetidinium groups form covalent crosslinks and covalent grafts to carboxyl groups on fiber surfaces – see Figure 1. The lowest molecular weight fractions of PAE can enter fiber wall pores, strengthening the fibers (Taylor 1968) (Andreasson et al. 2005).

***Corresponding author: Robert Pelton,** Chemical Engineering, McMaster University, 1280 Main St. West, Hamilton, ON L8S 4L7, Canada, e-mail: peltonrh@mcmaster.ca, ORCID: http://orcid.org/0000-0002-8006-0745
Dong Yang, Emil Gustafsson, Chemical Engineering, McMaster University, 1280 Main St. West, Hamilton, ON L8S 4L7, Canada, e-mails: yangd24@mcmaster.ca, emilgus@kth.se
John-Louis DiFlavio, The Lubrizol Corporation 29400 Lakeland Blvd, Wickliffe, OH 44092, USA, e-mail: loudiflavio@gmail.com

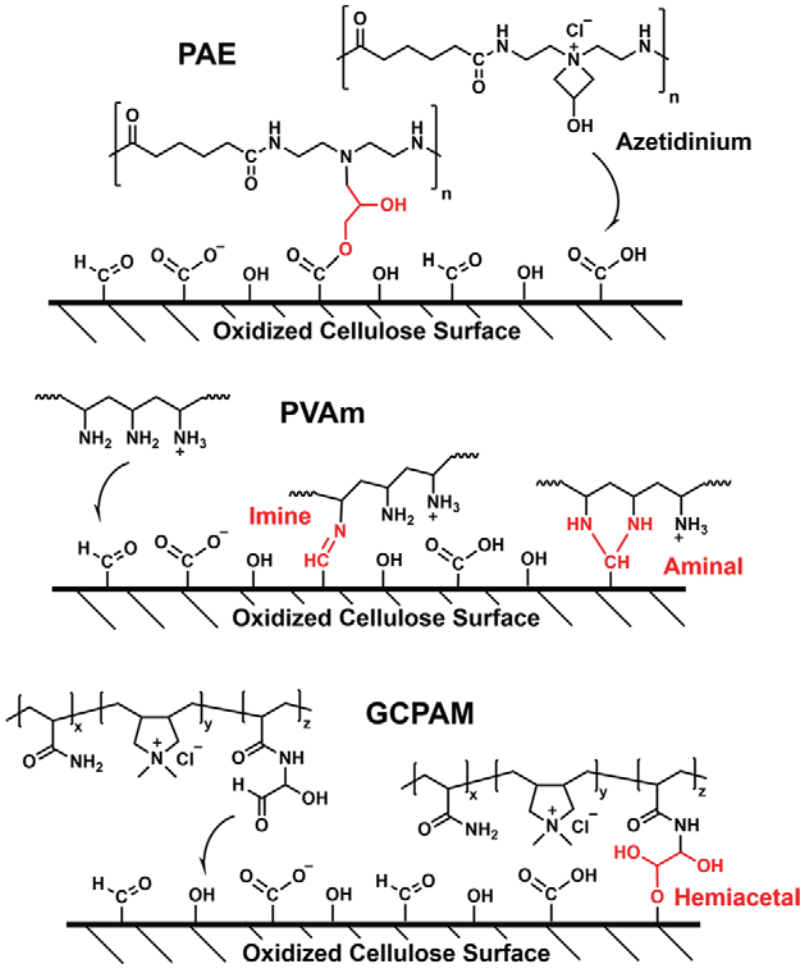

Figure 1: PAE, PVAm, and GCPAM grafting to oxidized cellulose. PAE reacts with carboxyls, PVAm reacts with aldehydes, and GCPAM react with alcohols.

PVAm is a linear, highly cationic (8 meq/g, hydrochloride salt and 50 % ionization), high molecular weight water-soluble polymer that, with drying, forms imine and aminal grafts to aldehyde groups on oxidized cellulose – see Figure 1. Finally, GCPAM is a modified cationic polyacrylamide, often with high molecular weights (106–107 Da) and intermediate charge contents. With drying, the glyoxal adducts form covalent hemiacetal bonds with cellulosic alcohol groups – see Figure 1.

In addition to grafting, PAE and GCPAM form covalent crosslinks within and between the polymer chains, contributing significantly to joint strength – example crosslinking chemical structures are given in Espy's review (Espy 1995). By contrast, PVAm molecules do not form covalent crosslinks so the cohesive strength of PVAm films depends upon physical interactions.

In summary, all three wet-strength resin types are cationic, promoting electrostatic adsorption of the resins onto anionic fiber surfaces. PAE may penetrate small pores in the fiber wall, whereas high molecular weight GCPAM and PVAm cannot. The grafting chemistries vary: PAE requires cellulosic carboxyls, drying and heating; PVAm requires cellulosic aldehydes and drying; and, GCPAM requires cellulosic hydroxyls, and drying. The specific products used in this work were chosen at random – no effort was made to identify a "best-of-breed".

Materials and methods

Materials

Regenerated cellulose membranes (Spectra/Por2, MWCO 12–14 kDa, 76 mm diameter tubing, product number 132684) were purchased from Spectrum Laboratories, US. TAPPI Standard blotter papers were purchased from Labtech Instruments Inc., Canada. Moisture-resistant double-sided medical tape 1522 was purchased from 3M, US. Glyoxalated cationic polyacrylamide (GCPAM) was Luredur Plus 555 provided by BASF, US. Polyamide-

epichlorohydrin (PAE) was Kymene 5221 provided by Solenis, US. Polyvinylamine (PVAm) samples were provided by BASF, Germany. Some PVAm samples were further hydrolyzed (DiFlavio et al. 2005) to remove residual formamide moieties and all PVAms were dialyzed for 1 week and freeze-dried before use. All other chemicals were used as received. TEMPO (2,2,6,6-tetramethylpiperidine 1-oxyl) and all other chemicals were purchased from Sigma-Aldrich, Canada. Carboxymethyl cellulose (CMC) used in this study was Mw 250 kDa with DS 0.9. Water type 1 (as per ASTM D1193-6, resistivity 18.2 MΩ/cm) was used in all experiments.

Pre-treatment of regenerated cellulose membranes

Regenerated cellulose dialysis tubes (12 cm diameter) were cut into strips, either 6 cm × 2 cm for the "top strips" or 6 cm × 3 cm for the "bottom strips", as shown in Figure S1. The membranes were cleaned by extraction in water at 60 °C for 1 h and stored in water at 4 °C.

TEMPO-mediated oxidation

The regenerated cellulose membranes were oxidized by TEMPO-mediated oxidation. In our standard method for membrane oxidation, 68 mg of TEMPO was dissolved in 2 L of water along with 680 mg NaBr and followed by the addition of 300 mg NaClO. The concentration of NaClO solution was determined by available chlorine titration (TAPPI, Test Method T 611 cm-07). The pH of the solution was adjusted to 10.5, after which wet cellulose membranes (10 g dry weight) were added. The solution was stirred and the pH maintained at 10.5 for 15 minutes, after which the oxidation was stopped by the addition of 10 mL ethanol. The oxidized membranes were washed thoroughly with water and stored at 4 °C.

Borohydride Reduction of Oxidized Cellulose Membranes. Sodium borohydride was used to reduce C6 aldehydes on oxidized cellulose to the corresponding alcohol. Wet, oxidized cellulose membranes (1 g dry weight) were immersed in 100 mL of 10 mM phosphate buffer at pH 8.5, followed by the addition of 0.5 g sodium borohydride. The pH of the suspension was adjusted to 8.5 using 1 M acetic acid. The reduction was carried out at room temperature and pH 8.5 for 48 hours. After the reaction, the cellulose membranes were washed with water and stored at 4 °C.

CMC-treated membranes

CMC was irreversibly adsorbed to cellulose membranes following the method (Laine et al. 2000). CMC was dissolved in water and followed by the addition of CaCl2 giving a final treatments solution composition of 1 g/L CMC in 50 mM CaCl2 at pH 8.0. Wet, regenerated cellulose membranes (10 g dry weight) were immersed in 400 mL of the treatments solution and the CMC was allowed to deposit to cellulose under mild stirring for 3 hours at 80 °C and pH 8. The CMC-treated cellulose membranes were washed with water and stored in 1 mM NaCl solution at 4 °C.

Lamination with wet-strength resins

In this work, two methods were used to apply resin in laminate joints, "adsorption application" and "direct application". In a typical adsorption application experiment, wet cellulose membranes (1 g dry weight) were soaked in 50 mL 0.2 g/L polymer solution with 1 mM NaCl at pH 7 in a plastic Petri dish for 30 min. Then the membranes were transferred to another Petri dish containing 50 mL rinsing solution (1 mM NaCl, pH 7) to rinse the non-adsorbed polymers from the membrane surfaces. The rinsing solutions were changed 3 times during the 10 min of rinsing. After the rinsing two wet cellulose membranes, each covered by a monolayer of polymer, were laminated. To permit easy separation at one end of the laminate, a piece of Teflon tape was applied across one end of the bottom membrane before lamination – see Figure S1. After lamination the Teflon tape was removed and the top membrane could easily be attached to the jaws of the Instron used to measure the peel force. The overall lamination procedure is illustrated in Figure S2.

In the direct application method, a top and a bottom membrane were blotted free of excess water, the water content was approximately 54 wt% after the blotting. 15 µL of wet-strength resin solution was carefully applied to the bottom membrane using a micropipette, after which a top membrane was applied, and the two membranes laminated using the Teflon spacer described above – see Figure S2. Normally, our resins are dissolved in 1 mM NaCl at pH 7. However, the pH and ion strength of the resin solution are variables which can be varied systematically to give mechanistic information. The polymer coverage in the laminate joints (mg/m^2) can be calculated from the laminate surface area (typically 10 cm^2) and the concentration and volume of the resin solution added.

Lamination and Wet-peeling. Wet laminates were placed between two 8 square inch TAPPI blotter papers and pressed in a Standard Auto CH Benchtop Press (Carver, Inc., US) with an applied pressure of 323 kPa for 5 min. The pressed laminates were then dried unrestrained at constant temperature and humidity (23 °C, 50 % RH) for 24 h.

For never-dried samples, lamination was performed at 23 °C. With once-dried laminates, hot pressing can be used to promote grafting and crosslinking. Most the results herein were with room temperature pressing and drying.

Wet peeling

Before delamination, the dried laminates were soaked in rewetting solution for 30 minutes. Our normal rewetting solution is 1 mM NaCl at pH 7. However, varying the pH and ionic strength can give mechanistic information. Dilute buffer solutions can give better pH control. We do not recommend deionized water for rewetting because the swelling and electrostatic forces are exaggerated.

The wet-peel force was measured with an Instron 4411 (Instron Corp., US) universal testing system. The lower jaw was replaced with a freely rotating 14 cm diameter aluminum peeling wheel running on SKF-6,8-2RS1 radial bearings (SKF, Scarborough, ON, Canada). The peel wheel has a 40 mm wide smooth outer surface. Our peel wheel is based on a design from Paprican (now FPInnovations), Point Claire, QC, Canada (Skowronski and Bichard 1987).

In a typical test, the rewetted laminate was removed from the soaking solution and excess water was removed by placing the laminate between two blotter papers and pressing once with a 2.4 kg hand roller. The wet laminate was fixed to the peeling wheel using moisture-resistant double-sided tape and the end of the top membrane was peeled off the Teflon tape spacer and fixed to the crosshead jaw of the Instron – see Figure S3. Our standard peel rate was 20 mm/min and the resulting peel force, measured with a 50 N load cell, was recorded as a function of displacement.

The Instron software was used to determine the average peel force over a user-defined displacement, corresponding to steady-state peeling. The steady state peel force is normalized with the width of the top membrane giving reported results with the unit N/m. At least three replicates were performed for each test and the average value and standard deviation were reported. The laminates were weighed wet before mounting on the wheel and after peeling, as well as after drying. The solids content of air-dried (23 °C, 50 % RH) membranes was 92–93 %, whereas the solids contents of the wet laminates were in the range of 47–54 wt% during the delamination. The solids contents increased a couple of percent during peeling because of evaporation.

Never-dried wet adhesion. Wet laminates were pressed (323 kPa) between two standard TAPPI blotter papers for times ranging between 0.1 min – 10 min; the longer the pressing time, the lower the laminate water content. The pressed wet laminates were put in a sealed plastic bag to prevent water evaporating and transferred immediately to the Instron. The wet-peel force was measured at a peel rate of 20 mm/min. The laminate wet weight was taken as the average value before and after testing – typically the wet mass decreased 2–3 wt% during peeling. The solids content is calculated as the oven-dry mass divided by the wet mass.

Cellulose membrane characterization

Mechanical properties of cellulose membranes were measured with an Instron 4411 (Instron Corp., US) universal testing system with 500 N load cell. The tensile rate was 20 mm/min and the grip distance was 3 cm. All membranes were cut to the size of 6 cm × 2 cm. For never-dried membranes, the samples were tested immediately out of water solution. For once-dried membranes, the samples were air-dried in a constant temperature and humidity room (23 °C, 50 % relative humidity) for one day, and thereafter rewetted in 1 mM NaCl solution at pH 7 for 1 hour before the measurement.

During tensile testing, the solids contents of the test specimens were typically in the range of 40–45 wt%. The reported results are the average of at least 3 replicates. The error bars depict the standard deviation.

The aldehyde content of oxidized membranes was measured from the fluorescence emission of dansylhydrazine labeled membranes, following Dementev's procedure (Dementev et al. 2009). Cellulose membranes were cut into 10 mm × 20 mm strips. In a typical reaction, wet cellulose (45 mg dry weight) was immersed in 30 mL of 0.14 mM dansyl hydrazide in methanol, followed by the addition of 1 mL of 1 M HCl. After 24 hours at room temperature and in the dark, labelled cellulose was rinsed with methanol and stored in the dark. The fluorescence intensity was determined using a ChemiDoc MP Imaging System (Bio-Rad Laboratories, Inc. US). The labelled cellulose strips were fixed to glass microscope slides (Precleaned, Corning) with 3M 1522 double sided medical tape.

UV Trans illumination (302 nm) was used as the excitation source and Standard Filter (580 ± 120 nm) was used as the emission filter. Images were analyzed using Image Lab version 4.1 (Bio-Rad Laboratories, Inc. US).

Calibration solutions of dansylhydrazine/acetone (1:2 molar ratio) in methanol were prepared with dansylhydrazine concentrations in a range of 0.2–4 mmol/L. 50 µL solution was applied to oxidized cellulose strips (10 mm × 20 mm) fixed to glass slides and air-dried in the dark. The resulting fluorescence intensities were a linear function of the dansylhydrazine contents.

Pulp treatment and handsheet testing

Pulp treatments and handsheet preparation: Unbeaten northern bleached softwood kraft pulp (SBK) suspensions were prepared from dried market pulp. CMC-treated pulps were prepared by treating a 2.5 % consistency pulp in 50 mM CaCl2 with CMC (50 mg per o.d. gm of pulp) and the pH was adjusted to 8. The suspension was heated to 95 °C and mixed for two hours.

TEMPO oxidized pulps were prepared as follows: Disintegrated pulp (25 g) was diluted to 4 L with DI water and TEMPO (60 mg) and NaBr (600 mg) were added. The mixture was stirred for about 30 min until the TEMPO dissolved. The reaction was initiated by addition of 12.5 mL NaClO (1.4 M) and the reaction pH was maintained at 10.5 by addition of NaOH (1 M). After 15 min, the reaction was quenched by addition of excess ethanol. The oxidized pulp was filtered and carefully washed multiple times and then stored at 10 wt% in refrigerator until further use.

Handsheets with a target basis weight of 60 g/m^2 were prepared using a semi-automatic sheet maker (Labtech Instruments Inc., Model 300-1, Canada) following TAPPI method T205 sp-95. Pulp with a consistency of 0.25 % were mixed with 2 % PAE, PVAm or GCPAM (based on dried-pulp weight) for 15 min at pH 7 prior to sheet-making. All of the handsheets were dried on a speed drier (Labtech Instruments Inc., Canada) at 120 °C for 10 min and stored at 23 °C and 50 % RH.

Paper wet tensile index: Wet tensile indices of handsheets were measured following TAPPI method T494 om-96. Paper specimens (150 mm × 15 mm) were rewetted in 1 mM NaCl at pH 7 for 5 min. Excess water was removed by blotter papers before the tensile test. Tensile strength was measured with the Instron fitted with a 50 N load cell at a stretching rate of 20 mm/min. Each experiment was repeated at least 4 times.

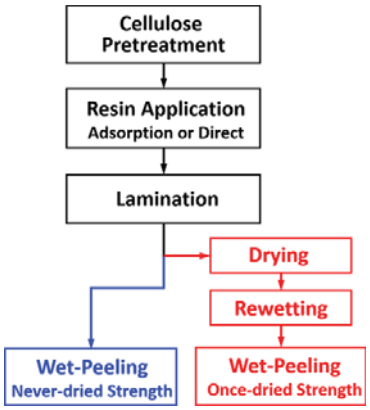

Figure 2: Workflow for wet-peel measurements.

Results

The results are presented in two parts: *The wet-peel methods* and *Demonstrating utility*. Whereas the experimental section describes the details, the following section describes the results of each step of the procedure, highlighting what we believe to be the most important issues. The second section, Demonstrating Utility, shows examples of experiments that can reveal features not accessible using traditional wet-tensile measurements on handsheets.

The Wet-peel methods

The steps for wet-peel methodology are summarized in Figure 2. This workflow measures either the once-dried wet adhesion or the never-dried wet adhesion. We propose that once-dried wet adhesion measurements are related to wet paper strength. In contrast, we propose that the never-dried wet adhesion measurements reflect the chemical contribution of polymers to wet-web strength. The detailed procedures corresponding to each step in Figure 2 are given in the experimental section, whereas the following paragraphs describe the key features of each step.

Cellulose membrane pretreatment

We used dialysis tubing as the source of regenerated cellulose membranes. Some membrane properties are summarized in Table 1. In all cases the cellulose membranes had to be pretreated. In the simplest case, pretreatment was water washing to remove glycerol and other water-soluble impurities. However, the regenerated cellulose membranes have insufficient non-hydroxyl surface groups

Table 1: Regenerated cellulose membrane properties before and after TEMPO oxidation or CMC treatment.

	Untreated	TEMPO-oxidation	CMC-treated
Dry roughness (nm)	7 ± 4	6 ± 3	-
Total aldehyde (μmol/m^2)	0	0.71	0
Estimated area per surface aldehyde (nm^2)	0	62	0
Never-dried			
Water content after blotting (wt%)	54 ± 1	56 ± 1	54 ± 1
Roughness (nm)	15 ± 6	8 ± 1	-
Elastic modulus (MPa)	93 ± 4	114 ± 8	92± 11
Tensile strength (MPa)	22 ± 1	18 ± 2	19 ± 1
Strain at break (%)	70 ± 9	47 ± 6	59 ± 9
Yield stress (MPa)	1-2	1-2	1-2
Once-dried and then rewetted			
Water content after blotting (wt%)	53 ± 1	51 ± 1	-
Elastic modulus (MPa)	91 ± 4	99 ± 5	-
Tensile strength (MPa)	24 ± 2	13 ± 1	-
Strain at break (%)	78 ± 6	34 ± 7	-
Yield stress (MPa)	~ 1	~ 1	~ 1

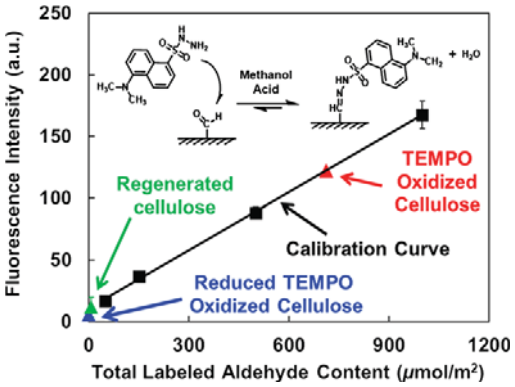

Figure 3: Comparing the aldehyde contents of untreated, TEMPO oxidized, and reduced cellulose membranes. Note the that fluorescent labels are distributed throughout the thickness of the membrane.

to give wet strength with most wet-strength enhancing polymers. Herein we present results for membranes with a surface layer of CMC and for TEMPO oxidized surfaces. Our CMC-treatment protocols are directly based on the work of Laine and Lindstrom who demonstrated that CMC could be deposited, virtually irreversibly onto cellulose fibers (Laine et al. 2000). By contrast, low temperature CMC solutions in low ionic strength solutions show little tendency to bind to clean wood pulp fibers.

Membrane treatments by TEMPO mediated oxidation follow Saito's early work (Saito and Isogai 2006). Both CMC treatment and TEMPO oxidation generate surface carboxyl groups that are grafting sites for PAE (see Figure 1) and that promote adsorption of cationic polymers. TEMPO mediated oxidation also generates aldehyde groups (Saito and Isogai 2006) that are grafting sites for PVAm (DiFlavio et al. 2005).

The surface treatments have little impact on the mechanical properties of the wet membranes under our standard conditions. We also measured membrane mechanical properties after exposure to PVAm and PAE. The results, summarized in Table S1, show that the polymers did not have a significant influence on the membrane mechanical properties. Therefore, we propose that wet-peel values from these treated membranes can be directly compared.

Measuring the density of surface functional groups is a challenge because of the very low total surface area in the membranes. We used dansyl hydrazine to label the aldehyde groups, and fluorescence to estimate the total aldehyde content of the labeled membranes. Figure 3 shows the labeling chemistry and superimposes on the calibration curve the properties of the unmodified membrane, TEMPO oxidized membrane, and, TEMPO oxidized membrane that was treated with sodium borohydride to reduce the aldehydes. Only the TEMPO mediated oxidation gave a significant aldehyde content of 0.71 μmol per square meter of membrane top surface (10 μmol per dry gram). However, we have shown previously that confocal images of membrane cross sections revealed a uniform distribution of fluorescent groups in the z-direction (Liu et al. 2013). Therefore, to estimate the surface density of aldehydes we assumed that the "surface aldehydes" corresponded to the top 5 nm layer of the membrane. We have expressed our estimate of the aldehyde density in Table 1 as the area per aldehyde group of approximately 62 nm^2. TEMPO mediated oxidation targets the C6 hydroxyl and the estimated area per exposed C6 hydroxyl on crystalline cellulose is 0.6 nm^2. (Fleming et al. 2001) Therefore, based on our estimate, only a small fraction of the accessible C6 hydroxyls are present as aldehydes in our experiments.

Wet membranes were 130 ± 10 μm thick. Once-dried membranes were dried at 23 °C. The surface aldehyde density is based on the assumption of a 5 nm surface layer. RMS roughness values measured by AFM (Yang 2018). Error limits depict the standard deviation based on at least 3 replicates. Above paragraph should move to Table 1 description

Finally, Liu et al. reported that the CMC (250 kDa, DS 0.9, 30 mM $CaCl_2$) adsorption density on regenerated cellulose was 0.34 mg/m^2 (Liu et al. 2011). This corresponds to an area per carboxyl group of 1.2 nm^2. Note that an adsorbed layer of CMC will have loops and tails extending into solutions. Therefore, the carboxyls are dispersed through the adsorbed layer thickness.

Wet-strength resin application

Two methods have been developed for applying wet-strength resins to the membranes – direct application and adsorption, as show in Figure S2. Direct application involves spreading 15 μL of polymer solution over a joint area of 10 cm^2. In early work we were concerned that pressing would squeeze out some of the wet-strength resin solutions. Figure S4 shows photographs of a laminate and the blotters after pressing. The laminate was formed with a Congo Red solution to facilitate the visualization of lost solution. There was no obvious leakage with pressing. The hand blotting of membranes just before adding the 15 μL of polymer solution is a critical step. The blotted membrane has the capacity to hold the directly added polymer solution.

We show below that direct application is useful for comparing a range of polymer types, while keeping constant the polymer content in the laminate joint. For much of our work the wet-strength resin coverage (dry polymer mass/joint area) was 15 mg/m^2 corresponding to a dry thickness of 15 nm, corresponding to approximately 15 layers of polymer molecules between the cellulose membranes. However, compared to conventional adhesive technologies, these are very thin adhesive layers.

In adsorption application one or both membrane surfaces are exposed to a polymer solution to give an adsorbed monolayer on each surface treated. Adsorption application is the closest to the situation in papermaking. However, adsorption has two serious drawbacks. First, the coverage (dry polymer mass/joint area) is difficult to measure. Second, it is impossible to control coverage which, in turn, means a series of polymers cannot be compared at the same coverage. Typically, adsorbed water-soluble polymers give coverages in the range 0.1–1 mg/m^2 on an individual surface. Forming a joint between two such surfaces doubles the polymer coverage in the joint.

For both direct and adsorption application, it is important to control the pH and ionic strength of the polymer solution. The degree of ionization and the polymer configuration are sensitive to aqueous solution conditions.

We believe the membranes are manufactured in an extrusion process that generated striations in the peeling direction. Atomic force microscopic reveals a wet RMS roughness of only 10–15 nm. However, the images suggest parallel striations – see Figure S5. We prepared a series of laminates with fluorescently labeled PVAm and used confocal microscopy to image the plane of maximum fluorescence between the cellulose membranes. The top image in Figure 4 shows a laminate made by direct application. The directly applied polymer is present as bands reflecting the striations in the membranes. By contrast, adsorption from solution gave a much more uniform distribution of polymer. Finally, the striations were parallel to the long axis of the parent dialysis tubing which was also our peeling direction.

Figure 4: Confocal micrographs of wet laminates prepared with fluorescently labeled PVAm. Image planes were chosen between the membranes giving maximum fluorescence.

Lamination. Pairs of polymer treated, wet membranes are pressed together between standard handsheet blotters to ensure good contact. Originally our pressing pressures were high (2150 kPa), for no particular reason. Our current standard pressing pressure is 323 kPa. Figure 5 shows that wet-peel force is not very sensitive to lamination pressure over a great range. The highest wet-peel forces corresponded to the highest lamination pressures.

For never-dried wet-peeling, the laminate water content is an important variable. Because pressing between dried blotters lowers the water content, pressing time is a convenient way to control never-dried water content.

Drying

GCPAM, PVAm, and PAE resins all require water removal for covalent bonds to form within in the resin (crosslinking) and to the cellulose surfaces (grafting). For GCPAM and PVAm the once-dried laminates were normally removed from the lamination press and dried at 23 °C, 50 % RH overnight. Under these conditions, the equilibrium laminate water content was about 7.5 %. PAE crosslink-

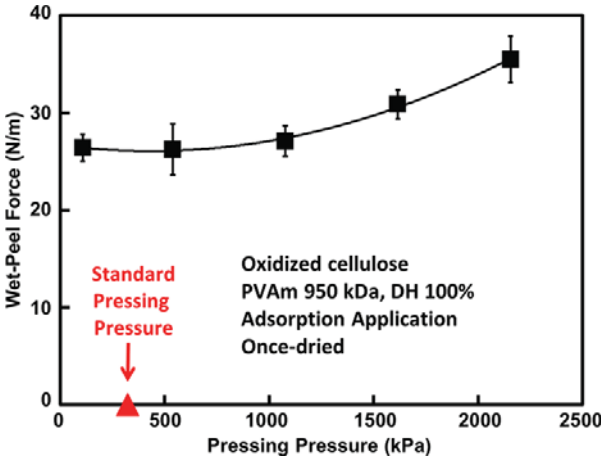

Figure 5: The influence of pressing load on the once-dried wet-peel force for 950 kDa PVAm adsorbed on one membrane.

ing reactions are facilitated by drying at elevated temperatures (Obokata and Isogai 2007). In these cases, we employed a heated lamination press, combining the heating and drying step. We have found that the upper temperature limit for the laminates is about 70 °C for PAE treated membranes. Above this, we observe membrane failure during the wet-peeling possibly indicating the joints were stronger than the membranes.

Rewetting

Once-dried laminates must be rewetted-before wet-peeling. The laminates are hydrogels and the degree of swelling will depend upon the pH and ionic strength of the rewetting solution – these properties should be controlled. Typically, we use 1 mM NaCl at neutral pH as the rewetting solution. Deionized water should not be used as it exaggerates joint swelling. A dilute buffer is recommended for pH sensitive adhesive chemistries.

Our standard rewetting time of 30 minutes is usually sufficient to saturate the laminate. In early work we were concerned that water soluble PVAm could diffuse out of laminates. We showed that laminates bonded with 7.5 mg/m^2 could be soaked for 2000 hours with no loss in wet-peel force (DiFlavio et al. 2005).

The laminates are removed from the soaking solution, hand blotted, and weighed just before and after wet-peeling. Typically, each laminate takes approximately 3 minutes to weigh and delaminate. The solids content increases about 1 % per minute at 23 °C, 50 % RH, giving an average of about 50 % during the delamination.

Wet-peeling

Laminate adhesion was measured as the ninety-degree peel delamination force values – see Figure S3 for photographs of a wet-peel experiment. The reported wet-peel results are expressed in units of N/m obtained by dividing the measured forces by the width of the top membrane. Note that wet-peel forces are dimensionally equivalent to J/m^2, corresponding to the total delamination work per area of laminate joint.

The mechanics of peeling has been studied and modeled in the pressure sensitive adhesives literature (Kendall 1975) (Gent and Hamed 1977) (Kinloch 1982) (Zhang Newby and Chaudhury 1998) (Pesika et al. 2007). Peel work is much greater than the thermodynamic work of adhesion (Zhang Newby and Chaudhury 1998) (Li et al. 2001) reflecting energy consumption by stretching the tape backing and viscoelastic deformation within thick adhesive layers. In the case of our experiments, non-adhesive contributions to the peel work could include stretching of the top membrane after separation, and dissipation within the two-sided medical tape fixing the bottom membrane to the peel wheel. Example stress/strain curves for wet cellulose membranes are shown in Figure S6. The strain corresponding to a wet-peel force of 40 N/m was less than 1 %, and the corresponding work of stretching was only 0.13 N/m when the overall wet-peel force was 40 N/m. Table 1 compares the mechanical properties of treated and untreated membranes. For the < 1 % membrane strains in the wet-peel experiments, changes in membrane properties due to surface treatments should have little impact on the membrane stretching contributions to peel work.

Peel rate

The peel forces for pressure sensitive adhesive tapes are a strong function of peeling rate because much energy is consumed deforming the thick (typically 100 μm) viscoelastic adhesive layer (Satas 1989). By contrast, the adhesive layers in our cellulose laminates are very thin (3–30 nm), mimicking fiber-fiber joints in paper. Figure 6 shows two examples of peel force versus peel rate curves. The thicker adhesive layer showed some rate effects, whereas the very thin layer did not. If we assume that the water content of the adhesive layer was 50 %, the corresponding thickness of the wet adhesive layers was about twice the dry PVAm coverage, 15 nm for thicker layer and 3 nm for the thin layer. Virtually all of our work has employed a fixed peeling rate of 20 min/min.

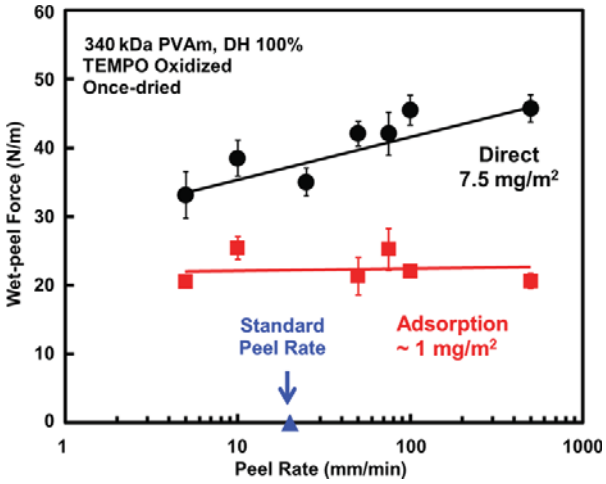

Figure 6: Peel rates showing limited impact on wet-peel forces.

Data quality

Figure 7 shows four replicates of raw peel-force versus displacement curves, as well as the mean and standard deviation plots. The mean peel force is calculated from the user-defined horizontal section of the curve; the values for the curves in Figure 7 were 32, 27, 28, and 29 N/m. The results in Figure 7 reveal two types of variation. Focusing on the steady-state portions beyond a displacement of 5 mm, each curve shows significant noise around a mean value. In addition, there is laminate-to-laminate variation. Normally we perform triplicated measurements and the steady-state portions of the curves are averaged and the curve-to-curve variation is a used as a measure of experimental error. Flawed experiments are usually obvious from the absence of a horizontal section in the peel curve. Such results are rejected and additional samples are measured.

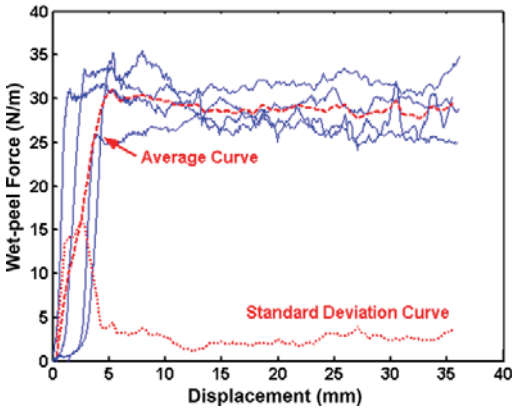

Figure 7: Example curves of wet-peel force monitored during the delamination. PVAm (950 kDa, 100 % hydrolyzed) was adsorbed on one membrane before lamination. The laminates were rewetted in 10 mM NaCl at neutral pH. The peel rate was 20 mm/min. (DiFlavio 2013).

Demonstrating utility

One of the most useful applications of wet-peeling is comparing the efficacy of wet-strength polymers at the same coverage. Table 2 summarizes unpublished early work (2003) where we compared some common polymers used in papermaking. None of the polymers gave significant wet adhesion with untreated regenerated cellulose membranes. On the other hand, with oxidized cellulose, PVAm gave adhesion values of 42 N/m. PAE laminates were weaker, however, PAE gives stronger laminates than PVAm if the laminates are heated, promoting crosslinking and grafting. It is not surprising that CMC (applied without calcium ions and elevated temperatures) and PolyDADMAC do not impart wet strength. PEI (polyethyleneimine) is known to give some wet strength (Espy 1995). The CPAM had a slight strengthening effect on TEMPO oxidized cellulose – similar results have been reported for handsheets (Saito and Isogai 2007).

Table 2: Comparison of polymers as wet-strength resins.

Polymer	Details	Average once-dried wet-peel force (N/m)			
		Untreated cellulose	Standard error	Oxidized cellulose	Standard error
PDADMAC	400–500 kDa	0.00	-	5.05	0.97
CMC	250 kDa, DS 0.9	0.00	-	6.09	1.30
PAE	Kymene 557H	2.13	0.24	31.6	1.80
PEI	Polymin SK	2.13	0.24	17.8	0.70
CPAM	Percol 175	2.36	0.40	7.78	0.99
PVAm	950 kDa	2.91	0.42	41.5	2.70

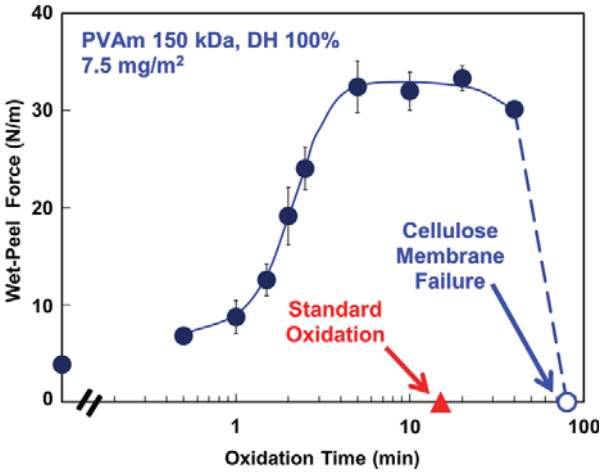

Figure 8: The influence of cellulose membrane oxidation time on the laminate wet-peel force. Conditions: TEMPO 0.034 g/L, NaBr 0.34 g/L, and NaClO 3 wt% based on dry cellulose. PVAm molecular weight was 150 kDa. The laminates were air dried at 50 % RH and rewetted for 30 min in pH 6.5, 5mM NaCl. Figure adapted from (Pelton et al. 2011).

Comparing cellulose surface treatments

Wet-peeling is also adept at showing how wet-strength resins respond to cellulose surface pretreatments. Figure 8 shows the influence of TEMPO oxidation time on the wet-peel force with PVAm. Adhesion increases with oxidation time, reflecting an increase of the concentration of carboxyl and aldehyde groups. The aldehyde groups are grafting sites for PVAm (see chemistry in Figure 1) whereas the carboxyl groups promote PVAm adsorption at the cellulose/water interface. However, these experiments employed the direct application procedure, giving a constant, high PVAm content in the laminates, removing the extent of PVAm adsorption as a factor. With conventional handsheet studies, the coverage of adsorbed PVAm would increase with oxidation time because of the increased carboxyl content. Finally, at very long oxidation times, cellulose degradation leads to membrane failure during the wet-peeling.

The polymer solutions contained 1 mM NaCl adjusted to pH 7 and direct application method gave a coverage of 11 mg/m^2. Laminates were dried at 23 °C in 50 % RH. The membranes were modified by TEMPO mediated oxidation. Above paragraph should move to Table 2 description.

Table 3 compares adhesion results from experiments comparing three wet-strength resin types (PAE, GCPAM, and PVAm) and two types of cellulose treatments, TEMPO oxidation and CMC treatment. In these experiments the resins were applied by adsorption. Therefore the surface treatment can impact both the coverage of resin in the laminate and the extent and type of bonding between the resin and the membrane. The results in the first three rows show that without a wet-strength resin, TEMPO oxidation gives some increase in wet strength, presumably due to the formation of hemiacetal bonds between the membranes. Similar results from wet handsheet testing have been reported (Jaschinski et al. 2003; Saito and Isogai 2005).

Unbeaten, bleached softwood pulp was treated with 2 wt% polymer based on dry fiber. The membranes were saturated with adsorbed polymer. The laminates were dried at room temperature, whereas the handsheets were dried at 120 °C. The handsheet results were published recently (Gustafsson et al. 2017). Above move to Table 3

With PAE, both TEMPO oxidized and CMC-treated membranes gave high strengths, whereas laminates from

Table 3: The influence of membrane and fiber pre-treatments on once-dried wet adhesion and handsheet wet tensile indices.

Cellulose membrane treatment	Adsorbed polymer	Once-dried wet-peel (N/m)	Handsheet wet tensile index (N·m/g)
-	-	1±1	1±0
TEMPO oxidized	-	11±2	4±1
CMC-treated	-	1±1	1±0
Untreated	PAE	1.4±0.1	4.5±0.1
TEMPO oxidized	PAE	37±4	9±1
Reduced TEMPO oxidized	PAE	32±3	-
CMC-treated	PAE	30±1	9±1
Untreated	PVAm	7±1.6	-
TEMPO oxid.	PVAm	24±4	6±0
Reduced TEMPO oxidized	PVAm	8±1	-
CMC-treated	PVAm	14±1.2	2±1
Untreated	GCPAM	17±4	3.8±0.2
TEMPO oxidized	GCPAM	20±1	9.3±0.2
CMC-treated	GCPAM	35±2	12±0.1

untreated membranes were weak, reflecting the lack of carboxyl groups on the regenerated cellulose membrane surfaces.

PVAm was most effective with TEMPO oxidized membranes, whereas the CMC-treated membrane laminates were only half as strong as the TEMPO oxidized membrane laminates – see Table 3. The amine groups on PVAm interact with CMC by forming polyelectrolyte complexes (Feng et al. 2007a, Gustafsson et al. 2016) whereas with drying, amines form covalent imine and aminal linkages with aldehydes.

The glyoxalated cationic polyacrylamide, GCPAM, was the only polymer to improve the wet-strength of laminates made with untreated regenerated cellulose membranes. TEMPO oxidation gave a small improvement whereas the CMC-treated membranes, treated with GCPAM, gave the highest wet-peel values in Table 3.

The contribution of aldehyde groups to wet-adhesion was illustrated by reducing the aldehydes on the TEMPO oxidized membrane before laminate formation. With PAE, removal of aldehydes had little impact because azetidinium groups on PAE resins do not react with aldehydes. On the other hand, the results in Table 3 show that TEMPO oxidized membranes, laminated with adsorbed PVAm lose about 2/3 of their strength when the aldehydes are reduced. This example shows how the wet-peel experiments can be used to test adhesion mechanistic hypotheses.

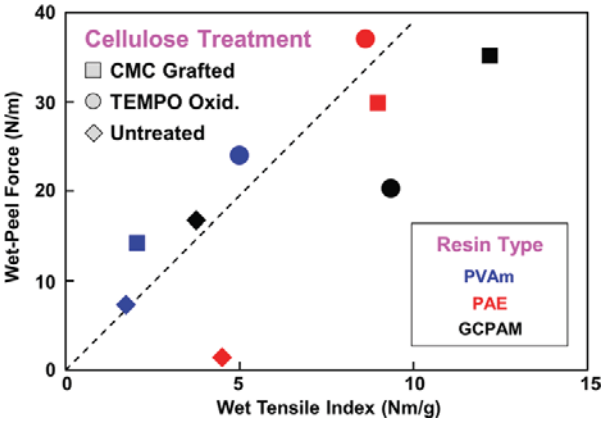

Figure 9: Relating wet-peel measurements to handsheet wet tensile indices. Cellulose membranes and SBK pulps were either untreated, TEMPO oxidized or CMC-treated cellulose membranes. All results come from Table 3.

For a given fiber type and sheet structure, there is a strong correlation between once-dried wet-peel and wet tensile index. Figure 9 shows the once-dried wet peel force as a function of handsheet wet tensile index for the results in Table 3. In spite of the wide range of fiber/membrane treatments and wet-strength resin chemistries, wet-peel force measured with laminates increases with wet tensile index measured on handsheets. Given the speed, ease, and reproducibility of wet-peel measurements, it might be tempting to replace handsheet testing completely. We do not recommend this because fiber treatments and polymers that give exceptional wet strength also can give extensive formation problems due to fiber flocculation. The roles of formation, retention, and fibrillation (beating) require paper testing.

Wet-strength resin coverage (thickness)

The influence of wet-strength resin coverage (resin mass/joint area) on wet cellulose adhesion is easily probed by wet-peeling laminates prepared using direct application of resin solution. Figure 10 compares three data sets showing once-dried wet-peel force as a function of coverage for PVAm laminated oxidized cellulose membranes. The PVAm coverage is expressed as mg of dry polymer per square meter of laminate. If the density of the dry polymer is 1 g/mL, the dry polymer thickness in nm is equal to the coverage. For example, a 10 mg/m^2 dried uniform film, coating a smooth surface has a thickness of about 10 nm. Note that the very highest coverage in Figure 10 correponds to a dry adhesive thickness of 100 nm,

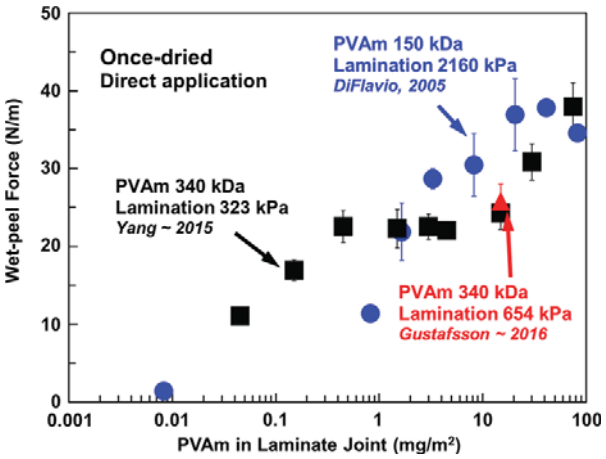

Figure 10: The influence of PVAm coverage on wet cellulose adhesion. All laminates were prepared by direct application with PVAm solution in 1 mM NaCl at pH ~7 and rewetted in 1 mM NaCl at pH 7 for 30 min before the delamination. Compared are results from three researchers over a 12-year period. Diflavio's results were published in 2005 whereas the other data is new.

whereas a typical pressure sensitive adhesive layer thickness is 100 μm (Satas 1989). Therefore in the context of the broader adhesive technologies, all the results in Figure 10 correspond to thin adhesive layers.

For our standard direct application procedure, the volume of polymer solution (15 μL) and the laminate bonded area (10 cm^2) are constant. Therefore in going from 0.01 mg/m^2 to 1000 mg/m^2, the polymer concentration ranged from 0.7 mg/L to 7 g/L. Thus the solutions of the applied polymer ranged from the dilute, low viscosity regime to the concentrated, high viscosity regime.

The major trend in Figure 10 is that wet-peel force increases with adhesive coverage. The two data sets and the individual experiments were obtained by three different researchers over a twelve year period. Although the PVAm molecular weights and the laminate pressing pressures varied, the results show reasonable agreement. There is no papermaking process that can apply wet-strength resin by direct application to the fiber-fiber joint. Therefore the utility of results such as those in Figure 10 are two-fold. First, one can compare different resins at exactly the same resin content and second, results from thicker layers (>10 nm) show the contributions of polymer-polymer cohesive interactions to the overall adhesion.

Never-dried adhesion: the chemical contribution to wet web strength

On some papermachines wet-web strength is an important requirement for efficient operation. Wet-web strength depends upon water content, the sheet structure and the adhesion/friction properties of fiber-fiber contacts (Page 1993). Polymeric additives have the potential to influence water content (drainage), sheet structure (formation) and possibly fiber-fiber adhesion. Never-dried wet-peel gives insight into the contribution of polymers to adhesion without the complications of varying paper sheet formation and sheet structure. Figure 11 shows the influence of cellulose pretreatment on the never-dried wet adhesion of cellulose membranes laminated with gyloxlated cationic polyacrylamide, GCPAM. In all cases wet-peel strength increases with the solids contents. The CMC-treated membranes gave spectacular never-dried wet adhesion, whereas TEMPO oxidized membranes showed little improvement compared to untreated membranes. We propose that adhesion is due to polyelectrolyte complexation between GCPAM and the surface CMC layer. We have shown that complexes formed between PVAm and CMC in solution give good once dried wet adhesion (Feng et al. 2007b) and have also shown that high never dried adhesion is achieved using CMC-treatment and PVAm (Gustafsson et al. 2016).

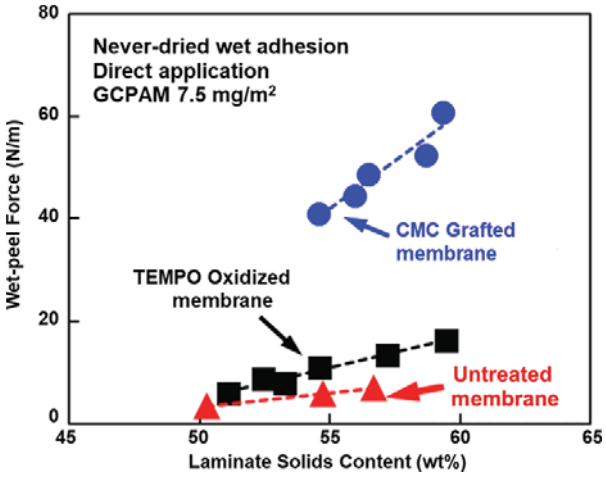

Figure 11: The influence of membrane pretreatment on never-dried wet-peel force with GCPAM wet-strength resin. Laminates using untreated cellulose membranes were prepared by the direct application with GCPAM (7.5 mg/m^2) whereas the other laminate types were prepared by the adsorption application.

With respect to the never-dried adhesion measurements, we have not settled on a standard procedure for sample preparation. The key property is the laminate water content. We recently reported never-dried wet-peel results where the lamination step was performed with a 2.4 kg hand roller pressing the laminates, sandwiched between blotters – water content was varied by blotter exposure time (Gustafsson et al. 2016). By contrast, the laminates for the results in Figure 11 were dewatered in a Carver press at 323 kPa. The water content was varied by adjusting the pressing times between 0.1 and 10 minutes.

Discussion

Our motivation herein is to promote the wet-peeling method for evaluating and comparing paper wet-strength resins. The most compelling application of wet-peeling is the "head-to-head" comparison of a series of wet-strength resin candidates using the once-dried method. With direct application, the comparison is made with exactly the same coverage (i. e. the mass of polymer/joint area). With adsorption application, the peel-force reflects both the ability of the polymer to adsorb and then to contribute to adhesion. Although adsorption application more closely mimics the situation in papermaking, it is difficult to determine

the amount of wet-strength resin adsorbed on the membrane surfaces.

Our wet, regenerated cellulose membrane laminates are physical models for the wet fiber-fiber joints in papermaking. The utility of any model is limited by the extent to which the model mimics its target. From the perspective of chemical composition, bleached kraft pulp fibers and the membranes are both mainly cellulose. The pulp will include some hemicellulose, whereas the membranes should not. Of course, fiber morphology is much more complex and diverse than is the case for the dialysis membranes. The pore volume fraction of the membranes, as judged by the water content, is about 50 %, which is less than most fiber pore volumes based on water retention values. Pulp fiber wall pore size estimation is complex issues and results depend upon the method. The introduction to Andreasson's paper gives a good summary of the issues (Andreasson et al. 2003). Typical radii estimates for bleached kraft pulp fibers are 10 nm as estimated by NMR (Maloney et al. 1999). On the other hand, the accessibility of fiber pores to soluble polymer suggest pore throat radii of 50 nm (Andreasson et al. 2003). By comparison, the effective pore size of dialysis membranes are smaller than those in pulp fibers; a 12 kDa pullulan molecular weight standard has a radius of about 3 nm (Dubin and Principi 1989). This analysis suggests that intermediate molecular weight wet-strength resins that can diffuse into fiber walls are unlikely to enter the dialysis membranes. The mechanical properties of individual membranes were little changed by polymer treatment (see Table S1), further supporting the claim that our PAE, PVAm and GCPAM polymers did not penetrate the wet cellulose membrane pores.

Our adhesion results suggest that untreated regenerated cellulose membranes have too few surface functional groups to promote grafting and adhesion. Regenerated cellulose fibers display the same behaviors. We recently have shown that handsheets prepared with regenerated cellulose (Lyocell) fibers treated with 2 % PAE resins had a low wet tensile index of 1.6 Nm/g, whereas when the fibers were pretreated by TEMPO oxidation, the wet tensile increased to 4.1 Nm/g (Gustafsson et al. 2017).

We propose that never-dried wet-peeling measurements give insight into the contributions of polymers to wet-web strength during papermaking. Historically, web-web strength on papermachines was explained by a fiber-fiber friction induced by capillary forces (Campbell 1933; Lyne and Gallay 1954; Page 1993). However, this view has been recently challenged (van de Ven 2008). The influence of polymer additives on wet-web strength is complicated. The most likely positive contributions are increased fiber-fiber wet adhesion/friction and increased sheet solids content (i. e. better drainage). Wet-web strength measurements are tedious, and meaningful comparisons require a series of measurements as functions of solids contents. Never-dried wet-peeling gives a direct measure of the adhesion contributions of polymer additives and is easily performed as a function of water content (see Figure 11 as an example). The application of never-dried wet-peeling to elucidate wet-web strengthening mechanisms is illustrated by the following example. PDADMAC is known to increase drainage rates in some types of pulp suspensions (Hubbe 2000). On the other hand, PDADMAC gave no never-dried wet adhesion on TEMPO oxidized cellulose membranes. This means that improved drainage and press dewatering are the only mechanisms by which PDADMAC is likely to enhance wet-web strength.

Finally, for more academic and mechanistic studies, wet-peeling has proved to be useful in evaluating more exotic joint structures such as layer-by-layer (Feng et al. 2009), microgels (Wen and Pelton 2012), and colloidal polyelectrolyte complexes (Feng et al. 2007b).

Conclusions

Laminated wet, regenerated cellulose membranes serve as a physical model for fiber-fiber joints in wet paper. Measurements of the wet delamination force (i. e. wet-peel measurements) augment conventional laboratory wet tensile strength measurements by:

1) Giving comparisons of wet-strength polymers at the same content of polymer in the laminate joint without the influences of varying fines contents, formation or paper density.
2) Providing measurement of both the wet-strength of cured, dried joints, and the strength of never-dried joints (i. e. analogous to wet-web strength).
3) Showing the influence of fiber surface chemistry, including oxidation and the presence of firmly bound polymers.
4) Permitting the evaluation of more exotic joint structures, including layer-by-layer assemblies, microgels and colloidal polyelectrolyte complexes.

For a given paper structure and surface chemistry, wet-peel forces are approximately linearly related to wet tensile strength when varying the wet strength chemicals. In our laboratory, wet-peel measurements have proven to be reproducible over 10+ years with multiple users. Wet-peel

data are sensitive to important chemical parameters, including adhesive composition, pH and drying temperature, while being relatively insensitive to experimental details, including sample width, peel rate and the lamination pressure. Finally, wet-peel experiments are rapid and require very low quantities of wet-strength resin, facilitating the comparison of large polymer libraries.

Acknowledgments: Dr. Anton Esser, BASF Ludwigshafen and Joel Soucy, BASF Canada, are acknowledged for useful discussions. Heera Marway is thanked for help with AFM experiments.

Funding: Some measurements were performed in the McMaster Biointerfaces Institute funded by the Canadian Foundation for Innovation. R.H.P. holds the Canada Research Chair in Interfacial Technologies. BASF Canada is acknowledged for funding this project through a grant to R.P. entitled "Understanding Cellulose Interactions with Reactive Polyvinylamines".

Conflict of interest: The authors declare no conflicts of interest.

References

Andreasson, B., Forsstrom, J., Wagberg, L. (2003) The Porous Structure of Pulp Fibres with Different Yields and Its Influence on Paper Strength. Cellul. 10(2):111–123.

Andreasson, B., Forsstrom, J., Wagberg, L. (2005) Determination of Fibre Pore Structure: Influence of Salt, pH and Conventional Wet Strength Resins. Cellul. 12(3):253–265.

Campbell, W. B. The Cellulose-Water Relation in Papermaking. Forest Service Bulletin, Dept. of Interior, Canada, (84), 1933.

Dementev, N., Feng, X., Borguet, E. (2009) Fluorescence Labeling and Quantification of Oxygen-Containing Functionalities on the Surface of Single-Walled Carbon Nanotubes. Langmuir 25(13):7573–7577.

DiFlavio, J.-L. The Wet Adhesion of Polyvinylamine to Cellulose. Chemical Engineering. McMaster University, Hamilton, Canada, 2013.

DiFlavio, J. L., Bertoia, R., Pelton, R., Leduc, M. (2005) The Mechanism of Polyvinylamine Wet-Strengthening. In: Advances in Paper Science and Technology: Transactions of the 13th Fundamental Research Symposium. Ed. SJ, I. A. Cambridge, UK. pp. 1293–1316.

Dubin, P. L., Principi, J. M. (1989) Failure of Universal Calibration for Size-Exclusion Chromatography of Rodlike Macromolecules Vs. Random Coils and Globular Proteins. Macromolecules 22(4):1891–1896.

Espy, H. H. (1995) The Mechanism of Wet-Strength Development in Paper: A Review. Tappi J. 78(4):90–99.

Feng, X., Pelton, R., Leduc, M., Champ, S. (2007a) Colloidal Complexes from Poly(vinyl Amine) and Carboxymethyl Cellulose Mixtures. Langmuir 23(6):2970–2976.

Feng, X., Pouw, K., Leung, V., Pelton, R. (2007b) Adhesion of Colloidal Polyelectrolyte Complexes to Wet Cellulose. Biomacromolecules 8(7):2161–2166.

Feng, X., Zhang, D., Pelton, R. (2009) Adhesion to Wet Cellulose – Comparing Adhesive Layer-by-Layer Assembly to Film Casting. Holzforschung 63:28–32.

Fleming, K., Gray, D. G., Matthews, S. (2001) Cellulose Crystallites. Chem. – Eur. J. 7(9):1831–1836.

Gent, A. N., Hamed, G. R. (1977) Peel Mechanics for an Elastic-Plastic Adherend. J. Appl. Polym. Sci. 21(10):2817–2831.

Gurnagul, N., Page, D. H. (1989) The Difference between Dry and Rewetted Zero-Span Tensile-Strength of Paper. Tappi J. 72(12):164–167.

Gustafsson, E., Pelton, R., Wågberg, L. (2016) Rapid Development of Wet Adhesion between Carboxymethylcellulose Modified Cellulose Surfaces Laminated with Polyvinylamine Adhesive. ACS Appl. Mater. Interfaces 8(36):24161–24167.

Gustafsson, E., Wang, Z., Polat, O., Ostendorf, W. W., Sheehan, J. G., Pelton, R. (2017) Towards Wet Resilient Paper – Fiber Modifications and Test Method Development. In: 16th Fundamental Research Symposium. Oxford. pp. 865–894.

Hubbe, M. A. (2000) Reversibility of Polymer-Induced Fiber Flocculation by Shear. 1. Experimental Methods. Nord. Pulp Pap. Res. J. 15(5):545–553.

Jaschinski, T., Gunnars, S., Besemer, A.C., Bragd, P. (2003) Oxidized Polymeric Carbohydrates and Products Made Thereof. SCA Hygiene Products GmbH, US 6,635,755 B1.

Kendall, K. (1975) Thin-Film Peeling-the Elastic Term. J. Phys. D, Appl. Phys. 8(13):1449.

Kinloch, A. J. (1982) The Science of Adhesion.2. Mechanics and Mechanisms of Failure. J. Mater. Sci. 17(3):617–651.

Laine, J., Lindstrom, T., Nordmark, G. G., Risinger, G. (2000) Studies on Topochemical Modification of Cellulosic Fibres Part 1. Chemical Conditions for the Attachment of Carboxymethyl Cellulose onto Fibres. Nord. Pulp Pap. Res. J. 15(5):520–526.

Li, L., Tirrell, M., Korba, G. A., Pocius, A. V. (2001) Surface Energy and Adhesion Studies on Acrylic Pressure Sensitive Adhesives. J. Adhes. 76(4):307–334.

Liu, Z., Choi, H., Gatenholm, P., Esker, A. R. (2011) Quartz Crystal Microbalance with Dissipation Monitoring and Surface Plasmon Resonance Studies of Carboxymethyl Cellulose Adsorption onto Regenerated Cellulose Surfaces. Langmuir 27(14):8718–8728.

Liu, J., Pelton, R., Obermeyer, J. M., Esser, A. (2013) Laccase Complex with Polyvinylamine Bearing Grafted TEMPO Is a Cellulose Adhesion Primer. Biomacromolecules 14:2953–2960.

Lyne, L. M., Gallay, W. (1954) Measurement of Wet Web Strength. Tappi J. 37(12):694–698.

Maloney, T. C., Laine, J. E., Paulapuro, H. (1999) Comments on the Measurement of Cell Wall Water. Tappi J. 82(9):125–127.

McLaren, A. D. (1948) Adhesion of High Polymers to Cellulose. Influence of Structure, Polarity, and Tack Temperature. J. Polym. Sci. 3(5):652–663.

Obokata, T., Isogai, A. (2007) The Mechanism of Wet-Strength Development of Cellulose Sheets Prepared with Polyamideamine-Epichlorohydrin (PAE) Resin. Colloids Surf. A 302(1–3):525–531.

Obokata, T., Yanagisawa, M., Isogai, A. (2005) Characterization of Polyamideamine-Epichlorohydrin (PAE) Resin: Roles of Azetidinium Groups and Molecular Mass of PAE in Wet Strength Development of Paper Prepared with PAE. J. Appl. Polym. Sci. 97(6):2249–2255.

Page, D. H. (1993) A Quantitative Theory of the Strength of Wet Webs. J. Pulp Pap. Sci. 19(4):175–176.

Pelton, R., Ren, P. R., Liu, J., Mijolovic, D. (2011) Polyvinylamine-Graft-TEMPO Adsorbs onto, Oxidizes and Covalently Bonds to Wet Cellulose. Biomacromolecules 12:942–948.

Pesika, N. S., Tian, Y., Zhao, B., Rosenberg, K., Zeng, H., Mcguiggan, P., Autumn, K., Israelachvili, J. N. (2007) Peel-Zone Model of Tape Peeling Based on the Gecko Adhesive System. J. Adhes. 83(4):383–401.

Saito, T., Isogai, A. (2005) A Novel Method to Improve Wet Strength of Paper. Tappi J. 4(3):3–8.

Saito, T., Isogai, A. (2006) Introduction of Aldehyde Groups on Surfaces of Native Cellulose Fibers by TEMPO-Mediated Oxidation. Colloids Surf. A 289(1–3):219–225.

Saito, T., Isogai, A. (2007) Wet Strength Improvement of TEMPO-Oxidized Cellulose Sheets Prepared with Cationic Polymers. Ind. Eng. Chem. Res. 46(3):773–780.

Satas, D. (1989) Peel. In: Handbook of Pressure Sensitive Adhesive Technology, Ed. Satas, D., Van Nostrand Reinhold, New York.

Skowronski, J., Bichard, W. (1987) Fibre-to-Fibre Bonds in Paper. Part 1. Measurement of Bond Strength and Specific Bond Strength. J. Pulp Pap. Sci. 13(5):165–169.

Taylor, D. L. (1968) Mechanism of Wet Tensile Failure. Tappi J. 51(9):410–413.

van de Ven, T. G. M. (2008) Capillary Forces in Wet Paper. Ind. Eng. Chem. Res. 47(19):7250–7256.

Wen, Q., Pelton, R. (2012) Microgel Adhesives for Wet Cellulose – Measurements and Modeling. Langmuir 28(12):5450–5457.

Yang, D. Degradable Wet Cellulose Adhesives. Ph.D. Thesis, Chemical Engineering McMaster. Hamilton, Canada, 2018.

Zhang Newby, B.-M., Chaudhury, M. K. (1998) Friction in Adhesion. Langmuir 14(17):4865–4872.

Supplemental Material: The online version of this article offers supplementary material (https://doi.org/10.1515/npprj-2018-0013).

WET-PEEL - A TOOL FOR COMPARING WET-STRENGTH RESINS.

Dong Yang, John-Louis DiFlavio, Emil Gustafsson, Robert Pelton

SUPPLEMENTARY INFORMATION

Table S1The influence of PAE and PVAm on the mechanical properties of wet TEMPO oxidized cellulose (TO-C) membranes. Once-dried membranes were dried at 23 ºC. The polymers were applied by adsorption. Error limits depict the standard deviation based on at least 3 replicates.

	TO-C	TO-C + PAE	TO-C + PVAm
Never-dried After Polymer Treatment			
Water content after blotting, wt%	56 ± 1	55 ± 1	55 ± 1
Elastic modulus, MPa	114 ± 8	114 ± 4	106 ± 4
Tensile strength, MPa	18 ± 2	17 ± 1	15 ± 2
Wet strain at break, %	47 ± 6	50 ± 6	40 ± 6
Yield stress, MPa	1-2	1-2	1-2
Once-dried at 23 °C and then rewetted			
Water content after blotting, wt%	51 ± 1	51 ± 2	51 ± 1
Elastic modulus, MPa	99 ± 5	95± 8	100 ± 8
Tensile strength, MPa	13 ± 1	18 ± 1	17 ± 1
Strain at break, %	34 ± 7	54 ± 1	49 ± 5
Yield stress, MPa	~ 1	~ 1	~ 1

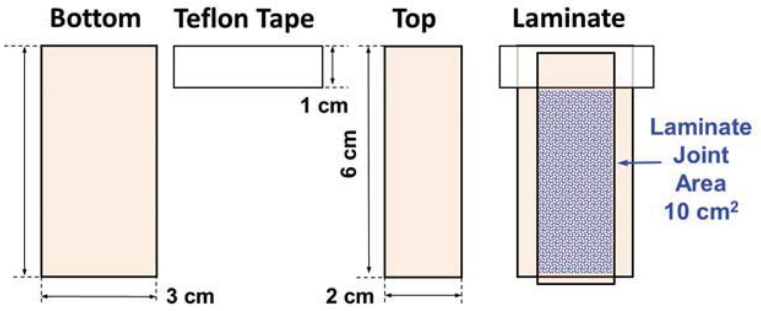

Figure S1 Dimensions of cellulose membranes and the release tape and their orientation in the assembled laminate.

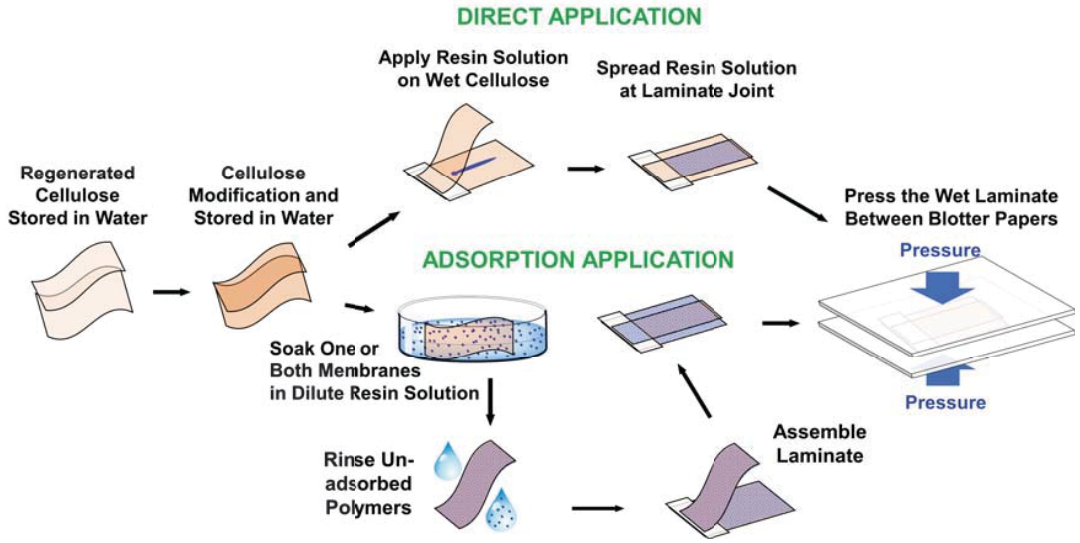

Figure S2 Schematic depiction of the "adsorption" and the "direct application" methods for applying wet-strength resin to cellulose surfaces.

Figure S3 Photographs of peeling assembly.

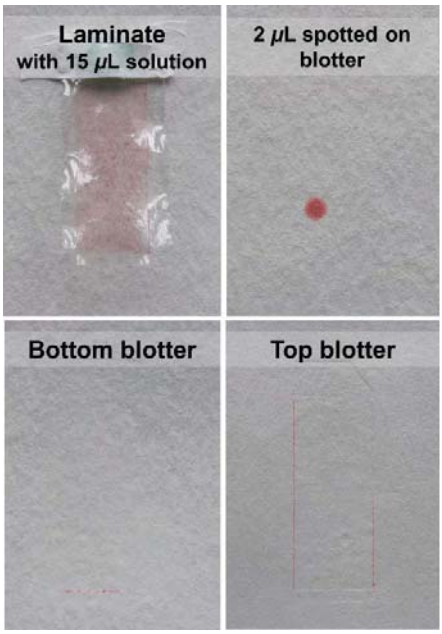

Figure S4 Photographs of a laminate and the blotters after pressing at 323 kPa for 5 min. The laminate was prepared with 15 μL of 1g/L Congo Red solution. There was no indication that pressing squeezed solution out of the laminate.

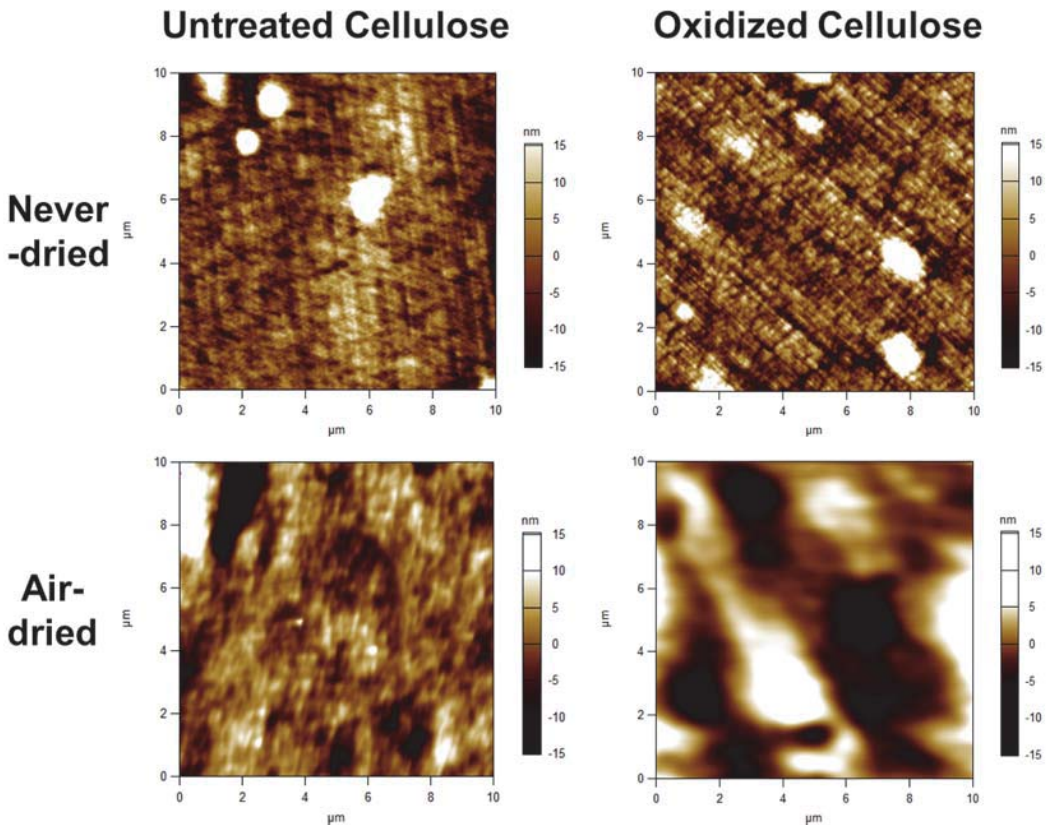

Figure S5 AFM images were collected using an Asylum MFP-3D instrument (Asylum Research, US). Images were processed in Igor Pro 6.37 running Asylum Research 13.03.17 software using the Magic Mask feature. Root mean squared roughness was calculated in an area of 5 µm × 5 µm using the analysis tool in Asylum Research software. For underwater imaging, a drop of 1 mM NaCl, pH 7 water solution was added on the surface of never-dried wet membranes. The images were collected underwater under ambient conditions using TR800PSA cantilevers with normal spring constants of a force constant of 0.57 ± 0.08 N/m and resonance frequencies of 70 ± 15 kHz. in tapping mode. For imaging of once-dried samples, the samples were dried in air. The images were collected in air under ambient conditions using FMR cantilevers with normal spring constants of 2.8 ± 0.3 N/m and resonance frequencies of 75 ± 15 kHz in tapping mode.

.

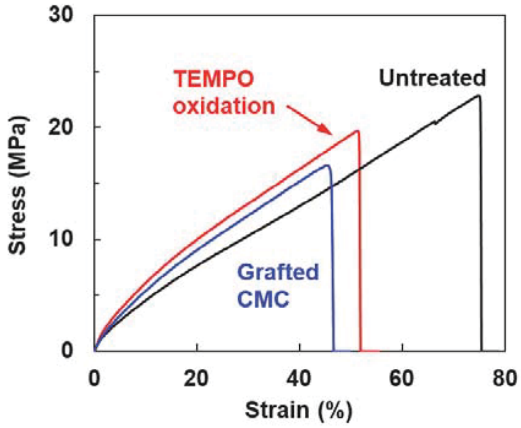

Figure S6 Stress-strain curves for never-dried wet cellulose membranes. Assume the wet-peel force is 40 N/m and the thickness of wet membrane is 130 μm. The corresponding stress in membrane is ~ 0.3 MPa during the wet peel and the strain is less than 1%.

Chapter 3

Hydrazide-derivatized Microgel Cellulose Wet Adhesives

In this chapter, hydrazide-derivatized microgels were applied as cellulose wet adhesives. Microgel adhesives were synthesized to have specific properties, including size, cross-linking density, and hydrazide content. The performance of the microgel adhesives was evaluated using wet-peel measurements. A mechanistic model was developed to analyze the contribution of microgel properties to the adhesive energy. This knowledge helped us in the design of microgel adhesives with controllable degradability, which is described in Chapters 4 and 5.

The data within this chapter have been collected by me with the assistance of Taylor Stimpson, who worked with me as a summer student. I summarized the data and wrote the draft myself. Dr. Emil Gustafsson, Dr. Anton Esser, and Dr. Robert Pelton helped me analyze the results. Dr. Pelton re-wrote parts of the draft as necessary.

This chapter and the supporting information are reprinted as they appear in *ACS Applied Materials & Interfaces* with permission from the American Chemical Society.

Hydrazide-Derivatized Microgels Bond to Wet, Oxidized Cellulose Giving Adhesion Without Drying or Curing

Dong Yang, Emil Gustafsson, Taylor C. Stimpson, Anton Esser, and Robert H. Pelton

ACS Applied Materials & Interfaces, 2017, 9 (24), 21000-21009

DOI: 10.1021/acsami.7b04700

ACS APPLIED MATERIALS & INTERFACES

Hydrazide-Derivatized Microgels Bond to Wet, Oxidized Cellulose Giving Adhesion Without Drying or Curing

Dong Yang,[†] Emil Gustafsson,[†] Taylor C. Stimpson,[†] Anton Esser,[‡] and Robert H. Pelton*[,†]

[†]Department of Chemical Engineering, McMaster University, 1280 Main St. West, Hamilton, Ontario Canada L8S 4L7

[‡]BASF AG, EVW/MI, 67056 Ludwigshafen, Germany

Supporting Information

ABSTRACT: Hydrazide-derivatized poly(*N*-isopropylacrylamide-*co*-acrylic acid) microgels gave strong adhesion to wet, TEMPO oxidized, regenerated cellulose membranes without a drying or heating step. Adhesion was attributed to hydrazone covalent bond formation with aldehyde groups present on the cellulose surfaces. This is one of only three chemistries we have found that gives significant never-dried adhesion between wet cellulose surfaces. By contrast, for cellulose joints that have been dried and heated before wet testing, the hydrazide-hydrazone chemistry offers no advantages over standard paper industry wet strength resins. The design rules for the hydrazide-microgel adhesives include: cationic microgels are superior to anionic gels; the lower the microgel cross-link density, the higher the adhesion; longer PEG-based hydrazide tethers offer no advantage over shorter attachments; and, adhesion is independent of microgel diameter. Many of these rules were in agreement with predictions of a simple adhesion model where the microgels were assumed to be ideal springs. We propose that the unexpected, high cohesion between neighboring microgels in multilayer films was a result of bond formation between hydrazide groups and residual NHS-carboxyl esters from the preparation of the hydrazide microgels.

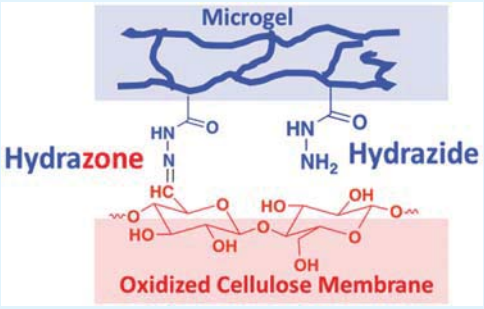

KEYWORDS: *wet adhesion, hydrazone, hydrazide, microgels, cellulose oxidation*

INTRODUCTION

The "Bioeconomy" is a vision in which many of the materials we use come from sustainable sources and are recyclable. Cellulose, the world's most abundant organic material, must play a major role in replacing conventional plastics, concrete and other materials we all use every day. Wood and paper materials have a long history. More recently there has been an explosion in activities around breaking wood down to cellulose nanocrystals and to cellulose nanofibers. The Achilles heel of wooden structures, paper-based materials, and the newest nanocellulose composites is moisture sensitivity. Amorphous cellulose sorbs water, changing properties as far ranging as stiffness and oxygen permeability. In addition, the hydrophilic nature of cellulose surfaces makes it difficult to achieve durable adhesive joints between wet cellulose surfaces. The long-term goal of our research is to develop new adhesive technologies specifically aimed at achieving durable joints between cellulose surfaces in water. Our aspirations include: adhesive joints that form spontaneously in water under ambient conditions giving what we call herein "never-dried adhesion"; adhesive joints in which adhesion can be turned off to promote recycling; adhesive materials based on green chemistry principles; and, adhesive materials that, like cellulose, are completely biodegradable.

Most of our adhesion research has focused on polyvinylamine (PVAm) as the adhesive in the form of linear polymers or as microgels. Microgels offer many advantages including: they are easily cleaned and characterized;[1] they can be deposited in well-defined arrangements in adhesive joints; their influence on adhesion can be modeled by simply treating them as springs;[2] and because microgels are larger than most linear polymers, an adsorbed layer of microgels puts more adhesive in cellulose-adhesive-cellulose joints, an important advantage when forming joints between rough surfaces.[3] Our most recent adhesive microgels were based on carboxylated poly(*N*-isopropylacrylamide) (PNIPAM) microgels with an adsorbed layer of PVAm.[2] These materials give significant wet adhesion to oxidized cellulose. However, the adhesive joint must first be dried to form covalent imine and aminal linkages. Without the drying step, the never-dried adhesion is minimal.

There are potential applications of cellulose adhesives where never-dried adhesion would be useful. In papermaking, methods of increasing the strength of the wet paper sheet on the papermachine (i.e., the wet web strength) help prevent the wet paper sheet from tearing and disrupting production.[4] Agricultural mulches based on sprayed wood pulp fibers is another example where instant wet, cold adhesion is an important property.[5]

In this work, we explore the utility of hydrazide-hydrazone chemistry as a route to never-dried adhesion in the presence of

Received: April 3, 2017
Accepted: May 31, 2017
Published: May 31, 2017

water (see Figure 1B). This is an attractive chemistry because hydrazone bonds form in water under ambient conditions,

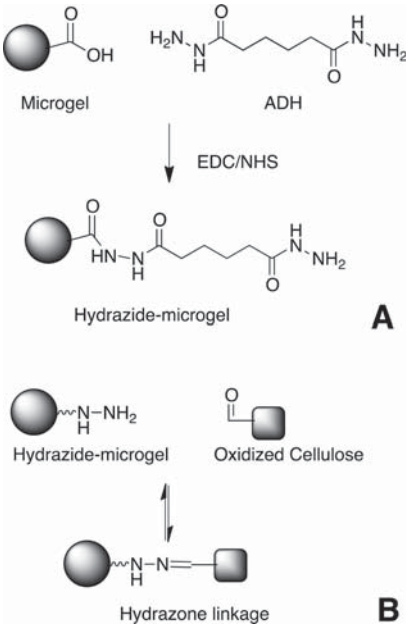

Figure 1. (A) Hydrazide derivatization of carboxylated microgels and (B) hydrazone bond formation between a hydrazide and an aldehyde in water. Although, hydrazone bond formation is acid-catalyzed, the reverse hydrolysis reaction dominates at low pH. Therefore, neutral pH is optimal for hydrazone bond formation.[9,10]

giving covalent hydrazone linkages.[6,7] Hydrazone bond formation requires aldehyde groups, and we generated these by mild TEMPO (2,2,6,6-tetramethylpiperidine 1-oxyl) oxidation of regenerated cellulose films.[8] Although most adhesives polymers are linear or branched, we chose poly(*N*-isopropylacrylamide-*co*-acrylic acid) microgels (poly(NIPAM-*co*-AA)) as the polymer platform onto which we grafted hydrazide groups (see Figure 1).

Cellulose−cellulose adhesion in the presence of water is an old problem. Most of the current technologies have been developed for use in the paper industry where small wood-pulp fibers are assembled into large structures. Two extremes that span the technology landscape are saturating papers and paper towels. Saturating papers are impregnated with thermosetting polymeric resins, producing materials that are used in flooring, furniture, and laminated panels. Such materials are strong, tough, water resistant, and commonly found in our homes and offices. They are neither sustainable nor recyclable.

The second example of wet-strengthened cellulosic materials is the paper towels we all use. Unlike products based on saturating papers, most of the material in paper towels is lignocellulosics. During the papermaking process, a small quantity of adhesive forms an adsorbed layer on wet fibers surfaces. When the fiber suspension is filtered to form wet paper, adhesive coated fibers are forced together, forming weak fiber−fiber joints. During the drying process at elevated temperatures, the polymer present in the fiber−fiber joints cross-links and forms covalent grafts to the fiber surfaces. In the paper industry, these materials are called wet-strength resins, and the most popular one is a material commonly called PAE resin (polyamide-epichlorohydrin).[11] We know from using premium paper towels or paper coffee filters that PAE resins give high wet strength. In terms of our goals: PAE fails to give never-dried adhesion; PAE strengthened papers cannot be recycled and do not decompose quickly; PAE adhesion cannot be switched off; and, PAE polymers are neither green nor from sustainable sources.

Possible but impractical approaches to never-dried adhesion are chitosan applied at high pH,[12] polymers bearing grafted cellulose binding domain proteins,[13] and polymers bearing grafted DNA aptamers.[14] A few years ago we showed that PVAm with grafted phenylboronic acid moieties gives never-dried adhesion when applied at pH > 8.[15] We proposed that the mechanism involved the formation of boronate esters with cellulose chain ends. If one is willing to pretreat cellulose fibers, followed by a second adhesive application, there are more options for never-dried cellulose-cellulose adhesion. Recently, we have shown that cellulose coated with grafted carboxymethyl cellulose (CMC), a process developed by Laine and Lindström,[16] gives very high never-dried adhesion when laminated with PVAm.[17] The never-dried adhesion was attributed to polyelectrolyte complex formation between cationic PVAm and anionic CMC.

The current work was inspired by the biotechnology literature, where hydrazide-hydrazone chemistry has been used to prepare hydrogels under mild, wet conditions for controlled drug release[18] and for the immobilization of biological cells.[19] In spite of these possibilities, there are surprisingly few publications or patents exploiting hydrazide/hydrazone cross-linking in the papermaking technology literature. More than 45 years ago Machida described the use of polyacrylamide-hydrazide as a flocculant for papermaking; there was no mention of exploiting the ability of the hydrazide groups to bond to oxidized cellulose.[20] By contrast, the patent literature contains many examples of hydrazone bond formation for modifying or cross-linking water-soluble polymers.[21−24] Finally, Tejado et al. recently described the use of adipic dihydrazide (ADH) to bond carboxylated cellulosic fibers.[25] Whereas hydrazides react spontaneously with aldehydes, coupling to carboxyl groups requires one or more activating agents such as carbodiimides.

Herein we link the properties of hydrazide-modified microgels to their performance as cellulose wet adhesives. The experimental results are interpreted within the framework of a mechanistic adhesion model, highlighting both the key microgel properties and the strengths and weaknesses of our model.

EXPERIMENTAL SECTION

Materials. Dihydrazide-polyethylene glycol (PEG) with Mw 1 kDa was purchased from Creative PEGWorks, U.S. Regenerated cellulose membranes (Spectra/Por2, MWCO 12−14 kDa, product number 132684) were purchased from Spectrum Laboratories, U.S. Blotter papers were purchased from Labtech Instruments Inc., Canada. All other chemicals were purchased from Sigma-Aldrich, Canada. Water type 1 (as per ASTM D1193-6, resistivity 18MΩ/cm) were used in all experiments. The hydroquinone inhibitor was removed from *N*,*N*′-dimethylaminoethyl methacrylate (DMAEMA) by passing it through a column (Sigma-Aldrich, U.S.).

Microgel Preparation. A series of poly(NIPAM-*co*-acrylic acid) microgels was synthesized based on the methods in the literature[26] and the recipes are summarized in the Supporting Information (see Table S1). In a typcial polymerization, NIPAM, *N*,*N*′-methylenebis-(acrylamide) (MBA), sodium dodecyl sulfate (SDS), and AA were dissolved in water and heated to 70 °C. The solution was agitated for

30 min with nitrogen gas purging. Ammonium persulfate was dissolved in 2 mL of water and injected into the solution.

For amphoteric microgels, NIPAM, MBA, cetyltrimethylammonium bromide (CTAB), DMAEMA and AA were dissolved in water and heated to 70 °C. The solution was adjusted to pH 3 with 0.1 M hydrochloric acid. The solution was agitated for 30 min with nitrogen gas purging. 2,2′-Azobis(2-methylpropionamidine) dihydrochloride (AAPH) was dissolved in 2 mL water and injected into the solution.

All polymerizations proceeded for 8 h at 70 °C with nitrogen gas purging. The microgels were purified by dialysis against water. The properties of the nine starting microgels are summarized in Table S2.

Hydrazide-Microgels. Hydrazide-derivatized microgels were prepared by the EDC/NHS mediated conjugation of ADH to poly(NIPAM-*co*-AA) microgels.[27] The conjugation chemistry is shown in Figure 1A and detailed conjugation recipes are given in Table S4. In a typical reaction, the molar ratio of ADH, 1-ethyl-3-(3-(dimethylamino)propyl)carbodiimide hydrochloride (EDC) and *N*-hydroxysuccinimide (NHS) was 2:2:1. 120 mg of dry microgels were dispersed in 24 mL water at room temperature and after 30 min stirring, the pH of solution was adjusted to 5. EDC was added and then NHS was added 2 min later. The dispersion was stirred and maintained at pH 5. After 10 min, the pH was adjusted to 7.2 and the grafting reagents ADH or dihydrazide-PEG were added. The modification proceeded for 2 h at room temperature with pH maintaining 7.2. The products were purified by dialysis and stored as aqueous solution at 4 °C.

Microgel Characterization. For most measurements, the microgels were dispersed in 1 mM NaCl solution at neutral pH at 23 °C. The electrophoretic mobilities of microgels were measured by ZetaPlus analyzer (Brookhaven Instruments, US) using the phase analysis light scattering mode. The reported mean electrophoretic mobility values and the corresponding standard errors were based on 10 cycles with 10 scans for each cycle.

Hydrodynamic diameters of microgels were measured by dynamic light scattering (DLS) (Model BI-APD, Brookhaven Instruments, US) with software version 1.0.0.1. The detection angle was 90° and we used a 633 nm wavelength laser. The DLS results were interpreted with the CONTIN algorithm providing a polydispersity index (PDI) and a mean diameter for each measurement. The reported average particle diameters and the corresponding standard deviations were based on at least three measurements.

Microgel carboxyl contents were determined by potentiometric titrations, carried out with a Burivar-I2 automatic buret (ManTech Associates, Canada). Thirty ±2 mg of dried microgel was dispersed in 50 mL 1 mM NaCl with initial pH 3.0 ± 0.1. All samples were titrated by 0.1 M NaOH with a target increment of 0.05 pH units/injection. The corresponding injection volumes were in the range 5−100 μL. The interval between injections was 90 s. The microgel carboxyl contents, before and after hydrazide conjugation, were calculated from potentiometric titration data. However, we were unable to use the potentiometric data directly from pH 3 because the hydrazide groups, with a $pK_a \approx 2.5$,[28] contribute to titration end points. Instead, the residual carboxyl contents were estimated from the portion of the potentiometric curve pH >4. This analysis was based on two assumptions: (1) the hydrazide groups do not contribute to the titration curve for pH > 4; and, the degree of ionization for microgel carboxyl groups at pH 4 was equal for both the hydrazide-microgels and the microgels before derivatization. Details of potentiometric data analysis are given in the Supporting Information, and the resulting microgel carboxyl contents are expressed herein as carboxyl equivalent weights (g/mol carboxyl).

The hydrazide contents of the derivatized microgels (see structure in Figure 1A) were expressed herein as the "DS value" (degree of substitution), which is the mole fraction of the carboxyl groups converted to hydrazide groups. The DS is related to the equivalent weights of the microgels, before, EW_O, and after, EW_H, derivatization by eq 1 where MW_H = 156.2 Da is the molecular weight of each hydrazide moiety. The hydrazide-microgel DS values are summarized in Table 1 and eq 1 is derived in the Supporting Information.

$$DS = \frac{EW_H - EW_O}{EW_H - MW_H} \quad (1)$$

Table 1. Properties of the Hydrazide Microgels[b]

microgel	cross-linker (mol %)	hydrazide DS (mol %)	diameter (nm)	PDI	mobility (10^{-8} m^2/(V s))
A1-H31	5.3	31	823 ± 37	0.09	−2.35 ± 0.05
A2-H75	5.3	75	372 ± 6	0.06	−2.14 ± 0.08
A2-H62	5.3	62	381 ± 6	0.01	−2.16 ± 0.07
A2-H45	5.3	45	399 ± 4	0.03	−2.32 ± 0.07
A2-H28	5.3	28	417 ± 6	0.01	−2.34 ± 0.07
A2-H19	5.3	19	438 ± 6	0.06	−2.33 ± 0.03
A2-H6	5.3	6	450 ± 14	0.09	−2.56 ± 0.07
A2-HPEG12	5.3	12	422 ± 7	0.12	−2.59 ± 0.03
A2-HPEG31	5.3	31	406 ± 6	0.08	−2.37 ± 0.10
A3-H30	5.3	30	231 ± 5	0.07	−2.08 ± 0.06
A4-H38	5.3	52	113 ± 14	0.39	−1.57 ± 0.06
A5-H72	16.0	72	493 ± 25	0.13	−2.07 ± 0.04
A6-H72	10.7	72	399 ± 9	0.03	−2.27 ± 0.04
A7-H68	1.5	68	393 ± 23	0.18	−1.73 ± 0.08
A8-H75	0.5	75	398 ± 37	0.41	−1.65 ± 0.15
AMP-H	5.3	29[a]	187 ± 6	0.22	−1.49 ± 0.11
AMP1-H	5.3	49[a]	132 ± 12	0.37	−1.04 ± 0.05

[a]Overestimates that include the unknown contribution of the tertiary amine monomer to the titration. [b]The hydrazide-microgel names combine the parent starting microgel name (A1, A2, AMP, or AMP1) with the percentage of carboxyl groups converted to hydrazides (H62, H28, etc.) Particle size and electrophoretic measurements were performed in 1 mM NaCl at pH 7, at 23 °C. The properties of the unmodified starting microgels are given in Table S3.

Cellulose Membrane Oxidation. Regenerated cellulose Spectra/Por2 (MWCO 12−14 kDa) dialysis tubing (120 mm diameter) was cut into 6 cm × 2 cm (top) and 6 cm × 3 cm (bottom) strips. The membranes were cleaned by agitating in water at 60 °C for 1 h. The clean membranes were oxidized as follows. 68 mg TEMPO (2,2,6,6-tetramethylpiperidine 1-oxyl) was dissolved in 2 L of water along with 680 mg NaBr and followed by 300 mg NaClO. The concentration of NaClO solution was determined by available chlorine titration (TAPPI, Test Method T 611 cm-07). The pH of the solution was adjusted to 10.5, after which 10 g cellulose membranes were mixed at room temperature while maintaining the pH at 10.5 by 1 M NaOH or HCl. After 15 min, the oxidation reaction was stopped by adding 10 mL ethanol. The oxidized membranes were washed with water and stored at 4 °C.

Once-Dried Wet Adhesion. The laminates were prepared by a method we call "direct application".[2] In this procedure, 15 μL microgel dispersion was carefully applied between two wet, oxidized cellulose membranes. The top membrane was 6 cm × 2 cm and the bottom one was 6 cm × 3 cm. A Teflon tape (1 cm wide) was put between two membranes at one end, making an effective adhesive area between two membranes of 5 cm × 2 cm. The adhesive coverage in laminate joints Γ (mg/m^2) was determined from the volume (15 μL), concentration of application solution, and the effective adhesive area of laminate. The adhesive concentration of application solution was changed to vary the adhesive coverage. For most cases, the adhesive dispersion consisted of 1 g/L microgel in 1 mM NaCl solution at pH 7, corresponding to 15 mg of dry microgel per square meter of laminate.

The laminates were place between two blotter papers and pressed under 334 kPa for 5 min at room temperature in Standard Auto CH Benchtop Press (Carver, Inc., US). The samples were then dried in a constant temperature and humidity room (23 °C, 50% relative humidity) for 1 day.

A freely rotating aluminum peel wheel with a diameter of 14 cm and width of 4 cm was attached to an Instron 4411 universal testing system with 50 N load cell (Instron Corp., Norwood, MA). Before testing, the laminates were soaked for 30 min in 1 mM NaCl at pH 7 and then blotted free of excess water. Wet membranes were fixed to the wheel with moisture-resistant double-sided tape (medical tape 1522, 3M, US). Delamination force was determined with a 90 deg peeling geometry using a peel rate was 20 mm/min. The wet laminates were weighed before and after peeling. The solid contents of the laminates were in the range of 47−54 wt % during the peeling. The reported delamination forces and standard deviations were based on at least 3 replicates.

Never-Dried Adhesion. 90-degree peel tests were used to determine never-dried adhesion. Laminates were prepared by the direct application, and then placed between two blotter papers, and pressed under 334 kPa at room temperature. The water contents of the laminates were controlled by varying the pressing time in the range of 0.1−10 min. Delamination force of never-dried laminates was tested immediately after pressing. The weight of each laminate was recorded before and after peeling. The reported solids contents of the laminates were the average of the values before and after delamination. In most of experiments, water contents decreased 8−14 wt % during delamination.

RESULTS

The Microgels. The adhesive microgels were prepared in a two-step process. First, nonadhesive, starting copolymer microgels containing carboxyl groups were prepared by standard batch polymerization. Second, some of the carboxyl groups were converted to adhesive hydrazide groups by coupling with the bifunctional hydrazide, ADH, see chemistry in Figure 1A.

Starting microgel series A1−A8 were anionic copolymers of *N*-isopropylacrylamide (NIPAM) and acrylic acid−see recipes in Table S1. Over the series, the acrylic acid mole fraction in the monomer mixture was 15 mol % for all of the microgels, whereas the cross-linker content ranged from 0.5 to 16 mol %. Amphoteric NIPAM copolymer microgels, AMP and AMP1, were also prepared, and the recipe is given in Table S2. The measured diameters, electrophoretic mobilities, and carboxyl contents of the starting microgels are given in Table S3. The carboxyl contents and electrophoretic mobilities were approximately constant, whereas the average microgel swollen diameters spanned the range of 100−1000 nm.

Hydrazide groups were coupled to the nine starting microgels, giving 17 hydrazide-microgels whose properties are summarized in Table 1. The hydrazide contents are expressed as DS (degree of substitution) values we define as the mole percent of carboxyls converted to hydrazides. The microgel designations include the parent microgel name and the hydrazide DS value. For example, microgel A2-H6 was starting microgel A2 with 6 mol % of the carboxyls derivatized to hydrazides.

Our hydrazide conjugation procedure (Figure 1A) could induce microgel/microgel attachments. However, the PDI values did not change significantly, and the microgel diameters actually decreased because of the conversion of ionized carboxyl groups to nonionized hydrazides. Example particle size distributions, before and after conjugation, are given in Figure S1.

In the next sections, we present the abilities of the hydrazide-microgels to promote the adhesion between wet cellulose surfaces. Our results describe two separate cases: "never-dried", where the adhesive joint is not allowed to dry, and "once-dried", where the adhesive joints were allowed to dry at room temperature before being rewetted for adhesion testing. The distinction between the two cases is important because drying is required to promote covalent bond formation in virtually all adhesive chemistries.

Strength of Never-Dried Joints. A potential advantage of the hydrazide chemistry is covalent bond formation in the presence of water. Wet adhesion experiments were performed with samples that were never dried−herein designated "never-dried adhesion". Regenerated cellulose membranes were TEMPO oxidized to introduce aldehyde groups and the wet membranes were laminated with a layer of microgels acting as an adhesive layer. The moisture content of the laminates was controlled by varying the room temperature pressing time. Ninety-degree peel tests were performed to give measures of wet adhesion. Figure 2 shows the results with oxidized cellulose membranes as a function of laminate solids contents. Note that before lamination, our swollen cellulose membranes had a solids content of 48−49 wt % after oxidation. In all cases the wet delamination force increased with the laminate solids content.

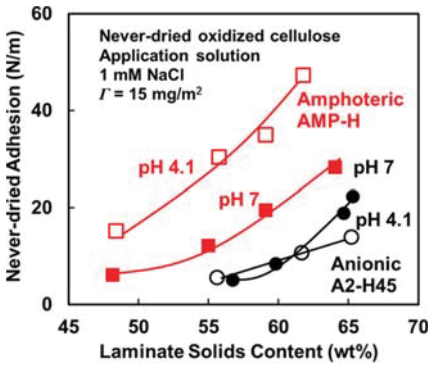

Figure 2. Never-dried adhesion of oxidized cellulose membranes laminated with hydrazide-microgel adhesives. The mass coverage was $\Gamma = 15$ mg/m^2; the corresponding number of layers of microgels in the laminate joint was 1.4 for AMP-H and 0.9 for A2-H45.

AMP-H, the amphoteric hydrazide microgel displayed high never-dried adhesion with oxidized cellulose, particularly at pH 4.1. By contrast, the hydrazide-microgels were ineffective with nonoxidized cellulose (see Figure S2), supporting the proposal that the hydrazide groups form covalent hydrazone bonds to cellulosic aldehydes—see chemical structures in Figure 1. Note that a second amphoteric microgel gave similar results—see Figure S3.

Anionic hydrazide microgel A2-H45 (Figure 2) gave low never-dried adhesion until the laminate was partially dried. Increasing microgel coverage did not improve adhesion to any extent—see Figure S4. Although hydrazide moieties should be able to couple with the cellulose aldehyde promoting adhesion, we propose that electrostatic repulsion between the anionic microgel and anionic cellulose inhibits intimate microgel/cellulose contact and thus hydrazone bond formation.

Strength of Once-Dried Joints. In the following experiments, the cellulose laminates were allowed to dry at room temperature before rewetting for peel delamination. Figure 3 shows the influences of pH and NaCl concentration on the properties of two microgels. A2-H75 was an anionic microgel with a high content of hydrazide groups, whereas AMP-H was the amphoteric microgel with lower hydrazide content. We consider first the anionic microgel A2-H75. As expected, the

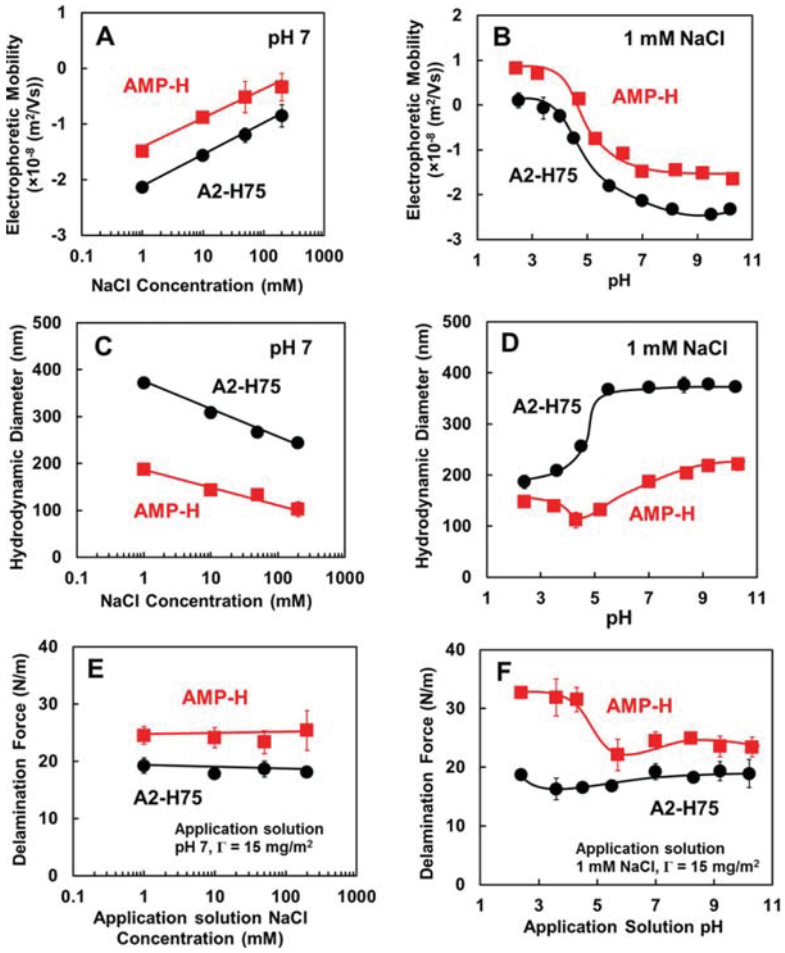

Figure 3. Influence of ionic strength and pH on (A and B) microgel electrophoretic mobility, (C and D) microgel size, and (E and F) once-dried wet adhesion.

anionic microgel shrank with increasing salt content and lowering pH, reflecting the electrostatic contribution to swelling.

Amphoteric microgel swelling and electrophoretic mobility values usually show complex behaviors over the pH range, and AMP-H is no exception. At low pH, the carboxyl groups were uncharged, whereas the tertiary amine groups on the cationic monomer (DMAEMA) were ionized. At high pH, the carboxyls were ionized and the amines were not. The corresponding electrophoretic mobility was positive below pH 5 and negative at higher pH values. Swelling was minimum around pH 4.5 corresponding to the isoelectric point.

After the laminates were formed, they were allowed to dry slowly at 23 °C and 50% relative humidity (i.e., once-dried). Before strength testing the laminates were soaked in water for 30 min giving water contents in the range 47−54 wt %. Figure 3E and F compare the adhesion characteristics of the microgels.

In contrast to the never-dried adhesion results (Figure 2), where the anionic hydrazide microgel gave poor adhesion, the anionic hydrazide microgel, A2-H75, gave once-dried wet adhesion values of about 20 N/m. In our experience, this is an intermediate strength. The very best adhesives give values of 30−45 N/m, above which cohesive failure of the oxidized cellulose membranes often occurs. By contrast, with unmodified microgels we were unable to measure a once-dried wet adhesion. Without adhesive microgels, TEMPO oxidized cellulose gave a cellulose/cellulose once-dried wet adhesion lower than 10 N/m after 30 min wetting.

A most striking observation was that the wet adhesion values with the anionic microgels were virtually constant over the large range of pH values and salt concentrations. Our cellulose-microgel-cellulose laminates were prepared by directly adding the adhesive during the laminate preparation. Although the anionic microgels may not spontaneously adsorb onto the cellulose, with drying the aldehydes and hydrazides will be brought together as the laminate dries, giving an opportunity for hydrazone bond formation. Ionic strength and pH effects that are important in solution, are probably attenuated when the adhesive joint dries.

The amphoteric microgel AMP-H gave consistently higher once-dried adhesion than the anionic microgel. We were surprised to observe a strong pH dependence in the adhesion properties of the amphoteric microgels (see Figure 3F). Above pH 5 the adhesion values were around 25 N/m, whereas at lower pH the adhesion increased to 35 N/m, a substantial change. Comparing Figure 3B and F it reveals that the highest amphoteric microgel once-dried wet adhesion corresponded to the pH range where the microgels had a positive electrophoretic mobility. A second hydrazide-amphoteric microgel AMP1-H also showed high cellulose-cellulose once-dried wet adhesion at low pH. The electrophoretic mobility and adhesion values for AMP1-H are summarized in Figure S5. We propose

that the positively charged polymer chains on the microgel surface promote molecular contact with the negatively charged cellulose surfaces, which in turn promotes hydrazone bond formation before drying when the tethered hydrazide groups are more mobile. By contrast, negatively charged microgel surface chains will be repelled from the cellulose until the water is removed.

Comparing Never-Dried and Once-Dried Adhesion. Results from two types of adhesion measurements should be compared at the same laminate water contents. The average solids contents in the once-dried laminates during testing was around 50 wt %. The corresponding never-dried adhesion results in Figure 2 at 50 wt % were about half the once-dried values in Figure 3 for the amphoteric microgel. The never-dried anionic microgel laminates were very weak at 55 wt %; we were unable to measure adhesion at lower solids contents with the anionic microgels.

Modeling the Influence of Microgel Properties. Parameters required to describe a microgel adhesive include: diameter, degree of swelling, type and density of cellulose affinity groups, cross-linker content, elastic modulus, etc. In an effort to guide thinking toward the critical parameters, we developed a simple model to relate microgel gel properties to the delamination force.[2,3] The essential features of the model are illustrated in Figure 4. The model assumptions included:

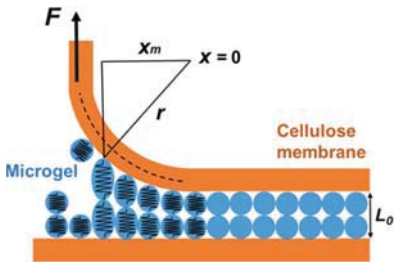

Figure 4. Illustrating the elements of the adhesion model. Figure adapted from Wen and Pelton.[2]

each microgel is treated as an ideal spring and failure only occurs at the adhesive contacts between the microgel and the cellulose interface; the membrane adopts a circular geometry with radius r at the peel front; and, the thickness of adhesive layer (L_o in Figure 4) is a function of unrestrained microgel diameter and the adhesive coverage.

Details of the adhesion model are illustrated in the Supporting Information. D, the microgel diameter and r, the radius of curvature at the peel front were measurable parameters. E, the elastic modulus of individual microgel particles and ε_m, the critical microgel extension at which a microgel particle detaches from cellulose, were unknown parameters and were treated as adjustable parameters. The model was able to simulate the influence of microgel coverage and cross-link density.[3] Herein, we have made the following two extensions to our model to describe better the hydrazide-microgels.

First, our new model no longer assumes failure only occurs at the microgel-cellulose interface. Instead, we replaced ε_m in our original work with two critical microgel extensions, ε_{gc} for the cellulose-microgel failure, and ε_{gg} for microgel-microgel adhesive failure. We anticipated that microgel-microgel adhesion for the hydrazide-microgels, would be low, requiring this change to the model. However, we will see below that microgel-microgel adhesion was high.

Second, r, the radius of curvature at the peel front is no longer assumed to be constant. Both the membrane mechanical properties and the adhesion forces determine peel-front curvature. For weak joints, r is large, whereas for strong joints r is small; photographs showing comparing a small and large r value are shown in Figure S6. We performed a series of experiments in which the delaminated force was varied by 3−25 N/m. Figure 5A shows the measured r values as functions of

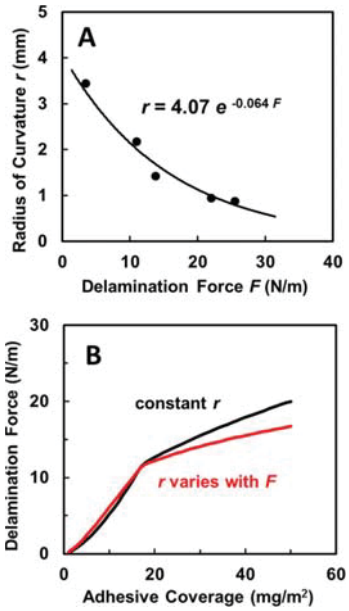

Figure 5. (A) Experimentally determined radius of curvature, r, at the delamination point as a function of delamination force of once-dried membranes. The solid line is an exponential fit to the data. (B) comparison of two simulated delamination force versus coverage curves, one with constant r and the other where r was a function of delamination force of once-dried membranes.

the delamination force, together with the exponential function used to fit the data. In the revised model, this exponential relationship was used to couple the delamination to r. However, the simulated curves for variable r were similar to those calculated assuming r was constant—see example comparison in Figure 5B.

Our revised model, implemented in MathCad Prime 3.1, is described in detail in the Supporting Information. The model was solved numerically and the results are compared with experimental results in the following sections. Peel mechanics are complicated and not captured in detail by our model. Nevertheless, it is instructive to see where the model and experiments diverge.

Influence of Microgel Coverage. A series of laminates was prepared with a range of adhesive coverages, Γ (dry mass/joint area). Figure 6 shows the once-dried wet adhesion as a function of the coverage of anionic A2-H75 microgel. The delamination force increased with microgel coverage up to a plateau value of about 25 N/m, which occurred for dry microgel coverages $\Gamma > 30$ mg/m^2. The vertical dashed line at $\Gamma = \Gamma_{sat} = 35$ mg/m^2 in Figure 6 depicts our estimate of the coverage given by two layers of A2-H75 microgels randomly deposited in the cellulose/cellulose joint. For this estimate, the

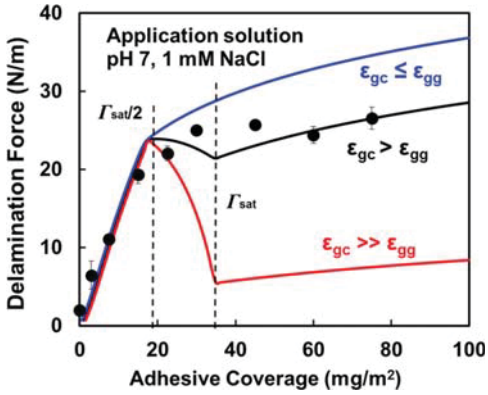

Figure 6. Influence of A2-H75 microgel coverage in laminate joints on once-dried wet adhesion. The solid lines were calculated with Version 2 of our model (see SI) with D = 372 nm, E = 100 kPa, and ε_{gc}= 10.5. The ε_{gg} values were 10.5 for the blue curve, 7.35 for the black curve, and 2.1 for the red curve. ε_{gc} is the microgel extension at which it detaches from cellulose, whereas ε_{gg} is the microgel extension leading to broken microgel/microgel contacts.

mass of polymer in an individual microgel particle was calculated from the diameter above the volume phase transition temperature,[1] assuming the ratio of water to polymer in the dehydrated gels was 0.4.[29]

The solid lines in in Figure 6 were calculated with our extended model (see SI file). Three cases are shown: (1) failure occurs only at gel/cellulose interface ($\varepsilon_{gc} \ll \varepsilon_{gg}$); (2) gel/cellulose contacts are slightly stronger than gel/gel contacts ($\varepsilon_{gc} \approx \varepsilon_{gg}$); and (3) gel/cellulose contacts are much stronger than gel/gel contacts ($\varepsilon_{gc} \gg \varepsilon_{gg}$). In these simulations, the absolute values of the delamination forces were not significant as they depended upon the assumed values of the microgel modulus. However, the simulations do highlight the observation that there is no evidence of microgel/microgel failure because there was no decrease in delamination force when moving from sub-monolayer coverage (i.e., Γ = 17 mg/m^2) to multilayer coverage where gel/gel contacts are bearing load during delamination. An unrelated observation suggesting strong adhesion between hydrazide-microgels involves their ability to be dispersed in water after drying. Whereas the parent poly(NIPAM) microgels spontaneously redisperse in water after drying, the hydrazide derivatives do not—see Figure S7.

Microgel Elasticity. A series of hydrazide-microgels was prepared with varying cross-link density but with constant diameters and hydrazone contents. Figure 7 shows the once-dried wet adhesion as a function of the ratio of cross-linking monomer (MBA) to linear polymer (NIPAM). The microgel coverage in these experiments was constant and roughly equivalent to a single layer of microgels in the laminate joints. The delamination forces decreased with increasing cross-linker density. We observed similar behavior in microgels with a surface layer of adsorbed PVAm.[3]

The solid curve in Figure 7 was from our model, which included the following approximations. Classical rubber elasticity theory predicts that the microgel elastic modulus should be proportional to the ratio of the cross-linking monomer content to the linear monomer content (λ = MBA/NIPAM) ratio. Therefore, we assumed that the microgel elastic modulus was a linear function of λ (E = 20·λ·kPa). Because the force required to detach a microgel from cellulose is proportional to the product $E{\cdot}\varepsilon_{gc}$,[3] this ratio was kept

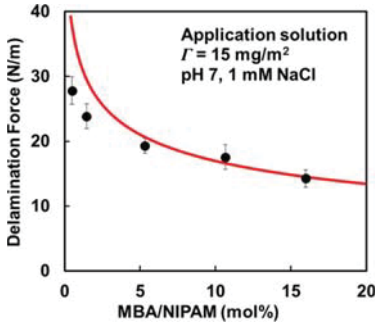

Figure 7. Influence of microgel cross-linker content on once-dried wet adhesion. All the microgel adhesives (A2-H75, A5-H72, A6-H72, A7-H68, and A8-H75) had similar sizes and hydrazide contents. The corresponding of number of layers of microgels in the laminate joint was 0.9. Cross-linking density is represented by the molar ratio of MBA cross-linker and NIPAM monomer in microgel synthesis. The red solid line was calculated by our model with parameters D = 372 nm, ε_{gc}= 10.5, and ε_{gg} = 7.35.

constant for the solid line in Figure 7—see calculations in the SI file.

The model showed the same features as the experimental results. Furthermore, the model points to the following explanation for higher delamination forces corresponding to lower microgel modulus. When peeling, only a few rows of microgels near the delamination crack are supporting the peeling load—see Figure 4. The lower the microgel modulus, the greater the number of microgels that are bearing the load. In terms of the model, the lower the microgel modulus, the greater is x_m, the length of load bearing region—see Figure 4.

Hydrazide Content. The A2 series of microgels (see Table 1) had hydrazide contents varying between 6% and 75% of A2 carboxyl groups being derivatized to give hydrazide groups. The once-dried wet adhesion performances of this series are compared in Figure 8, where delamination force is plotted

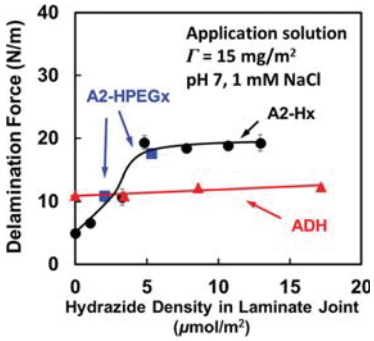

Figure 8. Once-dried wet adhesion for the A2-Hx microgels series as a function of the density of hydrazide groups in the laminates. The number of layers of microgels in the laminate joint was 0.9. The two blue square symbols represent laminate prepared with microgels grafted with dihydrazide PEG. The red triangles represent laminates prepared with ADH.

versus the hydrazide density (μmol/m^2). In these experiments the microgel coverage was 15 mg/m^2, which corresponds to about 90% of a single layer of microgels between the cellulose surfaces. The hydrazide densities in the laminates (i.e., the x-axis values) are the product of the dry mass coverage, Γ, the microgel DS (Table 1) and the carboxyl content of the starting

microgels (Table S3). These total hydrazide density values overestimate the number of hydrazides available for conjugation with cellulose because many of the hydrazides should be located in the interiors of the spherical microgels and thus not in contact with the cellulose surfaces.[30]

Figure 8 shows that the once-dried wet adhesion increased approximately linearly with hydrazide density up to about 5 μmol/m^2, above which the delamination force was constant with a plateau value of 20 N/m. We propose that a constant delamination force implies a constant density of hydrazone bonds between cellulose aldehydes and microgel hydrazides. Therefore, we propose that at hydrazide density above 5 μmol/m^2, many of the surface carboxyls have been derivatized and adhesion does not increase with further hydrazide functionalization.

The two blue square symbols in Figure 8 were for hydrazide groups coupled to the microgels via a 1 kDa PEG chain. We thought that there might be some advantage in attaching the hydrazide groups with more flexible tethers, however, the longer tethers did not increase adhesion. Finally, the results labeled ADH in Figure 8 were obtained with the very low molecular weight bifunctional hydrazide—see structure in Figure 1. ADH alone did not improve wet adhesion between wet cellulose surfaces.

Influence of Microgel Diameter. Once-dried wet adhesion experiments were performed with a series of microgels with a fixed hydrazide content but with microgel diameters varying between 113 and 823 nm. The laminates were prepared with a constant microgel coverage, which means the structures within the joints ranged from 2.8 layers of the smallest microgels to only 40% of monolayer coverage for the largest microgels. Figure 9 shows the experimental results. The

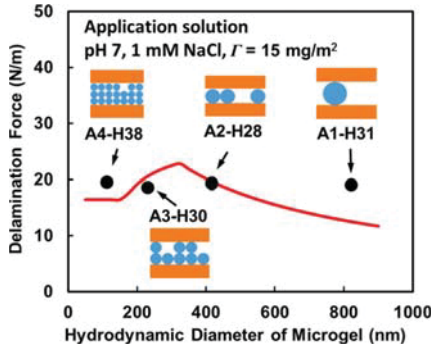

Figure 9. Influence of microgel size on once-dried wet adhesion. All the microgel adhesives have similar cross-linking densities and hydrazide contents. The red line was calculated from the model (see details in SI) assuming E = 100 kPa, ε_{gc}= 10.5, and ε_{gg} = 7.35.

illustration beside each data point shows the structure of the microgel layers and is approximately to scale. In spite of this enormous range of adhesive layer structures, the experimental results were independent of microgel diameter.

The solid curve in Figure 9 is the model prediction. Again, the absolute delamination forces have little significance as they are dependent upon the arbitrary elastic modulus, E, and the failure extension values, ε_{gc} and ε_{gg}. On the other hand, the model does predict some structure in the delamination force curve over the range of diameters that is completely absent from the experimental results. Clearly the simple spring model fails to give a complete description of microgel adhesion. An implied assumption of the model is that microgels completely swell when the laminate is soaked in water for adhesion testing. Complete reswelling may not occur because of new cross-link formation by a process described in the next section.

DISCUSSION

Never-dried cellulose adhesion is an unmet need. For example, breaks in the wet paper sheet during the papermaking process are a consequence of low adhesion forces between wet cellulose fibers. Currently there is no commercial water-soluble polymer adhesive that can significantly increase the strength of a never-dried sheet of wet paper made with untreated, conventional wood pulp fibers. Adhesion between cellulose surfaces in the presence of water is difficult to promote because cellulose is hydrophilic and offers little functionality for adhesive interaction. The physical adsorption of cationic water-soluble polymers onto untreated cellulose fibers, for example, does not give significant wet adhesion. Chemical bonds or very substantial physical bonding are required.

Herein we have demonstrated a novel, two-step approach consisting of cellulose oxidation followed by the application of hydrazide-microgels, resulting in significant adhesion between never-dried, wet cellulose surfaces. This approach exploits the well documented ability of hydrazide to form hydrazone linkages with aldehydes in water.[9] Over the years we have explored many polymer approaches to never-dried adhesion. On the basis of our experience, only two systems compared favorably with AMP-H as a never-dried adhesive: (1) polyvinylamine with pendant phenylboronate moieties at pH > 8[15] and (2) cellulose with a surface layer of grafted carboxymethyl cellulose and laminated with polyvinylamine.[17]

Two features of once-dried wet adhesion results require comment. First, the amphoteric hydrazide microgels gave strong joints (up to 30 N/m, Figure 3); however, we have seen similar results applying either commercial PAE or PVAm to oxidized cellulose surfaces. Hydrazide-hydrazone chemistry offers little advantage for dried joints, whereas hydrazide functionalized polymers are most promising as never-dried adhesives.

Second, we anticipated that multiple layers of hydrazide microgels would give weak joints, particularly when never dried because the microgel dispersions are colloidally stable, indicating microgel/microgel repulsion. However, our expectation of low microgel/microgel adhesion was incorrect. In our experiments, we controlled the coverage (dry microgel mass/area), and we calculated the corresponding number of microgel layers based on the coverage and microgel water-swollen diameter. There are many examples in our results where joints with multiple microgel layers gave strong adhesion. For example, the experimental data in Figure 6 shows strong joints when the coverage, Γ, is greater than Γ_{sat}, the coverage giving two layers of microgels in the joint. The role of microgel/microgel adhesion is further illustrated in the model curves. The red curve shows that in the case where microgel/microgel adhesion is low, the delamination force plummets once the coverage exceeds a single layer of microgels in the joint (i.e., $\Gamma = \Gamma_{sat}/2$). Other examples of experimental adhesion increasing above a monolayer coverage for never-dried laminates are given in Figures S3 and S4.

In a related observation, hydrazide microgels dried at room temperature did not redisperse as individual microgels (Figure S7). Taken as a whole, these results suggest that when the hydrazide microgels are forced together, covalent microgel/

microgel linkages are formed. Based on Lyon's work,[31] we propose that our hydrazide-microgels also contained low contents of residual NHS esters. If a surface hydrazide group on one microgel displaces a NHS ester on the surface of a neighboring microgel, the result would be a covalent linkage between the neighboring microgels, based on the chemistry shown in Figure 1A.

Finally, we employed microgels as the polymeric support for evaluating the potential of hydrazide chemistry in wet cellulose adhesion. From a mechanistic perspective, the microgels are attractive because: we can control their size and composition, we can assemble microgels on surfaces in well-defined layers; we can interpret our results in terms of the microgel peeling model previously developed; and, when adhesive is applied to cellulose surfaces by adsorption from dilute solution, saturated layers of adsorbed microgels contain far more material compared to a saturated adsorbed layer of linear polymer.[2] Nevertheless, hydrazide-based adhesives do not have to be microgels. Linear or branched hydrazide copolymers should also spontaneously form covalent linkages between cellulose surfaces in water.

CONCLUSIONS

In this Research Article, we demonstrate a new method for obtaining never-dried adhesion between wet oxidized cellulose surfaces without a drying or curing step. Our main conclusions are as follows: (1) Hydrazide-microgels with a net cationic charge gave significant never-dried adhesion between oxidized cellulose surfaces due to the formation of hydrazone covalent linkages. This is one of only three chemistries we found that gives significant never-dried adhesion between wet cellulose surfaces—the other two approaches are cellulose-*g*-CMC + PVAm,[17] and PVAm with pendant phenylboronic acid groups.[15] (2) For joints that have been dried, hydrazide-microgels offer no advantage compared to treating oxidized cellulose with conventional wet strength resin (PAE) or with PVAm. (2) The design rules for the hydrazide-microgels include: cationic microgels are superior to anionic gels; the lower the microgel cross-link density, the higher the adhesion; longer PEG-based hydrazide tethers offer no advantage over shorter attachments; and, adhesion is independent of microgel diameter. Many of these rules were in agreement with predictions of a simple adhesion model where the microgels were assumed to be ideal springs. (4) An unresolved mechanistic question is the origin of the high microgel/microgel cohesion within the adhesive joints based on hydrazide-microgels. We speculate that residual NHS ester groups near the surface of hydrazide-microgels serve as reaction sites, leading to interparticle coupling of hydrazide and carboxyl groups.

ASSOCIATED CONTENT

Supporting Information

The Supporting Information is available free of charge on the ACS Publications website at DOI: 10.1021/acsami.7b04700.

Detailed description of the delamination model (PDF)

Microgel preparation and characterization details, additional adhesion data, photographs illustrating the delamination radius, and example analysis of the potentiometric titrations (PDF)

AUTHOR INFORMATION

Corresponding Author

*E-mail: peltonrh@mcmaster.ca.

ORCID

Robert H. Pelton: 0000-0002-8006-0745

Notes

The authors declare no competing financial interest.

ACKNOWLEDGMENTS

BASF Canada is acknowledged for funding this project through a grant to R.P. entitled "Understanding Cellulose Interactions with Reactive Polyvinylamines". R.P. thanks Prof. Todd Hoare for introducing us to hydrazide−hydrazone chemistry. Some measurements were performed in the McMaster Biointerfaces Institute funded by the Canadian Foundation for Innovation. R.H.P. holds the Canada Research Chair in Interfacial Technologies.

REFERENCES

(1) Pelton, R. Temperature-Sensitive Aqueous Microgels. *Adv. Colloid Interface Sci.* **2000**, *85*, 1−33.

(2) Wen, Q.; Pelton, R. Microgel Adhesives for Wet Cellulose − Measurements and Modeling. *Langmuir* **2012**, *28*, 5450−5457.

(3) Wen, Q.; Pelton, R. Design Rules for Microgel-Supported Adhesives. *Ind. Eng. Chem. Res.* **2012**, *51*, 9564−9570.

(4) Belle, J.; Odermatt, J. Initial Wet Web Strength of Paper. *Cellulose* **2016**, *23*, 2249−2272.

(5) Masiunas, J.; Wahle, E.; Barmore, L.; Morgan, A. A Foam Mulching System to Control Weeds in Tomatoes and Sweet Basil. *HortTechnology* **2003**, *13*, 324−328.

(6) Nakayama, Y. Development of Novel Aqueous Coatings Which Meet the Requirements of Ecology-Conscious Society: Novel Cross-Linking System Based on the Carbonyl−Hydrazide Reaction and Its Applications. *Prog. Org. Coat.* **2004**, *51*, 280−299.

(7) Levrand, B.; Ruff, Y.; Lehn, J.-M.; Herrmann, A. Controlled Release of Volatile Aldehydes and Ketones by Reversible Hydrazone Formation - "Classical" Profragrances Are Getting Dynamic. *Chem. Commun.* **2006**, 2965−2967.

(8) Saito, T.; Isogai, A. Introduction of Aldehyde Groups on Surfaces of Native Cellulose Fibers by TEMPO-Mediated Oxidation. *Colloids Surf., A* **2006**, *289*, 219−225.

(9) Mckinnon, D. D.; Domaille, D. W.; Cha, J. N.; Anseth, K. S. Bis-Aliphatic Hydrazone-Linked Hydrogels Form Most Rapidly at Physiological pH: Identifying the Origin of Hydrogel Properties with Small Molecule Kinetic Studies. *Chem. Mater.* **2014**, *26*, 2382−2387.

(10) Bouhadir, K. H.; Hausman, D. S.; Mooney, D. J. Synthesis of Cross-Linked Poly(Aldehyde Guluronate) Hydrogels. *Polymer* **1999**, *40*, 3575−3584.

(11) Espy, H. H. The Mechanism of Wet-Strength Development in Paper: A Review. *Tappi J.* **1995**, *78*, 90−99.

(12) Laleg, M.; Pikulik, I. I. Wet-Web Strength Increase by Chitosan. *Nord. Pulp Pap. Res. J.* **1991**, *6*, 99−103.

(13) Levy, I.; Nussinovitch, A.; Shpigel, E.; Shoseyov, O. Recombinant Cellulose Crosslinking Protein: A Novel Paper-Modification Biomaterial. *Cellulose* **2002**, *9*, 91−98.

(14) Sato, T.; Ali, M. M.; Pelton, R.; Cranston, E. D. DNA Stickers Promote Polymer Adsorption onto Cellulose. *Biomacromolecules* **2012**, *13*, 3173−3180.

(15) Chen, W.; Leung, V.; Kroener, H.; Pelton, R. Polyvinylamine-Phenylboronic Acid Adhesion to Cellulose Hydrogel. *Langmuir* **2009**, *25*, 6863−6868.

(16) Laine, J.; Lindstrom, T.; Nordmark, G. G.; Risinger, G. Studies on Topochemical Modification of Cellulosic Fibres Part 1. Chemical Conditions for the Attachment of Carboxymethyl Cellulose onto Fibres. *Nord. Pulp Pap. Res. J.* **2000**, *15*, 520−526.

(17) Gustafsson, E.; Pelton, R.; Wågberg, L. Rapid Development of Wet Adhesion between Carboxymethylcellulose Modified Cellulose Surfaces Laminated with Polyvinylamine Adhesive. *ACS Appl. Mater. Interfaces* **2016**, *8*, 24161−24167.
(18) Patenaude, M.; Smeets, N. M. B.; Hoare, T. Designing Injectable, Covalently Cross- Linked Hydrogels for Biomedical Applications. *Macromol. Rapid Commun.* **2014**, *35*, 598−617.
(19) Freeman, A. Gel Entrapment of Whole Cells and Enzymes in Crosslinked, Prepolymerized Polyacrylamide Hydrazide. *Ann. N. Y. Acad. Sci.* **1984**, *434*, 418−426.
(20) Machida, S. Polyacrylic Hydrazide-a New Wet End Additive. *Tappi* **1969**, *52*, 1734−1738.
(21) Heath, H. D.; Hofreiter, B. T.; Ernst, A. J. Method of Making Nongelling Aqueous Cationic Dialdehyde Starch Compositions. U.S. Patent 4,001,032, 1977.
(22) Lowe, A.; Williams, G. Modification of the Properties of Fibrous Materials. U.S. Patent 2,795,517, 1957.
(23) Billmers, R. L.; Tessler, M. M.; Giudice, D. M. D.; Leake, C. Polysaccharide Derivatives Containing Aldehyde Groups on an Aromatic Ring, Their Preparation from the Corresponding Acetals and Use in Paper. U.S. Patent 4,788,280, November 29, 1988.
(24) Barcus, R. L.; Mohammadi, K. P.; Leimbach, A. M.; Kelly, S. R. Temporary Wet Strength Additives. U.S. Patent 7,691,233 B2, 2010.
(25) Tejado, A.; Antal, M.; Liu, X.; Van De Ven, T. G. M. Wet Cross-Linking of Cellulose Fibers Via a Bioconjugation Reaction. *Ind. Eng. Chem. Res.* **2011**, *50*, 5907−5913.
(26) Hoare, T.; Pelton, R. Charge-Switching, Amphoteric Glucose-Responsive Microgels with Physiological Swelling Activity. *Biomacromolecules* **2008**, *9*, 733−740.
(27) Sivakumaran, D.; Maitland, D.; Oszustowicz, T.; Hoare, T. Tuning Drug Release from Smart Microgel−Hydrogel Composites Via Cross-Linking. *J. Colloid Interface Sci.* **2013**, *392*, 422−430.
(28) Shafer, D. E.; Toll, B.; Schuman, R. F.; Nelson, B. L.; Mond, J. J.; Lees, A. Activation of Soluble Polysaccharides with 1-Cyano-4-Dimethylaminopyridinium Tetrafluoroborate (Cdap) for Use in Protein-Polysaccharide Conjugate Vaccines and Immunological Reagents. II. Selective Crosslinking of Proteins to Cdap-Activated Polysaccharides. *Vaccine* **2000**, *18*, 1273−1281.
(29) Lele, A. K.; Hirve, M. M.; Badiger, M. V.; Mashelkar, R. A. Predictions of Bound Water Content in Poly(N-Isopropylacrylamide) Gel. *Macromolecules* **1997**, *30*, 157−159.
(30) Hoare, T.; Mclean, D. Kinetic Prediction of Functional Group Distributions in Thermosensitive Microgels. *J. Phys. Chem. B* **2006**, *110*, 20327−20336.
(31) Debord, J. D.; Lyon, L. A. On the Unusual Stability of Succinimidyl Esters in Pnipam-Aac Microgels. *Bioconjugate Chem.* **2007**, *18*, 601−604.

SUPPORTING INFORMATION

Hydrazide-derivatized Microgels Bond to Wet, Oxidized Cellulose Giving Adhesion Without Drying or Curing

Dong Yang,[1] Emil Gustafsson,[1] Taylor C. Stimpson,[1] Anton Esser,[2] and Robert H. Pelton [1]*

[1] Department of Chemical Engineering, McMaster University, 1280 Main St. West, Hamilton, Ontario, Canada L8S 4L7

[2] BASF AG, EVW/MI, 67056 Ludwigshafen, Germany

*R. Pelton: peltonrh@mcmaster.ca

Table S1 Recipes for anionic poly(NIPAM-co-AA) microgel preparation.

Microgel	mmol in 100 mL solution				
	NIPAM	MBA	AA	APS	SDS
A1	4.13	0.22	0.62	0.15	0.02
A2	4.13	0.22	0.62	0.15	0.08
A3	4.13	0.22	0.62	0.15	0.17
A4	4.13	0.22	0.62	0.15	0.33
A5	4.13	0.66	0.62	0.15	0.04
A6	4.13	0.44	0.62	0.15	0.06
A7	4.13	0.06	0.62	0.15	0.10
A8	4.13	0.02	0.62	0.15	0.11

Table S2 Recipes for amphoteric poly(NIPAM-AA-DMAEMA) microgel preparation.

Microgel	mmol in 100 mL solution					
	NIPAM	MBA	AA	DMAEMA	AAPH	CTAB
AMP	4.13	0.22	0.62	0.08	0.20	0.01
AMP1	4.13	0.22	0.44	0.25	0.20	0.01

Table S3 Properties of the unmodified poly(NIPAM-co-AA) starting microgels.

Designation	MBA/NIPAM (mol%)	Diameter (nm)	PDI	Electrophoretic mobility (10^{-8} m^2/Vs)	Carboxyl Equivalent Wt. (Da)
A1	5.3	1048±36	0.06	-2.53±0.09	612±25
A2	5.3	458±14	0.05	-2.86±0.05	665±32
A3	5.3	283±8	0.08	-2.31±0.12	704±29
A4	5.3	98±22	0.42	-1.88±0.08	747±23
A5	16.0	587±21	0.14	-2.58±0.02	615±21
A6	10.7	482±3	0.03	-2.73±0.08	624±30
A7	1.5	465±6	0.16	-2.17±0.10	697±47
A8	0.5	436±23	0.33	-1.95±0.05	722±35
AMP	5.3	246±11	0.20	-1.98±0.06	-
AMP1	5.3	157±18	0.29	-1.17±0.12	-

Table S4 Conditions for microgel hydrazide derivatization.

Microgel	Starting microgel	Microgel (mg)	EDC (mg)	NHS (mg)	ADH (mg)	Dihydrazide PEG (mg)
A1-H31	A1	120	187.2	56.4	170.9	-
A2-H75	A2	120	187.2	56.4	170.9	-
A2-H62	A2	120	124.8	37.6	113.9	-
A2-H45	A2	120	62.4	18.8	57.0	-
A2-H28	A2	120	31.2	9.4	28.5	-
A2-H19	A2	120	9.4	2.8	8.5	-
A2-H7	A2	120	4.7	1.4	4.3	-
A2-HPEG12	A2	120	15.6	4.7	-	81.8
A2-HPEG31	A2	120	31.2	9.4	-	163.5
A3-H30	A3	120	187.2	56.4	170.9	-
A4-H38	A4	120	124.8	37.6	113.9	-
A5-H72	A5	120	124.8	37.6	113.9	-
A6-H72	A6	120	187.2	56.4	170.9	-
A7-H68	A7	120	187.2	56.4	170.9	-
A8-H75	A8	120	124.8	37.6	113.9	-
AMP-H	AMP	120	187.2	56.4	170.9	-
AMP1-H	AMP	120	187.2	56.4	170.9	-

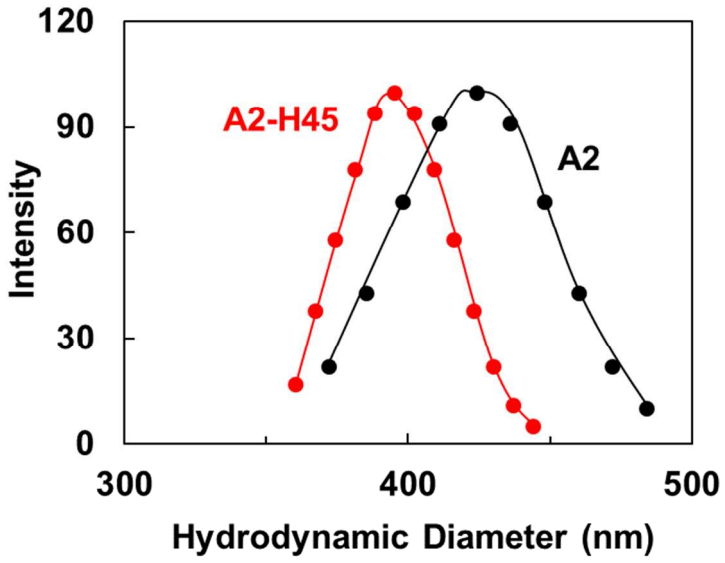

Figure S1 Particle size distributions of supporting microgel (A2) and hydrazide microgel (A2-H45) obtained by dynamic light scattering. Measurements were made in 1mM NaCl at neutral pH. Losing charge groups caused the microgels to shrink. There was no evidence of aggregation.

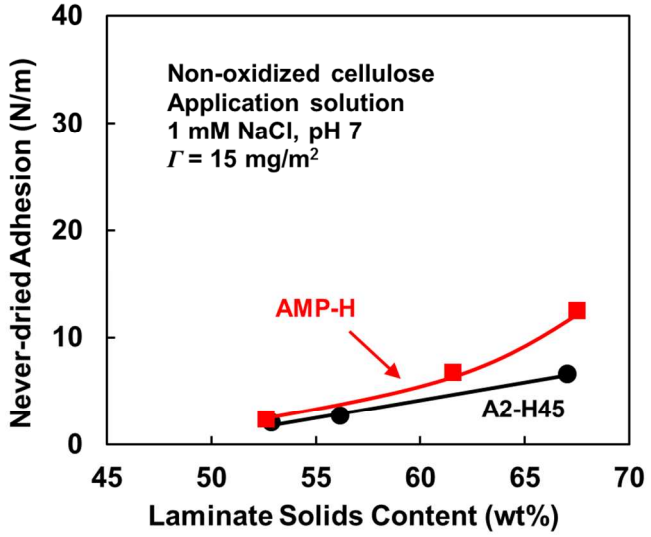

Figure S2 Never-dried adhesion of non-oxidized cellulose membranes laminated with hydrazide-microgels. The of number of layers of microgels in the laminate joint was 0.9 for A2-H45 and 1.4 for AMP-H. The never-dried adhesion of

microgels with non-oxidized cellulose was much lower than that with TEMPO oxidized cellulose, as shown in Figure 2. Hydrazone bonds did not form with cellulose that was not oxidized, and the adhesion was low.

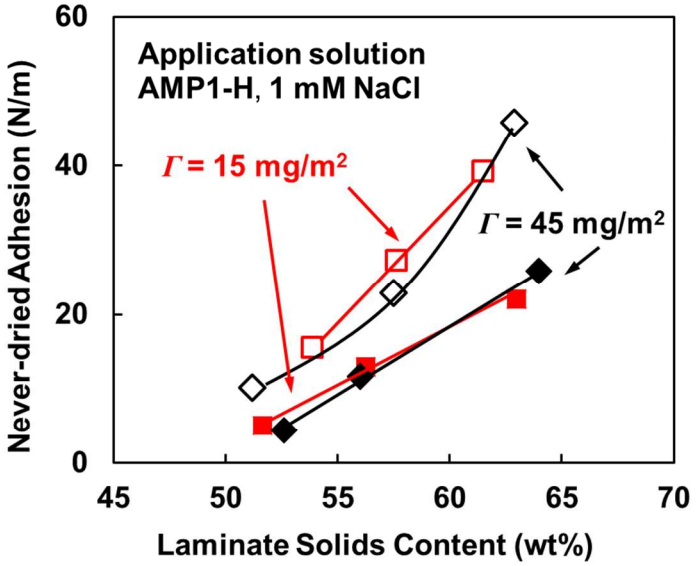

Figure S3 Never-dried adhesion of hydrazide-amphoteric microgel AMP1-H. Hollow symbols represent laminates prepared at pH 4.1 and solid ones represent pH 7. The corresponding of number of layers of microgels in the laminate joint was 2.0 for $\Gamma = 15$ mg/m^2 and 6.0 for $\Gamma = 45$ mg/m^2. The never-dried adhesion did not change over the range 2 to 6 microgel layers.

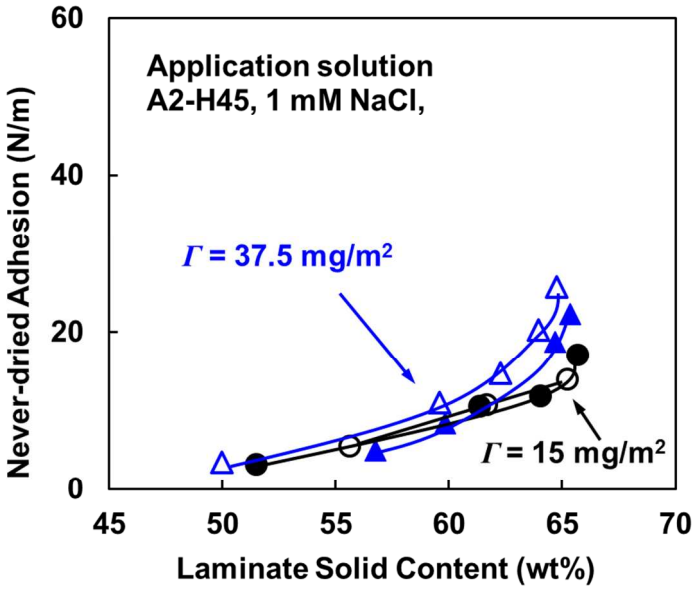

Figure S4 Never-dried adhesion of hydrazide-anionic microgel A2-H45. Hollow symbols represent laminates prepared at pH 4.1 and solid ones represent pH 7. The corresponding number of layers of microgels in the laminate joint was 0.9 for $\Gamma = 15$ mg/m^2 and 2.2 for $\Gamma = 37.5$ mg/m^2. Adhesion was sensitive to coverage of A2-H45 microgels for partially dried laminates.

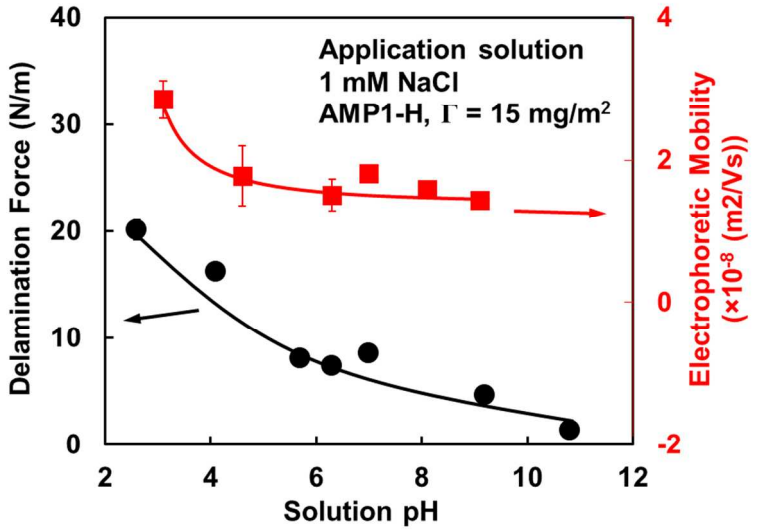

Figure S5 Once-dried wet adhesion (black) and electrophoretic mobility (red) of hydrazide-amphoteric microgel AMP1-H. The number of layers of microgels in the laminate joint was 2.0. The once-dried wet adhesion was stronger when the microgels were positively charged

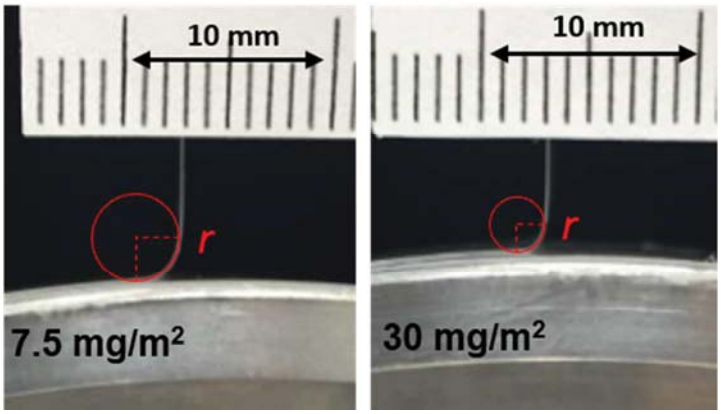

Figure S6 Photographs illustrating the peel radius of curvature. The lower the adhesive coverage, the lower the strength and the greater the resulting peel radius of curvature.

Figure S7 Microgel dispersions in 1 mM NaCl solution at pH ~7 prepared from room temperature dried powder. The photograph was taken one week after dispersion in water. The hydrazide microgels never fully dispersed.

Dong-Pelton 2017 Extending our original model (Wen 2010) by accounting for the variation of peel angle with peel force and by including gel-gel cohesion

Microgel Swelling and Packing Properties

$D := 372 \cdot nm$ Microgel diameter, at 25C A2-H62

$Dh := 179\ nm$ Microgel diameter T > VPTT

$r_w := 0.4$ Water mass /polymer mass in dehydrated gels, Dong Hoffman in Lele Macromolecules 1997, 30, 157

$\rho_p := \frac{1}{0.902}\ \frac{gm}{mL}$ Density of pnipam at 33 C Heskins and Guillet

$\rho_w := 0.9832 \cdot \frac{gm}{mL}$ Water density 60 C

Dry mass of a microgel particle

$$M_g(D, Dh) := \frac{\pi}{6} \cdot Dh^3 \cdot \frac{\rho_p \cdot \rho_w}{\rho_w + \rho_p \cdot r_w} \cdot (Dh > 0\ nm) + \frac{\pi}{6} \cdot D^3 \cdot 0.085\ \frac{gm}{mL} \cdot (Dh \le 0\ nm)$$

If Dh is unknown, it is set to zero and the polymer density in the swollen microgel is assumed equal to 0.085 gm/mL

$M_g(D, Dh) = (2.2944 \cdot 10^{-12})\ mg$ $M_g(D, 0\ nm) = (2.2911 \cdot 10^{-12})\ mg$

$MW := M_g(D, Dh) \cdot N_A = (1.3817 \cdot 10^9)\ Da$ Microgel MW 1000 greater than typical linear PNIPAM or PAM

$$\rho(D, Dh) := \frac{M_g(D, Dh)}{\frac{\pi}{6} \cdot D^3}$$

Polymer density in swollen gels. If Dh is not available, it is set to zero

Amp-H39

$\rho(D, Dh) = 0.0851\ \frac{gm}{mL}$ $\rho(187\ nm, 96\ nm) = 0.1034\ \frac{gm}{mL}$

$f_m := 0.82$ Maximum microgel packing fraction on a surface - random, non-overlaping circles

Structure of the Joint

$\Gamma := 15\ \frac{mg}{m^2}$ Coverage of adhesive in the joint between cellulose membranes

$$\Gamma_{sat}(D, Dh) := \frac{4}{3} \cdot D \cdot \rho(D, Dh) \cdot f_m$$

This is the dry mass coverage of microgel giving two layers of spheres in the joint, **Wen eq. 1,** if we do not have Dh values, set Dh =0nm

$$n_{max}(D) := \frac{f_m}{\pi \cdot \left(\frac{D}{2}\right)^2}$$

This is the number density of spheres in a single layers of gels **Wen eq. 7**

$$\Gamma_{sat} = 2\left(\frac{2}{3} D \rho \lambda_m\right) = 38 \frac{mg}{m^2} \quad (1)$$

$$n_{max} = \frac{4}{\pi D^2} \lambda_m \quad (7)$$

$$n(D, Dh, \Gamma) := \frac{\Gamma}{M_g(D, Dh)}$$

Density of microgels in the joint. **Note this definition differs from n in the Wen paper** where n was the density of springs (gels) in contact with one of the cellulose surfaces in the laminate, defined as:

$$n = 2\frac{\Gamma}{\Gamma_{sat}} n_{max} = \frac{\Gamma}{\Gamma_{sat}} \frac{8}{\pi D^2} \lambda_m \quad \text{for } \Gamma/\Gamma_{sat} < 0.5$$

$$n = n_{max} = \frac{4}{\pi D^2} \lambda_m \quad \text{for } \Gamma/\Gamma_{sat} \ge 0.5 \quad (8)$$

The following function gives the Wen n value calculated in eq 8

$$n_{wen}(D, Dh, \Gamma) := n_{max}(D) \left(\frac{\Gamma}{\Gamma_{sat}(D, Dh)} \ge 0.5\right) + 2 \cdot \frac{\Gamma}{\Gamma_{sat}(D, Dh)} \cdot n_{max}(D) \cdot \left(\frac{\Gamma}{\Gamma_{sat}(D, Dh)} < 0.5\right)$$

$$NL(D, Dh, \Gamma) := \left(\frac{n(D, Dh, \Gamma)}{n_{max}(D)}\right)$$

Number of layers of microgels in the joint,

$NL(D, Dh, \Gamma_{sat}(D, Dh)) = 2$

$L_o(D, Dh, \Gamma) := D \cdot NL(D, Dh, \Gamma)$ The thickness of the water swollen joint, Wen eq. 9

$$Lo = D \cdot NL = D \cdot \frac{n}{n_{max}} = D \cdot \frac{\frac{\Gamma}{Mg}}{\frac{4 \cdot fm}{\pi D^2}} = D \cdot \frac{\frac{\Gamma}{k \cdot D^3}}{\frac{4 \cdot fm}{\pi D^2}} = D \cdot \frac{\frac{\Gamma}{k \cdot D}}{\frac{4 \cdot fm}{\pi}} = \frac{\frac{\Gamma}{k}}{\frac{4 \cdot fm}{\pi}}$$

Lo is independent of D if Γ is constant

For the new modeling, we consider two types of microgels in the laminate. Type **gc** gels adhere to both cellulose films. Type gc gels can only be present if the total microgel coverage in the joint is less than two monolayers

Type **gg** gels are present in a stack of two or more gels in the z direction. Type gg gels can have both gel/cellulose bonds and gel/gel bonds - the weaker type will break first.

Brown is cellulose film
Pink gels are type gg
Green gel is type gc

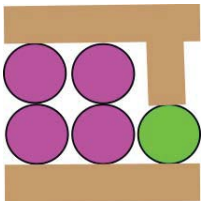

Coverage of gc gels, only contacting two cellulose surfaces

$$n_{gc}(D,Dh,\Gamma) := n(D,Dh,\Gamma)\cdot(NL(D,Dh,\Gamma)<1)+(1<NL(D,Dh,\Gamma)<2)\cdot(n_{max}(D)\cdot(2-NL(D,Dh,\Gamma)))$$

$$n_{gg}(D,Dh,\Gamma) := n(D,Dh,\Gamma)-n_{gc}(D,Dh,\Gamma)$$

Coverage of gg microgels present in z-direction stacks with both gel/gel and gel cellulose bonds in the stack

Summarizing structural parmeters

	Γ / Γ_{sat}	NL = n/n_{max} = Lo/D	n_{gc}/n_{max}	n_{gg}/n_{max}	S_{gg}/ n_{max}
	2/6	2/3	2/3	0/3	0
	3/6	1	3/3	0/3	0
	5/6	5/3	1/3	4/3	(3-1)/3 = 2/3
	6/6	6/3	0/3	6/3	3/3
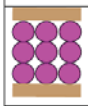	9/6	9/3	0/3	9/3	3/3

Γ mass coverage of dry microgels (mg/m2)

Γ_{sat} mass coverage corresponding to two monolayers in joint

NL is the number of layers

nmax number density of a single layer of gels (1/m2)

ngc is the number density of gc type gels

ngg is the number density

Sgg number density of gel stacks containing more than 1 gel

Lo is the thickness of the gel layer in the joint

$\Gamma\Gamma := 1 \frac{mg}{m^2}, 2 \frac{mg}{m^2} .. 70 \frac{mg}{m^2}$

Illustrating the contributions of various types of gels as a function of coverage

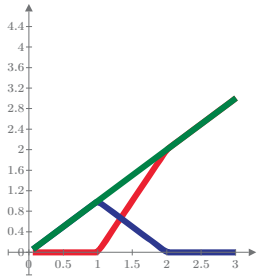

$NL(D, Dh, \Gamma\Gamma)$

Number of layers

Coverage/monolayer coverage

$\frac{n_{gg}(D, Dh, \Gamma\Gamma)}{n_{max}(D)}$

Coverage of type gg gels divided by monolayer coverage

$\frac{n_{gc}(D, Dh, \Gamma\Gamma)}{n_{max}(D)}$

Coverage type gc gel divided by monolayer coverage

$\frac{n(D, Dh, \Gamma\Gamma)}{n_{max}(D)}$

Total microgel coverage divided by monolayer coverage

Our modeling treats the joint as a set of vertical springs formed by stacks of microgels.
For the force calculation we need the density of springs.

$S_{gc}(D, Dh, \Gamma) := n_{gc}(D, Dh, \Gamma)$

Density of springs, consisting of single microgels adsorbed on both films

$S_{gg}(D, Dh, \Gamma) := (n_{max}(D) - n_{gc}(D, Dh, \Gamma)) \cdot (NL(D, Dh, \Gamma) > 1)$

Density of springs with two or more stacked microgels

Corresponding spring densities

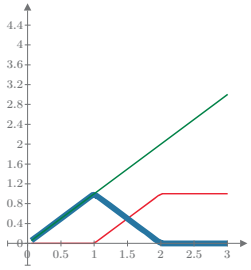

$NL(D, Dh, \Gamma\Gamma)$

$\frac{S_{gg}(D, Dh, \Gamma\Gamma)}{n_{max}(D)}$

$\frac{S_{gc}(D, Dh, \Gamma\Gamma)}{n_{max}(D)}$

$\frac{n(D, Dh, \Gamma\Gamma)}{n_{max}(D)}$

NL - number of microgel layers

n - the total microgel coverage in the laminate, m-2

ngg - the number density of microgels present as stacks of two or more gels in the z direction

Sgg - the density of stacks of gels with two or more stacked gels in the z direction

nmax - the number density corresponding to a monolayer of gels on a surface

Mechanical properties of microgels

$E := 100 \cdot kPa$ Elastic modulus of microgel,

$\varepsilon_m := 5$ Microgel strain at break, Wen-Pelton model

ε_{gc} Gel/cellulose strain at break, Dong-Pelton model

ε_{gg} Gel/gel strain at break

$k_{mg}(E, D) := E \cdot \pi \cdot \left(\frac{D}{2}\right)^2$ Hooke's law spring constant, Wen eq. 5

Case 1 - the Wen-Pelton model

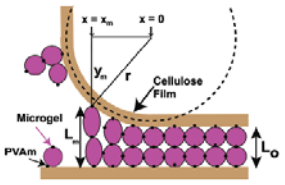

Figure 4. A schematic illustration of the peel front in our delamination experiments. The microgels are treated as ideal springs and the PVAm as stickers that fail at a critical stress.

Illustrating the model parameters originally described in Quan Wen; Robert Pelton, Microgel Adhesives for Wet Cellulose – Measurements and Modeling. *Langmuir* **2012,** *28* (12), 5450–5457

$r := 2\ mm$ Peel front radius, a variable

$x_m(D, Dh, \Gamma, r, \varepsilon_m) := \sqrt{r^2 - (r - \varepsilon_m \cdot L_o(D, Dh, \Gamma))^2}$ Length of zone with elongated springs, **Wen eq.11**

$F_p(D, Dh, \Gamma, r, \varepsilon_m, E) := \frac{n_{wen}(D, Dh, \Gamma) \cdot k_{mg}(E, D)}{L_o(D, Dh, \Gamma)} \cdot \int_{0 \cdot m}^{x_m(D, Dh, \Gamma, r, \varepsilon_m)} r - \sqrt{r^2 - x^2}\ dx$ Peel force, **Wen eq. 6**

Accounting for Variable Peel Angle

In our original work we assumed a constant value for r when varying coverage or other parameters. However, we know from observation that r gets larger as F gets smaller. This is a problem in mechanics that involves the membrane properties. **Herein, we assume that for our standard membrane with a given water content, there is a unique relationship between F and r.** .

$r_e(F) := 4.07 \cdot e^{-0.064 \frac{F}{\frac{N}{m}}}\ mm$ Fit of experimental data

$F_e(r) := \frac{\ln\left(\frac{r}{mm \cdot 4.07}\right)}{-0.064} \cdot \frac{N}{m}$ inverse of fit function

$F_e(2\ mm) = 11.1015\ \frac{N}{m}$ $r_e\left(22\ \frac{N}{m}\right) = 0.9957\ mm$

Experimental relation between F and r

$PFe := \begin{bmatrix} 3.37 \\ 10.9 \\ 13.7 \\ 22.0 \\ 25.5 \end{bmatrix} \cdot \frac{N}{m}$ $Ra := \begin{bmatrix} 3.45 \\ 2.175 \\ 1.425 \\ 0.95 \\ 0.875 \end{bmatrix} \cdot mm$

$FF := 1\ \frac{N}{m}, 2\ \frac{N}{m} .. 50\ \frac{N}{m}$

Figure 5A

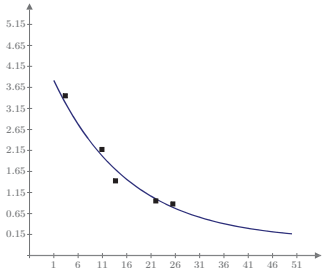

$\frac{r_e(FF)\ (mm)}{Ra\ (mm)}$

$\frac{FF\ \left(\frac{N}{m}\right)}{PFe\ \left(\frac{N}{m}\right)}$

Here we show peel radius, r, as a function of peel force. The experimental points and fit were from Dong Yang

$r_r(D, Dh, \Gamma, \varepsilon_m, E) := \mathbf{root}(r_e(F_p(D, Dh, \Gamma, r, \varepsilon_m, E)) - r, r)$ Using the solver to find r value for Wen model parameters

$r_r(D, Dh, \Gamma, \varepsilon_m, E) = 2.1622\ mm$

Corresponding force

$F_r(D, Dh, \Gamma, \varepsilon_m, E) := F_e(r_r(D, Dh, \Gamma, \varepsilon_m, E))$

$F_r(D, Dh, \Gamma, \varepsilon_m, E) = 9.8834\ \frac{kg}{s^2}$

$\Gamma\Gamma := 1\ \frac{mg}{m^2}, 2\ \frac{mg}{m^2} .. 50\ \frac{mg}{m^2}$

Black line uses experimental r versus Fp function
Red line is the old model, where r is assumed constant

Not a big difference

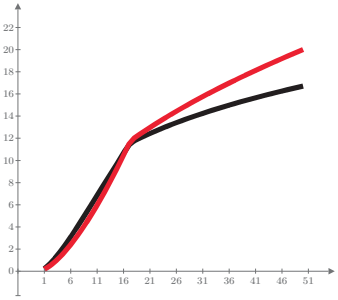

$\frac{F_r(D, Dh, \Gamma\Gamma, \varepsilon_m, E)}{F_p(D, Dh, \Gamma\Gamma, r, \varepsilon_m, E)} \left(\frac{kg}{s^2}\right)$

$\frac{\Gamma\Gamma}{\frac{mg}{m^2}}$

$D = 372\ nm$
$Dh = 179\ nm$
$\varepsilon_m = 5$
$r = 2\ mm$
$E = (1 \cdot 10^5)\ Pa$

Figure 5B

Yang-Pelton model - Expanding model to account for separate mg/mg and mg/cellulose adhesion

$\varepsilon_{gg} := 1.5$ Extension to break gel/gel bonds

$\varepsilon_{gc} := 5$ Extension to break gel/cellulose bonds

Calculating peel force when we know r

$$F_{p2}(E, D, Dh, \Gamma, r, \varepsilon_{gg}, \varepsilon_{gc}) := \frac{k_{mg}(E, D)}{L_o(D, Dh, \Gamma)} \cdot \left(S_{gg}(D, Dh, \Gamma) \cdot \int_{0 \cdot m}^{x_m(D, Dh, \Gamma, r, \min(\varepsilon_{gg}, \varepsilon_{gc}))} r - \sqrt{r^2 - x^2}\ dx + S_{gc}(D, Dh, \Gamma) \cdot \int_{0 \cdot m}^{x_m(D, Dh, \Gamma, r, \varepsilon_{gc})} r - \sqrt{r^2 - x^2}\ dx \right)$$

gg contribution **gc contribution**

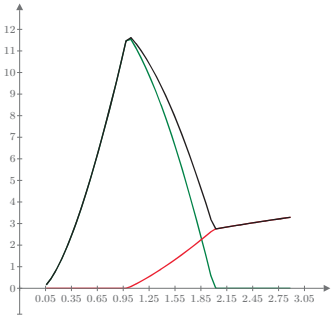

$NL(D, Dh, \Gamma\Gamma)$

Number of microgel layers in laminate

$\frac{k_{mg}(E, D)}{L_o(D, Dh, \Gamma\Gamma)} \cdot S_{gc}(D, Dh, \Gamma\Gamma) \cdot \int_{0 \cdot m}^{x_m(D, Dh, \Gamma\Gamma, r, \varepsilon_{gc})} r - \sqrt{r^2 - x^2}\ dx \left(\frac{N}{m}\right)$

contribution of gc microgels bridging both membranes

$\frac{k_{mg}(E, D)}{L_o(D, Dh, \Gamma\Gamma)} \cdot S_{gg}(D, Dh, \Gamma\Gamma) \cdot \int_{0 \cdot m}^{x_m(D, Dh, \Gamma\Gamma, r, \min(\varepsilon_{gg}, \varepsilon_{gc}))} r - \sqrt{r^2 - x^2}\ dx \left(\frac{N}{m}\right)$

contribution of gg stacked gel where the weaker of gel/cel or gel/gel breaks

$F_{p2}(E, D, Dh, \Gamma\Gamma, r, \varepsilon_{gg}, \varepsilon_{gc}) \left(\frac{kg}{s^2}\right)$

Total peel force

In the above calculation, the peel radius is assumed constant. The next page accounts for variable peel radius

Using solver to find peel force and corresponding peel radius, r

$$r_{rr}(E,D,Dh,\Gamma,\varepsilon_{gg},\varepsilon_{gc}) := \text{root}\left(r_e\left(F_{p2}(E,D,Dh,\Gamma,r,\varepsilon_{gg},\varepsilon_{gc})\right)-r,r\right)$$

$$F_{pr}(E,D,Dh,\Gamma,\varepsilon_{gg},\varepsilon_{gc}) := F_e\left(r_{rr}(E,D,Dh,\Gamma,\varepsilon_{gg},\varepsilon_{gc})\right)$$

Corresponding force, this function accounts for gel/cellulose and ge/gel adhesion through the extensions at break

Figure 6

Influence of coverage

$Dh = 179\ nm$

$\Gamma\Gamma := 1\ \frac{mg}{m^2}, 2\ \frac{mg}{m^2} .. 100\ \frac{mg}{m^2}$ $\quad \varepsilon_{gc} := 10.5$ $\quad D = 372\ nm$ $\quad E = (1\cdot 10^5)\ Pa$

$\Gamma_{sat}(D,Dh) = 34.6211\ \frac{mg}{m^2}$

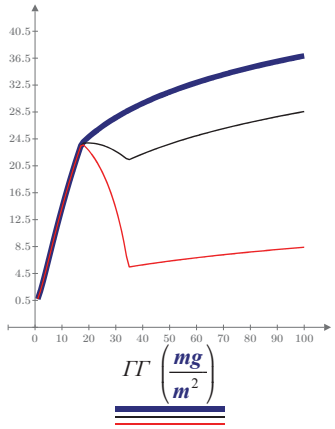

$\Gamma\Gamma\ \left(\frac{mg}{m^2}\right)$

$F_{pr}(E,D,Dh,\Gamma\Gamma,\varepsilon_{gc}\cdot 1,\varepsilon_{gc})\ \left(\frac{kg}{s^2}\right)$

$F_{pr}(E,D,Dh,\Gamma\Gamma,\varepsilon_{gc}\cdot 0.7,\varepsilon_{gc})\ \left(\frac{kg}{s^2}\right)$

$F_{pr}(E,D,Dh,\Gamma\Gamma,\varepsilon_{gc}\cdot 0.2,\varepsilon_{gc})\ \left(\frac{kg}{s^2}\right)$

The model most closely corresponds to the experimental if the gel/gel bonds are slightly weaker than the gel/cellulose bonds

Influence of microgel Modulus

$\varepsilon_{gg} := 0.7\cdot\varepsilon_{gc}$ $\quad \varepsilon_{gc} = 10.5$ $\quad E = 100\ kPa$

$jj := -1.1, -1 .. 0.6$ $\quad D = 372\ nm$ $\quad \Gamma = 15\ \frac{mg}{m^2}$

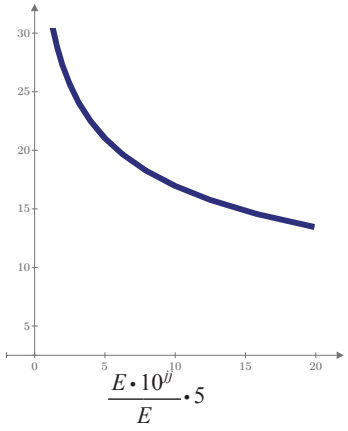

$\frac{E\cdot 10^{jj}}{E}\cdot 5$

$F_{pr}\left(E\cdot 10^{jj}, D, Dh, \Gamma, \frac{\varepsilon_{gg}}{10^{jj}}, \frac{\varepsilon_{gc}}{10^{jj}}\right)\ \left(\frac{N}{m}\right)$

In this plot we vary D and the ε values in opposite ways because adhesion forces between the gel and surface is proportional to the product Dε **- see the Wen papers for equations.**

Figure 7

Variation of microgel diameter, assuming constant swollen density

$\varepsilon_{gc} = 10.5$

$dd := 50\ nm, 75\ nm .. 900\ nm$ $\quad \varepsilon_{gg} := 0.7\ \varepsilon_{gc}$ $\quad E = 100\ kPa$ $\quad \Gamma = 15\ \frac{mg}{m^2}$

$F_{pr}(E, D, Dh, \Gamma, \varepsilon_{gg}, \varepsilon_{gc})$

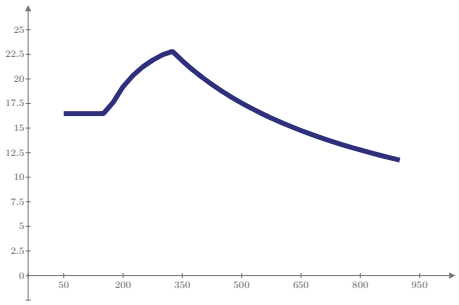

$F_{pr}(E, dd, 0\ nm, \Gamma, \varepsilon_{gg}, \varepsilon_{gc})\ \left(\frac{kg}{s^2}\right)$

$d := nm$

$\frac{dd}{nm}$

root$(NL(d, 0\ nm, \Gamma) - 1, d) = 322.8121\ nm$

root$(NL(d, 0\ nm, \Gamma) - 2, d) = 161.406\ nm$

Figure 9

Number of layers versus the microgel diameter

$NL(dd, 0\ nm, \Gamma)$

2

1

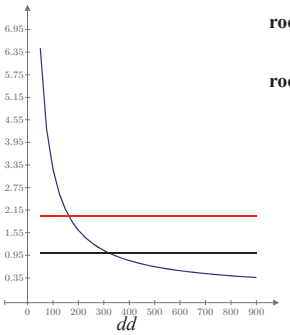

$\frac{dd}{nm}$

The goal of this calculation is to derive the relationship between microgel hydrazide DS and the titration results

Carboxyl content of starting microgels

$$EW_o = \frac{m_o}{n_{cooh}}$$

EW_o is equivalent wt.of starting microgel

m_o is the mass of dry microgel titrated

n_{cooh} is mols of COOH titrated

rearranging

Eq 1 $$n_{cooh} = \frac{m_o}{EW_o}$$

Charge content of derivatized micogels

Eq 2 $$EW_H = \frac{m_H}{nH_{cooh}}$$

Mass of microgels after hydrazide derivatization

$$m_h = m_o + DS \cdot n_{cooh} \cdot MW_H$$ mass balance

where

Eq 3 $$DS = 1 - \frac{nH_{cooh}}{n_{cooh}}$$ the fraction of carboxyls converted to hydrazides

nH_{cooh} is the carboxyl content after derivatization

MW_H molecular weight increase per added hydrazide

substituting Eq 1

Eq 4 $$m_h = m_o + DS \cdot \frac{m_o}{EW_o} \cdot MW_H = m_o\left(1 + DS \cdot \frac{MW_H}{EW_o}\right)$$

Charge content of derivatized micogels

Eq 2 $$EW_H = \frac{m_H}{nH_{cooh}}$$

rearranging Eq 3

Eq 5 $$DS = 1 - \frac{nH_{cooh}}{n_{cooh}} \xrightarrow{solve,\, nH_{cooh}} -\left(n_{cooh} \cdot (DS - 1)\right)$$

substituting into Eq 5 into Eq 2

$$EW_H = \frac{m_H}{n_{cooh} \cdot (1 - DS)}$$

substituting Eq 1

$$EW_H = \frac{m_H}{\frac{m_o}{EW_o} \cdot (1 - DS)}$$

substituting Eq 4

$$EW_H = \frac{m_o\left(1 + DS \cdot \frac{MW_H}{EW_o}\right)}{\frac{m_o}{EW_o} \cdot (1 - DS)} = \frac{EW_o\left(1 + DS \cdot \frac{MW_H}{EW_o}\right)}{(1 - DS)}$$

$$EW_H = \frac{\left(EW_o + DS \cdot MW_H\right)}{(1 - DS)}$$

solving for DS

$$EW_H = \frac{\left(EW_o + DS \cdot MW_H\right)}{(1 - DS)} \xrightarrow{solve,\, DS} \frac{EW_H - EW_o}{EW_H + MW_H}$$

Eq 6 $$DS = \frac{EW_H - EW_o}{EW_H + MW_H}$$

This expression gives the DS as a function of the two experimental equivalent weights.

Determing equivalent weights

The issue is to avoid contributions of the hydrazides tothe titration results.
In this analysis the two main assumptions are:

1) hydrazides make no contribution for pH>4
2) the degree of carboxyl ionization at pH = 4 is the same for both the starting and the final microgels

Figure A, below, show the analysis of the A6 potentiometric titration to give the carboxyl equivalent weight for A6 and α, the degree of ionization of A6 at pH =4

Figure B, shows the corresponding determination of the equivalent wt of microgel A6-H72, EW_o.

Note the x-axis is expressed as moles of NaOH added per mass titrated (~30mg). The x-axis for the blank curve was calculated by dividing the NaOH moles by 30 mg

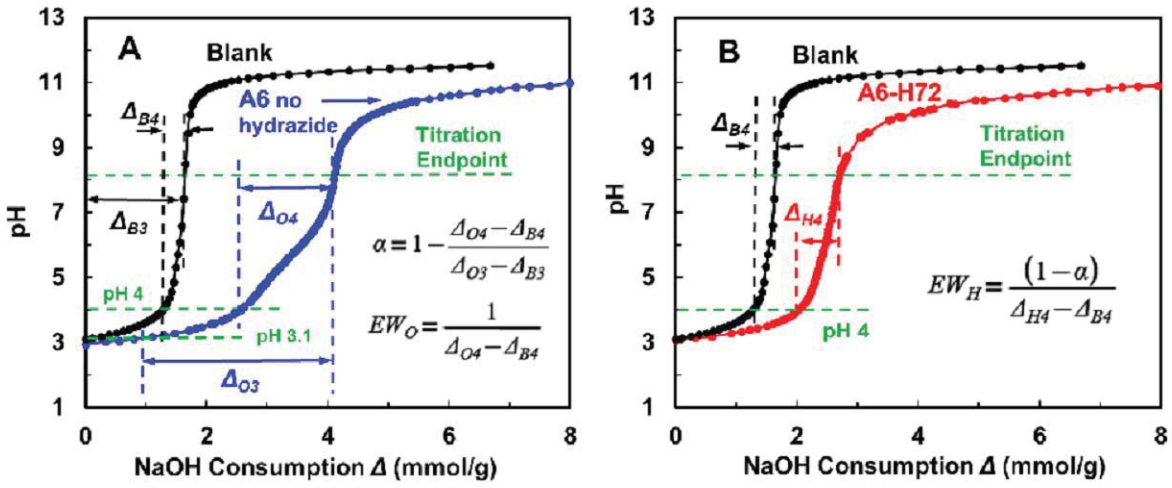

Calculations based on Figure A

Eq 7 $$EW_o = \frac{1}{\Delta_3} = \frac{1}{\Delta_{o3} - \Delta_{B3}}$$

$$EW_o := \frac{1}{(3.313 - 1.656) \cdot \frac{mmol}{gm}} = 603.5003 \ Da$$

Equivalent weight of microgel A6

Eq 8 $$\alpha = 1 - \frac{\Delta_4}{\Delta_3} = 1 - \frac{\Delta_{o4} - \Delta_{B4}}{\Delta_{o3} - \Delta_{B3}}$$

$$\alpha := 1 - \frac{(1.566 - 0.390) \cdot \frac{mmol}{gm}}{(3.313 - 1.656) \cdot \frac{mmol}{gm}} = 0.2903$$

Degree of ionization at pH 4 for microgel A6

Calculations based on Figure B

Eq 9 $$EW_H = \frac{1 - \alpha}{\Delta_{H4}} = \frac{1 - \alpha}{\Delta_{H4} - \Delta_{B4}}$$

Calculating the equivalent weight of hydrazide derivatized microgels from the pH 4 titration data based on α (degree of ionization of carboxyls at pH 4).

$$EW_H := \frac{1 - \alpha}{(0.672 - 0.390) \cdot \frac{mmol}{gm}} = (2.5167 \cdot 10^3) \ Da$$

Equivalent weight of A6-H62

$$MW_H := 156.2 \ Da$$

Molecular weight per hydrazide is MW of ADH minus 1 water molecule

Determining hydrazide DS

$$DS_H := \frac{EW_H - EW_o}{EW_H + MW_H} = 0.7158$$

Applying equation 6. Corresponding DH value using equation 1 from paper.

Chapter 4

Hydrazide-derivatized Microgel Adhesives with Reductant-responsive Degradability

In this chapter, reductant-responsive, hydrazide-derivatized microgels were applied as cellulose wet adhesives providing controllable degradability. Two strategies were used to design the degradable microgels: labile disulfide linkages were synthesized either in the chains tethering the adhesive hydrazide groups or as crosslinks within the microgels. In both scenarios, the cellulose wet adhesion was "switched off" in response to the presence of a reductant. This work was a proof of concept to facilitate the recycling of wet strength paper.

The data within this chapter were collected by me. I summarized the data and wrote the draft myself. Dr. Robert Pelton helped me analyze the results and re-write parts of the draft as necessary.

This chapter and the supporting information are reprinted as it appears in *ACS Sustainable Chemistry & Engineering* with permission from the American Chemical Society.

Degradable Microgel Wet-Strength Adhesives: A Route to Enhanced Paper Recycling

Dong Yang and Robert H. Pelton

ACS Sustainable Chemistry & Engineering, 2017, 5 (11), 10544-10550

DOI: 10.1021/acssuschemeng.7b02541

ACS Sustainable Chemistry & Engineering

Research Article

Cite This: ACS Sustainable Chem. Eng. 2017, 5, 10544-10550

pubs.acs.org/journal/ascecg

Degradable Microgel Wet-Strength Adhesives: A Route to Enhanced Paper Recycling

Dong Yang and Robert H. Pelton*

Department of Chemical Engineering, McMaster University, 1280 Main Street West, Hamilton, Ontario L8S 4L7, Canada

Supporting Information

ABSTRACT: Demonstrated is a new approach to cellulose fiber-based materials that are strong when wet, yet can be recycled after exposure to a weak reducing agent. Poly(*N*-isopropylacrylamide-*co*-acrylic acid) microgels were transformed into wet cellulose adhesives by incorporation of hydrazide groups that can form hydrazone linkages to oxidized cellulose. Reductant responsivity was obtained by introducing cleavable disulfide linkages, either in the chains tethering the adhesive hydrazide groups, or by using disulfide cross-links in the microgels. Both types of disulfide derivatives gave about 75% reduction in cellulose wet adhesion after exposure to a reductant. Truly sustainable wood-fiber replacements for plastic packaging must be insensitive to water while being fully recyclable; this work demonstrates two routes to reversible wet cellulose adhesives, facilitating recycling.

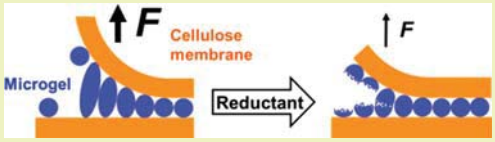

KEYWORDS: *Cellulose wet adhesion, Reductant-responsive, Controllable degradation, Microgels, Paper recycling*

INTRODUCTION

Generally, paper, wood pulp, lumber, and other forest products score very high in terms of sustainability and environmental stewardship. For example, we have seen major fast-food chains convert from plastic- to paper-based food packaging. However, not all lignocellulosic materials are equally sustainable. Two examples of problematic materials are paper coffee filters and premium paper towels. In both cases, the cellulose fiber matrices are impregnated with cross-linked polymers, called wet-strength resins, that are required to maintain paper strength in the presence of water.[1] These resin treatments permit one to safely pick up a coffee filter, filled with hot, wet coffee grounds. However, this enhanced wet paper strength also makes it very difficult to regenerate useful wood pulp fibers in conventional paper recycling processes.[2] Although the global consumption of paper coffee filters and paper towels is a small fraction of forest products, the shift from plastic packaging to cellulosic water-resistant and waterproof packaging will increase as we migrate from a petroleum-based to a biobased economy. In anticipation of the bioeconomy revolution, we have started a research program to develop fully recyclable wet strength chemistries for cellulose-based packaging.

The main wet-strength resin currently used by the North American paper industry for permanent wet strength is polyamide-epichlorohydrin (PAE), a cationic, water-borne polymer.[1] In the papermakng process, PAE is added to dilute aqueous fiber suspensions and spontaneously forms an adsorbed monolayer at the cellulose/water interface. The treated pulp suspension is then filtered to form wet paper. PAE cross-links and grafts onto carboxyl groups on fiber surfaces during high temperature (~120 °C) paper drying. PAE and related products have been used for decades. One feature that sets wet-strength resins apart from most adhesive technologies is that PAE is present in fiber−fiber adhesive joints as very thin layers. For example, if the PAE content of dry paper is 2 wt %/wt, a high value, and if the specific surface area of the pulp fiber suspension is 5 m^2/g, the PAE thickness is ~8 nm. PAE is an old technology, is there nothing better?

The scientific literature describes innovative wet adhesives based on gecko-inspired nanostructured surface structures, and mussel-inspired phenolic chemistries.[3,4] Although promising for high end applications such as tissue adhesives,[5] these approaches may not be practical for the inexpensive commodity products that are filling our landfills. Similarly, switchable light-responsive[6] or shape memory adhesives[7] are unlikely to be applicable in packaging applications.

Our approach wet-strengthened papers that are recyclable and more compostable is to build labile (i.e., cleavable) bonds into the wet strength polymer networks that can be severed by a physical or chemical stimulus. However, instead of developing completely new wet-strength resins, we are investigating a more modular approach. Our ultimate goal is to transform conventional wet-strength resins into labile adhesives by adsorbing them onto degradable supporting particles that will degrade under a specific stimulus. Decoupling the wet-strength resin adhesion chemistry from the degradable supporting particle chemistry facilitates optimization of both wet strength during use and adhesive joint cleavage during recycling.

In this work, we have chosen poly(*N*-isopropylacrylamide) (PNIPAM) copolymer microgels as degradable supporting particles because we have much experience controlling their properties. For example, we have shown that commercial polyvinylamine (PVAm) strongly adsorbs onto nonlabile, PNIPAM carboxylated microgels.[8] The PVAm coated micro-

Received: July 26, 2017
Revised: September 22, 2017
Published: September 25, 2017

gels function as good wet cellulose adhesives, particularly with rough cellulose surfaces where coated microgels give much thicker adsorbed layers resulting in better contact between two rough surfaces. Thus, the microgels are good model particles for mechanistic studies. Ultimately, degradable particles such as colloidal starch gels, might be environmentally and economically preferable.

Herein we present our first results on the development of labile supporting microgels. From a microgel design perspective, there are two approaches to labile microgel structures: (1) employ labile cross-linkers forming the microgel network; and (2) employ labile linkages to the surface carboxyl groups that interact with the wet strength resins. These two approaches are compared in this work.

The literature describes many approaches to covalent linkages that can be cleaved by stimuli such as heat, light, pH change, and redox processes.[9] We chose disulfide linkages that are cleaved under mild reducing conditions. Disulfide linkages have been employed to produce self-healing materials,[10] recyclable materials,[11] and have been incorporated into microgels.[12,13] The reduction of disulfide bonds has also been shown to weaken joints based on protein adhesives.[14]

To determine the best strategy for disulfide bond incorporation, we have employed supporting microgels have been converted to wet-strength adhesives by covalently linking hydrazide groups that can form covalent hydrazone bonds with aldehyde groups present on oxidized cellulose.[15] For the current mechanistic studies, this approach is cleaner compared with adsorbing commercial wet-strength resins on the microgels.

Figure 1 illustrates the two types of hydrazide-microgels bound to oxidized cellulose we have prepared. In the "Labile Hydrazide" case, the hydrazide groups are attached to the microgel particles by labile tethers containing disulfide linkages, whereas in the "Labile Microgel Crosslinks", the disulfide groups are present as labile cross-links in the microgel structure.

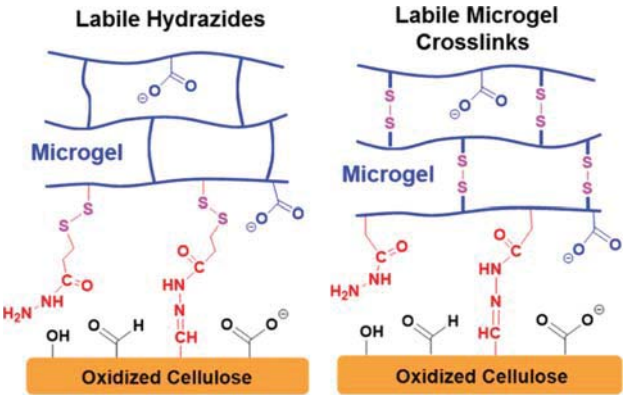

Figure 1. Hydrazone bond formation at the interface between oxidized cellulose and hydrazide-microgels. Disulfide linkages are broken by exposure to reductants, decreasing adhesive joint strength.

In summary, this work compares the two strategies for cleavable cellulose wet adhesive, Labile Hydrazides and Labile Microgel Cross-links. In addition, we report the influence of reductant type and pH on the microgel degradation and adhesion loss.

EXPERIMENTAL SECTION

Materials. Regenerated cellulose membranes (Spectra/Por2, MWCO 12−14 kDa, product number 132684) were purchased from Spectrum Laboratories, US. Blotter papers were purchased from Labtech Instruments Inc., Canada. All other chemicals were purchased from Sigma-Aldrich, Canada. Water type 1 (as per ASTM D1193-6, resistivity 18.2 MΩ/cm) was used in all experiments.

Microgel Preparation. A series of poly(NIPAM-*co*-acrylic acid) microgels was synthesized based on the methods in the literature.[16] The recipes are summarized in Table S1. *N*-Isopropylacrylamide (NIPAM) was purified by recrystallization from toluene and washed with hexane, whereas acrylic acid (AA) and the two cross-linkers, *N*,*N*′-methylenebis(acrylamide) (MBA) and reductant-responsive cross-linker *N*,*N*′-bis(acryloyl)cystamine (BAC), were used as received. The chemical structures of the monomers are shown in the Supporting Information (Figure S1).

In a typical polymerization, NIPAM, sodium dodecyl sulfate (SDS), AA, and MBA were dissolved in 100 mL of water. The solution was heated to 70 °C and agitated for 30 min with nitrogen gas purging. BAC in 2 mL of dimethylformamide and ammonium persulfate (APS) in 2 mL water were injected into the solution. The polymerization proceeded for 8 h at 70 °C with nitrogen gas purging. The microgels were purified by dialysis against water and stored as an aqueous dispersion at 4 °C. The solids contents of the dialyzed solutions, determined gravimetrically after drying at 60 °C, were in the range 6−10 mg/mL

Dithiodipropionic Acid Dihydrazide (DTDH) Synthesis. DTDH (see structure in Figure S1) was required to conjugate labile hydrazide functional groups onto the microgels. Following the literature,[17] 4.2 mmol 3,3′-dithiopropionic acid dimethyl ester dissolved in 15 mL of methanol was slowly added to a 100 mL round-bottomed flask containing 25 mmol hydrazine hydrate dissolved in 10 mL of dry methanol. The flask was sealed and placed on a magnetic stirrer at room temperature for 12 h. The product was present as crystals that were filtered and purified with methanol and hexane. The NMR spectrum of the product is shown in the Supporting Information (Figure S2).

Hydrazide Derivatized Microgels. Hydrazide derivatized microgels were prepared by the conjugation of dihydrazides with microgel carboxyls.[18] Two dihydrazide reagents were employed, adipic acid dihydrazide (ADH) and the reductant-responsive dihydrazide DTDH. The detailed conjugation recipes are given in Table S2 and the dihydrazide reagent structures are given in Figure S1. In a typical reaction, the molar ratio of dihydrazide reagent, 1-ethyl-3-(3-(dimethylamino)propyl)carbodiimide hydrochloride (EDC) and *N*-hydroxysuccinimide (NHS) was 2:2:1. Stock microgel dispersion was diluted with water to give 24 mL containing 120 mg of dry microgel. After 30 min of stirring at room temperature, the pH of solution was adjusted to 5. EDC was added and then NHS was added 2 min later. The dispersion was stirred and maintained at pH 5. After 10 min, the pH was adjusted to 7.2. ADH and DTDH were added into the solution. The modification proceeded for 2 h at room temperature with pH maintained at 7.2. The products were purified by dialysis and stored as aqueous dispersions (3−5 mg/mL) at 4 °C. The concentrations of derivatized microgels were determined gravimetrically.

Microgel Characterization. For most characterization experiments, the microgels were dispersed in 1 mM NaCl solution at neutral pH at 23 °C. The electrophoretic mobilities of microgels were measured by ZetaPlus analyzer (Brookhaven Instrument Corp., US) using the phase analysis light scattering mode. Reported values were averaged over 10 cycles with 10 scans for each cycle. The error bars represent the standard error.

Hydrodynamic diameters of microgels were measured by dynamic light scattering (DLS) (Model BI-APD, Brookhaven Instrument Corp., US) with software version 1.0.0.1. The detection angle was 90° and the laser source was 633 nm wavelength. At least 3 runs were recorded for each sample and error bars represented the standard deviation. The

Table 1. Supporting Microgel Properties[a]

Microgel designation	[BAC]/[BAC]+[MBA]	COOH equiv. wt[b] (Da)	Diameter (nm)	PDI	Electrophoretic mobility (10^{-8} $m^2/(V\ s)$)
M0	0	665 ± 32	458 ± 14	0.05	−2.86 ± 0.05
M41	0.41	674 ± 17	525 ± 22	0.12	−2.42 ± 0.06
M68	0.68	639 ± 38	520 ± 25	0.08	−2.47 ± 0.05
M100	1.00	653 ± 34	438 ± 24	0.06	−2.42 ± 0.08

[a]BAC is a labile cross-linker whereas MBA is not; see Figure S1 for monomer structures. The supporting microgels designation reflects the mole percentage of labile cross-links. M*xx*, where *xx* is the mole percentage of crosslinks that are labile. Particle size and electrophoretic measurements were performed in 1 mM NaCl at pH 7, at 23 °C. [b]Microgel carboxyl content expressed as an equivalent weight.

Table 2. Reductant-Responsive Adhesives Prepared by Conjugating Hydrazide Groups to the Supporting Microgels

Microgel designation	ADH (mol %)[a]	DTDH (mol %)[a]	Diameter (nm)	PDI	Electrophoretic mobility (10^{-8} $m^2/(V\ s)$)
Labile-hydrazide microgels					
M0-H62	62	0	372 ± 6	0.06	−2.14 ± 0.08
M0-H41-Hs21	41	21	353 ± 11	0.02	−1.96 ± 0.07
M0-H23-Hs45	23	45	347 ± 4	0.02	−1.89 ± 0.08
M0-H0-Hs64	0	64	334 ± 18	0.08	−2.09 ± 0.03
Labile-cross-link microgels					
M0-H62	62	–	372 ± 6	0.06	−2.14 ± 0.08
M41-H71	71	–	509 ± 14	0.04	−1.91 ± 0.04
M68-H65	65	–	509 ± 16	0.08	−2.26 ± 0.07
M100-H65	65	–	407 ± 6	0.01	−2.17 ± 0.07

[a]Molar percentage of carboxyl groups converted to hydrazides.

corresponding polydispersity indices (PDI) were recorded as a measure of the particle size distribution.

The hydrazide contents were determined by comparing the potentiometric titrations before and after dihydrazide conjugation. The methods and analysis were described in detail recently.[15] In those cases where mixtures of ADH and DTDH were employed, we assumed that the reactivity of ADH and DTDH was equal toward carboxyls.

Wet Cellulose Adhesion. Regenerated cellulose membranes (effective adhesive area between two membranes 5 cm × 2 cm, 80 ± 5 μm thick), derived from commercial dialysis tubing, were prepared and 2,2,6,6-tetramethylpiperidine 1-oxyl (TEMPO)are oxidized by the methods recently described.[15] Laminates were prepared by pressing (334 kPa for 5 min) together two wet, cellulose membranes, bonded with a very thin layer (15 mg dry adhesive per square meter of cellulose/cellulose interface) of microgel adhesive. The laminates were allowed to dry at 23 °C and 50% RH for 1 day.

For adhesion measurements, the laminates were soaked in a rewetting solution, usually for 30 min, followed by measurement of the force required to peel apart the laminates. The peel angle was 90° and the peel rate was 20 mm/min. The cellulose membranes are water-swollen hydrogels. During the peeling, the overall solid contents of laminates were in the range of 47−54 wt %, determined gravimetrically before and after peeling. The reported delamination forces were the average of at least 3 replicates. The error bars depict the standard deviation. The many details of the sample preparation and testing procedure were recently described.[15]

RESULTS

Supporting Microgel Properties. Our reductive-responsive adhesives consisted of poly(NIPAM-*co*-AA) microgels decorated with hydrazide adhesive groups. Four supporting microgels were synthesized by precipitation polymerization. The recipes are given in Table S1 and the microgel properties are summarized in Table 1. All except microgel M0 contain some labile disulfide cross-links, introduced by BAC, see structure in Figure S1. The carboxyl contents, diameters, and electrophoretic mobilities of the four supporting microgels were approximately constant, see Table 1. Our previous work with hydrazide-microgels showed that microgels with positive electrophoretic mobilities gave stronger adhesion than negative ones.[15] Since the oxidized cellulose is negatively charged, we explained the charge effect as an electrostatic contribution to wet adhesion. In this work, we employed negatively charged microgels to ensure that hydrazone covalent bond formation was the only contribution to wet adhesion.

Adhesive Hydrazide Microgels. The four supporting microgels have no cellulose wet-adhesive properties. The nonadhesive supporting microgels were converted to adhesive by grafting aldehyde reactive hydrazide functional groups in and on the microgels,[15] see Figure 1. As a result, two families of reductant responsive adhesive microgels were prepared, labile-hydrazide microgels and labile-cross-link microgels. The key features are illustrated in Figure 1, and microgel compositions and properties are given in Table 2.

For the labile-hydrazide microgels, some of the acrylic acid groups on supporting microgel M0 were condensed with ADH to give stable hydrazide groups, and/or with DTDH (see structure in Figure S1), which includes a labile disulfide linkage. The labile-hydrazide microgels are designated M0-H*yy*-Hs*zz*, where *yy* mol % of the carboxyls were converted to nonlabile hydrazide and *zz* mol % of the carboxyls were converted to labile hydrazides. Since the entire labile-hydrazide series was based on a common parent supporting microgel, the diameters and electrophoretic mobilities are similar. Note that M0, the parent microgel is larger (Table 1), reflecting a higher degree of swelling. Hydrazide conjugation replaces ionized carboxyls with uncharged hydrazides, lowering the swelling.

The labile-cross-linked microgels are designated M*xx*-H*yy*, where *xx* mol % of the cross-links that were labile cross-linking monomer BAC and *yy* mol % of the carboxyls were converted to stable hydrazides. This series of microgels is based on the four supporting microgels and shows more variation in properties than the labile-hydrazide series.

Previously, we investigated the design criteria for nonlabile, adhesive microgels and we reported that with PVAm adsorbed onto carboxylated PNIPAM microgels, wet cellulose adhesion

was not very sensitive to microgel diameters with microgels larger than the roughness scale of cellulose substrate.[19] Therefore, we did evaluate the role of microgel diameter herein.

PNIPAM microgels shrink when heated above the volume phase transition temperature (VPTT) of ~32 °C. The introduction of carboxyl containing monomers raises the transition temperature[20] and microgels with high carboxyl contents tend to exhibit two phase transition temperatures, one near 32 °C for PNIPAM-rich domains and one at 45 °C for acid-rich domains.[21,22] For the microgels in Tables 1 and 2, the VPTT values are expected to fall in the range approximately 34–45 °C.[23] None of the lamination or adhesion experiments were conducted with shrunken microgels. We do not postulate that temperature is a useful tool for switching on or off wet adhesion because our previous, unpublished results with the PVAm coated microgels did not show significant temperature sensitivity in wet adhesion.

Reductant-Responsive Microgel Swelling. For most of our studies, we employed dithiothreitol (DTT), a reductant that cleaves disulfide bonds by thiol–disulfide exchange. DTT has two thiol groups (see DTT structure in Figure 2A) with pK_a values of 9.2 and 10.1. The reduction of disulfides in microgels is initiated by thiolates in DTT. Therefore, rapid disulfide cleavage with DTT requires pH values >8.[24]

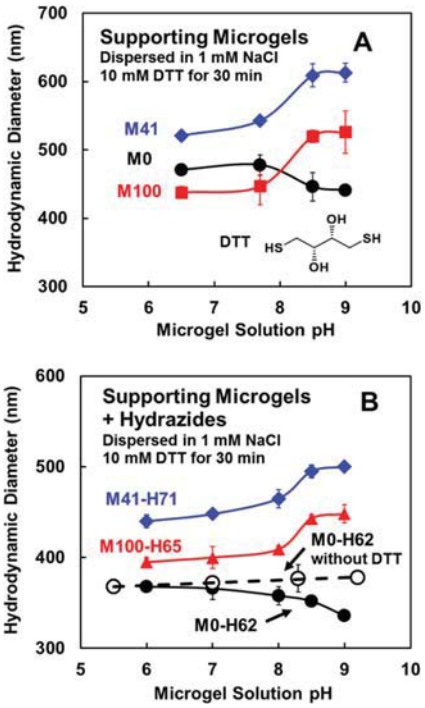

Figure 2. Influence of DTT reduction pH on microgel swelling. Above pH 8, cross-linker cleavage increases swelling. Microgel M0 has no disulfide cross-links, and the open circles were obtained with microgels not exposed to DTT. The pH values were adjusted with 0.1 M NaOH or 0.1 M HCl.

Supporting microgels M41, M68 and M100 (see Table 1) should be sensitive to the presence of a reducing agent because of the disulfide cross-links. We treated the microgels with the reductant DTT solution for 30 min and Figure 2A shows that the diameters of microgels M41 and M100 increased at pH > 8.5 in the presence of DTT, indicating increased swelling in the absence of cross-linking. Although one might expect the microgel M100 to completely dissolve when reduced, it does not. A recent paper from Serpe's group also showed the incomplete dissolution of similar disulfide cross-linked PNIPAM microgels.[13] Gao and Frisken presented evidence for PNIPAM microgel cross-linking in the absence of added bifunctional monomer.[25] They proposed branched structures arising from hydrogen abstraction. Perhaps the best explanation comes from Lyon's group who propose that the disulfide groups can interfere with free radical polymerization at elevated temperature, yielding some nondegradable cross-links.[12]

The M0 microgel has no disulfide cross-links and thus does not increase swelling in the presence of DTT. In fact, the swelling decreases with DTT at high pH because of the increase in ionic strength.

Figure 2B shows the corresponding results for the hydrazide modified supporting microgels. The trends are the same except the changes are somewhat attenuated compared to the unmodified microgels. The conversion of acrylic acid groups to the corresponding hydrazides lowers the net charge in the gels, decreasing the swelling. In summary, the cleavage of disulfide cross-links gives increased microgel swelling; however, the microgels do not dissolve.

Reductant-Responsive Adhesion. We evaluated wet cellulose adhesion by measuring the peel delamination force required to separate wet regenerated cellulose membranes, laminated with a microgel wet-strength adhesive, Figure 3. The

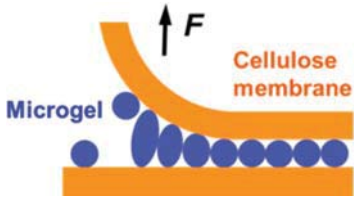

Figure 3. Cross-sectional illustration of the 90° peel delamination geometry for measuring wet cellulose adhesion. The microgel coverage corresponded to a monolayer of microgels between the membranes. The diagram is not to scale; water-swollen membranes (50 ± 3% water) were 80 ± 5 μm thick and the microgel diameters were ~500 nm.

laminates serve as physical models for fiber–fiber joints in paper. In these experiments, regenerated cellulose membranes were TEMPO oxidized, converting some C6 primary hydroxyls to aldehyde and carboxyl groups. Pairs of wet membranes were laminated with microgel-supported adhesives with adhesive coverage of 15 mg/m^2. and were allowed to dry at 50% relative humidity at 23 °C. Before measuring the peel delamination forces, the laminates were soaked in a rewetting solution, typically for 30 min.

The quantity of microgels in the laminates was 15 mg/m^2, which approximately corresponds to a monolayer microgels in the adhesive joints. Previously, we have shown that hydrazide-microgels show substantial microgel/microgel adhesion and the reasons are not obvious. In an extensive discussion, we proposed that covalent bonds formed when a hydrazide on an microgel reacts with a residual NHS ester on a neighboring microgel.[15]

Figure 4 compares the adhesion characteristic of all hydrazide-based microgels in the presence of the reductant DTT. The results are shown as functions of pH. At low pH, DTT is not ionized and all of the microgels gave delamination forces of about 20 N/m. Above pH 8, the DTT reduces the

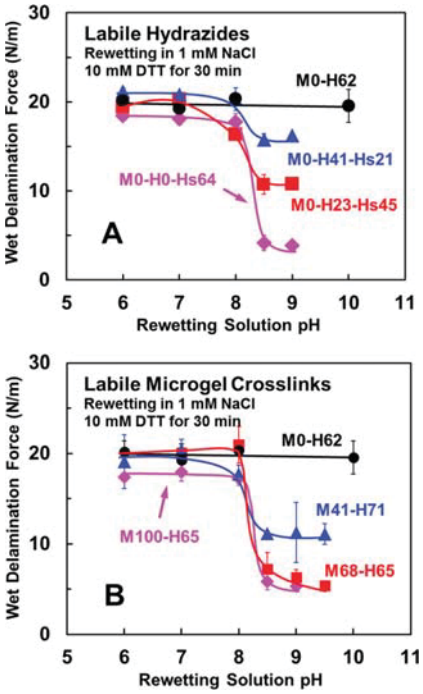

Figure 4. Influence of DTT reductant rewetting solution pH on the wet adhesion between oxidized cellulose membranes laminated with 15 mg/m^2 of (A) labile-hydrazide and (B) labile-cross-link microgel adhesives. Laminates were soaked in 1 mM NaCl, 10 mM DTT for 30 min before measuring the wet delamination force.

disulfide bonds. Results for the labile-hydrazide microgels are shown in Figure 4A. The extent of adhesion decrease under reducing conditions was greatest for M0-H0-Hs64 where all of the hydrazide groups were attached by labile tethers. At the other extreme, the wet adhesion of disulfide-free M0-H62 was not influenced by DTT.

The responses of the hydrazide microgels with labile cross-links to DTT are shown in Figure 4B. The M68 and M100 supporting microgels gave similar decreases in adhesion with reduction, even though M68 has 32% nonlabile MBA cross-links, whereas M100 has no MBA cross-links. Our microgels were prepared by batch polymerization, which gives nonuniform cross-linker distribution within microgel particles: MBA tends to concentrate in the microgel core.[26] If for example, the disulfide cross-links were more concentrated toward the microgel surfaces, the adhesion decrease with reduction should be insensitive to permanent cross-links in the microgel core.

The kinetics of DDT reduction of disulfide bonds is reflected in the adhesion properties. Figure 5 shows wet delamination strength as functions of rewetting time in DTT or NaCl solutions. The DDT kinetics were pH dependent. At pH 8.5, the adhesion decreased as quickly as we could measure it, whereas at pH 7, more than 10 h were required for a low adhesion. The adhesion also slowly decreased in NaCl solution at neutral pH. This trend reflects the known behavior of hydrazone linkages; they slowly hydrolyze.[27] Another example of hydrazone slow hydrolysis is given in Figure S3, which shows that cellulose laminates made with microgel M0-H62 lose most of their wet strength when soaked in 1 mM NaCl for 100 h. Since there are no disulfide linkages in microgel M0-H62, this decay in adhesion must be due to the reversible nature of hydrazone bonds. By contrast, two commercial wet-strength

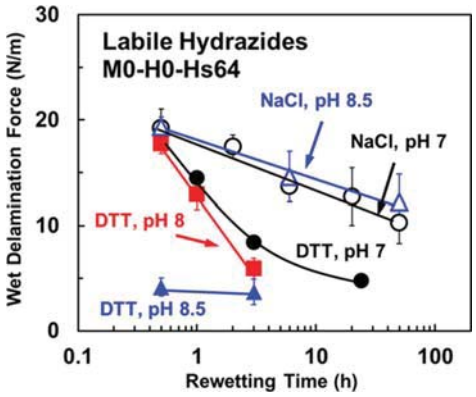

Figure 5. Influence of rewetting solution pH on the degradation rate of wet adhesion. The solid symbols denote laminates rewetted in 1 mM NaCl, 10 mM DTT solution whereas the open symbols represent the laminate was rewetted in 1 mM NaCl without DTT.

resins, PVAm (polyvinylamine) and polyamide-epichlorohydrin (PAE), show little strength loss over this extended rewetting time, see Figure S3.

Reductant Type. The minimum pH required to reduce disulfide bonds, degrading adhesion, depends upon the properties of the reductant. Figure 6 compares the influence

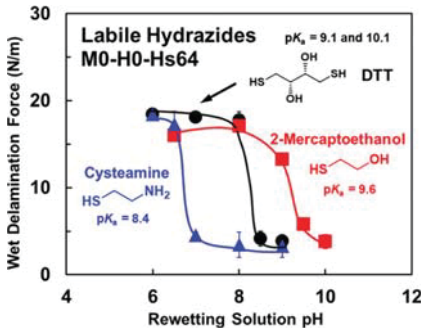

Figure 6. Influence of reductant type on the pH required to reduce adhesion of wet, oxidized cellulose, laminated with M0-H0-Hs64 adhesive. Laminates were rewetted in 1 mM NaCl, 10 mM reductant for 30 min before measuring the wet delamination force.

of three reductant types on wet adhesion of cellulose laminated with the labile-hydrazide microgel M0-H0-Hs64. All three reductants gave the same strength after reduction when the reductant solution pH was close to the first pK_a of the reductant. Thus, the required pH for degrading adhesion can be tailored by choice of reductant.

DISCUSSION

This initial investigation demonstrates the potential of reductant-responsive microgel-based paper wet-strength resins to give high wet adhesion between cellulose surfaces before reductant exposure, and high recyclability after reductant exposure. We have compared two strategies for inducing cleavable linkages into microgel-based wet cellulose adhesive-labile cross-links within the supporting microgel, versus labile tethers to the adhesive hydrazide functional groups. Both strategies were effective with almost a complete loss of wet strength upon exposure to reductant (Figure 4). This result demonstrates that it is possible to design reversible wet

adhesives for lignocellulosic materials, greatly enhancing recyclability.

Our initial hypothesis was that the labile-hydrazide microgels would give the most dramatic responses to reductants, because without hydrazides the supporting microgels give no wet adhesion. By contrast, the labile-cross-link microgels did not dissolve after reduction (Figure 2), suggesting they still would be adhesive after reduction. We were surprised that the labile-cross-link microgels gave essentially the same degree of adhesion lowering as the labile-hydrazide microgels. Since both approaches work, which is better?

In terms of technology development, the labile microgel cross-links are very attractive because the labile function is decoupled from the adhesive function. For example, with an effective labile supporting microgel, one could fabricate a wide range of labile adhesives simply by changing the adhesive component on the microgel surfaces. Herein we employed hydrazides as the adhesive functional groups. Hydrazides react with aldehydes in water at neutral pH forming hydrazone bonds, giving adhesion without drying.[15] However, hydrazone bonds give a slow loss in adhesion when wet (Figure 5), which would not be acceptable in many applications. Instead, more robust commercial wet-strength resins, that do not require cellulose oxidation, would be more attractive adhesive components to combine with labile-cross-link microgels. We will show in a future publication that a commercial PAE wet-strength resin became reductant-responsive when supported on disulfide cross-linked microgels. In the longer term, truly sustainable wet adhesives that are responsive to reductants, or some other stimulus, should be based upon fully degradable polymers originating from the biomass.

Finally, from a mechanistic perspective, the reduced microgels represent a limiting case of near zero cross-link density when considering the influence of microgel cross-linking on adhesion. Based on our previous modeling, supported by experiments, we argued that the delamination force increases with decreasing cross-link density.[8,19] This is because only a narrow band of microgels near the peel front support the peeling load, see Figure 3. The width of this band increases with increasing microgel extensibility, resulting in more microgels sharing the load. However, these arguments were based on the assumption that failure did not occur within the microgel network. Obviously as the cross-link density approaches zero, the locus of failure switches from the microgel/cellulose interface to cohesive failure within the microgels.

CONCLUSIONS

(1) Microgels with labile disulfide cross-links or with labile adhesive hydrazide groups, give up to 75% strength loss in the presence of reducing agents, providing routes to reductant-responsive wet cellulose adhesives. Degradable adhesives are a new way to enhance the recycling of wet-strengthened cellulose-based materials. (2) The optimal pH for adhesion reduction can be varied by the choice of reductants. (3) Although both labile-hydrazide and labile-cross-link microgels gave large decreases in adhesion with disulfide cleavage, disulfide cross-linked microgels is the preferred approach because a wide range of cellulose reactive materials can be adsorbed or grafted onto the labile supporting microgel, expanding the potential property space of degradable adhesives. By contrast, replacing labile hydrazide groups with other cellulose reactive groups would require synthesis of unique disulfide tethers for every additional type of cellulose-reactive functional group. (4) In special cases where degradation to a limited degree is required, mixtures labile and nonlabile tethered hydrazides (Figure 4A) gave more accurate control than mixtures of labile and nonlabile cross-links (Figure 4B)

ASSOCIATED CONTENT

Supporting Information

The Supporting Information is available free of charge on the ACS Publications website at DOI: 10.1021/acssuschemeng.7b02541.

Microgel recipes, chemical structures of monomers and hydrazide reagents, proton NMR of difunctional hydrazides, tabulated hydrazide-microgel properties, plot of adhesion degradation with storage time comparing PAE, PVAm and a hydrazide-microgel (PDF)

AUTHOR INFORMATION

Corresponding Author

*R. H. Pelton. E-mail: peltonrh@mcmaster.ca.

ORCID

Robert H. Pelton: 0000-0002-8006-0745

Notes

The authors declare no competing financial interest.

ACKNOWLEDGMENTS

BASF Canada is acknowledged for funding this project through a grant to R.P. entitled "Understanding Cellulose Interactions with Reactive Polyvinylamines". Dr. Emil Gustafsson, McMaster University, Dr. Anton Esser, BASF Ludwigshafen and Joel Soucy, BASF Canada, are acknowledged for useful discussions. Some measurements were performed in the McMaster Biointerfaces Institute funded by the Canadian Foundation for Innovation. R.H.P. holds the Canada Research Chair in Interfacial Technologies.

REFERENCES

(1) Espy, H. H. The Mechanism of Wet-Strength Development in Paper: A Review. *Tappi J.* **1995**, *78*, 90−99.

(2) Darlington, W. B.; Lanier, W. G. Repulpable Wet Strength Paper. Patent US5,427,652, June 27, 1995.

(3) Lee, H.; Lee, B. P.; Messersmith, P. B. A Reversible Wet/Dry Adhesive Inspired by Mussels and Geckos. *Nature* **2007**, *448*, 338−341.

(4) Hwang, D. S.; Zeng, H.; Srivastava, A.; Krogstad, D. V.; Tirrell, M.; Israelachvili, J. N.; Waite, J. H. Viscosity and Interfacial Properties in a Mussel-Inspired Adhesive Coacervate. *Soft Matter* **2010**, *6*, 3232−3236.

(5) Mahdavi, A.; Ferreira, L.; Sundback, C.; Nichol, J. W.; Chan, E. P.; Carter, D. J. D.; Bettinger, C. J.; Patanavanich, S.; Chignozha, L.; Ben-Joseph, E.; Galakatos, A.; Pryor, H.; Pomerantseva, I.; Masiakos, P. T.; Faquin, W.; Zumbuehl, A.; Hong, S.; Borenstein, J.; Vacanti, J.; Langer, R.; Karp, J. M. A Biodegradable and Biocompatible Gecko-Inspired Tissue Adhesive. *Proc. Natl. Acad. Sci. U. S. A.* **2008**, *105*, 2307−2312.

(6) Akiyama, H.; Kanazawa, S.; Okuyama, Y.; Yoshida, M.; Kihara, H.; Nagai, H.; Norikane, Y.; Azumi, R. Photochemically Reversible Liquefaction and Solidification of Multiazobenzene Sugar-Alcohol Derivatives and Application to Reworkable Adhesives. *ACS Appl. Mater. Interfaces* **2014**, *6*, 7933−7941.

(7) Reddy, S.; Arzt, E.; Del Campo, A. Bioinspired Surfaces with Switchable Adhesion. *Adv. Mater.* **2007**, *19*, 3833−3837.

(8) Wen, Q.; Pelton, R. Microgel Adhesives for Wet Cellulose – Measurements and Modeling. *Langmuir* **2012**, *28*, 5450–5457.
(9) Hermanson, G. T. *Bioconjugate Techniques*; Academic Press: San Diego, CA, 1996.
(10) Lei, Z. Q.; Xiang, H. P.; Yuan, Y. J.; Rong, M. Z.; Zhang, M. Q. Room-Temperature Self-Healable and Remoldable Cross-Linked Polymer Based on the Dynamic Exchange of Disulfide Bonds. *Chem. Mater.* **2014**, *26*, 2038–2046.
(11) Imbernon, L.; Oikonomou, E. K.; Norvez, S.; Leibler, L. Chemically Crosslinked yet Reprocessable Epoxidized Natural Rubber Via Thermo-Activated Disulfide Rearrangements. *Polym. Chem.* **2015**, *6*, 4271–4278.
(12) Gaulding, J. C.; Smith, M. H.; Hyatt, J. S.; Fernandez-Nieves, A.; Lyon, L. A. Reversible Inter- and Intra-Microgel Cross-Linking Using Disulfides. *Macromolecules* **2012**, *45*, 39–45.
(13) Li, X.; Gao, Y.; Serpe, M. J. Reductant-Responsive Poly(N-Isopropylacrylamide) Microgels and Microgel-Based Optical Materials. *Can. J. Chem.* **2015**, *93*, 685–689.
(14) Kalapathy, U.; Hettiarachchy, N. S.; Myers, D.; Rhee, K. C. Alkali-Modified Soy Proteins: Effect of Salts and Disulfide Bond Cleavage on Adhesion and Viscosity. *J. Am. Oil Chem. Soc.* **1996**, *73*, 1063–1066.
(15) Yang, D.; Gustafsson, E.; Stimpson, T. C.; Esser, A.; Pelton, R. H. Hydrazide-Derivatized Microgels Bond to Wet, Oxidized Cellulose Giving Adhesion without Drying or Curing. *ACS Appl. Mater. Interfaces* **2017**, *9*, 21000–21009.
(16) Pelton, R. H.; Chibante, P. Preparation of Aqueous Latices with N-Isopropylacrylamide. *Colloids Surf.* **1986**, *20*, 247–256.
(17) Rodriguez-Docampo, Z.; Otto, S. Orthogonal or Simultaneous Use of Disulfide and Hydrazone Exchange in Dynamic Covalent Chemistry in Aqueous Solution. *Chem. Commun.* **2008**, 5301–5303.
(18) Sivakumaran, D.; Maitland, D.; Oszustowicz, T.; Hoare, T. Tuning Drug Release from Smart Microgel–Hydrogel Composites Via Cross-Linking. *J. Colloid Interface Sci.* **2013**, *392*, 422–430.
(19) Wen, Q.; Pelton, R. Design Rules for Microgel-Supported Adhesives. *Ind. Eng. Chem. Res.* **2012**, *51*, 9564–9570.
(20) Snowden, M. J.; Chowdhry, B. Z.; Vincent, B.; Morris, G. E. Colloidal Copolymer Microgels of N-Isopropylacrylamide and Acrylic Acid: pH, Ionic Strength and Temperature Effects. *J. Chem. Soc., Faraday Trans.* **1996**, *92*, 5013–5016.
(21) Kratz, K.; Hellweg, T.; Eimer, W. Influence of Charge Density on the Swelling of Colloidal Poly(N-Isopropylacrylamide-Co-Acrylic Acid) Microgels. *Colloids Surf., A* **2000**, *170*, 137–149.
(22) Hoare, T.; Pelton, R. Functional Group Distributions in Carboxylic Acid Containing Poly(N-Isopropylacrylamide) Microgels. *Langmuir* **2004**, *20*, 2123–2133.
(23) Pelton, R. Temperature-Sensitive Aqueous Microgels. *Adv. Colloid Interface Sci.* **2000**, *85*, 1–33.
(24) Lukesh, J. C.; Palte, M. J.; Raines, R. T. A Potent, Versatile Disulfide-Reducing Agent from Aspartic Acid. *J. Am. Chem. Soc.* **2012**, *134*, 4057–4059.
(25) Gao, J.; Frisken, B. J. Cross-Linker-Free N-Isopropylacrylamide Gel Nanospheres. *Langmuir* **2003**, *19*, 5212–5216.
(26) Wu, X.; Pelton, R. H.; Hamielec, A. E.; Woods, D. R.; Mcphee, W. The Kinetics of Poly(N-Isopropylacrylamide) Microgel Latex Formation. *Colloid Polym. Sci.* **1994**, *272*, 467–477.
(27) Kalia, J.; Raines, R. T. Hydrolytic Stability of Hydrazones and Oximes. *Angew. Chem.* **2008**, *120*, 7633–7636.

SUPPORTING INFORMATION

Degradable Microgel Wet-Strength Adhesives - A Route to Enhanced Paper Recycling

Dong Yang[1] and Robert H. Pelton [1]*

[1] Department of Chemical Engineering, McMaster University, 1280 Main St. West, Hamilton, Ontario, Canada L8S 4L7

*peltonrh@mcmaster.ca

This file contains 3 figures, 2 tables and 4 pages

Table S1 Preparation of poly(NIPAM-co-AA) supporting microgels. Monomer structures are shown in Figure S1

Microgel	mmol in 100 mL solution					
	NIPAM	MBA	BAC	AA	APS	SDS
M0	4.13	0.22	0	0.62	0.15	0.08
M41	4.13	0.13	0.09	0.62	0.15	0.06
M68	4.13	0.07	0.15	0.62	0.15	0.06
M100	4.13	0	0.22	0.62	0.15	0.06

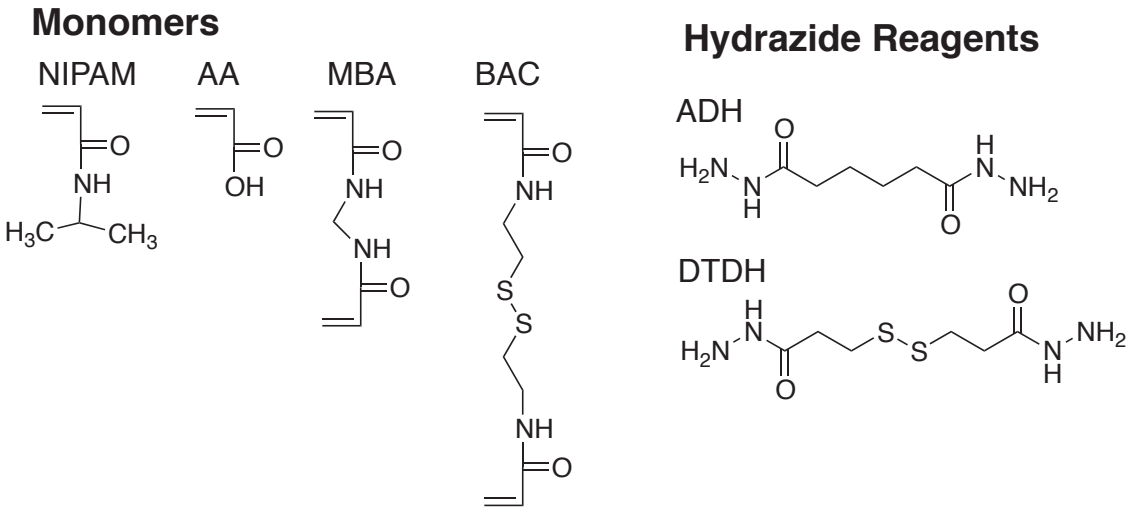

Figure S1 Structures of monomers and hydrazide reagents

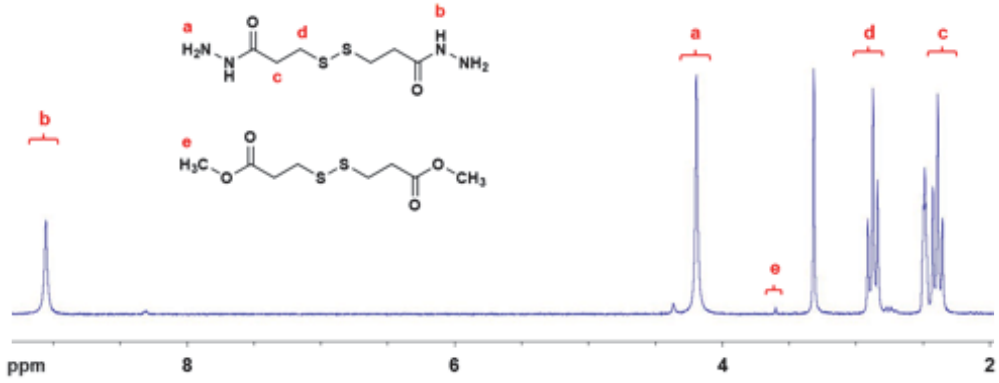

Figure S2 NMR spectrum of DTDH. ^{1}H NMR was performed using an NMR Spectrometer (Bruker AVANCE 600 MHz, US) at room temperature in DMSO-d_6 solvent. The peaks at 2.5 ppm and 3.3 ppm correspond to DMSO and water, respectively.

Table S2 Preparation of hydrazide derivatized microgels

Microgel adhesive	Microgel (mg)	ADH (mg)	DTDH (mg)	EDC (mg)	NHS (mg)	Total hydrazide DS (mol%)
M0-H62	120	141	0	187	56	62
M0-H41-Hs21	120	94	78	187	56	62
M0-H23-Hs45	120	47	156	187	56	68
M0-H0-Hs64	120	0	234	187	56	64
M41-H71	120	141	0	187	56	71
M68-H65	120	141	0	187	56	65
M100-H65	120	141	0	187	56	65

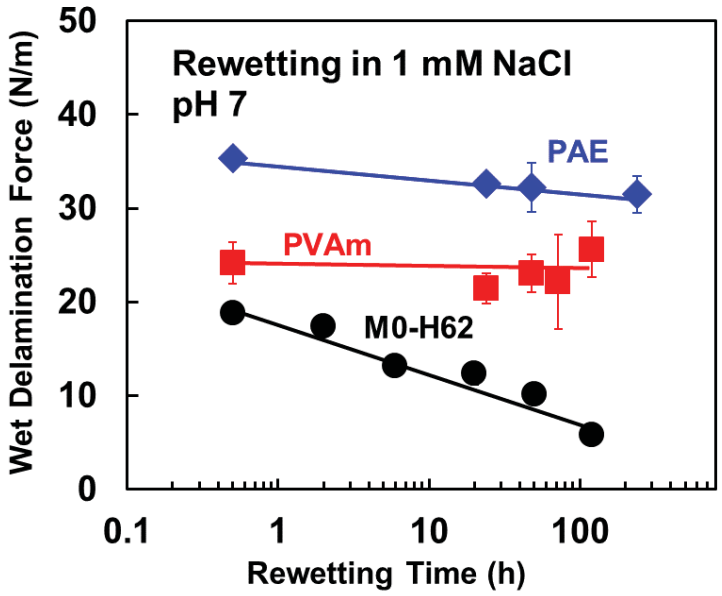

Figure S3 Degradation rate of wet adhesion. PVAm (red) with Mw 340 kDa were provided by BASF, Germany. PAE (blue) was Kymene 5221 from Solenis, US. The coverages of PAE, PVAm and M0-H62 were 15 mg/m^2 at laminate joints.

Chapter 5

Microgel-supported PAE — a Degradable Cellulose Wet Adhesive to Enhance Paper Recycling

In this chapter, a commercial cellulose wet adhesive, polyamide-epichlorohydrin (PAE), was loaded on microgels with labile disulfide crosslinks via electrostatic attraction. Compared to using hydrazides to bond with cellulose (as in Chapter 3 and 4), PAE adhesive shows many advantages: 1) it is widely used in paper manufacturing; 2) loading it on microgels is much easier than hydrazide functionalization; 3) it provides cellulose a stronger and more reliable wet adhesion. This concept is a promising start to manufacture wet-strength papers with enhanced recyclability.

The data within this chapter were collected by me with the assistance of Alexander Sotra, who worked with me as a summer student. I summarized the data and wrote the draft myself. Dr. Robert Pelton helped me analyze the results and edit the manuscript.

This chapter is to be submitted to Nordic Pulp and Paper Research Journal.

5.1 Introduction

Cellulosic materials, such as paper, pulp, and wood-based products, have a great reputation for their excellent renewability and recyclability.[1, 2] Pristine cellulose materials are hydrophilic. In water, a hydrogel layer will form near cellulose surfaces that can drastically change the interfacial property of the material.[3]

Generally, pre-treatments and additives are necessities to enhance the reliability of cellulosic materials in moist and water environments. Take wood products as an example: acrylic protective coatings with 10–100 μm thickness are commonly used to enhance their durability under weathering such as water spray.[4, 5] In some applications, glues such as phenol-formaldehyde resins and isocyanates are used to stabilize wood composite structures.[6, 7] The possible toxic residual from coatings and glues is a great concern in the reuse and recycling of wood materials.[8]

In paper products, wet-strength resins are important additives to manufacture wet strength papers such as premium paper towels and coffee filter papers.[9] The most commonly used wet-strength resin is PAE. In the paper manufacturing process, cationic PAE first adsorbs on anionic cellulose fibers in aqueous solutions, forming a saturated adsorbed layer on the fiber surface with a coverage < 5 mg/m^2.[9] A typical PAE chemical structure is shown in Figure 5-1. During drying, PAE both covalently grafts to cellulose fibers and forms crosslinks with carboxyls at the end of other PAE chains via the azetidinium groups, providing paper wet strength.[10, 11] However, wet-strength resins have a negative impact on the recycling of paper products. Su *et al.* reported the addition of 0.5–2 wt % PAE lowered the recyclability of paper products from 100% to ~ 20%.[12] According to Kanie *et al.*,[13] with the PAE and polyvinylamine (PVAm) addition, only approximate 10-15% of papers was degraded after 10 days in soil, compared with 50% weight loss of papers without wet-strength resins.

In Chapter 4, we demonstrated the concept of using microgel adhesives as degradable cellulose wet adhesives.[9] In that work, hydrazide-derivatized poly(NIPAM-co-AA) microgels were synthesized with labile disulfide bonds. Hydrazides can conjugate with aldehydes on oxidized cellulose surfaces, providing cellulose wet adhesion, while disulfides were reductant-responsive, providing the degradability. [9, 14, 15]

In this work, the goal was to further improve the design of degradable microgel adhesives for wet cellulose. Microgels with labile disulfide crosslinks were synthesized to support the wet-strength resin PAE. Microgel-supported PAE has great potential to perform as a degradable cellulose wet adhesive due to its excellent adsorption on cellulose surfaces, the high degradability of the microgel, the presence of adhesive azetidiniums, and the lack of chemical conjugation and organic solvents during the synthesis. The colloidal properties of this new microgel adhesive, such as electrophoretic mobilities and diameters, were measured and discussed. The wet adhesion performance and degradability were evaluated with wet-peel measurements.

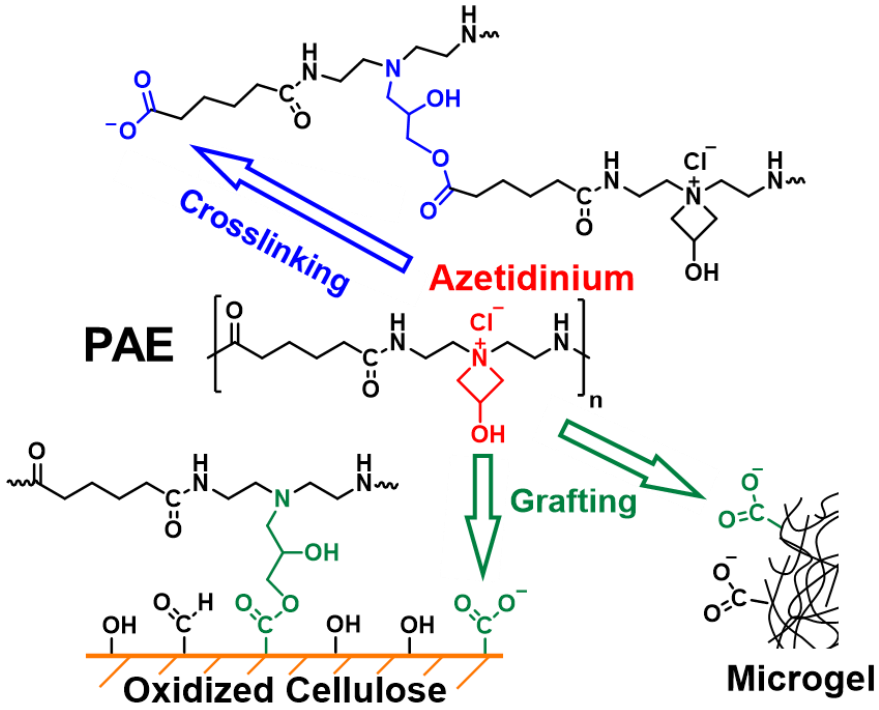

Figure 5-1 PAE structure and covalent bonding to carboxyls at the end of other PAE chains, on supporting microgels and on cellulose surfaces. Curing reactions require water removal and progress much faster if heated.[10]

5.2 Experimental Section

Materials. Regenerated cellulose membranes (Spectra/Por2, MWCO 12–14 kDa, product number 132684) were purchased from Spectrum Laboratories, US. TAPPI standard blotter papers were purchased from Labtech Instruments Inc., Canada. PAE was FENNOSTRENGTH 4063 provided by Kemira, US. PVAm with Mw 15 kDa and ~ 90% degree of hydrolysis was LUPAMIN 1595 provided by BASF, Germany. All other chemicals were purchased from Sigma-Aldrich, Canada. Water type 1 (as per ASTM D1193-6, resistivity 18MΩ/cm) were used in all experiments.

N-isopropylmethacrylamide (NIPMAm) was recrystallized with toluene/hexane (6/4, v/v) mixture solution and dried under nitrogen gas purge. The inhibitor (monomethyl ether hydroquinone) in acrylic acid (AA) was removed by passing the AA through an inhibitor remover column (Sigma-Aldrich, US). PAE was dialyzed against water for 8 hours using Spectra/Por3 dialysis tubes with MWCO 3.5 kDa (Spectrum Laboratories, US) and stored in aqueous solution at 4 °C. PVAm was dialyzed against water for one week and freeze-dried. Other chemicals were used as received.

Supporting Microgel Preparation. A series of poly(NIPMAm-co-AA) microgels was synthesized by redox-initiated precipitation polymerization.[16] The recipes are summarized in Table 5-S1. In a typical polymerization, 11.2 mmol NIPMAm, 0.15 mmol sodium dodecyl sulphate (SDS) and 0.56 mmol AA were dissolved in 80 mL water in a 250 mL round bottom flask. The mixture solution was adjusted to pH 3 with 0.1 M HCl and heated to 50 °C. The mixture solution was agitated with a magnetic stirrer bar for one hour with nitrogen gas purging, followed by the addition of 0.16 mmol *N,N,N',N'*-tetramethylethylenediamine (TEMED) in 10% water solution. After 10 minutes of agitation, 0.4 mmol ammonium persulfate (APS) in 2 mL water and 0.59 mmol *N,N'*-bis(acryloyl)cystamine (BAC) in 3 mL methanol were added into the mixture. The polymerization proceeded for six hours at 50 °C with nitrogen gas purging. The microgels were purified by dialysis against water for one week. The properties of the four synthesized supporting microgels are summarized in Table 5-1. Ax represents the supporting microgels containing x/10 mmol/g titratable carboxyls.

PAE Loading on Supporting Microgels. PAE loading recipes are shown in Table 5-S2 and the properties of microgel-supported PAE are listed in Table 5-1. In a typical process, 80 mg purified PAE was added in 60 mL 1 mM NaCl solutions at pH 7 in a 200 mL beaker. The solution was agitated vigorously with a magnetic stirrer bar for one hour. 50 mg Ax microgels were dispersed in 10 mL 1 mM NaCl solutions at pH 7 in a 20 mL glass vial. Microgel solutions were slowly added into PAE solutions at a rate of 1 mL/min with strong agitation to avoid aggregation. After the mixing, the mixture solution was agitated mildly overnight. Unloaded free PAE in the supernatant was removed by ultracentrifugation at 45,000 rpm for 30 minutes. The microgels were re-dispersed in 1 mM NaCl solutions at pH 7. The centrifugation and re-dispersion were repeated three times. Microgel-supported PAE solutions (Py-Ax) with a concentration of ~ 5 g/L were stored in aqueous solution at 4 °C.

The fraction of PAE loading on supporting microgels (y wt %, a mass ratio of PAE loading to supporting microgels) was determined by comparing the content of the total mass of PAE used in loading and the unloaded PAE separated from ultracentrifugation.[17] PAE content in solution was measured by polyelectrolyte titration. The polyelectrolyte titrations were performed using a Mutek PCD T3 titrator fitted with a Mutek PCD 03 streaming current detector (SCD) according to the method in Cui *et al.*[18] In a typical experiment, a 10 mL sample solution with 1 mM NaCl at pH 7 was loaded into the cell and was allowed to equilibrate for 5 minutes before the titration. The mixture was titrated with 1 meq/L polyvinyl sulfuric acid potassium salt (PVSK) standard solution (BTG, US). The apparatus automatically added 0.02–0.10 mL of PVSK per injection, and the SCD signal was recorded when the drift rate was below 8 mV in 10 seconds. The titration ended once the SCD signal was lower than zero. The PVSK consumption at end point was recorded. Reported values are averages of three repeated experiments and the standard deviation is reported. PAE content was determined based on a calibration curve. The calibration curve and calculation details are shown in Figure 5-S1.

Microgel-supported PVAm-A8 was prepared using the same process (Table 5-S2). In 1 mM NaCl solutions at pH 7, its hydrodynamic diameter was 357 ± 15 nm and electrophoretic mobility was 1.58 ± 0.23 (10^{-8} m^2/Vs).

Microgel Characterization. The electrophoretic mobilities of microgels were measured with a ZetaPlus analyzer (Brookhaven Instruments, US) using the phase analysis light scattering mode. Microgels were dispersed in 1 mM NaCl solution at pH 7 at 23 ºC. Reported values were averaged over 10 cycles with 10 scans for each cycle. The standard error is reported for each result.

Hydrodynamic diameters of microgels were measured by dynamic light scattering (Model BI-APD, Brookhaven Instruments, US) at 23 ºC with software version 1.0.0.1. The detection angle was 90°, and we used a 633 nm wavelength laser. At least three runs were recorded for each sample, and the standard deviation is reported. The polydispersity index was provided by the software. Microgels were measured in 1 mM NaCl solution at pH 7, unless specified.

Microgel carboxyl contents were determined by conductometric titrations, carried out with a Burivar-I2 automatic burette (ManTech Associates, Canada). 50 ± 2 mg of microgels was dispersed in 50 mL 1 mM NaCl with initial pH 2.7 ± 0.1. All samples were titrated by 0.1 M NaOH with a target increment of 0.05 pH units/injection. The corresponding injection volumes were in the range of 5–100 μL. The interval between injections was 90 seconds. Details of conductometric data analysis are given in Figure 5-S 2.

Once-dried Wet Adhesion. Regenerated cellulose membranes were prepared and 2,2,6,6-tetramethylpiperidine-1-yl)oxyl (TEMPO) oxidized according to our previous work.[14] The membranes were cut into strips, cleaned by agitating in water at 60 °C for 1 hour and then TEMPO oxidized at pH 10.5 for 15 minutes with the addition of TEMPO (6.8 mg per gram cellulose), NaBr (68 mg per gram cellulose), and NaClO (30 mg per gram cellulose). The oxidized membranes were rinsed with water and stored at 4 °C.

The laminates were prepared by “adsorption application” method described in a previous work in our lab.[19] The top membrane was 6 cm × 2 cm and the bottom one was 6 cm × 3 cm. Teflon tape (1 cm wide) was put between the two membranes at one end, making an effective adhesive area of 5 cm × 2 cm between the two membranes. In a typical adsorption application, 1 g cellulose membrane was soaked in 50 mL 0.2 g/L adhesive solution with 1 mM NaCl at pH 7 in plastic Petri dishes for 30 minutes. The non-adsorbed polymers were rinsed by soaking in rinsing solution with 1 mM NaCl at pH 7. The rinsing solution was changed three times during 10 minutes of rinsing. Two wet membranes with adsorbed polymers were laminated immediately.

The laminates were place between two blotter papers and pressed under 334 kPa for 5 minutes in a Standard Auto CH Benchtop Press (Carver, Inc., US). In this study, laminates were pressed at either room temperature or 85 °C. The samples were then dried in a room with constant temperature and humidity (23 °C, 50% relative humidity) for one day.

A freely rotating aluminum peel wheel with a diameter of 14 cm and width of 4 cm was attached to an Instron 4411 universal testing system with a 50 N load cell (Instron Corp., US). Before the wet-peeling, the laminates were rewetted for 30 minutes and then blotted free of excess water. The rewetting solution is specified in each set of results. Wet membranes were fixed to the wheel with moisture-resistant double-sided tape (medical tape 1522, 3M, US). The wet-peel force was determined as once-dried wet adhesion with a peel rate of 20 mm/min. The wet laminates were weighed before and after the delamination. The solid contents of the laminates were in the range of 47–54 wt % during the delamination. The reported wet-peel forces were the average of at least three replicates. The standard deviation is reported in the results as error bars.

Table 5-1 Properties of supporting microgels and microgels-supported PAE. All measurements were conducted in 1 mM NaCl at pH 7 at room temperature.

Microgel	PAE Loading (g PAE/g Ax)	Hydrodynamic Diameter (nm)	Poly-dispersity Index	Electrophoretic Mobility (10^{-8} m^2/Vs)	COOH Content (mmol/g)
A1	0	292±2	0.20	-0.84±0.07	0.11±0.00
A3	0	446±8	0.06	-1.57±0.05	0.33±0.01
A8	0	407±8	0.03	-1.83±0.07	0.81±0.05
A12	0	293±2	0.04	-2.27±0.09	1.15±0.01
P10-A1	9.5±3.1	249±3	0.24	1.69±0.11	-
P34-A3	34.0±2.2	415±14	0.12	2.42±0.17	-
P53-A8	52.9±4.0	461±8	0.14	2.52±0.13	-
P69-A12	69.2±5.9	395±10	0.18	2.70±0.09	-

5.3 Results

Four types of poly(NIPMAm-co-AA) microgels were synthesized as supporting microgels by redox-initiated precipitation polymerization. The supporting microgels were purified by dialysis and stored as water solutions after the synthesis. As shown in Table 5-1, the supporting microgels had particle sizes ranging from 290–450 nm, and all synthesized with 5 mol% of crosslinker (based on NIPMAm + AA). The major difference among microgels was the carboxyl content. Supporting microgels are named using the format “Ax”, where x/10 represents their carboxyl content (mmol/g). For example, A3 had a carboxyl content of 0.3 mmol/g. Carboxyl contents were measured by conductometric titrations.

In this work, redox initiation was used in polymerization to avoid the uncontrolled self-crosslinking of BAC crosslinkers, which is a common problem in thermal-initiated polymerization.[9, 16] As shown in Figure 5-2, supporting microgels with disulfide crosslinks showed excellent degradability. In exposure to the reductant dithiothreitol (DTT) at pH 9, microgels disintegrated into invisible parts in 30 minutes due to the reduction of disulfide crosslinks. The light absorbency of microgel solutions at 860 nm

decreased to almost zero in response to DTT. The reduction of disulfide facilitated by DTT is illustrated in Figure 5-3.

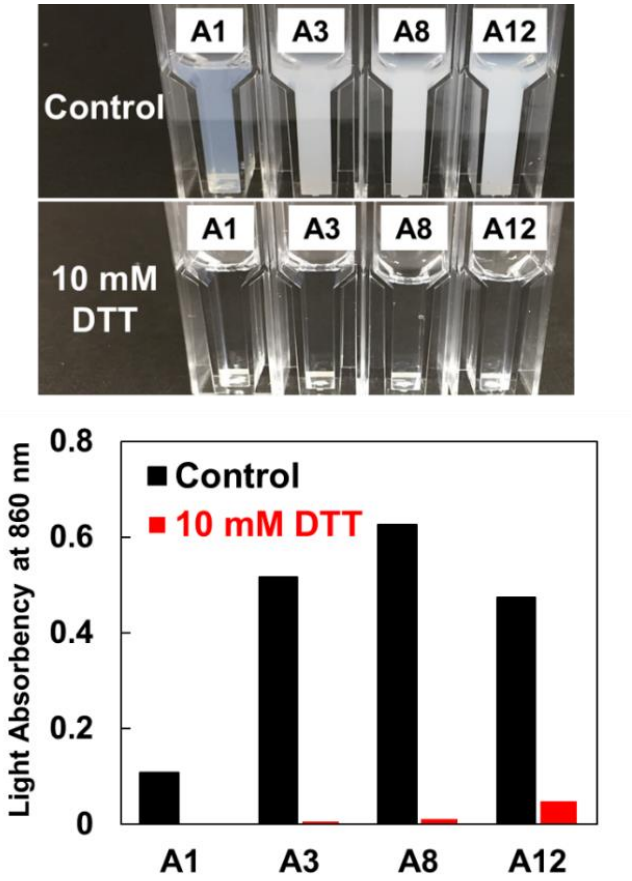

Figure 5-2 Supporting microgel solutions before (control) and after reduction (10 mM DTT). In the control group, 2 g/L microgels were dispersed in 1 mM NaCl solutions at pH 9 for 30 minutes. In 10 mM DTT group, 2 g/L microgels were dispersed in an aqueous solution of 10 mM DTT and 1 mM NaCl at pH 9 for 30 minutes. Light absorption was measured with a DU 800 Spectrophotometer (Beckman Coulter, US) at a wavelength of 860 nm.

In this work, industry-grade PAE samples were purified with dialysis and stored as solutions before the application. From the NMR spectra (Figure 5-S3), we found the content of the reactive azetidinium was 47 mol% in purified PAE. In addition to azetidinium groups, there were secondary amines (44 mol%) and tertiary amines (9 mol%) in the PAE backbone chain, along with one primary amine and one carboxyl at the end of each chain.

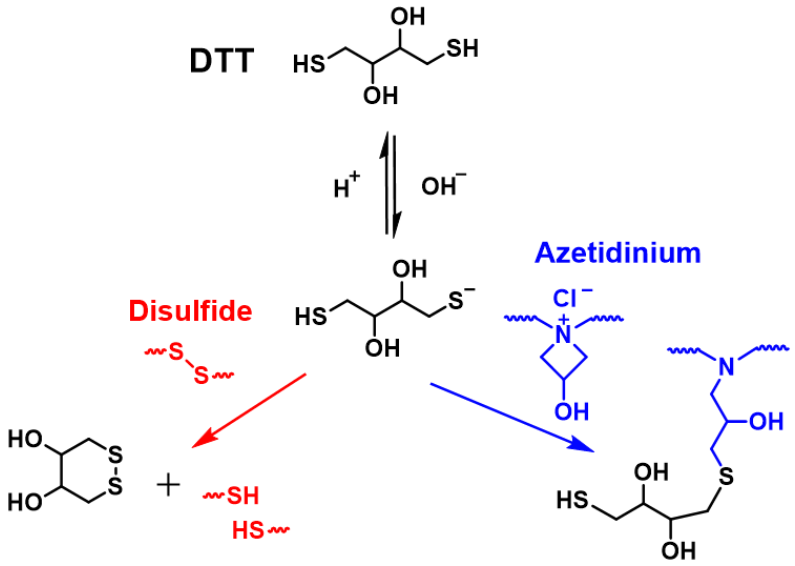

Figure 5-3 DTT structure and its reactions with disulfide and PAE in water.

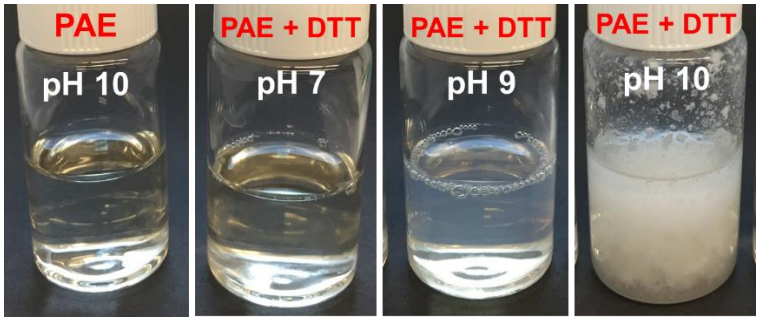

Figure 5-4 PAE precipitates in the presence of DTT at pH 10. In all the samples, 500 mg PAE was dissolved in 10 mL, 3 mM NaCl solution. In PAE + DTT samples, 200 mg DTT was dissolved in PAE solutions with the pH adjusted by 1 M NaOH. The solutions were agitated mildly for one hour before imaging.

The interaction between PAE and DTT was observed as shown in Figure 5-4. PAE solutions were mixed with DTT at various pH values. PAE formed colloids with DTT at pH 9 and formed aggregates at pH 10. It was reported that the azetidinium of PAE can react with the nucleophilic thiol group through the ring opening reaction and form a thioether bond in water.[20] The p*K*a of the first and second thiol group of DTT are 9.2 and 10.1, respectively.[15] As illustrated in Figure 5-3, at pH 9 one thiol group of DTT started to deprotonate and became reactive towards PAE. Under these conditions, DTT would

graft on PAE backbone chains via thioether bonding, which lowered the water solubility of PAE. When the pH increased to 10, both thiols of DTT became deprotonated. The fully deprotonated DTT started to crosslink PAE chains, leading to the formation of aggregates. When the solution adjusted to neutral pH, we found the aggregates did not convert back to soluble polymers.

Would DTT treatment enhance the PAE laminated cellulose joint via crosslinking? Wet adhesion of laminates with PAE adhesive layers were measured after rewetting with or without DTT. As shown in Figure 5-5, after DTT rewetting at pH 9, no significant improvement in wet adhesion was observed. These results demonstrated that rewetting in DTT solution at pH 9 did not significantly crosslink the PAE at laminate joints.

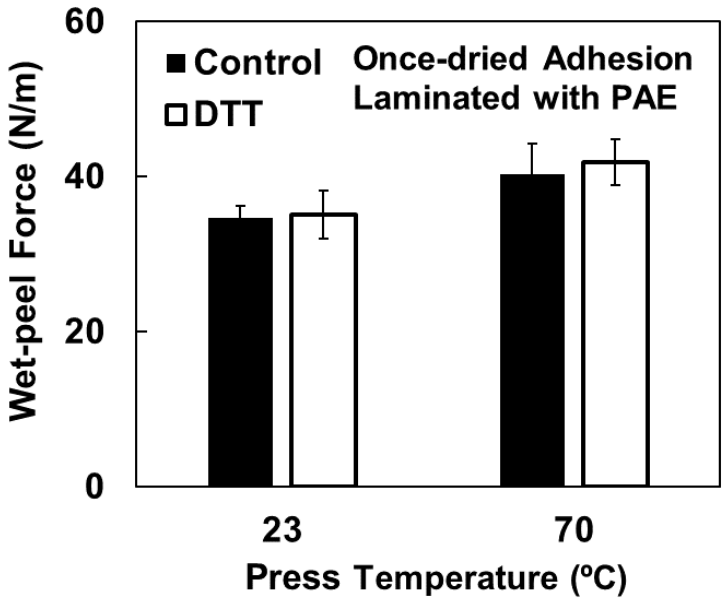

Figure 5-5 Wet adhesion of laminates prepared with PAE. The black bar represents the laminate rewetted in 1 mM NaCl at pH 9, and the white bar represents the laminate rewetted in the reducing mixture of 10 mM DTT, 1 mM NaCl at pH 9.

Cationic PAE was loaded on anionic poly(NIPMAm-co-AA) supporting microgels in 1 mM NaCl solution at pH 7, according to the recipe in Table 5-S2. PAE loading on the supporting microgels was measured by polyelectrolyte titrations. As illustrated in Figure 5-6, a higher carboxyl content of the supporting microgels led to a higher PAE loading. Since we knew the mass ratio of PAE to Ax and the charge densities of PAE and Ax, the net charge of all four Py-Ax microgels was predicted to be positive according to the calculation in Table 5-2. The same results were observed from the electrophoretic mobility measurement, where we found the mobilities positive.

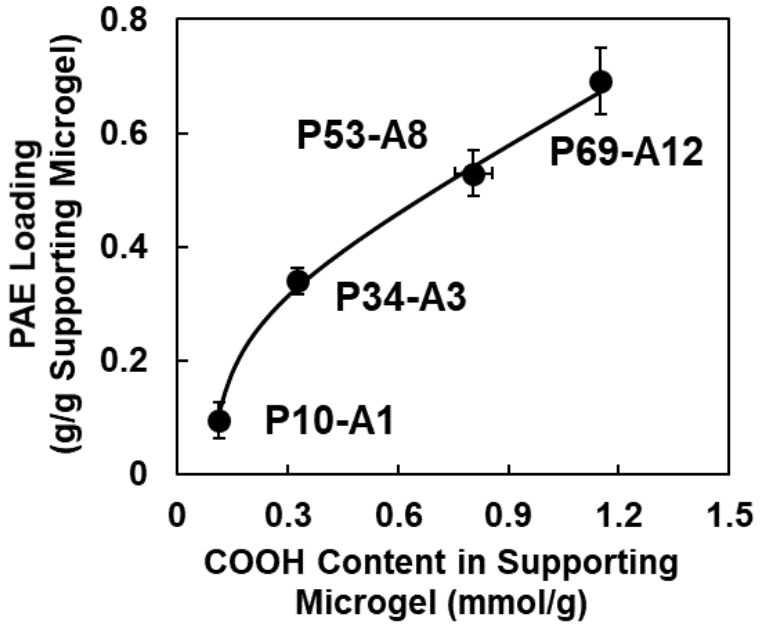

Figure 5-6 PAE binding capacity of microgels increases with carboxylic acid content of the supporting microgel. The figure is based on the results in Table 5-1.

Table 5-2 Loaded PAE overcompensates the anionic charge on supporting microgels. All results are millimoles per gram of microgel-supported PAE.

Microgel	Carboxyls in Supporting Microgel (mmol)	Titratable Cationic Charge in Loaded PAE (mmol)	Excess Cationic Group Content (mmol)
	Per Gram of Microgel-supported PAE		
P10-A1	0.100	0.186	0.086
P34-A3	0.246	0.544	0.297
P53-A8	0.530	0.741	0.211
P69-A12	0.680	0.876	0.196

PAE loading had a significant effect on hydrodynamic diameters of microgels (Table 5-1). With loaded PAE, the size of microgel particles with low carboxyl content (A1 and A3) became smaller. In contrast, the size of microgels with high carboxyl content (A8 and A12) became larger after the PAE loading. As the size distribution of Py-Ax microgels was more dispersed compared with the corresponding supporting microgels (Figure 5-S4), we believed a mild aggregation happened after the PAE loading.

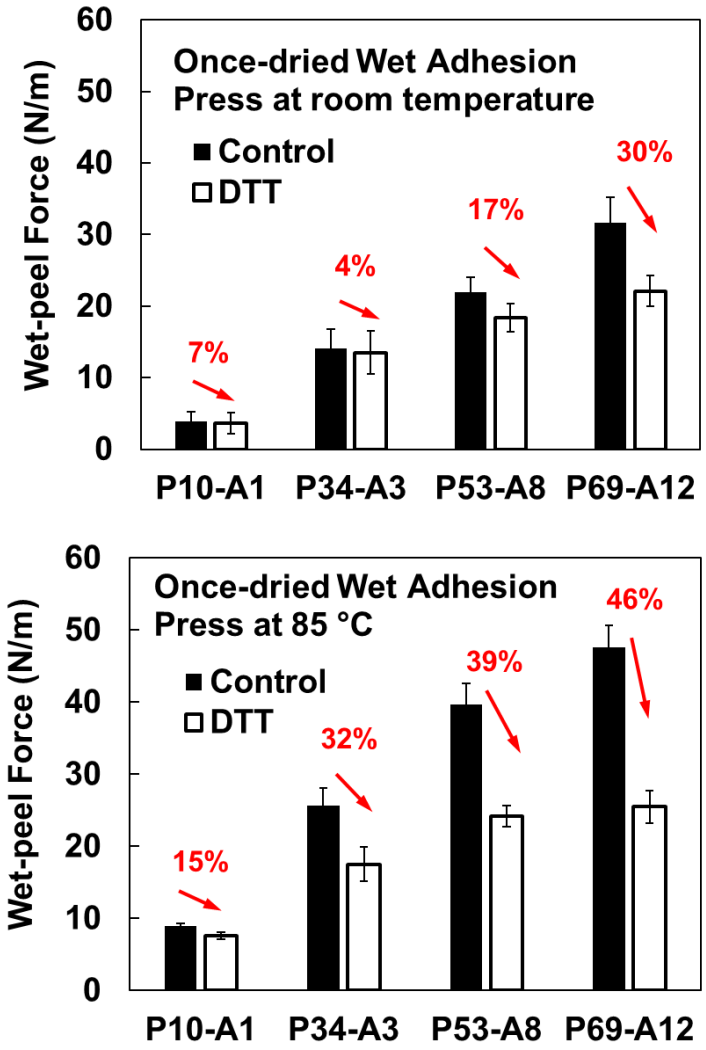

Figure 5-7 Wet adhesion of laminates rewetted with or without reductants. The control group (black) was rewetted in 1 mM NaCl at pH 9, while the DTT group (white) was rewetted in 10 mM DTT, 1 mM NaCl at pH 9. Red numbers represent the percentage decrease in wet adhesion of the DTT group compared to the control group.

In this study, cationic, PAE-loaded microgels were applied on wet, anionic cellulose membrane via the adsorption application. In each laminate, there were two layers of adsorbed microgels between cellulose surfaces. The microgel adhesive coverage was approximately 30 mg/m^2 at the laminate joint.[14] As shown in Figure 5-7, cellulose wet adhesion increased with a higher PAE loading on microgels and a higher lamination temperature. These results align with the findings reported by other researchers: 1) the higher dose of PAE led to a stronger cellulose wet adhesion until a plateau was

reached;[10, 12] 2) the higher curing temperature provided an enhanced wet cellulose joint due to a higher reactivity of azetidiniums.[10]

We predicted that a higher PAE loading on microgels would introduce a higher density of stable crosslinks within microgel structures, which would compromise the degradability of wet adhesion.[9] However, as shown in Figure 5-7, the wet adhesion of the microgel with the lowest PAE loading (P10-A1) only decreased 15% in response to DTT, whereas the wet adhesion of P69-A12 with the highest PAE loading decreased as much as 46%.

5.4 Discussion

The goal of this work was to develop a cellulose wet adhesive that provides strong wet adhesion and is degradable in the presence of reductants. Anionic poly(NIPMAm-co-AA) microgels with labile disulfide crosslinks were first synthesized as supporting microgels. Microgel-supported PAE was synthesized by loading cationic PAE on these degradable microgels via electrostatic attraction. Owing to its positive surface charge, the microgel-supported PAE can load on anionic cellulose surfaces non-selectively, making this adhesive applicable in the papermaking processes.

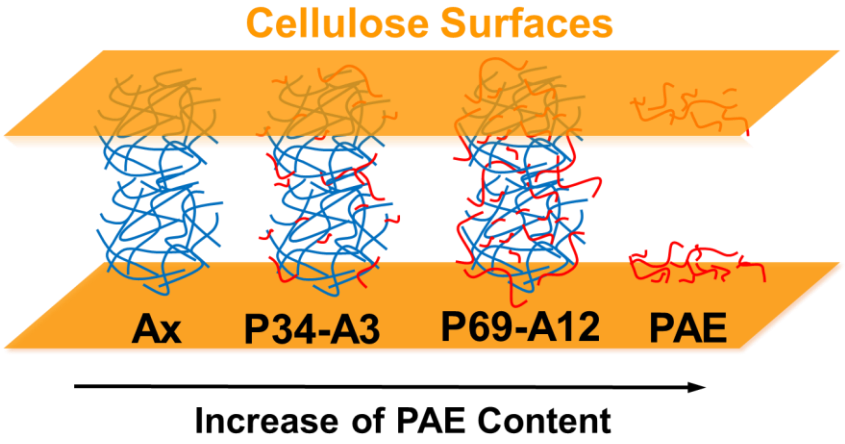

Figure 5-8 Schematic diagram of microgel-supported PAE as cellulose wet adhesives.

Microgel-supported PAE provided excellent wet adhesion especially with high-temperature lamination (Figure 5-7). Also, we found the wet adhesion increased with a higher loading of PAE. However, its wet adhesion was still not as strong as that of pure PAE. Take the laminates prepared at room temperature as an example. P69-A12 showed a wet adhesion of 32 N/m with an estimated PAE dosage of 12 mg/m^2 (assuming 30 mg/m^2 of P69-A12 at laminate joints [14]). In contrast, pure PAE provided a slightly higher

wet adhesion (35 N/m) with a lower PAE dosage, since the adsorption coverage of PAE on a smooth cellulose surface is approximately 2–3 mg/m^2.[21]

The organization of wet adhesives between cellulose surfaces are illustrated in Figure 5-8. In one extreme case, when there is only supporting microgels between cellulose, the wet adhesion should be nearly zero and the degradability should be 100%. In the other extreme case, when only PAE is applied, the wet adhesion is high (Figure 5-5) and the degradability is very limited. In Py-Ax adhesives, the PAE component provides the cellulose wet adhesion and the disulfide-crosslinked microgel provides the degradability. In this work, the most interesting phenomenon was that the highest cellulose wet adhesion (48 N/m) and the best degradability (46%) among all Py-Ax microgels were observed in one microgel (P69-A12 microgel).

The P69-A12 microgel had the highest PAE loading among all Py-Ax microgels, which guaranteed the high wet adhesion. Why did P69-A12 microgel provide a high degradability as well? We found the P69-A12 microgel also had the highest percentage of the loaded PAE located near the microgel surface, which may contribute to its good degradability. According to Hoare *et al.*,[22] acrylic acid monomers provide a uniform carboxyl distribution in microgels. When PAE and microgel mixed in an aqueous solution during the PAE loading, a part of PAE diffuses into microgel pores to form a polyelectrolyte complex with mobile anionic chains of the microgel. Based on the pore sizes of swollen microgels reported in previous works,[23-25] the supporting microgel A12 was estimated to have an average pore size of 5–10 nm. The diffusion of PAE into the microgel porous structure was possible due to the polydisperse nature of the PAE chains.[26] However, with a high carboxyl content in A12, the diffusion may become difficult due to the competition and repulsion between PAE chains.

Take P34-A3 and P69-A12 as examples. The PAE loading was proportional to the carboxyl content of the supporting microgels. The size of P34-A3 particles shrank after the PAE loading due to the formation of polyelectrolyte complexes within the microgel networks. As our lab reported earlier, the decreased osmotic pressure in microgels lowers the particle diameter.[27] By contrast, the PAE loading on A12 increased the microgel size. Besides the contribution of aggregation, according to Greinert *et al.*, this phenomenon occurs when a large amount of charged polymer is located near the microgel surface.[28] A highly charged PAE shell on the surface of P69-A12 enhances the swelling of the microgels.

We find the strong binding between microgels may be another important factor for the high degradability of wet adhesion. Both a higher PAE loading and higher lamination temperature led to a strong binding between microgels, showing a better degradability of wet adhesion in the presence of DTT. This observation was confirmed when we used PVAm in place of PAE. In this experiment, microgel-supported PVAm (PVAm-A8) was synthesized as described in Wen *et al.*[27] PVAm was loaded on anionic microgels via electrostatic attraction. The interaction between microgels was mainly electrostatic attraction, which was weaker than the covalent bonding formed between microgel-

supported PAE. As shown in Figure 5-S5, although PVAm-A8 provided a medium cellulose wet adhesion (~ 18 N/m), no degradability was observed.

Microgel-supported PAE is a promising start to create adhesives providing a strong cellulose wet adhesion that can be degraded by nearly a factor of two in the presence of reductants. As these results demonstrate, the concept of the microgel-loaded PAE offers many advantages over the degradable hydrazide-derivatized microgel adhesives (Chapter 4): 1) no hydrazide grafting required, 2) easy tuning of the adhesive chemistry by changing the loaded polymer, 3) the application of commercial polymers and 4) a higher wet adhesion. In another set of experiment, PAE was mixed with anionic microgels directly to obtain a PAE/microgel mixture adhesive, as shown in Figure 5-S6. We find the microgel-supported PAE showed a much better colloidal stability in aqueous dispersion and a higher degradability compared to this PAE/microgel mixture adhesive.

5.5 Conclusion

1. A microgel adhesive for wet cellulose was synthesized by loading PAE on carboxylated, disulfide-crosslinked microgels. Cellulose wet adhesion can be degraded by nearly a factor of two by severing the microgel crosslinks with reductants.
2. Both the cellulose wet adhesion and the degradability of the wet adhesion increased with a higher PAE loading, a higher mass ratio of PAE located near the microgel surface and a higher lamination temperature.
3. The PAE loading capacity increased with the carboxyl content of the supporting microgels. The cationic, microgel-supported PAE showed good colloidal stability in aqueous dispersion.
4. When the adsorption application was used to prepare laminates, microgel-supported PAE put more PAE in cellulose-celluloses joint compared with PAE alone. However, the cellulose wet adhesion was not improved.

References

(1) Klemm, D.; Kramer, F.; Moritz, S.; Lindström, T.; Ankerfors, M.; Gray, D.; Dorris, A. Nanocelluloses: A New Family of Nature-Based Materials. *Angewandte Chemie International Edition* **2011,** *50*, 5438-5466.

(2) Zhu, M.; Li, T.; Davis, C. S.; Yao, Y.; Dai, J.; Wang, Y.; Alqatari, F.; Gilman, J. W.; Hu, L. Transparent and Haze Wood Composites for Highly Efficient Broadband Light Management in Solar Cells. *Nano Energy* **2016,** *26*, 332-339.

(3) Pelton, R. A Model of the External Surface of Wood Pulp Fibers. *Nordic Pulp and Paper Research Journal (Sweden)* **1993**.

(4) Vlad Cristea, M.; Riedl, B.; Blanchet, P. Enhancing the Performance of Exterior Waterborne Coatings for Wood by Inorganic Nanosized Uv Absorbers. *Progress in Organic Coatings* **2010,** *69*, 432-441.

(5) Grüll, G.; Tscherne, F.; Spitaler, I.; Forsthuber, B. Comparison of Wood Coating Durability in Natural Weathering and Artificial Weathering Using Fluorescent Uv-Lamps and Water. *Eur. J. Wood Prod.* **2014,** *72*, 367-376.

(6) Gindl, W.; Schöberl, T.; Jeronimidis, G. The Interphase in Phenol–Formaldehyde and Polymeric Methylene Di-Phenyl-Di-Isocyanate Glue Lines in Wood. *International Journal of Adhesion and Adhesives* **2004,** *24*, 279-286.

(7) Kamke, F. A.; Lee, J. N. Adhesive Penetration in Wood—a Review. *Wood and Fiber Science* **2007,** *39*, 205-220.

(8) Werner, F.; Althaus, H.-J.; Richter, K. Post-Consumer Wood in Environmental Decision-Support Tools. *Schweizerische Zeitschrift fur Forstwesen* **2002,** *153*, 97-106.

(9) Yang, D.; Pelton, R. H. Degradable Microgel Wet-Strength Adhesives: A Route to Enhanced Paper Recycling. *ACS Sustainable Chemistry & Engineering* **2017,** *5*, 10544-10550.

(10) Obokata, T.; Isogai, A. The Mechanism of Wet-Strength Development of Cellulose Sheets Prepared with Polyamideamine-Epichlorohydrin (Pae) Resin. *Colloids and Surfaces A: Physicochemical and Engineering Aspects* **2007,** *302*, 525-531.

(11) Espy, H. H. The Mechanism of Wet-Strength Development in Paper: A Review. *Tappi Journal* **1995,** *78*, 90-100.

(12) Su, J.; Mosse, W. K.; Sharman, S.; Batchelor, W.; Garnier, G. Paper Strength Development and Recyclability with Polyamideamine-Epichlorohydrin (Pae). *BioResources* **2012,** *7*, 0913-0924.

(13) Kanie, O.; Tanaka, H.; Mayumi, A.; Kitaoka, T.; Wariishi, H. Composite Sheets with Biodegradable Polymers and Paper, the Effect of Paper Strengthening Agents on Strength Enhancement, and an Evaluation of Biodegradability. *Journal of Applied Polymer Science* **2005,** *96*, 861-866.

(14) Yang, D.; Gustafsson, E.; Stimpson, T. C.; Esser, A.; Pelton, R. H. Hydrazide-Derivatized Microgels Bond to Wet, Oxidized Cellulose Giving Adhesion without Drying or Curing. *ACS Applied Materials & Interfaces* **2017,** *9*, 21000-21009.

(15) Lukesh, J. C.; Palte, M. J.; Raines, R. T. A Potent, Versatile Disulfide-Reducing Agent from Aspartic Acid. *Journal of the American Chemical Society* **2012,** *134*, 4057-4059.

(16) Gaulding, J. C.; Smith, M. H.; Hyatt, J. S.; Fernandez-Nieves, A.; Lyon, L. A. Reversible Inter-and Intra-Microgel Cross-Linking Using Disulfides. *Macromolecules* **2011,** *45*, 39-45.

(17) Wen, Q.; Pelton, R. Microgel Adhesives for Wet Cellulose: Measurements and Modeling. *Langmuir* **2012,** *28*, 5450-5457.

(18) Cui, Y.; Pelton, R.; Ketelson, H. Shapes of Polyelectrolyte Titration Curves. 2. The Deviant Behavior of Labile Polyelectrolytes. *Macromolecules* **2008,** *41*, 8198-8203.

(19) Chen, W.; Leung, V.; Kroener, H.; Pelton, R. Polyvinylamine− Phenylboronic Acid Adhesion to Cellulose Hydrogel. *Langmuir* **2009,** *25*, 6863-6868.

(20) Burkinshaw, S. M.; Lei, X. P.; Lewis, D. M.; Easton, J. R.; Parton, B.; Phillips, D. a. S. Modification of Cotton to Improve Its Dyeability. Part 2 – Pretreating Cotton with a Thiourea Derivative of Polyamide–Epichlorohydrin Resins. *Journal of the Society of Dyers and Colourists* **1990,** *106*, 307-315.

(21) Ahola, S.; Österberg, M.; Laine, J. Cellulose Nanofibrils—Adsorption with Poly(Amideamine) Epichlorohydrin Studied by Qcm-D and Application as a Paper Strength Additive. *Cellulose* **2007,** *15*, 303-314.

(22) Hoare, T.; Pelton, R. Characterizing Charge and Crosslinker Distributions in Polyelectrolyte Microgels. *Current Opinion in Colloid & Interface Science* **2008,** *13*, 413-428.

(23) Bradley, M.; Vincent, B. Interaction of Nonionic Surfactants with Copolymer Microgel Particles of Nipam and Acrylic Acid. *Langmuir* **2005,** *21*, 8630-8634.

(24) Eichenbaum, G. M.; Kiser, P. F.; Dobrynin, A. V.; Simon, S. A.; Needham, D. Investigation of the Swelling Response and Loading of Ionic Microgels with Drugs and Proteins: The Dependence on Cross-Link Density. *Macromolecules* **1999,** *32*, 4867-4878.

(25) Sierra-Martin, B.; Retama, J. R.; Laurenti, M.; Fernández Barbero, A.; López Cabarcos, E. Structure and Polymer Dynamics within Pnipam-Based Microgel Particles. *Advances in Colloid and Interface Science* **2014,** *205*, 113-123.

(26) Obokata, T.; Yanagisawa, M.; Isogai, A. Characterization of Polyamideamine-Epichlorohydrin (Pae) Resin: Roles of Azetidinium Groups and Molecular Mass of Pae in Wet Strength Development of Paper Prepared with Pae. *Journal of Applied Polymer Science* **2005,** *97*, 2249-2255.

(27) Wen, Q.; Vincelli, A. M.; Pelton, R. Cationic Polyvinylamine Binding to Anionic Microgels Yields Kinetically Controlled Structures. *Journal of Colloid and Interface Science* **2012,** *369*, 223-230.

(28) Greinert, N.; Richtering, W. Influence of Polyelectrolyte Multilayer Adsorption on the Temperature Sensitivity of Poly(N-Isopropylacrylamide) (Pnipam) Microgels. *Colloid Polym Sci* **2004,** *282*, 1146-1149.

(29) Obokata, T.; Isogai, A. 1h- and 13c-Nmr Analyses of Aqueous Polyamideamine–Epichlorohydrin Resin Solutions. *Journal of Applied Polymer Science* **2004,** *92*, 1847-1854.

Supporting Information

Table 5-S1 Recipes for anionic poly(NIPMAm-co-AA) supporting microgel preparation.

Microgel	mmol in 80 mL solution					
	NIPMAm	BAC	AA	APS	TEMED	SDS
A1	11.20	0.57	0.11	0.40	0.16	0.20
A3	11.20	0.59	0.56	0.40	0.16	0.15
A8	11.20	0.64	1.68	0.40	0.16	0.12
A12	11.20	0.70	2.80	0.40	0.16	0. 15

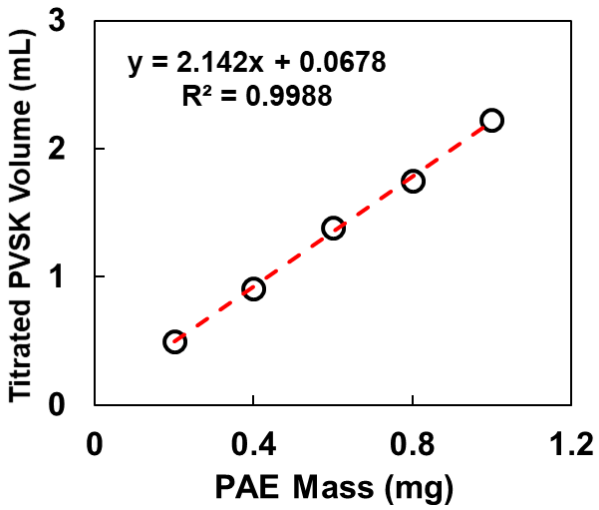

Figure 5-S1 Calibration curve of PAE titrated by 1 meq/L PVSK standard solution. Different weights of PAE were added in 10 mL 1 mM NaCl at pH 7 for titration. The charge density of PAE was calculated to be 2.14 meq/g.

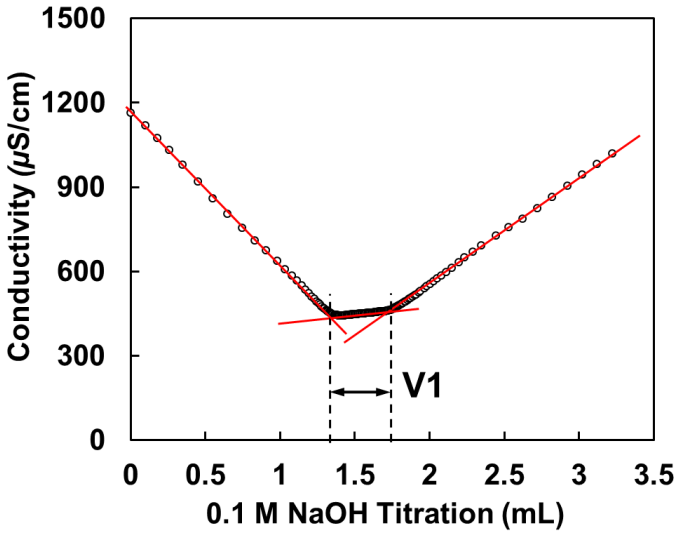

Figure 5-S2 Conductometric titration curve of A8 microgel. V1 is the volume of the consumed NaOH solution required to deprotonate carboxyl groups on the microgel. The carboxyl content of A8 microgels was calculated using V1.

Table 5-S2 Recipes for polymer loading on poly(NIPMAm-co-AA) supporting microgels.

Microgel	Microgel Addition (mg)	Polymer Addition (mg)	Polymer Loaded (mg)
P10-A1	50	40	4.7±1.5
P34-A3	50	80	17.0±0.9
P53-A8	50	120	26.5±1.4
P69-A12	50	180	34.6±1.8
PVAm-A8	50	40	4.4±0.3

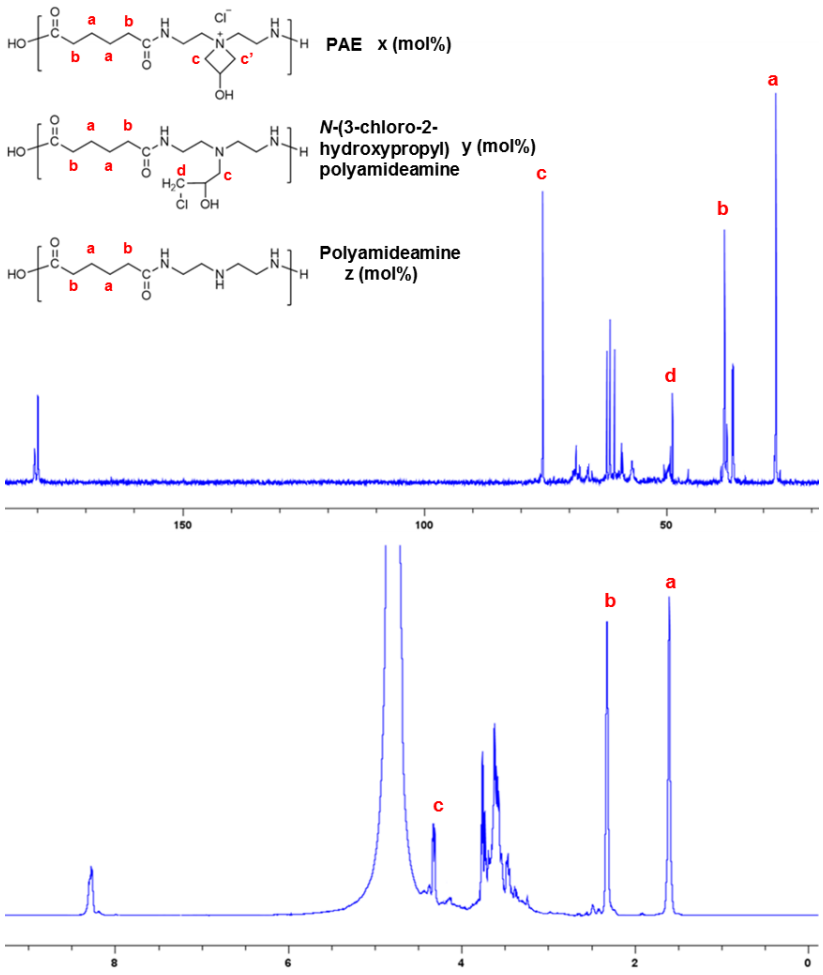

Figure 5-S3 ^{13}C (top) and ^{1}H (bottom) NMR spectra of PAE at pH 3. NMR spectra were recorded on an NMR Spectrometer (Bruker AVANCE 600 MHz, US) at room temperature with the method described in Obokata *et al.*[29] A small amount of D_2O was added into 5 wt % PAE aqueous solution for signal locking. TopSpin 3.2 software was used to analyze the spectra. We assume there are three major components in the PAE sample: PAE, *N*-(3-chloro-2-hydroxypropyl) polyamideamine and polyamideamine. The average value of x was calculated to be 47 mol %, y was 9 mol % and z was 44 mol %.

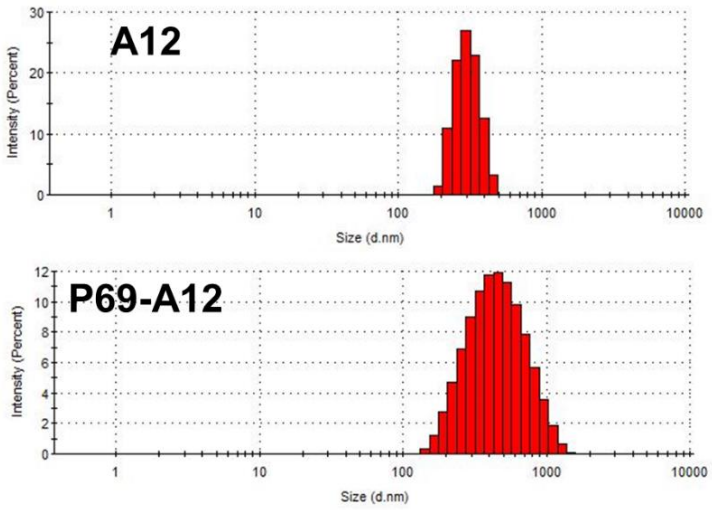

Figure 5-S4 Size distribution of microgels. Microgels were dissolved in 1 mM NaCl, pH 7 solutions for measurement at room temperature.

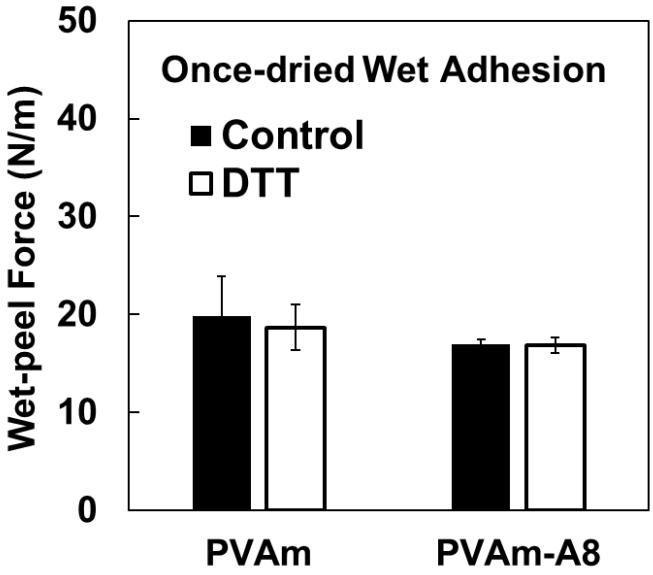

Figure 5-S5 Wet adhesion of laminates prepared with PVAm and PVAm-A8 at room temperature. The black bar represents the laminates rewetted in 1 mM NaCl at pH 9, and the white bar represents the laminates rewetted in 10 mM DTT, 1 mM NaCl at pH 9.

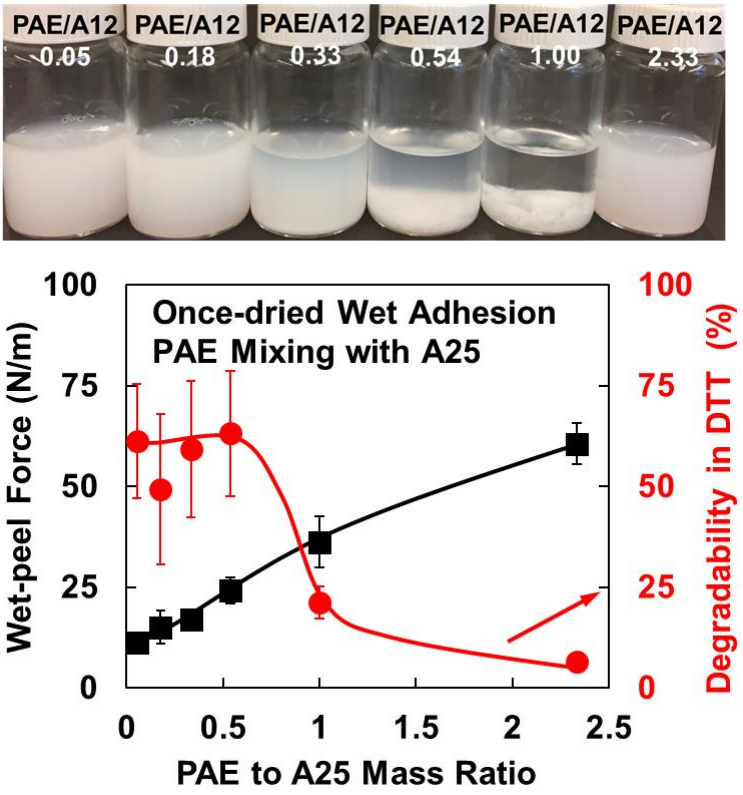

Figure 5-S6 Wet adhesion of laminates prepared with PAE/microgel mixture adhesive. The PAE/microgel mixture adhesive was prepared by directly mixing PAE solutions with supporting microgel solutions with different ratios. The mixture solutions with a concentration of 3 g/L (PAE + A25) were dispersed in 1 mM NaCl at pH 7 and agitated for one hour before the lamination. The mixture solution was applied at the laminate joint using the "direct application" as described in Chapter 4. The degradability (second y-axis) represents the ratio of laminate wet adhesion after rewetting in 10 mM DTT, 1 mM NaCl solution at pH 9 to the wet adhesion after rewetting in 1 mM NaCl at pH 9.

Chapter 6

Polyelectrolyte Adhesives for Wet Cellulose

In this chapter, the performance of a commercial cellulose wet adhesive, PVAm, was evaluated using wet-peel measurements. Many factors that influenced the cellulose wet adhesion were discussed, such as lamination methods, cellulose pre-treatments, polymer solution conditions, polymer dosage and rewetting durations. The phenomena in this chapter gave us a better understanding of thin-layer cellulose adhesives. Based on this knowledge, a novel degradable cellulose wet adhesive was developed, as described in the following chapter.

The data within this chapter were collected by me with the assistance of Taylor Stimpson, who worked with me as a summer student; Heera Marway, who conducted the AFM imaging; and Lina Liu, who conducted the radiolabeling. I summarized the data and wrote the draft myself. Dr. Joel Soucy, Dr. Anton Esser and Dr. Robert Pelton helped me analyze the results. Dr. Pelton help me re-wrote some parts of the draft.

This chapter has been submitted to *Cellulose* as an invited paper.

Polyelectrolyte Adhesion Promoters for Cellulose Hydrogel Surfaces

Dong Yang, Taylor C. Stimpson, Joel Soucy, Anton Esser, and Robert H. Pelton

POLYELECTROLYTE ADHESION PROMOTERS FOR CELLULOSE HYDROGEL SURFACES

Dong Yang,[1] Taylor C. Stimpson,[1] Joel Soucy,[2] Anton Esser,[3] and Robert H. Pelton [1]*

[1] Department of Chemical Engineering, McMaster University, 1280 Main St. West, Hamilton, Ontario, Canada L8S 4L7

[2] BASF Canada 100 Milverton Drive, 5th Floor Mississauga, ON L5R 4H1

[3] BASF AG, EVW/MI, 67056 Ludwigshafen, Germany

*R. Pelton. Email:peltonrh@mcmaster.ca

KEYWORDS

Adhesion, hydrogel, polyvinylamine, green strength, polyelectrolyte

ABSTRACT

The conditions are elucidated whereby strong adhesive joints between two wet cellulose surfaces can be achieved with a polyelectrolyte adhesive. The adhesive must be covalently grafted (or an equivalent strong bonding) to the cellulose surface – physically adsorbed polymers give weak polymer/cellulose interfaces in water. There are two cases which are remarkably different – never-dried joints versus dried and rewetted joints, we call once-dried. The strength of never-dried joints, or "green strength", is important in paper manufacturing and is likely to be critical in the manufacture of the new nanocellulose composites and foams described in the recent literature. We have observed only one adhesive joint architecture giving significant never-dried green strength - joints with only a monolayer of polyelectrolyte adhesive sandwiched between two cellulose surfaces. We propose that polymeric chains are simultaneously covalently grafted onto both cellulose surfaces. In the usual case of bringing together two polymer coated cellulose surfaces in water, there is no never-dried wet adhesion because electrosteric stabilization inhibits significant molecular contact between opposing adsorbed polymers. By contrast, high once-dried wet adhesion is easier to achieve because polymer-polymer molecular contact is promoted by water removal. The requirements for once-dried adhesion are polyelectrolyte grafting to cellulose and cohesion within polymer layers, either due to covalent crosslinking, or attractive physical interactions.

INTRODUCTION

The environmental impacts of plastic packaging, coupled with the introduction of new nanocellulose raw materials [1] have stimulated a resurgence in the development of cellulosic films, [2] foams [3] and composites.[4] In spite of the absolute water insolubility of crystalline cellulose, the Achilles heel of cellulosic materials is the impact of water. Paper and cardboard boxes are weaker when wet, nanocellulose films swell in humid conditions, and the gas permeability of cellulose films is moisture sensitive. The poor mechanical properties of wet cellulosic materials are problems during manufacture. For example, low density cellulose foams have been prepared from nanocellulose using aqueous processing. However, complex drying processes, such as critical point drying, [5] freeze-drying, [3] freeze-casting, [6]or solvent exchange [7] are required to prevent collapse of the fragile wet structures due to capillary forces during water removal. In other words, the "green strength" of materials assembled from wet nano and microscale cellulose building blocks is too low. In this paper we develop design rules for thin polymer layers promoting adhesion between cellulose hydrogel surfaces.

In nature, moisture sensitivity of cellulosic materials is a solved problem. Wood consists of strong cellulose fibers coated with hemicellulose and embedded in crosslinked lignin networks, giving tall trees and wooden ships. Man-made cellulosic materials tend to be composites made with pulp fibers, regenerated cellulose fibers and films, and more recently, various forms of nanocellulose. Paper coffee filters, wallpaper and paper kitchen towels are examples of cellulose based products that are sufficiently strong when wet because they have been strengthened by polymers called wet-strength resins that crosslink after high temperature (100-120 ºC) drying. Wet-strength resins give zero never-dried green strength because vital polymer crosslinking and grafting to cellulose does not occur in water. Therefore, when considering the adhesion between wet cellulose hydrogel surfaces, it is critical to distinguish between joints that are "never-dried", or "green joints", versus joints that have at least been "once-dried", facilitating curing of polymeric adhesives.

Developing polymer treatments giving never-dried cellulose wet strength is a real challenge. Treatment with starch aldehyde [8] is the only example in the papermaking technology literature of an individual water-soluble polymer giving never-dried wet adhesion between wood pulp fibers. Although authors have reported that chitosan gives never-dried strength, [9, 10] the strengthening is mainly at high pH where chitosan is insoluble and present on the surfaces as sticky/tacky particles. [11, 12] Herein we show for the first time that under the right conditions, polyvinylamine (PVAm - see Figure 1) promotes never-dried wet adhesion between regenerated cellulose hydrogel membranes if the membranes were mildly oxidized by TEMPO mediated oxidation. [13, 14] It has us taken more than 15 years to identify a polymer giving significant never-dried wet adhesion – we briefly summarize the milestones and the unanswered questions leading to the current work.

In 2004, we reported [15] that PVAm gives strong once-dried wet-adhesion if the cellulose were TEMPO oxidized. Based on the work of Isogai, Saito and their colleagues, [13, 14] we

knew that TEMPO mediated oxidation generates aldehydes and carboxyls on the cellulose C6. From the beginning, we proposed that imine and aminal bonding between PVAm and cellulosic aldehyde/hemiacetals was critical for wet adhesion – see structures in Figure 1.

Drying, before wet adhesion measurements, was required for strong rewetted wet joints in spite of our very mild drying conditions (23 ºC in a 50% relative humidity atmosphere) – a process we call "damp drying" because the process is slow and the final "dried samples" still contain 7 wt% water. For years we assumed and proposed that removing most of the water was required for imine and aminal bond formation. Subsequently we used XPS to quantify the aldehyde/hemiacetal contents after oxidation and showed that these values correlated with the once-dried wet adhesion, [16] supporting the hypothesis that PVAm formed covalent imine and aminal linkages with aldehyde/hemiacetal groups on the oxidized cellulose hydrogel surfaces. Further early results, published in the papermaking technology literature, suggested that once-dried wet adhesion is insensitive to PVAm molecular weight or pH from 3-9. [17]

There are lingering questions about the PVAm-oxidized wet cellulose hydrogel system. The biggest question is why is it necessary to nearly dry the joints under very mild conditions (23 ºC and 50% relative humidity) to achieve wet strength? Furthermore, is it possible to circumvent the drying step and achieve green strength with PVAm? Herein we provide answers for these questions and expose the general requirements for a polyelectrolyte adhesive giving strong never-dried cellulose/cellulose joints.

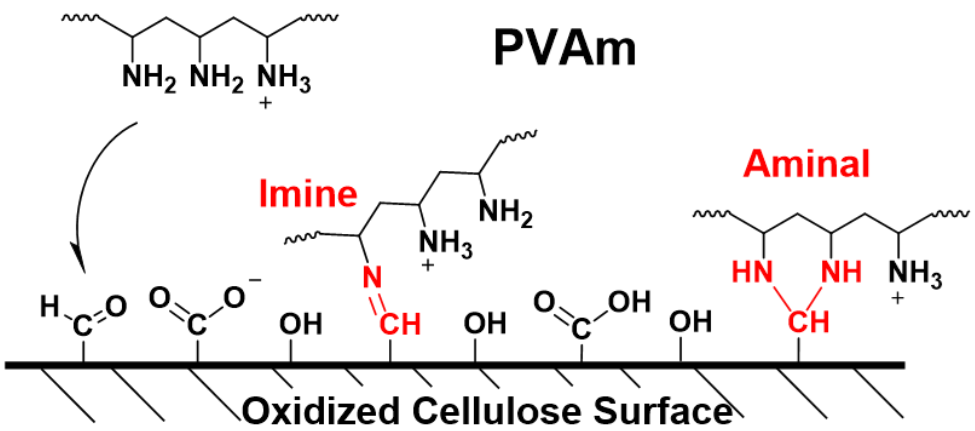

Figure 1 PVAm grafting to oxidized cellulose.

EXPERIMENTAL

Materials. Regenerated cellulose membranes (Spectra/Por2, MWCO 12-14 kDa, product number 132684) were purchased from Spectrum Laboratories, US. Blotter papers were purchased from Labtech Instruments Inc., Canada. PVAm 340 kDa (Lupamin 9095) and PVAm 15 kDa (Lupamin 1595), both with degree of hydrolysis >90%, were provided by BASF, Germany. Iodine-125 (800-1200 mCi/mL) was obtained from the McMaster University Nuclear Reactor group. All other chemicals were purchased from Sigma-Aldrich, Canada. Water type 1 (as per ASTM D1193-6, resistivity 18.2 MΩ/cm) was used in all experiments.

PVAm was purified by dialysis in water for one week and freeze-dried. Other chemicals were used as provided.

Regenerated Cellulose Membranes (C). Regenerated cellulose dialysis tubes were cut into strips, with the size of 6 cm × 2 cm for top membranes and 6 cm × 3 cm for bottom ones. The membranes were cleaned by agitating in water at 60 °C for 1 h and stored in water at 4 ºC.

TEMPO Oxidized Cellulose Membranes (TO-C). The regenerated cellulose membranes were oxidized by the method described in our previous work.[18] 68 mg TEMPO (2,2,6,6-tetramethylpiperidine 1-oxyl) was dissolved in 2 L of water along with 680 mg NaBr and followed by 300 mg NaClO. The concentration of NaClO solution was determined by available chlorine titration (TAPPI, Test Method T 611 cm-07). The pH of the solution was adjusted to 10.5, after which wet cellulose membranes (10 g dry weight) were mixed at room temperature while maintaining the pH at 10.5. After 15 minutes, the oxidation reaction was stopped by adding 10 mL ethanol. The oxidized membranes were washed by water and stored at 4 °C.

Borohydride Reduced TEMPO Oxidized Cellulose Membranes (*r*TO-C). Aldehydes of TEMPO oxidized cellulose membranes were reduced to hydroxyls by sodium borohydride treatment. Wet oxidized cellulose with a dry weight of 1 g was dispersed in 100 mL 10 mM phosphate buffer at pH 8.5, followed by the addition of 0.5 g sodium borohydride. The pH of the suspension was adjusted to 8.5 by 1 M acetic acid. The reduction proceeded at room temperature at pH 8.5 for 48 hours. After the reaction, the cellulose membranes were washed with water and stored at 4 °C.

Lamination. Polymers were applied in laminate joints by two methods, “adsorption application” and “direct application”. In a typical adsorption application, wet cellulose membranes with 1 g dry weight were soaked in 50 mL 0.2 g/L polymer solution in a plastic Petri dish for 30 min, in 1 mM NaCl at pH 7, if not specified. Non-adsorbed polymer was removed by soaking the membranes in 1 mM NaCl rinsing solution at pH 7. The rinsing solution was changed three times during 10 min of rinsing and the treated membranes were used immediately after this step. The direct application (d-Γ) was used to apply polymer solutions directly in the laminate joints. In a typical direct application experiment, 15 μL of polymer solution in 1 mM NaCl at pH 7 was carefully applied between two wet cellulose membranes. A Teflon tape (1 cm wide) separated the two wet

membranes at one end, making the effective adhesive area between the two membranes 5 cm × 2 cm.

Delamination Force Measurements – The "Wet-peel" Method. In once-dried adhesion measurements, the wet laminates were placed between two blotter papers after the lamination and pressed at 315 kPa for 5 minutes in Standard Auto CH Benchtop Press (Carver, Inc., US). The laminates were pressed at room temperature, if not specified. The samples were then dried at constant temperature and humidity (23 °C, 50% relative humidity) for one day. The wet peel force was measured using a freely rotating aluminum peel wheel with a diameter of 14 cm and width of 4 cm attached to an Instron 4411 universal testing system with 50 N load cell (Instron Corp., US). Before testing, the once-dried laminates were rewetted in 1 mM NaCl solution at pH 7 for 30 min and then blotted free of excess water. The rewetted membranes were fixed to the wheel using moisture-resistant double-sided tape (medical tape 1522, 3M, US). The peel rate was 20 mm/min. During the peeling, the solids contents of the laminates were in the range of 47 - 54 wt%. The reported wet-peel forces were the average of at least 3 replicates. The error bars of the reported results depict the standard deviation.

For never-dried adhesion measurements, wet laminates were placed between two blotter papers and pressed at 315 kPa at room temperature. The solids content of the wet laminate was controlled by varying the pressing time between 0.1 min and 8 min. The wet laminates were attached to the peel wheel immediately after the pressing step and the wet-peel force was measured using the same setup as for once-dried laminates. The reported solids content was the average value before and after the wet-peeling.

Characterization of Adsorbed PVAm. Radiolabeled PVAm was used to determine the surface coverage (mg/m^2) of adsorbed 340 kDa PVAm on cellulose membranes. First, PVAm was grafted with 4-hydroxybenzoic acid (HBA) by 1-ethyl-3-(3-dimethylaminopropyl)carbodiimide hydrochloride (EDC) mediated conjugation. 6 mg of HBA was dissolved in 30 mL of water at pH 4.7. After the dissolution of HBA, 100 mg EDC was added, followed by the addition of PVAm solution (172 mg in 20 mL water). The reaction time was 2 hours, and during the reaction the solution pH was maintained at pH 4.7. After the reaction, PVAm-HBA was dialyzed against water for 1 week. Then, PVAm-HBA with HBA DS 0.3% was radiolabeled with ^{125}I using the iodine monochloride (ICl) method developed by Brash and Sheardown. [19] The details of the ICl method are described in the supporting information. After the reaction, unbound ^{125}I was removed by passing the reaction mixture through a 3 mL syringe packed with AG1-X4 anionic exchange resins (chloride form, 100 - 200 mesh, Bio-Rad, US). Then the radiolabeled PVAm was dialyzed against water at pH 12 until the supernatant showed no radioactivity.

In a typical adsorption experiment, cellulose membranes were cut into disks with a diameter of 10 mm. The cellulose disks (6.5 mg) were soaked in 2 mL of the radiolabelled PVAm adsorption solution in a 24 well-plate for 30 min with occasional gentle shaking. The treated cellulose disks were rinsed by changing rinsing solution without polymer 3 times over 10 min. After the rinsing, excess water on the wet

membranes was blotted using a Kimwipe tissue. The radioactivity of the adsorbed PVAm was counted using a Wizard 3 1480 Automatic Gamma Counter (Perkin-Elmer, US). The coverage of radio-labelled PVAm (mg/m^2) on membranes was determined using calibration curves – see Figure S1.

RESULTS

Cellulose Hydrogel Membranes. Although our interests lie in materials based on wood pulp fibers and nanocellulose, the following adhesion experiments employ model adhesive joints in which the cellulose hydrogel substrates are regenerated cellulose membranes sold as dialysis tubing. The model joints consist of two wet membranes which are laminated with a layer of PVAm. Adhesion was characterized as the ninety-degree peel force required to separate the wet membranes. The workflow is schematically illustrated in Figure 2. We recently published a review of this technique, summarizing the impacts of the various experimental parameters. [20]

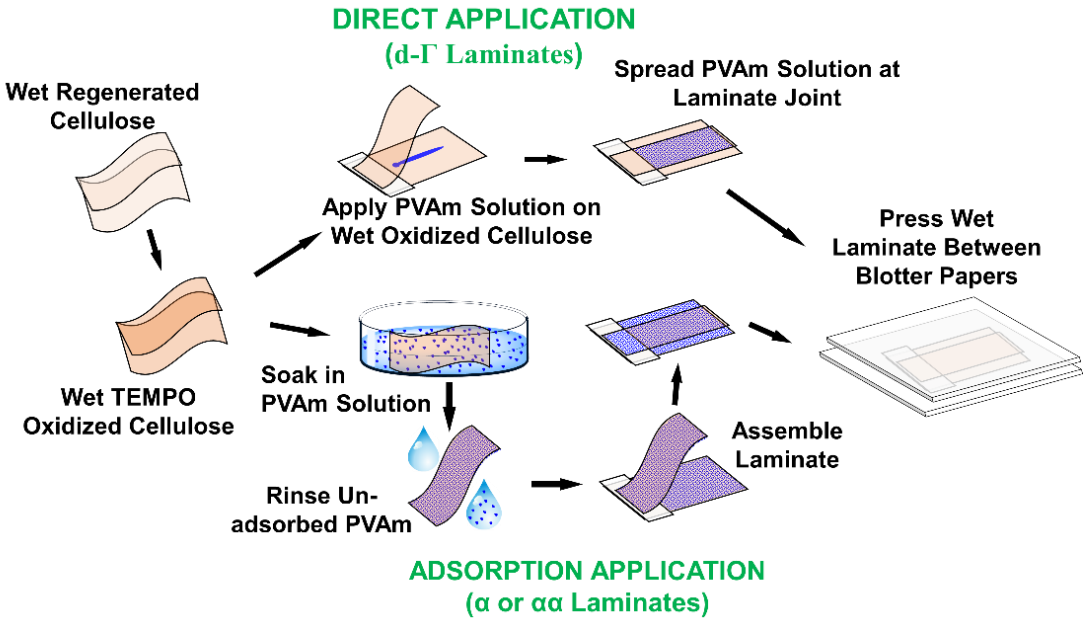

Figure 2 Never-dried laminate preparation. For once-dried experiments, the pressed laminates are dried (23 ºC and 50% RH) and then rewetted before wet peeling.

Most of the current results employed membranes pretreated by TEMPO mediated oxidation giving "TO-C membranes" with carboxyl and aldehyde/hemiacetal groups. Control experiments involved unmodified "C membranes", or oxidized membranes that were subsequently selectively reduced to convert aldehydes back to alcohols without impacting the carboxyl groups [14] giving "rTO-C membranes". Some properties of the membranes are summarized in Table S1. With a water content of 52 wt% the membranes are hydrogels.

The density of aldehyde groups on the hydrogel membrane surfaces is important. We employed a fluorescent probe assay to measure the total membrane aldehyde content, which was 9.6 μmol/g. [20] We have published images of oxidized membrane cross

sections, after treatment with an aldehyde reactive dye, suggesting a uniform aldehyde distribution. [21] To estimate the corresponding surface density, we assumed: 1) the aldehydes were uniformly distributed in the membranes; and 2) that the surface zone extended 5 nm into the membrane. Based on these assumptions, the area per surface aldehyde was 62 nm^2. For an adsorbed monolayer of PVAm 340 kDa, this corresponds to 6 surface aldehydes available for each adsorbed PVAm molecule.

Surface carboxylate groups promote PVAm adsorption. For example, exposure of unmodified C membranes to 0.2 g/L PVAm in 1 mM NaCl at pH 7, gave a saturated coverage of only 0.44 ± 0.02 mg/m^2, based on radio-labeled PVAm. Whereas for T-OC membranes the coverage was 1.90 ± 0.18 mg/m^2. We could not determine the density of carboxyl groups on our membranes. However, under similar oxidation conditions, the surface carboxyl content of wood pulp fibers was about 5 times greater than the aldehyde content. [14]

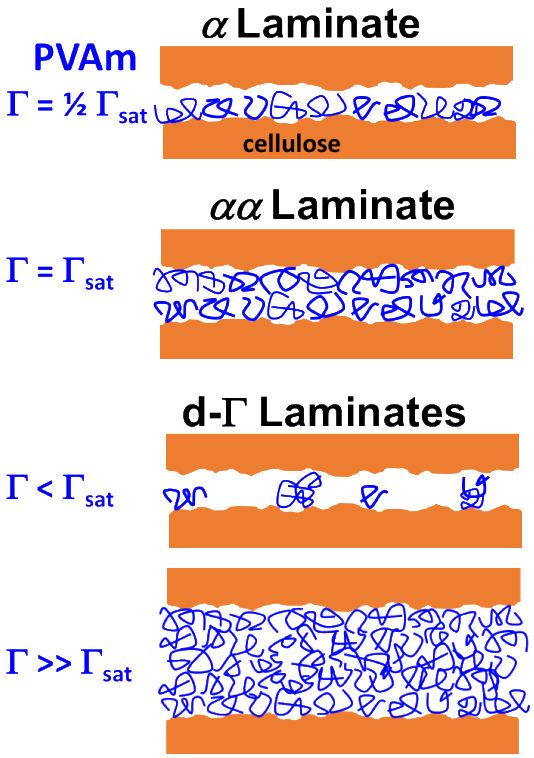

Figure 3 Schematic illustration of three types of cellulose-PVAm-cellulose laminates. The α and αα laminates were prepared by adsorbing PVAm on one (α) or both (αα) cellulose membranes, before lamination. The d-Γ laminates were prepared by directly applying concentrated PVAm solutions between the membranes. For most experiments Γ_{sat} =3.8 mg/m^2.

Adhesive Distributions in Laminates. Most of the following adhesion results involve TO-C membranes laminated with 340 kDa PVAm. Herein we define the quantity of PVAm in the joint as the coverage (Γ mg/m^2), which is the dry mass of polymer per joint area. We employed two methods for introducing PVAm into the joints – adsorption application (α or $\alpha\alpha$) and direct application (d-Γ). In the adsorption applications, one or both membranes are exposed to a PVAm solution before lamination, generating a saturated adsorbed monolayer of PVAm on the cellulose surfaces. Laminates in which both membranes are treated are called $\alpha\alpha$ laminates, whereas laminates prepared with one treated and one untreated membrane are called α laminates – see Figure 3. Under the standard adsorption conditions of 0.2 g/L PVAm in 1 mM NaCl at pH 7, the PVAm coverage in an $\alpha\alpha$ laminate was Γ_{sat} = 3.8 mg/m^2. The coverage of adsorbed PVAm was measured using PVAm radiolabeled with ^{125}I.
In direct application, a small volume of polymer solution was placed between wet membranes just before lamination. Laminates prepared by direct application are called d-Γ where Γ is coverage of dry PVAm in the joint expressed as mg/m^2. For example, a d-20 laminate was prepared by direct application giving a dry PVAm coverage in the joint of 20 mg/m^2. Figure 3 illustrates the joint architectures. Since the density of PVAm layers is close to 1 g/mL, PVAm coverages expressed as mg/m^2 also correspond to the PVAm film average dry thickness in nanometers.

Never-dried Adhesion - a Measure of Green Strength. Figure 4 compares the never-dried wet adhesion for different joint architectures. The y-axis shows the wet-peel force divided by the width of the laminate. These values represent the work per joint area required to separate the membranes. Wet-peel values below 5 N/m are low and difficult to measure accurately, whereas values approaching 60 N/m are high and often reflect membrane failure instead of delamination.

The x-axis is the overall solids content of the laminate. Most published never-dried adhesion results for cellulosic materials are expressed as a function of solids content. For example, the strength of never-dried wet paper often follows a power law relationship. [22] In our case, it is important to recognize that actual water content in the "interphase region" [23] between the membranes is unlikely to equal the overall content. To illustrate this point we measured the solids content of a membrane and of cast PVAm film as a function of relative humidity. The results showed PVAm takes up more water than cellulose (see Figure S2). Therefore, we suspect that the water content in the PVAm interphase is always higher than in the bulk cellulose membranes.

The most spectacular results in Figure 4 are the α laminates in which only one membrane surface was saturated with adsorbed PVAm. The PVAm content in these joints was only ½ Γ_{sat} = 1.9 mg/m^2. By contrast, the $\alpha\alpha$ laminates were very weak, only slightly stronger than the no PVAm data. The direct application joints, d-4.5 and d-30, were stronger than the $\alpha\alpha$ joints but were much weaker than the α laminates in spite of having high adhesive coverages. The joints with low solids content were the most challenging, and only α laminates were strong when very wet. The key distinction between α joints and the others

is that α joints have no PVAm-PVAm interfaces parallel to the membrane surfaces – see Figure 3.

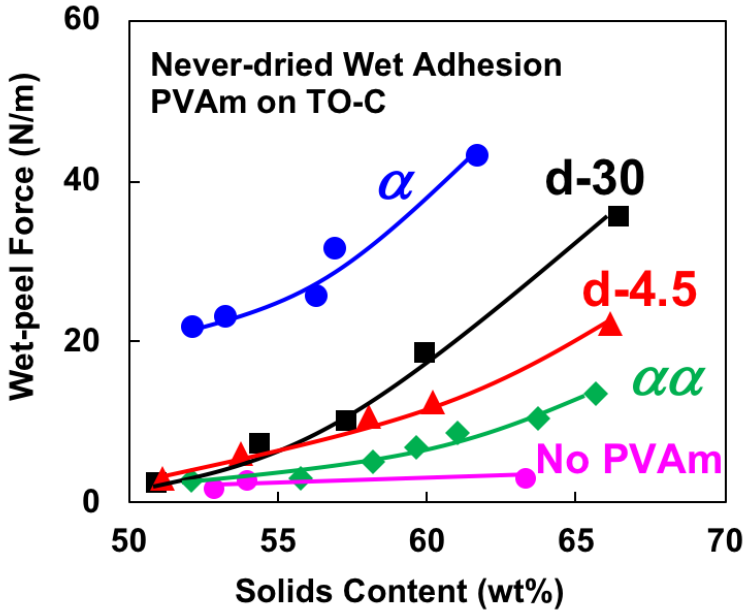

Figure 4 The strength of never-dried TEMPO oxidized cellulose membranes, laminated with PVAm 340 kDa, as a function of laminate water content, which was varied by pressing the wet laminates for various times between adsorbent blotters. The corresponding structures of the various laminate types are illustrated in Figure 3.

Finally, the α laminate results in Figure 4 illustrate the conclusion that PVAm can form covalent linkages with oxidized cellulose in water at neutral pH and room temperature. The never-dried wet-peel force for PVAm on untreated membranes are too weak to measure.

The Wet Strength of Once-dried Laminates. In our once-dried experiments, the wet laminates were stored at 23 ºC at 50% relative humidity for 24 h to dry the laminates. Under these conditions, the resulting laminates have a typical water content of 7%. Before testing they were rewetted for 30 min in 1 mM NaCl solution at pH 7.

With the adsorption application, we show below that it is possible to slightly vary the PVAm coverage in α and αα joints by varying the pH and ionic strength of the adsorption solution. With the direct application, we easily change adhesive coverages by orders of magnitude. Figure 5 shows the once-dried wet-peel delamination forces as a function of the PVAm coverage.

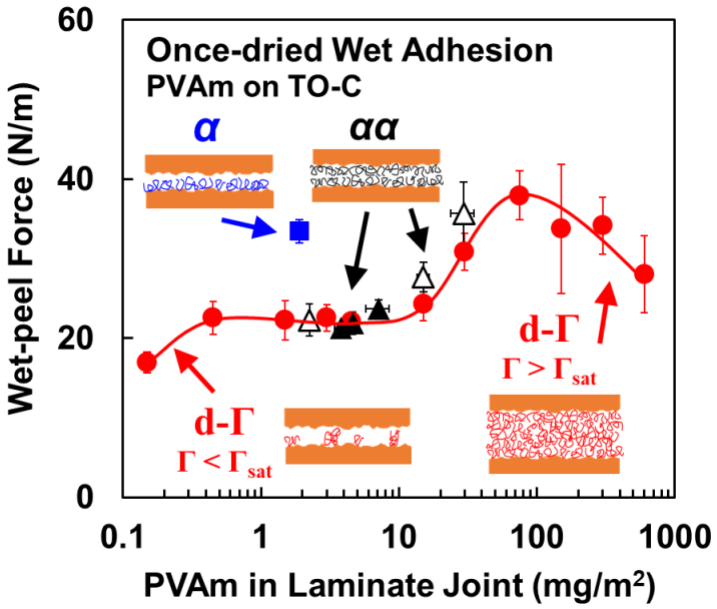

Figure 5 Once-dried wet adhesion as a function of PVAm coverage. α laminates were prepared with 0.2 g/L PVAm 340 kDa at neutral pH. αα are laminates prepared from two series of experiments; one series in which the adsorption pH was varied (open triangles – see Figure 8) and another series in which the NaCl concentration in the adsorption solution was varied (solid triangles - Figure S 5)

Mirroring the never-dried results (Figure 4), the once-dried α laminate was nearly twice as strong as the αα and d-Γ joints at the same PVAm coverage. The solids contents of the once-dried samples were about 48% after rewetting. Comparing extrapolated never-dried α results at 48 % to the once-dried α results in Figure 5 show that the drying step doubles the strength of the α laminates.

The highest wet-peel force in Figure 5 corresponded to the very high adhesive coverage of 100 mg/m^2. With thick adhesive layers, the viscoelastic dissipation in the PVAm film contributes to the delamination work. To further illustrate the relative contributions of adhesive bonds between PVAm and TO-C versus dissipation within the PVAm layer, we performed experiments where we "turned off" PVAm-cellulose adhesive bonds. Figure 6 compares wet-peel versus coverage for the three types of cellulose substrates: 1) TO-C, our standard TEMPO oxidized cellulose bearing carboxyl and aldehyde groups; 2) rTO-C, reduced TEMPO oxidized removing aldehydes but leaving carboxyls; and, 3) C, untreated cellulose membranes with neither aldehydes or carboxyls. With the unreactive substrates, (C & rTO-C) there is essentially no adhesion until PVAm coverage is above 20 mg/m^2. This result emphasizes the need for aldehyde bonding sites for PVAm. Saito

and Isogai reported a similar aldehyde reduction result for once-dried wet strength of paper sheets, strengthened with PVAm. [24]

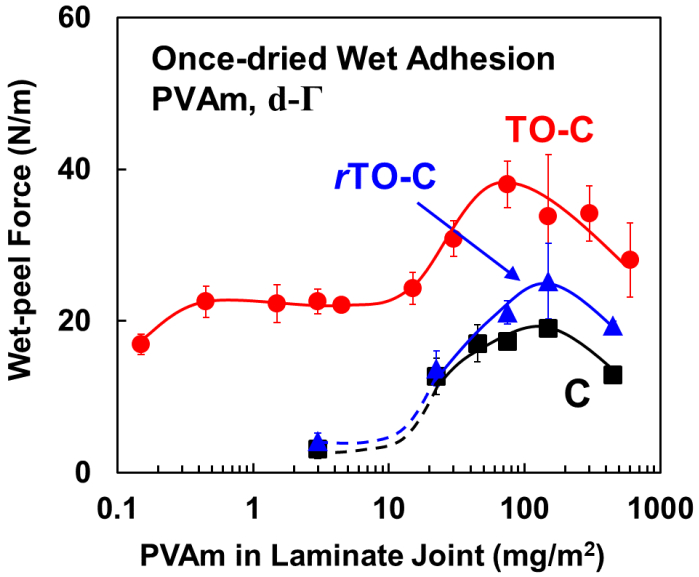

Figure 6 Once-dried wet adhesion of PVAm on cellulose surfaces: C is untreated cellulose, TO-C is TEMPO oxidize cellulose; and, rTO-C is reduced TEMPO oxidized cellulose. PVAm was applied by direct application with different PVAm concentrations in 1 mM NaCl, at pH 7.

The *r*TO-C membranes have carboxyl groups whereas the C membranes do not. Therefore, the results in Figure 6 suggest that carboxyls do not impact the cellulose/PVAm adhesion or the PVAm /PVAm cohesion. The direct application experiments do not depend upon electrostatically driven adsorption. Of course, with the adsorption application, the coverage of adsorbed PVAm does depend upon the presence of carboxyls.

Whereas aldehyde groups are critical for wet adhesion with PVAm, the following results reveal that once-dried PVAm wet adhesion is remarkably insensitive to PVAm MW, and the pH and the ionic strength of the PVAm solutions, used either for direct or adsorption application. Consider first the PVAm molecular weight. Figure 7 compares the once-dried wet adhesion for a high and low molecular weight PVAm. For low coverages ($\Gamma <$ 10 mg/m^2) the 15 kDa laminates were slightly weaker than the 340 kDa laminates. Both curves show an increase in adhesion at high coverages owing to the viscoelastic contribution of thicker PVAm layers. However, the coverage corresponding to the onset of viscoelastic contributions for PVAm 15 kDa was more than 10 times greater than for PVAm 340 kDa polymer.

For the results shown in Figure 7, we varied the concentration of PVAm solution used to prepare the d-Γ laminates. We estimated the overlap concentration, c*, from measurements of viscosity as a function concentration (see Figure S3). Joints prepared with PVAm solutions with concentrations above c* should have more entangled chains at the outset of drying, and thus may be more viscoelastic when rewetted. The coverages corresponding to the c* values are indicated on the x-axis in Figure 7. The c* values of the application solutions do not relate to any transition in adhesion behaviors of the dried and subsequently rewetted laminates.

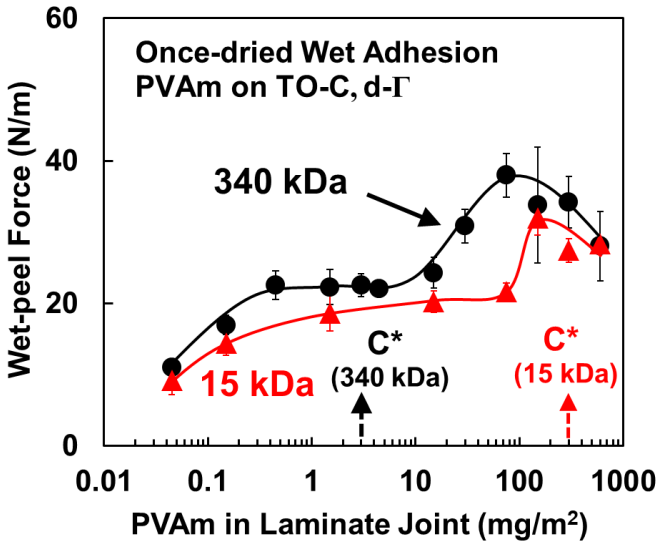

Figure 7 The influence of PVAm molecular weight on once-dried adhesion. Laminates were prepared by direct application using a range of PVAm concentrations in 1 mM NaCl solutions at pH 7. The c* values correspond to PVAm overlap concentrations.

The degree of PVAm ionization decreases almost linearly from 0.9 at pH 4 to 0.07 at pH 9.5, [25] an extreme example of the polyelectrolyte effect. Thus, one might predict a strong pH dependence on wet adhesion. However, Figure 8 shows that for the direct application experiments (d-7.5 on TO-C and d-15 on C) adhesion increased only slightly with application pH over the range pH 4 - 9.5. With adsorption application (i.e. the αα laminates) the coverage was substantially higher at pH 10.5, giving stronger joints. Also we have investigated the effects of the PVAm concentration in the adsorption solution (Figure S4), the ionic strength of PVAm solutions (see Figure S5), and, the rewetting pH (see Figure S6); none of these are very sensitive parameters.

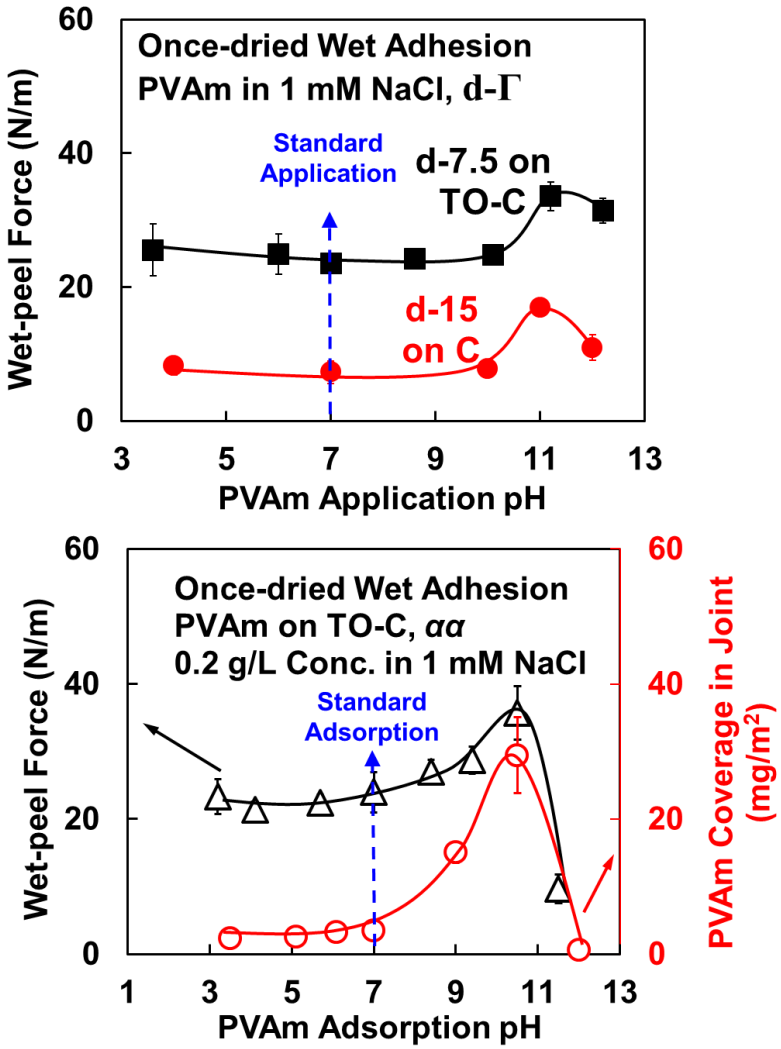

Figure 8 The influence of PVAm 340 kDa solution pH for d-7.5 laminates (top) and αα laminates (bottom). In all cases the laminates were rewetted in 1 mM NaCl, at neutral pH. Note the d-15 results were obtained using untreated cellulose membranes.

DISCUSSION

Cellulose composites include a broad range of materials from reinforced plastics to nanocellulose composite films. However, our interests herein were focused on the extreme of composite space where the materials are almost entirely cellulose with a low content of polymeric binder. In addition, we have focused on wet mechanical properties, either immediately after aqueous assembly, the never-dried green strength, or strength of materials once-dried and then rewetted. We employed laminates of TEMPO oxidized, regenerated cellulose hydrogel membranes, acting as physical models for wet cellulose-cellulose joints in paper and in other high cellulose-content composites. We now discuss the main features pointing to conclusions that extend beyond the specific PVAm/oxidized cellulose chemistry.

The only significant improvement in never-dried green strength in the presence of a polyelectrolyte binder (Figure 4) corresponded to α laminates, prepared from one membrane with a saturated adsorbed layer of PVAm laminated with a pristine oxidized membrane. High never-dried strength implies PVAm bonding to oxidized cellulose occurs in water at room temperature. Since the wet laminate strength was measured within minutes of the lamination process, PVAm covalent bonding must be rapid. We therefore propose that the strength of α laminates was due to PVAm chains being simultaneously covalently bonded to both membranes. PVAm chains simultaneously adsorbed on two glass surfaces have been shown to promote adhesion. [26]

The implication of our results is that wet cellulose composites with high green strength can be achieved by exclusively employing α joint structures in all cellulose-cellulose contacts. However, manufacturing cellulose composites solely based on α joints is an enormous challenge. In papermaking, essentially a continuous filtration operation, one could imagine adding just enough polymeric adhesive to coat half the fiber surfaces before filtration. However, the resulting paper structure would have a combination of α fiber-fiber joints, αα joints, and joints with no polymer. Similarly, when casting or templating nanocellulose suspensions into macroscopic bodies, it is impossible to generate only α joints. Therefore, we conclude that never-dried strength from α joints although mechanistically interesting, has little practical significance.

By contrast, αα joints are easy to manufacture – simply saturate the available surfaces with adsorbed polymer before forcing the surfaces into contact. However, another important lesson illustrated in this work, and reported by others, [27, 28] is that cellulose surfaces coated with hydrophilic polyelectrolyte adhesives have low never-dried strength because electrosteric stabilization prevents never-dried surfaces from establishing sufficiently close contact for adhesive interactions to take place. We believe that green strength from αα joint structures is possible. For example, never-dried polymer cohesion could be achieved by reducing the electrosteric repulsion by employing grafted surface polymers that have a low excess charge and are close to being water insoluble. Both the electrostatic and the osmotic contributions to repulsion would be less than with highly

water-swollen and polyelectrolytes. Green strength from αα joints remains an open challenge.

For completeness, we acknowledge that we [29] and others [30] [31] have shown that the sequential addition of a second polymer can lead to green strength by forming αββα joint structures. Similarly, thick layer-by-layer assemblies giving green strength have been reported. [31] Our focus herein however is on achieving strong wet adhesion with a single polymeric binder.

For once-dried wet adhesion, commercial papermaking wet strength resins that can give excellent once-dried wet adhesion, employ reactive aldehyde [32] or azetidinium groups [33] that give inter and intramolecular crosslinks, as well as covalent grafts to cellulose. PVAm grafted to oxidized cellulose also gives significant once-dried adhesion (Figure 5). However, PVAm does not form crosslinks with itself. We used to believe that drying αα laminates was required to drive covalent bonding of PVAm to oxidized cellulose (Figure 1). However, as discussed above, we now have evidence that bonding is spontaneous in water at room temperature. Instead, we propose that partial drying of αα PVAm laminates is required to eliminate the electrosteric repulsion between facing layers of cellulose grafted PVAm. With water removal the PVAm layers can intermix developing cohesive physical interactions. Not all grafted polyelectrolytes are sufficiently cohesive to give once-dried wet adhesion. For example, firmly attached carboxymethylcellulose gives αα joints without never-dried or once-dried wet strength. [34]

The directly applied d-Γ joints can have high PVAm coverages, giving thick PVAm layers in the joints. Such materials could be prepared by casting fiber or nanocellulose suspensions in concentrated polymer solutions, or by spraying application after the forming section on the paper machine.[35] As with αα joints, d-Γ laminates give poor never-dried wet strength (see Figure 4), however, the once-dried laminates required the most work to induce laminate failure when the PVAm coverage was 100 mg/m^2, which was about 50 times greater than the coverage for an α laminate. In general, the laminates with PVAm coverages less than 10 mg/m^2 could be left in water indefinitely (2000 h is our longest datum [36]) without strength loss whereas the strength of high PVAm coverage laminates rapidly declined with soaking time – see Figure S7.

In summary, we have demonstrated that the wet adhesion, once-dried and never-dried, is sensitive to adhesive distribution (α vs αα vs d-Γ) in wet cellulose joints. An unanswered challenge is the design of polymers that give strong, never-dried αα joints.

CONCLUSION

Determined were some factors influencing the wet strength of never-dried and once-dried adhesives joints prepared from wet, TEMPO oxidized, regenerated cellulose membranes laminated with PVAm. These results illustrate the following general requirements for cellulose hydrogel adhesives:

1. The polymer in contact with the cellulose surface must form covalent grafts or some other linkage with equivalent strength. For never-dried joints, grafting must occur in the presence of water.
2. The only way to achieve never-dried strength with a hydrophilic polyelectrolyte is by forming α joints that have a single layer of grafting polymer simultaneously attached to both substrate surfaces. With αα joints, where both surfaces are polymer coated, electrosteric stabilization (repulsion) inhibits polymer-polymer contact and thus cohesion within the polymer layer.
3. Once-dried joints with strong wet strength are easier to achieve because drying removes the electrosteric repulsion, allowing polymer coated surfaces to come into molecular contact. However, the contacting polymer layers must have significant cohesion after rewetting in water. Not all water-soluble polymers are cohesive. For example, once-dried PVAm gives intermediate wet cohesion, whereas grafted carboxymethylcellulose gives none. [34]
4. With thick adhesive layers obtainable by casting cellulose with adhesive solutions, viscous dissipation within the water swollen polymer layer contributes to the work required for once-dried joint failure. However, thick layers of non-crosslinked polymer slowly swell, weakening the joints with time.

ASSOCIATED CONTENT

Supporting Information

The Supporting Information is available free of charge on the Publications website

The file contains - a table of membrane physical properties – details for the aldehyde assay – moisture content vs relative humidity for a membrane and a PVAm film – viscosity data used to estimate c* - the influence of PVAm adsorption concentration of αα wet adhesion – the influence of NaCl concentration of adsorption and adhesion – the influence of rewetting solution pH – the influence of rewetting time on wet adhesion.

ACKNOWLEDGEMENT

BASF Canada is acknowledged for funding this project through a grant to RP entitled "Understanding Cellulose Interactions with Reactive Polyvinylamines". Dr. Emil Gustafsson is thanked for useful discussions and Dr. Lina Liu for help with the radio isotope experiments in Professor Sheardown's laboratory. Some measurements were performed in the McMaster Biointerfaces Institute funded by the Canadian Foundation for Innovation. R.P. holds the Canada Research Chair in Interfacial Technologies.

REFERENCES

(1) Klemm, D.; Kramer, F.; Moritz, S.; Lindström, T.; Ankerfors, M.; Gray, D.; Dorris, A. Nanocelluloses: A New Family of Nature-Based Materials. *Angew. Chem., Int. Ed.* **2011,** *50*, 5438-5466.

(2) Capron, I.; Rojas, O. J.; Bordes, R. Behavior of Nanocelluloses at Interfaces. *Curr. Opin. Colloid Interface Sci.* **2017,** *29*, 83-95.

(3) Cervin, N. T.; Aulin, C.; Larsson, P. T.; Wagberg, L. Ultra Porous Nanocellulose Aerogels as Separation Medium for Mixtures of Oil/Water Liquids. *Cellulose* **2012,** *19*, 401-410.

(4) Dufresne, A., *Nanocellulose: From Nature to High Performance Tailored Materials*. Walter de Gruyter: 2012.

(5) Sehaqui, H.; Zhou, Q.; Ikkala, O.; Berglund, L. A. Strong and Tough Cellulose Nanopaper with High Specific Surface Area and Porosity. *Biomacromolecules* **2011,** *12*, 3638-3644.

(6) Wicklein, B.; Kocjan, A.; Salazar-Alvarez, G.; Carosio, F.; Camino, G.; Antonietti, M.; Bergström, L. Thermally Insulating and Fire-Retardant Lightweight Anisotropic Foams Based on Nanocellulose and Graphene Oxide. *Nat Nano* **2015,** *10*, 277-283.

(7) Jin, H.; Nishiyama, Y.; Wada, M.; Kuga, S. Nanofibrillar Cellulose Aerogels. *Colloids and Surfaces A: Physicochemical and Engineering Aspects* **2004,** *240*, 63-67.

(8) Laleg, M.; Pikulik, I. I. Improving Paper Machine Runnability and Paper Properties by a Polymeric Additive. *J. Pulp Paper Sci.* **1991,** *17*, J206-J216.

(9) Allan, G. G.; Fox, J. R.; Crosby, G. D.; Sarkanen, K. V. In *Chitosan, a Mediator for Fibre-Water Interactions in Paper*, Fibre-Water Interactions in Papermaking, Oxford, UK, Committee, F. R., Ed. Technical Division, The British Paper and Board Fed., London, UK Oxford, UK, 1978; pp 765-794.

(10) Laleg, M.; Pikulik, I. I. Wet-Web Strength Increase by Chitosan. *Nordic Pulp & Paper Research Journal* **1991,** *6*, 99-103, 109.

(11) Myllytie, P.; Holappa, J.; Laine, J. Effect of Polymers on Aggregation of Cellulose Fibrils and Its Implication on Strength Development in Wet Paper Web. *Nordic Pulp and Paper Research Journal* **2009,** *24*, 125-134

(12) Myllytie, P.; Salmi, J.; Laine, J., *The Influence of Ph on the Adsorption and Interaction of Chitosan with Cellulose*. 2009; Vol. 4.

(13) Kitaoka, T.; Isogai, A.; Onabe, F. Chemical Modification of Pulp Fibers by Tempo-Mediated Oxidation. *Nordic Pulp & Paper Research Journal* **1999,** *14*, 279-284.

(14) Saito, T.; Isogai, A. Introduction of Aldehyde Groups on Surfaces of Native Cellulose Fibers by Tempo-Mediated Oxidation. *Colloids Surf. A* **2006,** *289*, 219-225.

(15) Kurosu, K.; Pelton, R. Simple Lysine-Containing Polypeptide and Polyvinylamine Adhesives for Wet Cellulose. *J. Pulp Paper Sci.* **2004,** *30*, 228-232.

(16) Diflavio, J. L.; Pelton, R.; Leduc, M.; Champ, S.; Essig, M.; Frechen, T. The Role of Mild Tempo-Nabr-Naclo Oxidation on the Wet Adhesion of Regenerated Cellulose Membranes with Polyvinylamine. *Cellulose* **2007,** *14*, 257-268.

(17) Diflavio, J. L.; Bertoia, R.; Pelton, R.; Leduc, M., The Mechanism of Polyvinylamine Wet-Strengthening. In *Advances in Paper Science and Technology: Transactions of the 13th Fundamental Research Symposium*, SJ, I. A., Ed. Pulp & Paper Fundamental Research Society: Cambridge, UK, 2005; Vol. 1, pp 1293-1316.

(18) Yang, D.; Gustafsson, E.; Stimpson, T. C.; Esser, A.; Pelton, R. H. Hydrazide-Derivatized Microgels Bond to Wet, Oxidized Cellulose Giving Adhesion without Drying or Curing. *ACS Applied Materials & Interfaces* **2017,** *9*, 21000-21009.

(19) Weeks, A.; Boone, A.; Luensmann, D.; Jones, L.; Sheardown, H. The Effects of Hyaluronic Acid Incorporated as a Wetting Agent on Lysozyme Denaturation in Model Contact Lens Materials. *Journal of Biomaterials Applications* **2013,** *28*, 323-333.

(20) Yang, D.; Diflavio, J.; Gustafsson, E.; Pelton, R. Wet-Peel: A Tool for Comparing Wet-Strength Resins. *Nordic Pulp & Paper Research Journal* **2018**.

(21) Liu, J.; Pelton, R.; Obermeyer, J. M.; Esser, A. Laccase Complex with Polyvinylamine Bearing Grafted Tempo Is a Cellulose Adhesion Primer. *Biomacromolecules* **2013,** *14*, 2953−2960.

(22) Shallhorn, P. M. Effect of Moisture Content on Wet-Web Tensile Properties. *J. Pulp Paper Sci.* **2002,** *28*, 384-387.

(23) Sharpe, L. H. Some Fundamental Issues in Adhesion: A Conceptual View. *J. Adhesion* **1998,** *67*, 277-289.

(24) Saito, T.; Isogai, A. Wet Strength Improvement of Tempo-Oxidized Cellulose Sheets Prepared with Cationic Polymers. *Ind. Eng. Chem. Res.* **2007,** *46*, 773-780.

(25) Katchalsky, A.; Mazur, J.; Spitnik, P. Polybase Properties of Polyvinylamine. *J. Polym. Sci.* **1957,** *23*, 513-530.

(26) Poptoshev, E.; Rutland, M. W.; Claesson, P. M. Surface Forces in Aqueous Polyvinylamine Solutions. I. Glass Surfaces. *Langmuir* **1999,** *15*, 7789-7794.

(27) Alince, B.; Vanerek, A.; De Oliveira, M. H.; Van De Ven, T. G. M. The Effect of Polyelectrolytes on the Wet-Web Strength of Paper. *Nordic Pulp & Paper Research Journal* **2006,** *21*, 653-658.

(28) Österberg, M. The Effect of a Cationic Polyelectrolyte on the Forces between Two Cellulose Surfaces and between One Cellulose and One Mineral Surface. *Journal of colloid and interface science* **2000,** *229*, 620-627.

(29) Gustafsson, E.; Pelton, R.; Wågberg, L. Rapid Development of Wet Adhesion between Carboxymethylcellulose Modified Cellulose Surfaces Laminated with Polyvinylamine Adhesive. *ACS Applied Materials & Interfaces* **2016,** *8*, 24161-24167.

(30) Aarne, N.; Vesterinen, A.-H.; Kontturi, E.; Seppälä, J. V.; Laine, J. A Systematic Study of Non-Crosslinking Wet Strength Agents. *Ind. Eng. Chem. Res.* **2013**.

(31) Wu, T.; Farnood, R. Cellulose Fibre Networks Reinforced with Carboxymethyl Cellulose/Chitosan Complex Layer-by-Layer. *Carbohydrate Polymers* **2014,** *114*, 500-505.

(32) Espy, H. H. The Mechanism of Wet-Strength Development in Paper: A Review. *Tappi Journal* **1995,** *78*, 90-99.

(33) Wagberg, L.; Bjorklund, M. On the Mechanism Behind Wet Strength Development in Papers Containing Wet Strength Resins. *Nordic Pulp & Paper Research Journal* **1993,** *8*, 53-58.

(34) Myllytie, P.; Yin, J.; Holappa, S.; Laine, J. The Effect of Different Polysacharides on the Development of Paper Strength During Drying. *Nordic Pulp and Paper Research Journal* **2009,** *24*, 469-477.

(35) Vishtal, A.; Retulainen, E. Improving the Extensibility, Wet Web and Dry Strength of Paper by Addition of Agar. *Nordic Pulp and Paper Research Journal* **2014,** *29*, 434-444.

(36) Diflavio, J.-L. The Wet Adhesion of Polyvinylamine to Cellulose. Ph.D. Thesis, McMaster University, Hamilton, Canada, 2013.

SUPPORTING INFORMATION

POLYELECTROLYTE ADHESION PROMOTERS FOR CELLULOSE HYDROGEL SURFACES

Dong Yang,[1] Taylor C. Stimpson,[1] Joel Soucy,[2] Anton Esser,[3] and Robert H. Pelton [1]*

[1] Department of Chemical Engineering, McMaster University, 1280 Main St. West, Hamilton, Ontario, Canada L8S 4L7

[2] BASF Canada 100 Milverton Drive, 5th Floor Mississauga, ON L5R 4H1

[3] BASF AG, EVW/MI, 67056 Ludwigshafen, Germany

*R. Pelton. Email:peltonrh@mcmaster.ca

Table S1 Properties of wet cellulose membranes. C and TO-C membranes were dried at room temperature. PVAm-ads-TO-C was prepared by PVAm adsorption on TO-C membranes and then air-dried. All membranes were rewetted before the measurement and had a wet thickness of 130 ± 10 μm.

	C	TO-C	PVAm-ads-TO-C
Wet roughness, nm	15 ± 6[a]	8 ± 1[a]	-
Dry roughness, nm	7 ± 1[a] 302 ± 14 [b]	6 ± 3[a]	-
Water content after blotting, wt%	53 ± 1	51 ± 1	51 ± 1
Elastic modulus, MPa	91 ± 4	99 ± 5	100 ± 8
Tensile strength, MPa	24 ± 2	13 ± 1	17 ± 1
Strain at break	78 ± 6 %	34 ± 7 %	49 ± 5 %
Area per surface aldehyde	0	62 nm^2	NA

[a] Root mean squared roughness calculated by AFM imaging in an area 5 µm × 5 µm. [b] Root mean squared roughness calculated from profilometer image (0.9 mm × 1.2 mm) in Appendix B, DiFlavio et al. [36]

Preparation of ICl Solution. 150 mg NaI was dissolved in 8 mL of 6 M HCl. 108 mg $NaIO_3 \cdot H_2O$ was dissolved in 2 mL water. The two solutions were mixed, and water was added to make the final volume 40 mL. 5 mL CCl_4 was added and shaken vigorously. This step was repeated until there was no pink color in the organic phase. The residual CCl_4 was removed by aerating the solution. Water was added to make the final volume 45 mL. For the labeling procedure 1 part of the above ICl solution was mixed with 9 parts of 2 M NaCl. The final solution was 0.0033 M ICl in 1.8 M NaCl.

ICl Method. 2 M glycine solution in 2 M NaCl at pH 8.8 was prepared and the pH was adjusted by adding NaOH. Solution A was prepared by mixing 1 mL 5 g/L PVAm-HBA and 200 µL glycine buffer. Solution B was prepared by mixing 565 µL ICl solution and 2260 µL glycine buffer. Then solutions A and B were mixed for 2 min. 10 µL ^{125}I was added to the mixture and stirred for 15 min. After the reaction, the radiolabeled PVAm was purified as described in method section.

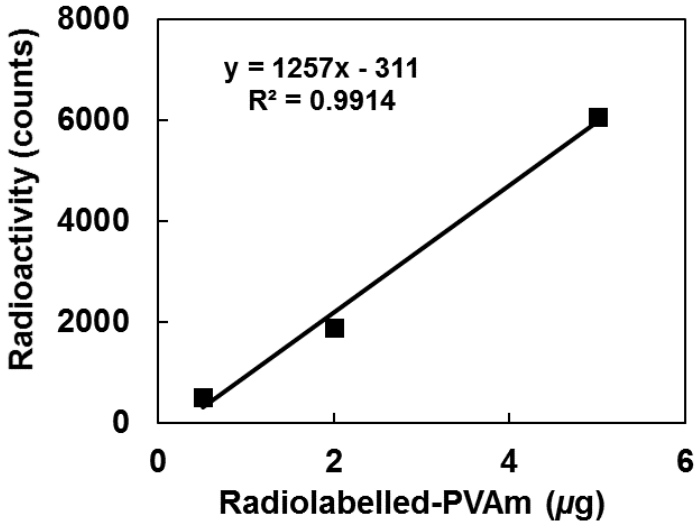

Figure S1 The calibration curve determining the mass of radiolabelled-PVAm adsorbed on cellulose membranes.

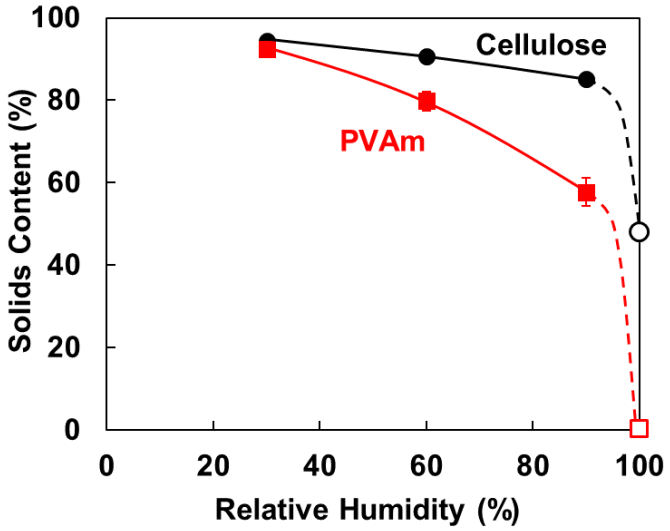

Figure S2 The solids content of cast PVAm films and TEMPO oxidized regenerated cellulose membranes as functions of the relative humidity. The extrapolated values at 100% RH were based on water content of fully wetted membranes (Table S1) and c* for PVAm.

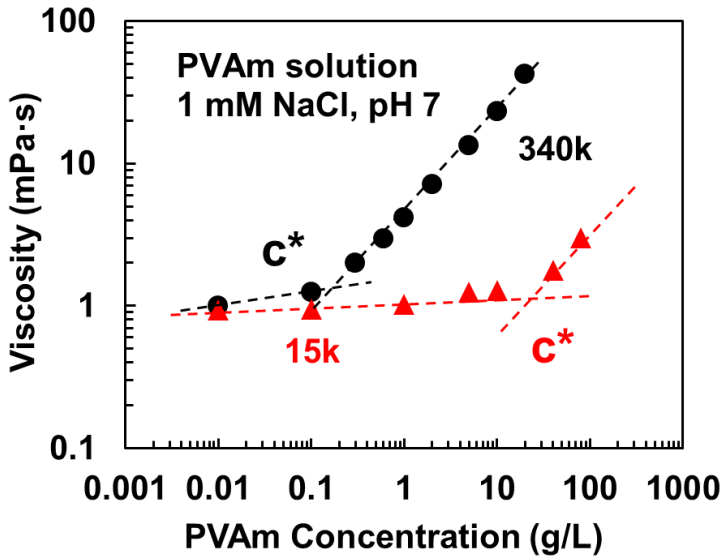

Figure S3 The viscosity of PVAm solutions as functions of concentration. Measurements were made with a Sine-Wave Vibro Viscometer (SV-10, A&D Company) at 23.5 °C. The inflection point in the viscosity curves gave the overlap concentration, c*, which was 0.2 g/L for PVAm 340 kDa and 20 g/L for PVAm 15 kDa.

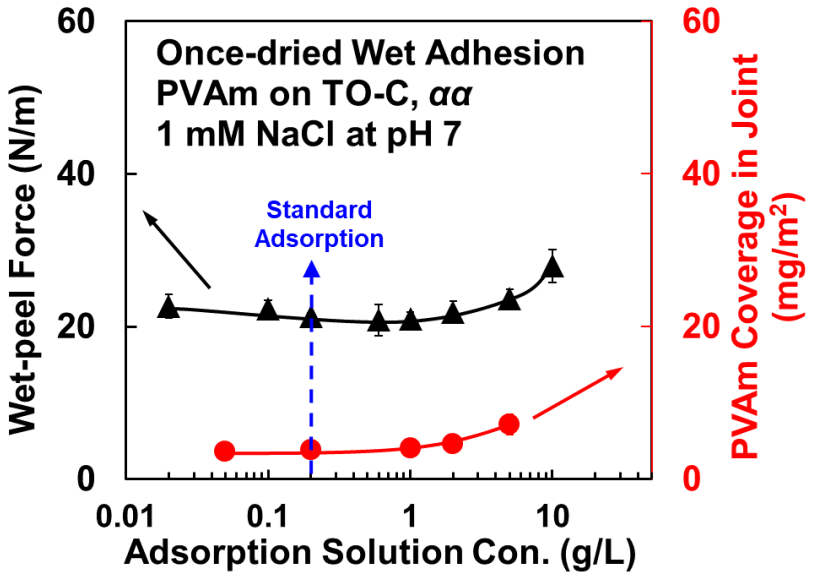

Figure S4 PVAm coverage and the corresponding once-dried wet-peel strengths for αα laminates as a function of the PVAm 340 kDa concentration in the adsorption solution.

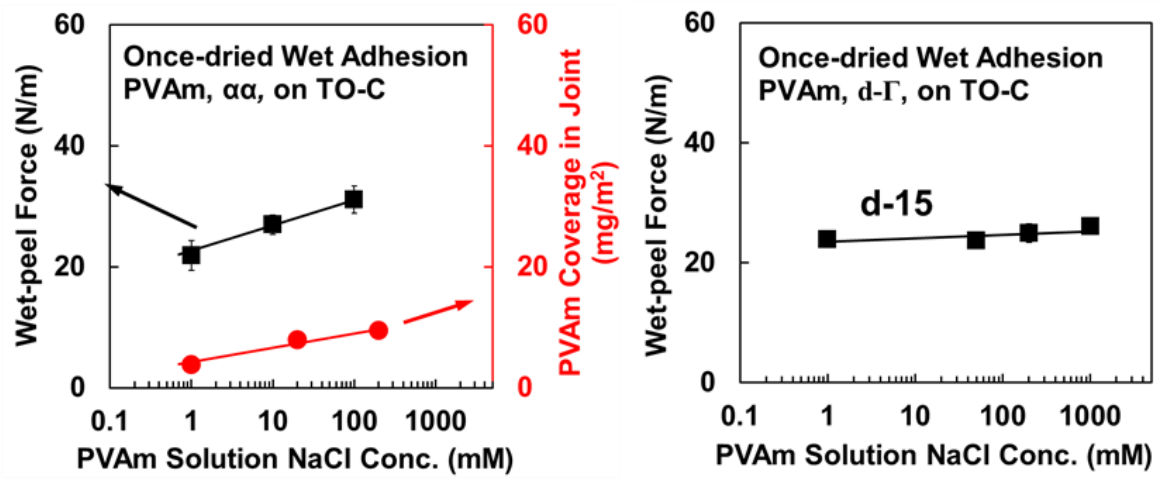

Figure S5 The influence of NaCl concentration in the PVAm treatment solutions on the once-dried wet adhesion. The PVAm 340 kDa concentrations were 0.2 g/L for the αα laminates and 1 g/L for the d-15 laminates.

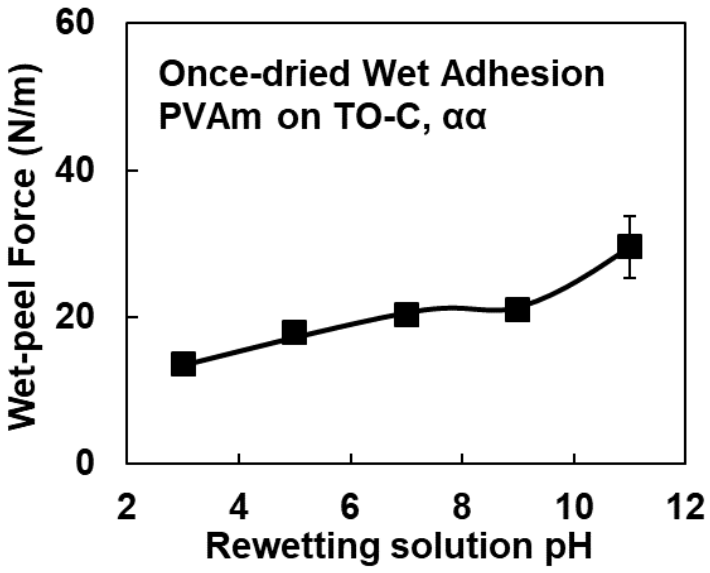

Figure S6 The influence of rewetting pH on once-dried wet adhesion. Laminates were rewetted in 5 mM phosphate buffer for 30 min before the wet-peeling.

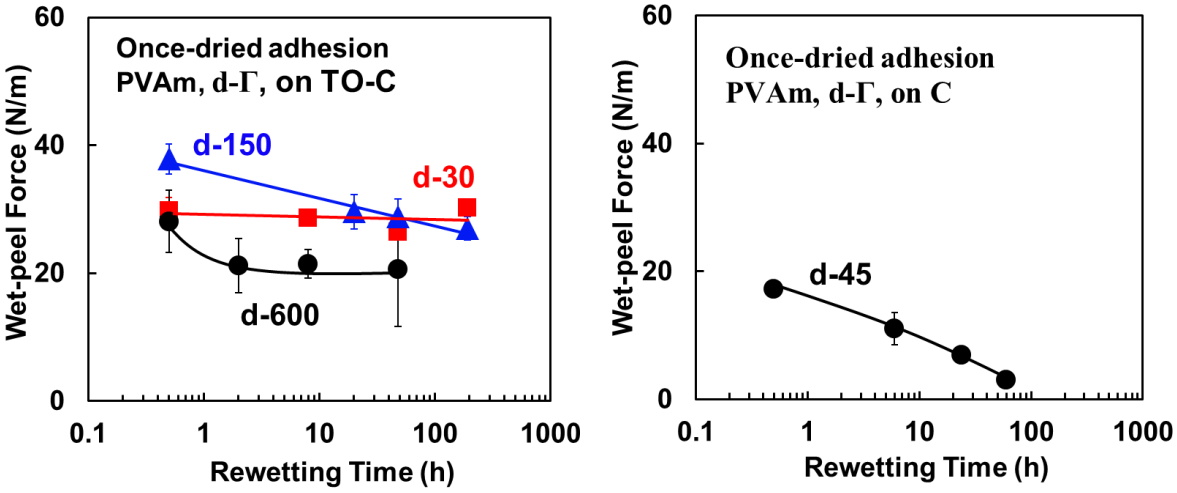

Figure S7 The influence of rewetting time on wet-peel force.

Chapter 7

Cellulose Wet Adhesives with Degradable Cohesive Bonds — a Route to Enhanced Paper Recycling

Unmodified Polyvinylamine (PVAm) showed a weak cohesion at the polymer-polymer interface in water. In this chapter, boronate-derivatized PVAm and dextran-derivatized PVAm were synthesized to enhance the cellulose wet adhesion by introducing new cohesive bonds. The wet adhesion of the cohesive PVAm showed an excellent degradability in response to pH and sugar levels due to the dissociation of the introduced cohesive bonds. We demonstrated that the cohesion of the cellulose adhesive was important for both wet adhesion and degradability.

The data within this chapter have been collected by me. I summarized the data and wrote the draft myself. Dr. Robert Pelton helped me analyze the results and proofread the manuscript.

This chapter is under preparation for future publication.

7.1 Introduction

Wet strength is an important property for many paper products, especially for those applied in moist or humid environments, such as coffee filter papers, paper towels and paper packaging.[1] Due to the weak wet adhesion between unmodified cellulose fibers, wet adhesives are applied in paper manufacturing to enhance the wet fiber joint. This involves laminating two layers of adsorbed polymeric adhesives between two cellulose surfaces. However, with the current techonology, it is difficult to recycle papers that are enhanced by commercial cellulose wet adhesives.[2] The development of a next-generation wet adhesive is required to manufacture wet strength papers with enhanced recyclability.

PVAm has been proved to be a great wet adhesive for cellulose materials containing surface aldehydes.[3, 4] As demonstrated in the last chapter, after the lamination of two PVAm-adsorbed, wet oxidized cellulose surfaces, there were two types of interfaces in the laminate joint: cellulose-PVAm interfaces and PVAm-PVAm interfaces. The wet adhesion at cellulose-PVAm interfaces is strong due to the formation of covalent imine and aminal bonds.[5] By contrast, the cohesion at PVAm-PVAm interfaces is low, which compromises the measured cellulose wet adhesion.

Many reports describe the formation of boronate-carbohydrate in water.[6, 7] However, so far the boronate-dextran complex has only been observed to form in anhydrous conditions or during dewatering.[8, 9] In this work, we synthesized boronate-derivatized PVAm and dextran-derivatized PVAm to promote the cohesion at the PVAm-PVAm interface and thereby enhance cellulose wet adhesion. Boronic ester bonds were expected to form between grafted boronic acids and dextran chains at the PVAm-PVAm interface after curing. As a proof of concept, we used subtle pH changes and monosaccharides to degrade the cellulose wet adhesion by "switching off" the cohesive boronic ester bonding at the PVAm-PVAm interface.

7.2 Experimental Section

Materials. Regenerated cellulose membranes (Spectra/Por2, MWCO 12-14 kDa, product number 132684) were purchased from Spectrum Laboratories, US. Blotter papers were purchased from Labtech Instruments Inc., Canada. PVAm with 340 kDa and 83 mol % degree of hydrolysis were Lupamin 9095 provided by BASF, Germany. All other chemicals were purchased from Sigma-Aldrich, Canada.

Water type 1 (as per ASTM D1193-6, resistivity 18MΩ/cm) was used in all experiments. PVAm was dialyzed against water for one week and freeze-dried. Other chemicals were used as received.

Lactonization of Dextran. Lactonization of dextran was conducted according to the method described by Hashimoto *et al*.[10] First, 3 g dextran with Mw 6,000 (DP 37) was dissolved in 15 mL water. 0.51 g iodine was dissolved in 20 mL water. 0.45 g potassium hydroxide was dissolved in 10 mL water. Then, the iodine and potassium hydroxide

solutions were added dropwise to the dextran solution. The reaction proceeded for 24 hours at room temperature with stirring. Dextran lactone was dialyzed for 3 days using dialysis tube with MWCO 3 kD.

Preparation of PVAm-D. Dextran lactone was grafted onto PVAm to form PVAm-D as shown in Figure 7-S1. The reaction was conducted according to the method described by Holland *et al.*[11] 50 mg PVAm was dissolved in 10 mL DMSO/methanol (2/1, v/v) co-solvent at 80 °C overnight. 357 mg dextran lactone was dissolved in 30 mL DMSO. The dextran lactone solution was added slowly into the PVAm solution. The reaction proceeded at 80 °C for 24 hours. PVAm-D was dialyzed for one week using dialysis tube with MWCO 25 kD.

Preparation of PVAm-PBAx. PVAm-PBAx represents PVAm grafted with 4-carboxyphenylboronic acid (PBA). The details of the reactions are listed in Figure 7-S2 and Table 7-S1. In a typical reaction, 4-carboxyphenylboronic acid was dissolved in pH 5.5 water at room temperature. 1-Ethyl-3-(3-dimethylaminopropyl)carbodiimide (EDC) was added, and *N*-hydroxysuccinimide (NHS) was added 2 minutes later. The solution was stirred and maintained at pH 5.5. After 15 minutes, the solution was adjusted to pH 7.2, followed by the addition of PVAm. The reaction was allowed to proceed for 1 hour at room temperature with the pH maintained at 7.2. PVAm-PBAx was purified by dialysis and stored as an aqueous solution at 4 °C.

Electrophoretic Mobility. The electrophoretic mobilities of PVAm-PBA were measured with a ZetaPlus analyzer (Brookhaven Instruments, US) at 23 ºC using the phase analysis light scattering mode. For all measurements, PVAm-PBA was dissolved in 3 mM NaCl solution. Reported values were averaged over 10 cycles with 10 scans for each cycle. The standard error is reported for each result.

Polymer Adsorption Measurement. Adsorption measurements were performed with an E4 quartz crystal microbalance with dissipation (QCM-D) from Q-Sense, Sweden at 23 °C. In all measurements, crystal chips with a sputtered silica surface (Q-Sense, Sweden) were used and 1 mM NaCl solutions were injected at a flow rate of 100 μL/min. Chips were cleaned by UV/ozone treatment and 2% sodium dodecyl sulfate solution before the measurement. In a typical experiment, an aqueous solution at a designated pH was injected until the baseline frequency shift was less than 0.5 Hz over 10 minutes. Then 0.2 g/L PVAm or its derivative solution at the same pH was injected until the baseline stabilized, typically after 30 minutes. The sample was rinsed with aqueous solution without polymer until the baseline stabilized. An example of the QCM-D data is shown in Figure 7-S3. The adsorption results are calculated and listed in Table 7-1.

Cellulose Membrane Oxidation. Regenerated cellulose dialysis tubing was cut into strips measuring 6 cm × 2 cm (top) and 6 cm × 3 cm (bottom). The membranes were cleaned by agitating in water at 60 °C for 1 hour. The clean membranes were oxidized as follows. 68 mg 2,2,6,6-tetramethylpiperidine-1-yl)oxyl (TEMPO) was dissolved in 2 L of water along with 680 mg NaBr, followed by 300 mg NaClO. The concentration of NaClO solution was determined by the available chlorine titration (TAPPI, Test Method T 611

cm-07). The pH of the solution was adjusted to 10.5, and then 10 g of cellulose membranes were added. During the oxidation, the pH was maintained at 10.5 at room temperature. The oxidation reaction was allowed to proceed for 15 minutes and then stopped by adding 10 mL ethanol. The oxidized membranes were washed with water and stored at 4 °C.

Once-dried Wet Adhesion. The laminates were prepared by a method we call "adsorption application." In this method, 1 g of oxidized cellulose membranes were soaked in 50 mL 0.2 g/L adhesive solution (either PVAm or PVAm derivatives) containing 1 mM NaCl at specific pH values in plastic Petri dishes for 30 minutes. The non-adsorbed polymers were rinsed off by soaking the membranes in rinsing solutions. The rinsing solutions were 1 mM NaCl solutions with the same pH value as the corresponding adsorption solutions. The rinsing solutions were changed three times during the 10-minute rinsing. After the rinsing, two wet, oxidized cellulose membranes were laminated. When both membranes were adsorbed with polymers, the resulting laminates contained two saturated layers of adsorbed polymer ($\alpha\alpha$ or $\alpha\beta$) at the laminate joints, as shown in Figure 7-1. When only the bottom membrane was adsorbed with polymers, the resulting laminates contained only one layer of polymers (α) at the laminate joints.

The laminates were placed between two blotter papers and pressed under 334 kPa for 5 minutes at room temperature in a Standard Auto CH Benchtop Press (Carver, Inc., US). The samples were then dried in a room with constant temperature and humidity (23 °C, 50% relative humidity) for one day.

A freely rotating aluminum peel wheel with a diameter of 14 cm and width of 4 cm was attached to an Instron 4411 universal testing system with a 50 N load cell (Instron Corp., Norwood, US). Before delamination, the laminates were rewetted in 5 mM phosphate buffer for 30 minutes and then blotted free of excess water. Each set of experiments was conducted using rewetting solution with a different pH. The wet membranes were fixed to the wheel with moisture-resistant double-sided tape (medical tape 1522, 3M, US). Wet-peel force was determined as once-dried wet adhesion with using a peel rate of 20 mm/min. The wet laminates were weighed before and after peeling. The solid contents of the laminates were in the range of 47–54 wt % during the peeling. The reported delamination forces were the average of at least three replicates. The standard deviation is reported for the results.

NMR Spectra. In a typical experiment, 2–3 mg of freeze-dried sample was dissolved in 1 mL D_2O. A small amount of DCl was used to increase the solubility of PVAm-PBAx in D_2O. ^1H NMR was performed using an NMR Spectrometer (Bruker AVANCE 600 MHz, US) at room temperature. Example spectra and calculations are shown in Figure 7-S4. PVAm showed a degree of hydrolysis of 0.83. The DS of dextran on PVAm-D was 0.05 per monomer, producing a glucose ring/amine molar ratio of 2.3. The DS of PVAm-PBA represents the number of grafted boronic acid groups per monomer. The calculation is shown in Table 7-S1.

7.3 Results

Wet adhesion at cellulose fiber-fiber joints is critical for paper wet strength. In this study, regenerated cellulose membranes were used as a model substrate to simulate wet adhesion at fiber-fiber joints. The cellulose membranes were pretreated by TEMPO oxidation to introduce aldehyde and carboxyl surface groups.

Cationic charged PVAm and its derivatives were used as cellulose wet adhesives in this work. The polymers were applied on wet oxidized cellulose membranes using the "adsorption application" method. The polymer adsorbed on the cellulose surface in the form of a single saturated layer mostly due to electrostatic attraction.[12] The cellulose membranes used in this work were dialysis tubes with a molecular weight cut-off of 12–14 kDa. PVAm (340 kDa) stayed mainly on the surface, instead of penetrating into porous structures.

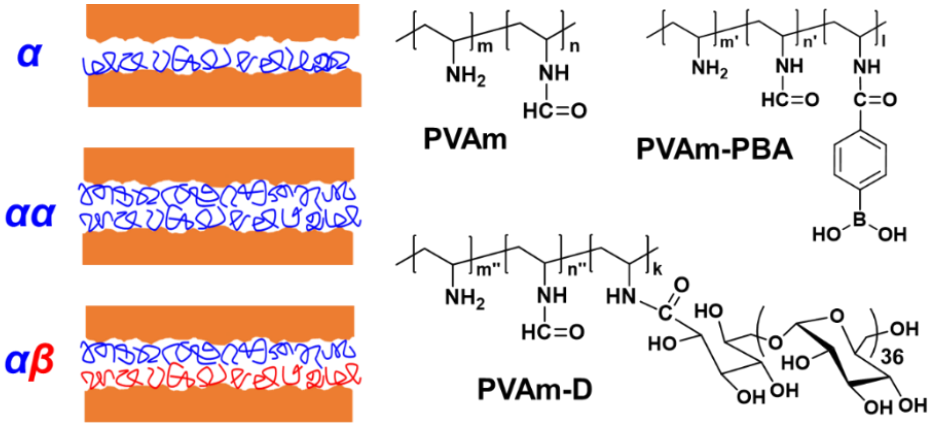

Figure 7-1 The schematic diagram of the three different laminate joints prepared and the two derivatives synthesized from PVAm.

In this work, two wet, oxidized cellulose membranes with adsorbed polymers were laminated and dried for one day. As shown in Figure 7-1, three different types of laminates were prepared: *α*, *αα* and *αβ* laminates. In *α* laminates, one cellulose membrane with adsorbed polymer was laminated with another membrane without adsorbed polymer, producing only one adsorbed layer of polymer at laminate joints. In *αα* laminates, there were two polymer layers. In *αβ* laminates, there were two layers of polymers at laminate joints, but the two polymers were different types, an asymmetrical structure. After one day, the dried laminates were fully rewetted and then subjected to a 90-degree wet-peel test to determine the wet adhesion between cellulose membranes.

The compositions of PVAm and PVAm derivatives were determined by NMR spectra (Figure 7-S4). The degree of hydrolysis of unmodified PVAm was 83 mol%. Two types

of PVAm derivatives were synthesized, including PVAm-PBAx and PVAm-D (see Figure 7-1). PVAm-PBAx was PVAm grafted with phenylboronic acid groups, with DS varying from 4 mol% to 26 mol%. PVAm-D was synthesized by grafting dextran with a DS of 5 mol%. Since the grafted dextran had an average DP of 37, the molar ratio of glucose units and amines in PVAm-D was 2.3:1. The synthesis details are shown in Table 7-S1.

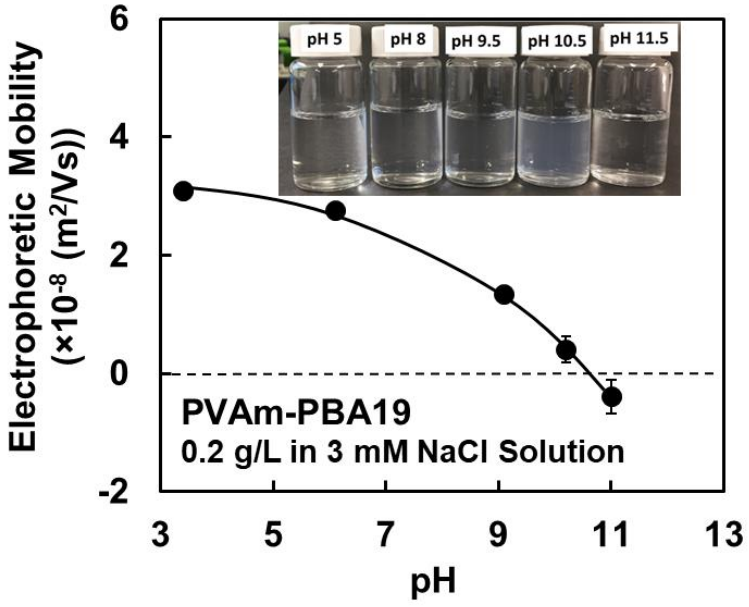

Figure 7-2 Electrophoretic mobility and solubility of PVAm-PBA19 solutions at different pH values.

PVAm and PVAm-D were positively charged over a wide range of pH values, while PVAm-PBA19 was an amphoteric polymer.[4, 6] The electrophoretic mobility of PVAm-PBA19 at various pH values was measured at a concentration of 0.2 g/L in 3 mM NaCl solution. As shown in Figure 7-2, the isoelectric point of PVAm-PBA19 was approximately pH 10.5. Amines in PVAm became less cationic with a higher pH, and grafted boronic acid started to convert to negatively charged boronate with the environmental pH approaching its p*K*a.[4, 6] PVAm-PBA19 solutions were water dispersible (soluble or colloidal) in the pH range of 5–11.5.

The adsorption of PVAm and its derivatives on silica were measured by QCM-D. Silica surfaces are negatively charged at pH > 2.[13] As presented in Table 7-1, untreated PVAm showed a relatively low adsorption coverage (0.6 mg/m^2) on silica. After boronic acid groups or dextran chains were grafted on, the resulting PVAm derivatives showed a much higher adsorption. The adsorption of PVAm-PBA19 increased significantly with a higher

pH. Although the PVAm adsorption on silica is different from adsorption on cellulose, the result is still very helpful for analyzing cellulose wet adhesion under different conditions.

Table 7-1 The adsorption of PVAm and its derivatives on silica surfaces measured by QCM-D. All experiments were performed in 1 mM NaCl solution at 23 ºC, and the adsorption of PVAm-PBA19 was tested at three different pH values. The adsorption coverage was calculated based on the third overtone using the Sauerbrey relationship, as described in Figure 7-S3.

Polymer	Adsorption pH	Adsorption (mg/m^2)
PVAm	8	0.6
PVAm-D	8	5.7
PVAm-PBA9	8	1.5
PVAm-PBA19	5	1.7
PVAm-PBA19	8	5.0
PVAm-PBA19	10	13.4

Table 7-2 Once-dried wet adhesion of PVAm derivatives. Laminates were prepared using the adsorption application method at pH 8. Laminates were rewetted at pH 7 before wet-peeling. The error bars denote the standard deviation of at least three repetitions.

Laminates	Polymers		Once-dried Wet Adhesion (N/m)
	α	***β***	
Control	-	-	11±2
α	PVAm	-	33±2
	PVAm-D	-	34±3
	PVAm-PBA19	-	35±2
αα	PVAm	-	22±3
	PVAm-D	-	13±3
	PVAm-PBA19	-	33±2
αβ	PVAm-PBA19	PVAm	29±2
	PVAm-PBA19	PVAm-D	39±4

Oxidized cellulose membranes were laminated with PVAm, PVAm-D or PVAm-PBA19 using the adsorption application method at pH 8 (Table 7-2). In Chapter 6, we showed that in *α* laminate PVAm, single chains bridge two cellulose surfaces by forming covalent linkages with cellulose aldehydes. It was interesting to find that *α* laminates of the PVAm derivatives showed a similar degree of wet adhesion to unmodified PVAm (33–35 N/m). In *αα* laminates, PVAm provided a medium degree of cellulose wet adhesion (22 N/m),

while PVAm-D provided a much weaker adhesion (13 N/m), showing that the pendant dextran chains decreased wet adhesion by a factor of 2. The *αα* laminates with PVAm-PBA showed high wet adhesion (33 N/m), which was 50% stronger compared to unmodified PVAm.

The highest cellulose wet adhesion (39 N/m) came from the asymmetrical *αβ* laminates with one layer of adsorbed PVAm-PBA19 and one layer of PVAm-D. The *αβ* laminate with PVAm-PBA19 and PVAm showed a much lower wet adhesion (29 N/m). This result illustrated the importance of the dextran grafting for the wet adhesion of *αβ* laminates.

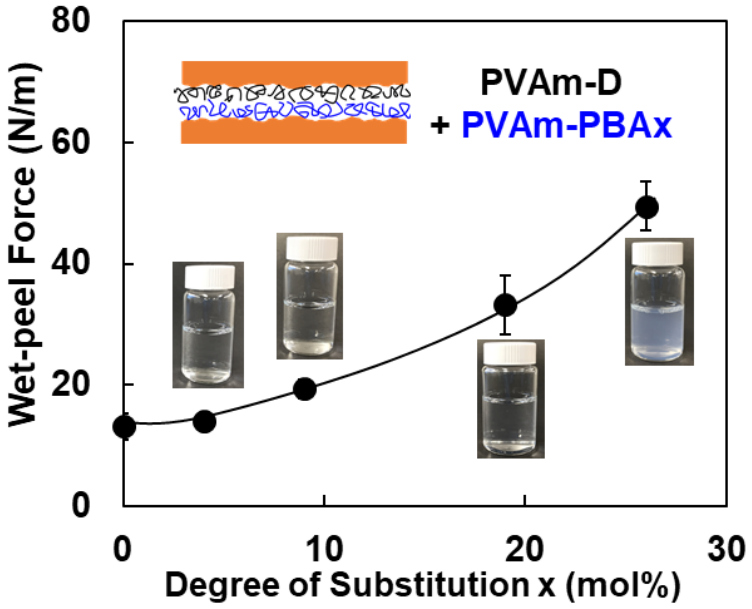

Figure 7-3 The influence of PBA content in PVAm-PBA on the once-dried wet adhesion of *αβ* laminates (PVAm-PBA+ PVAm-D). The polymers were applied on TEMPO-oxidized cellulose using the adsorption application method. Laminates were rewetted at pH 7 for 30 minutes before the wet-peel. PVAm-PBAx (0.2 g/L) was water dispersible (soluble or colloidal) in 1 mM NaCl at pH 8.

PVAm-PBA was synthesized with various DS of boronate grafting, ranging from 4 mol% to 26 mol%. PVAm-PBA with a DS > 26 mol% was also synthesized, but it was water insoluble. As shown in Figure 7-3, the wet adhesion of the *αβ* laminates increased as the DS of PVAm-PBAx increased. The same phenomena were reported in Chen *et al.*[6, 14] — a higher DS of boronate grafting led to a lower water solubility; it also led to a higher wet adhesion as long as the PVAm-PBAx was water dispersible (soluble or colloidal).

As shown in Figure 7-4, the wet adhesion of PVAm *αα* laminates remained constant (19–23 N/m) when the adsorption/lamination pH fell in the range of pH 4–9, corresponding to the result in Chapter 6. Earlier studies have shown that PVAm is very surface active in water at approximately pH 10.[3, 15] Its wet adhesion showed a peak value (31 N/m) at pH 10, which was mainly due to the high adsorption of PVAm on cellulose, same as described in Chapter 6. Compared to PVAm *αα* laminates, the wet adhesion of *αβ* laminates (PVAm-PBA + PVAm-D) was higher, especially when they were laminated under basic conditions. The wet adhesion of *αβ* laminates increased significantly as the adsorption/lamination pH increased until pH 10.5. Above that pH value, wet adhesion started to drop.

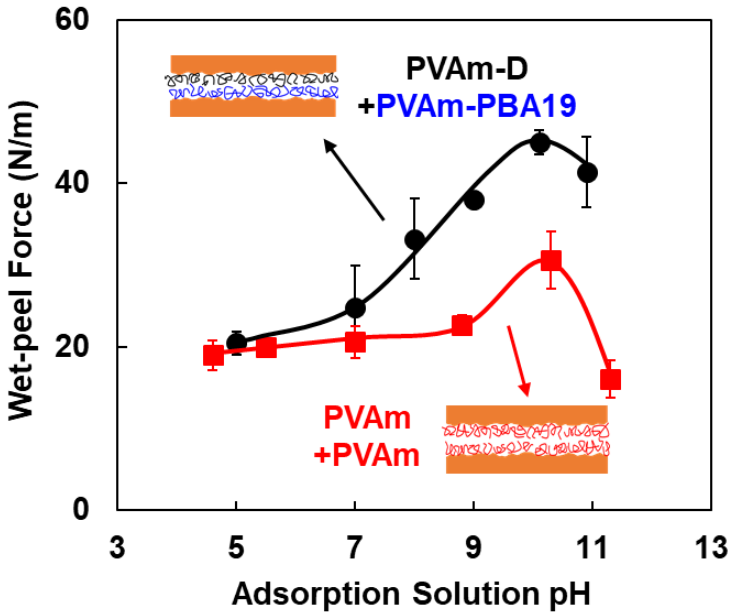

Figure 7-4 The influence of adsorption/lamination pH on the once-dried wet adhesion of *αβ* laminates (PVAm-PBA+ PVAm-D) compared to PVAm *αα* laminates. The polymers were applied on TEMPO-oxidized cellulose with the adsorption application at different pH values. Laminates were rewetted at pH 7 for 30 minutes before the wet-peel.

The *αβ* laminates (PVAm-PBA + PVAm-D) not only showed a high wet adhesion but also provided degradability to cellulose wet adhesion. As control, the *αα* laminates with unmodified PVAm showed a stable wet adhesion after rewetting at pH values between 4 and 10 (Figure 7-5). For *αβ* laminates (PVAm-PBA + PVAm-D), the wet adhesion was high when rewetted under basic conditions but significantly lower when rewetted under acidic or neutral conditions. For example, after rewetting at pH 5, wet adhesion (23 N/m) was 52% lower compared to laminate rewetted at pH 9 (48 N/m).

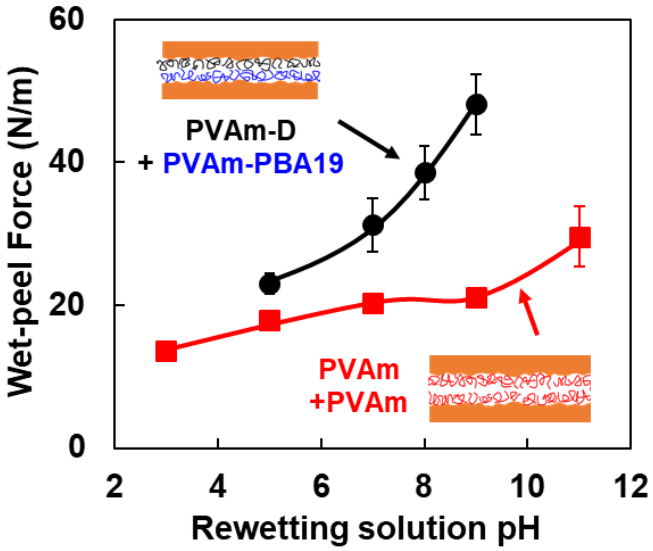

Figure 7-5 The influence of rewetting solution pH levels on the once-dried wet adhesion of *αβ* laminates (PVAm-PBA+ PVAm-D). Polymers were applied on TEMPO-oxidized cellulose membranes using the adsorption application method at pH 8.

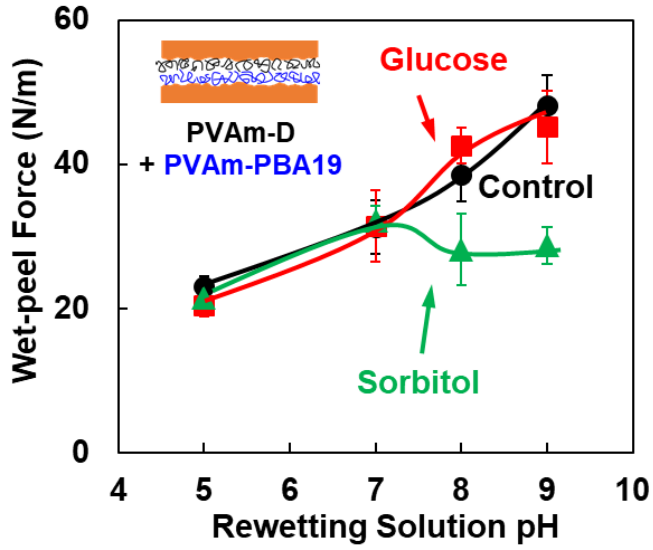

Figure 7-6 The effect of monosaccharides on wet adhesion of *αβ* laminates containing PVAm-PBA and PVAm-D. Polymers were applied on TEMPO-oxidized cellulose using the adsorption application methods at pH 8. Laminates were rewetted either with 10 mM monosaccharides (glucose or sorbitol) or without (control).

Monosaccharides serve as an stimulus to degrade the wet adhesion of *αβ* laminates (PVAm-PBA + PVAm-D). When sorbitol is added to the rewetting solution, wet adhesion can be significantly degraded under basic conditions. As shown in Figure 7-6, the wet adhesion (29 N/m) was 40% lower after rewetting in sorbitol solution at pH 9, compared to laminate rewetted without sorbitol (48 N/m). This decrease of wet adhesion was due to the dissociation of boronate-dextran complexes in the presence of sorbitols. This reaction is illustrated in Figure 7-7. By contrast, glucose failed to degrade the wet adhesion. Springsteen and Wang have reported that at pH 8.5, boronate-sorbitol ester bonding shows a higher association constant (1000 mol^{-1}) than boronate-glucose ester bonding (11 mol^{-1}), using PBA as the model molecule.[16] Meanwhile, Zhang *et al.* have reported that glucose shows a slightly lower affinity to boronates than dextran in water.[17] Thus, the affinity to boronates should rank as sorbitol >> dextran > glucose, which explains why the wet adhesion can be degraded by sorbitol, but not by glucose.

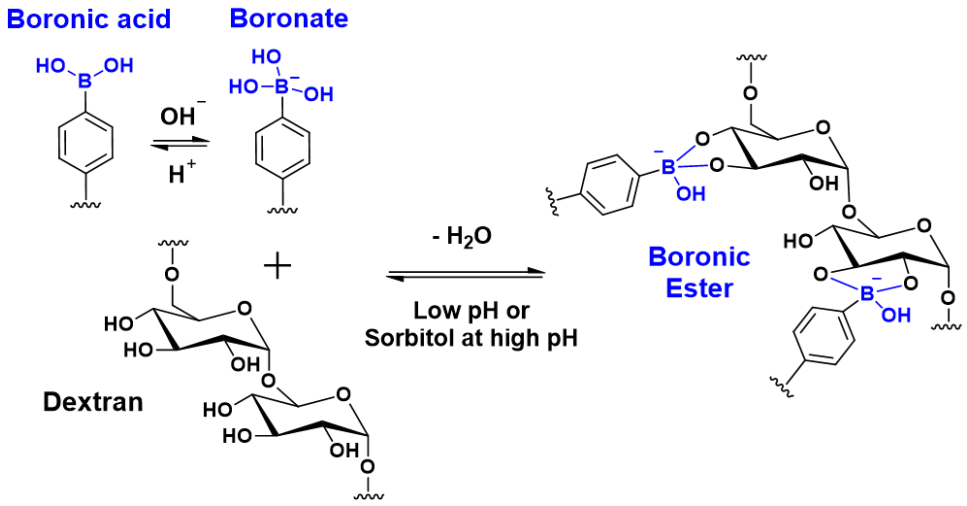

Figure 7-7 Reaction of boronate with dextran. Boronic ester bonding forms after drying and dissociates in low pH solutions or in sorbitol solutions at high pH.

7.4 Discussion

PVAm is a promising cellulose wet adhesive. In water, PVAm adsorbs on oxidized cellulose via electrostatic attraction.[18] After drying, wet adhesion forms between two PVAm-adsorbed cellulose surfaces due to covalent bonding.[5] However, as we observed in Chapter 6, the low cohesion at PVAm-PVAm interfaces limits the further improvement of the cellulose wet adhesion.

How does the wet adhesion form between PVAm-adsorbed cellulose surfaces? At the beginning of the lamination process, with much free water at laminate joints, van der Waals attraction between surfaces is negligible due to the long distance and the low Hamaker constant in water.[19] Capillary attraction is the driving force pushing the two surfaces towards each other. This is counteracted by the electro-steric stabilization effect, preventing two surfaces from achieving molecular-level contact. In the presence of free water, we believe two PVAm-adsorbed cellulose surfaces cannot reach "real" contact. As described in Chapter 6, a very low degree of wet adhesion in never-dried PVAm $\alpha\alpha$ laminates was observed when the solids content was < 45%. When the solids content reaches 47–49%, most of free water in laminates is removed. Under this condition, capillary attraction and the electro-steric stabilization effect will decrease significantly — ultimately to zero; the long-range van der Waals attraction increases; hydrogen bonds and covalent bonds start to form.

In this work, the $\alpha\beta$ laminate prepared with PVAm-PBA and PVAm-D showed much higher cellulose wet adhesion compared with the corresponding unmodified PVAm $\alpha\alpha$ laminate, mainly due to 1) the introduction of enhanced cohesion at PVAm-PVAm interfaces, and 2) the higher adsorption of PVAm derivatives on oxidized cellulose.

The covalent boronic ester bonding was the major contribution for the enhanced adhesion of the asymmetrical PVAm-PBA + PVAm-D laminates. Boronic acid groups ionize to boronates at neutral or basic conditions, depending on their pK_a.[16] Furthermore, Notley *et al.* reported that the ionization of boronate is enhanced when it is surrounded with PVAm.[20] After dewatering, anionic boronates form ester linkages with grafted dextran chains via 1,2-diols.[9, 21, 22] As shown in Figure 7-6, cellulose wet adhesion was much lower after rewetting in sorbitol solutions at pH 9 (29 N/m), comparing to that without sorbitol (48 N/m). This decrease in wet adhesion was entirely due to the dissociation of the boronate-dextran complexes in presence of sorbitol.

Under basic conditions, the anionic charge of boronates on PVAm-PBA also contributed to the formation of cohesion. PVAm-adsorbed layers are highly positively charged, leading to a strong repulsive force between surfaces in water.[20] The negatively charged, grafted boronates converted PVAm-PBA into an amphoteric polymer, which reduced the electrostatic repulsion between PVAm adsorbed surfaces. The isoelectric point of PVAm-PBA19 was approximately pH 10.5 (Figure 7-2), when the electrostatic repulsion reached zero. A previous study showed that wet adhesion between PVAm-PBA adsorbed cellulose in pH 8 aqueous solution was one order of magnitude greater compared to adhesion between PVAm-adsorbed cellulose.[20] As shown in Figure 7-5, the wet adhesion

of the *αβ* laminate (PVAm-PBA + PVAm-D) after rewetting at pH 9 was 48 N/m, while the wet adhesion was much lower (23 N/m) after rewetting at pH 5. Springsteen and Wang report that as pH drops from 9 to 5, boronates convert back to boronic acid groups, the boronate-dextran complexes dissociate and PVAm-PBA become fully positively charged, leading to a higher repulsive force.[16] Meanwhile, an earlier study in our lab showed no significant dative boron-nitrogen bonding was observed between amines and boronates.[6]

The high adsorption coverage of PVAm derivatives was another important reason for the extraordinary wet adhesion of the *αβ* laminate (PVAm-PBA + PVAm-D). The PVAm used in this work was a highly positively charged polymer. PVAm-PBA and PVAm-D both possessed a lower charge density due to the grafting. Typically, for highly charged polymers like PVAm, adsorption increases with a lower charge density.[12] We observed this phenomenon in our QCM-D results (Table 7-1): PVAm derivatives showed a much higher adsorption coverage on the anionic silica surface in pH 8 aqueous solutions compared to unmodified PVAm. The higher adsorption coverage contributed to the higher wet adhesion of the PVAm-PBA *αα* laminate. Surprisingly, we found the wet adhesion of the PVAm-D *αα* laminate was very low (13 N/m), showing that the pendant dextran chains interfered with the bridging of PVAm between two PVAm adsorbed surfaces. By contrast, in *α* laminates, all PVAm and PVAm derivatives showed a similar wet adhesion (33–35 N/m), showing that 1) the dextran chains did not interfere with covalent coupling of PVAm to cellulose, and 2) the grafted boronic acid did not form extra bonding with cellulose.

The adsorption coverage of PVAm-PBA on oxidized cellulose depended on both the DS of the grafting and the environmental pH. With a higher DS, the adsorption of PVAm-PBA is higher. This was one reason why wet adhesion increased with a higher DS in Figure 7-3. Also, we found that the adsorption coverage of PVAm-PBA increased with pH in the range of pH 5–10. From pH 5 to 10, cationic amines gradually became neutral and boronic acids converted to negatively charged boronates. We believe the increase of wet adhesion of *αβ* laminates that occurred as lamination pH increased (Figure 7-4) was due to not only the formation of boronate-dextran complex, but also a higher adsorption coverage at laminate joints. At an adsorption/lamination pH > 10.5, PVAm-PBA became neutrally charged or slightly negatively charged. Under this condition, the PVAm-PBA adsorption on negatively charged cellulose surfaces would be compromised, which corresponds to the drop of wet adhesion at pH 11 seen in Figure 7-4.

As a proof of concept, we demonstrated that cellulose wet adhesion was reduced significantly by “switching off” the PVAm-PVAm cohesion in response of pH changes and sugar levels, as shown in Figure 7-5 and Figure 7-6. However, it is important to mention that the polymer-enhanced asymmetric *αβ* laminate joints are easy to prepare for bench-top wet-peel measurements but hard in real paper manufacturing. In next step, the design of the degradable wet adhesive will be improved and evaluated in paper handsheets. The requirements of the adhesive are: stable in water, reactive to cellulose, and able to form degradable self-crosslinks.

7.5 Conclusion

1. When one adsorbed layer of boronate-derivatized PVAm and one adsorbed layer of dextran-derivatized PVAm formed an asymmetrical $\alpha\beta$ laminate between TEMPO-oxidized cellulose, the wet adhesion was 80% stronger than a symmetrical laminate with unmodified PVAm.
2. The high wet adhesion of the $\alpha\beta$ laminate was the result of the enhanced cohesion at PVAm-PVAm interfaces (primarily due to the boronic ester bonding) and a high adsorption coverage of PVAm derivatives.
3. The enhanced PVAm cohesion can be "switched off" in water by subtle pH changes or in the presence of sorbitol, providing controllable degradability to cellulose wet adhesion.
4. When laminated at the isoelectric point of the boronate-derivatized PVAm, the $\alpha\beta$ laminate showed the strongest wet adhesion. A higher DS of boronic acid led to a higher cellulose wet adhesion until the derivative became insoluble in water.

References

(1) Yang, D.; Pelton, R. H. Degradable Microgel Wet-Strength Adhesives: A Route to Enhanced Paper Recycling. *ACS Sustainable Chemistry & Engineering* **2017,** *5*, 10544-10550.

(2) Su, J.; Mosse, W. K.; Sharman, S.; Batchelor, W.; Garnier, G. Paper Strength Development and Recyclability with Polyamideamine-Epichlorohydrin (Pae). *BioResources* **2012,** *7*, 0913-0924.

(3) Chen, X.; Wang, Y.; Pelton, R. Ph-Dependence of the Properties of Hydrophobically Modified Polyvinylamine. *Langmuir* **2005,** *21*, 11673-11677.

(4) Pelton, R. Polyvinylamine: A Tool for Engineering Interfaces. *Langmuir* **2014**.

(5) Diflavio, J.-L. The Wet Adhesion of Polyvinylamine to Cellulose. McMaster University, 2013.

(6) Chen, W.; Pelton, R.; Leung, V. Solution Properties of Polyvinylamine Derivatized with Phenylboronic Acid. *Macromolecules* **2009,** *42*, 1300-1305.

(7) Pelton, R.; Hu, Z.; Ketelson, H.; Meadows, D. Reversible Flocculation with Hydroxypropyl Guar−Borate, a Labile Anionic Polyelectrolyte. *Langmuir* **2008,** *25*, 192-195.

(8) Yao, H.; Chang, F.; Hu, N. Ph-Switchable Bioelectrocatalysis Based on Layer-by-Layer Films Assembled through Specific Boronic Acid-Diol Recognition. *Electrochimica Acta* **2010,** *55*, 9185-9192.

(9) Li, L.; Bai, Z.; Levkin, P. A. Boronate–Dextran: An Acid-Responsive Biodegradable Polymer for Drug Delivery. *Biomaterials* **2013,** *34*, 8504-8510.

(10) Hashimoto, K.; Imanishi, S.-I.; Okada, M.; Sumitomo, H. Chemical Modification of the Reducing Chain End in Dextrans and Trimethylsilylation of Its Hydroxyl Groups. *Journal of Polymer Science Part A: Polymer Chemistry* **1991,** *29*, 1271-1279.

(11) Holland, N. B.; Qiu, Y.; Ruegsegger, M.; Marchant, R. E. Biomimetic Engineering of Non-Adhesive Glycocalyx-Like Surfaces Using Oligosaccharide Surfactant Polymers. *Nature* **1998,** *392*, 799-801.

(12) Enarsson, L.-E.; Wågberg, L. Polyelectrolyte Adsorption on Thin Cellulose Films Studied with Reflectometry and Quartz Crystal Microgravimetry with Dissipation. *Biomacromolecules* **2009,** *10*, 134-141.

(13) Parks, G. A. The Isoelectric Points of Solid Oxides, Solid Hydroxides, and Aqueous Hydroxo Complex Systems. *Chemical Reviews* **1965,** *65*, 177-198.

(14) Chen, W.; Leung, V.; Kroener, H.; Pelton, R. Polyvinylamine− Phenylboronic Acid Adhesion to Cellulose Hydrogel. *Langmuir* **2009,** *25*, 6863-6868.

(15) Romero Nieto, D.; Lindbråthen, A.; HäGg, M.-B. Effect of Water Interactions on Polyvinylamine at Different Phs for Membrane Gas Separation. *ACS Omega* **2017,** *2*, 8388-8400.

(16) Springsteen, G.; Wang, B. A Detailed Examination of Boronic Acid–Diol Complexation. *Tetrahedron* **2002,** *58*, 5291-5300.

(17) Zhang, J.; Geddes, C. D.; Lakowicz, J. R. Complexation of Polysaccharide and Monosaccharide with Thiolate Boronic Acid Capped on Silver Nanoparticle. *Analytical Biochemistry* **2004,** *332*, 253-260.

(18) Pelton, R.; Ren, P.; Liu, J.; Mijolovic, D. Polyvinylamine-Graft-Tempo Adsorbs onto, Oxidizes, and Covalently Bonds to Wet Cellulose. *Biomacromolecules* **2011,** *12*, 942-948.

(19) Notley, S. M.; Pettersson, B.; Wågberg, L. Direct Measurement of Attractive Van Der Waals' Forces between Regenerated Cellulose Surfaces in an Aqueous Environment. *Journal of the American Chemical Society* **2004,** *126*, 13930-13931.

(20) Notley, S. M.; Chen, W.; Pelton, R. Extraordinary Adhesion of Phenylboronic Acid Derivatives of Polyvinylamine to Wet Cellulose: A Colloidal Probe Microscopy Investigation. *Langmuir* **2009,** *25*, 6898-6904.

(21) Zhu, J.-Y.; Lei, Q.; Yang, B.; Jia, H.-Z.; Qiu, W.-X.; Wang, X.; Zeng, X.; Zhuo, R.-X.; Feng, J.; Zhang, X.-Z. Efficient Nuclear Drug Translocation and Improved Drug Efficacy Mediated by Acidity-Responsive Boronate-Linked Dextran/Cholesterol Nanoassembly. *Biomaterials* **2015,** *52*, 281-290.

(22) Xu, W.; Ding, J.; Li, L.; Xiao, C.; Zhuang, X.; Chen, X. Acid-Labile Boronate-Bridged Dextran–Bortezomib Conjugate with up-Regulated Hypoxic Tumor Suppression. *Chem. Commun.* **2015,** *51*, 17775-17776.

(23) Gu, L.; Zhu, S.; Hrymak, A. N. Acidic and Basic Hydrolysis of Poly(N-Vinylformamide). *Journal of Applied Polymer Science* **2002,** *86*, 3412-3419.

(24) Sun, Y.-X.; Zhang, X.-Z.; Cheng, H.; Cheng, S.-X.; Zhuo, R.-X. A Low-Toxic and Efficient Gene Vector: Carboxymethyl Dextran-Graft-Polyethylenimine. *Journal of Biomedical Materials Research Part A* **2008,** *84A*, 1102-1110.

Supporting Information

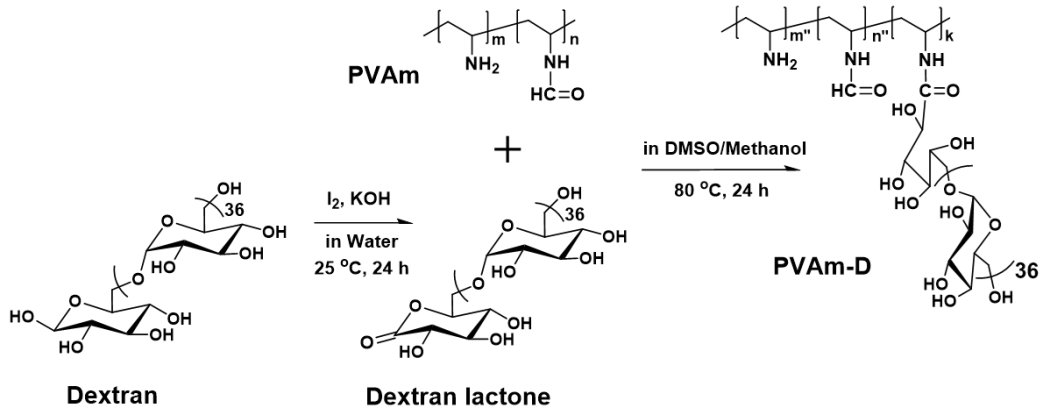

Figure 7-S1 Synthesis of dextran-derivatized PVAm (PVAm-D).

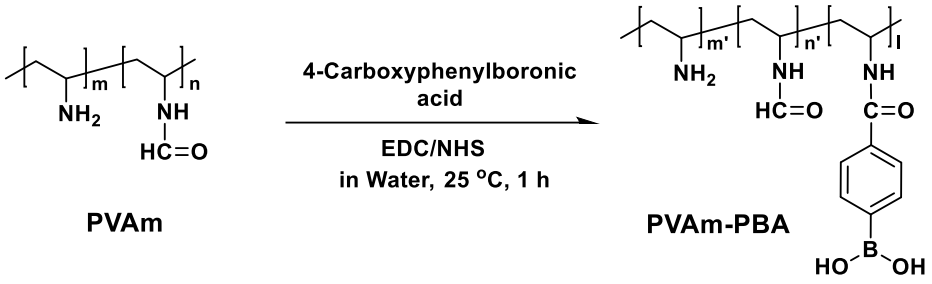

Figure 7-S2 Synthesis of boronate-derivatized PVAm (PVAm-PBA).

Table 7-S1 Preparation of boronate-derivatized PVAm, i.e. PVAm-PBAx. DS of PVAm-PBAx was calculated from ^{1}H NMR spectra. DS represents the number of boronic acid groups per monomer. The solubility of PVAm-PBA-P in D_2O was too low to obtain the NMR spectrum.

Polymer	PVAm (mg)	PBA (mg)	EDC (mg)	NHS (mg)	DS (mol %)
PVAm-PBA0	-	-	-	-	0
PVAm-PBA4	86	40	92	28	4
PVAm-PBA9	86	66	154	46	9
PVAm-PBA19	86	83	193	58	19
PVAm-PBA26	86	99	231	69	26
PVAm-PBA-P	86	132	308	92	-

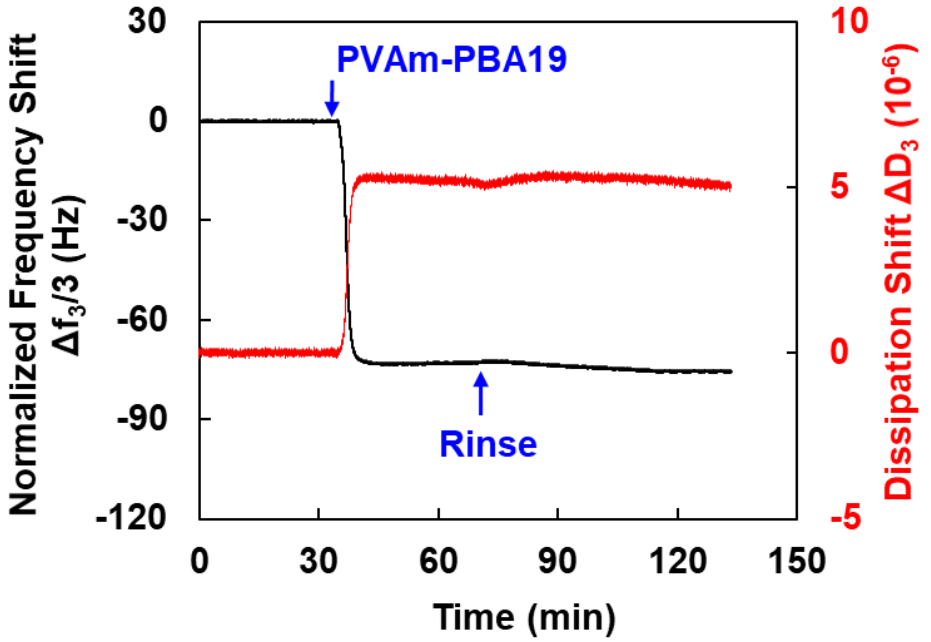

Figure 7-S3 QCM-D data for the adsorption of PVAm-PBA19 on silica chips at pH 10. The experiment started with the addition of 1 mM NaCl solution at pH 10, followed by PVAm-PBA19 adsorption in 1 mM NaCl at pH 10 and rinsing with 1 mM NaCl solution at pH 10. The stable normalized frequency shift after the rinsing was used for the calculation of the adsorbed mass using the Sauerbrey relationship.[12] The third overtone was shown and was used for the calculation.

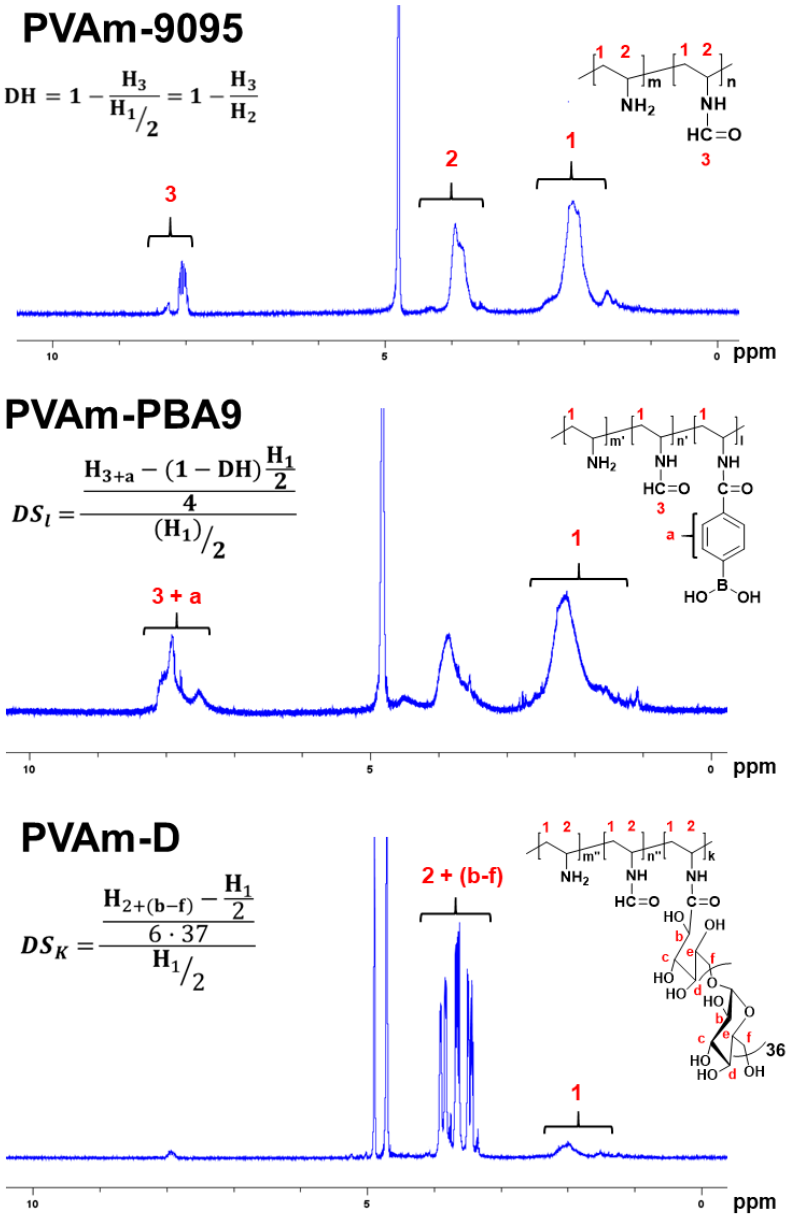

Figure 7-S4 ^{1}H NMR spectra of PVAm and its derivatives. The degree of hydrolysis of PVAm, DS of PVAm-PBA9 and DS of PVAm-D were calculated according to the methods described by other researchers.[6, 23, 24] The equations used are shown above. Purified PVAm showed a degree of hydrolysis of 0.83. The DS of dextran on PVAm-D was 0.05, which represented a molar ratio of glucose ring:amine of 2.3:1. The calculation results of PVAm-PBAx are shown in Table 7-S1.

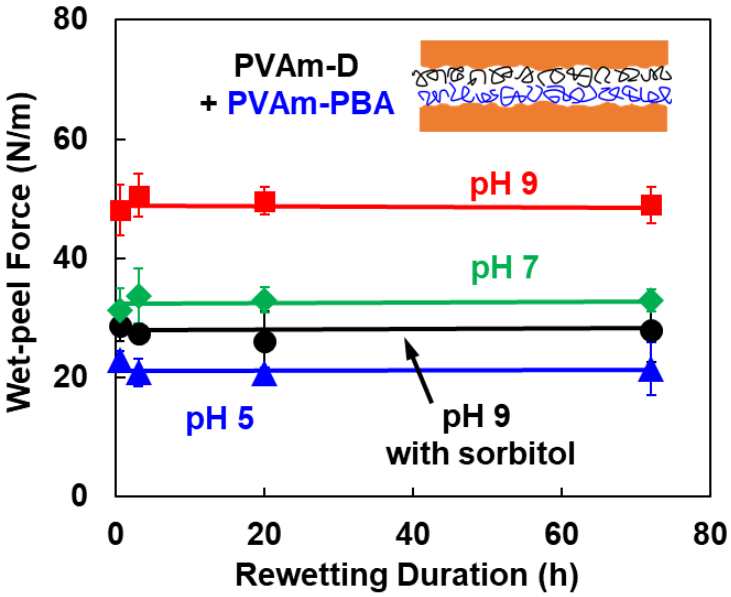

Figure 7-S5 Wet adhesion degradation of laminates prepared from PVAm-D and PVAm-PBA rewetted at different pH values with or without sorbitol. Polymers were applied on TEMPO-oxidized cellulose by the adsorption application at pH 8.

Chapter 8

My Contributions

In this thesis, wet-peel measurements were used to evaluate the performance of cellulose wet adhesives between two wet, regenerated cellulose membranes. Potential next generation of cellulose wet adhesives were designed to provide both strong wet adhesion and excellent degradability, to enhance the recycling of wet strength papers. The major contributions of this thesis are:

1. For the first time, I demonstrated the influence of the organization of polyvinylamine (PVAm) adhesive layer on the wet adhesion between two cellulose surfaces. I found that a single layer of grafting PVAm at the cellulose interface can simultaneously attached to both substrate surfaces, providing high wet adhesion with or without drying.
2. The importance of PVAm cohesion on cellulose wet adhesion was demonstrated for the first time. For unmodified PVAm, the wet adhesion between the two PVAm grafted cellulose surfaces was significantly lowered by the weak cohesion of PVAm. When cohesive PVAm derivatives were used, the cellulose wet adhesion was enhanced by as much as 80%.
3. For the first time, the design rules for the microgel adhesives with controllable degradability were demonstrated. Significant degradability of wet adhesion can be achieved by either incorporating labile crosslinks in microgels or grafting adhesive groups on microgels via labile linkages.
4. I demonstrated two new strategies for designing cellulose wet adhesives that provided both strong wet adhesion and excellent degradability in response to stimuli: a) boronate derivatized PVAm that gave strong and stimuli responsive cohesive bonding, and b) degradable microgels supported polyamide epichlorohydrin (PAE) that enhanced the recyclability of the commercial wet strength resin PAE.

APPENDIX A

Temporary Cellulose Wet Adhesives

The data within Appendix A have been collected by myself. I summarized the data and wrote the draft myself.

Introduction

Temporary wet-strength resins are widely used in paper and tissue products. The most commonly used temporary wet-strength resins are glyoxalated polyacrylamide and aldehyde-containing polysaccharides.[1, 2] Aldehydes of these wet-strength resins react with hydroxyls on cellulose surface after drying, forming hemiacetal bonds that provide paper wet strength. The formation of hemiacetal is enhanced by curing at high temperature and the catalysis of metal/ammonium salts.[3-5] The performance of aldehyde containing temporary wet-strength resins can also be improved by the incorporation of cationic groups and homo-crosslinking groups.[6, 7]

Temporary paper wet strength decays in water. The decay rate of the temporary wet strength is related to many factors, such as the process of paper manufacturing, the chemistry of wet-strength resins and the application environment of paper products. For example, the high drying temperature and the addition of catalysts in paper manufacturing would result in a slow decay of wet strength in water.[3] A slower decay rate can also be achieved by the addition of resin with a higher dosage and a higher molecular weight, or applying paper products in water environment with a lower temperature and a milder pH.[7-9] It was reported that the ratio of labile and stable bonds in wet-strength resins was tuned to control the decay rate of paper wet strength.[10]

Starch additives are widely used in paper manufacturing. In this study, dextran was used as the model of starch. Hydrophobic modification [11] and periodate oxidation [12] were used to synthesize dextran derivatives that provided paper temporary wet strength with a controllable decay rate.

Experimental Section

Materials. Dextran from *Leuconostoc* spp. with Mr 450 -650 kDa was purchased from Sigma-Aldrich, Canada. Polyvinyl alcohol (PVA) with Mw 146 - 186 kDa and > 99% DH was purchased from Sigma-Aldrich, Canada. PAE was Kymene 5221 provided by Solenis, US. PVAm with 340 kDa were Lupamin 9095 provided by BASF, Germany. All other chemicals were purchased from Sigma-Aldrich, Canada. Water type 1 (as per

ASTM D1193-6, resistivity 18MΩ/cm) were used in all experiments. PVAm was purified by dialysis in water for one week and freeze-dried. Other chemicals were used as it is.

Hydrophobic Modification of Dextran. Hydrophobic dextran (D-Cx) was prepared by esterification with fatty acid, as shown in Figure A-1A. The recipes are listed in Table A-1. Caproic acid (C6), caprylic acid (C8), lauric acid (C12) and myristic acid (C14) were used in dextran esterification as hydrophobic grafting. In a typical experiment, dextran powder was slowly added into anhydrous DMSO. After the total dissolution of dextran, fatty acid and 4-dimethylaminopyridine (DMAP) were added. The solution was stirred for 10 min, followed by the addition of 1-ethyl-3-(3-dimethylaminopropyl)carbodiimide (EDC). The reaction was proceeded at room temperature with stirring for one day, and terminated by precipitating the hydrophobic dextran with methanol (> 3 times of the reaction volume). The precipitated dextran was centrifuged and dissolved by small amount of water. Then the product was dialyzed against water and freeze-dried. The DS was measured by ^{1}H- NMR spectroscopy (Bruker AVANCE 200MHz, US) with samples dissolved in D_2O. An example of NMR spectra is shown in Figure A-3 and the results are listed in Table A-1. The y in D-Cx-y represents the DS of Cx grafting on dextran (mol%, based on glucose unit).

Dextran Oxidation. The chemistry of dextran oxidation is shown in Figure A-1A. 1 mmol (based on glucose unit) dextran or hydrophobic dextran was completely dissolved in 6 mL water. 0.5 mmol sodium periodate was dissolved in 2 mL water and added into dextran solution. The mixed solution was stirred at room temperature in dark for eight hours. The oxidized dextran was purified by dialysis against water and then freeze-dried.

The oxidation degree of dextran was determined by potentiometric titration as described in Zhao *et al.*[13] Oxidized dextran (30 mg) was dissolved in 10 mL of water and then mixed with 10 mL, 0.2 M hydroxylamine hydrochloride solution. The mixed solution was sealed in container and stirred for one day in dark. 30 mL water was mixed into the solution one hour before the titration. The potentiometric titration was carried out with Burivar-I2 automatic burette (ManTech Associates, Canada). All samples were titrated by 0.1 M NaOH with a target increment of 0.05 pH units/injection. The corresponding injection volumes were in the range 5 - 100 μL. The interval between injections was 30 seconds. The titration was repeated at least twice for each sample.

A control solution was used to determine the titration end point (pH_E). The control solution was prepared by the same method as described above, but the corresponding non-oxidized dextran/hydrophobic dextran was dissolved and mixed with hydroxylamine hydrochloride. The aldehyde content of oxidized dextran (mmol/g) can be calculated by the base consumption V_E at the titration end point pH_E, as described in Zhao *et al.*[13] The calculated aldehyde contents of oxidized dextran are shown in Table A-1.

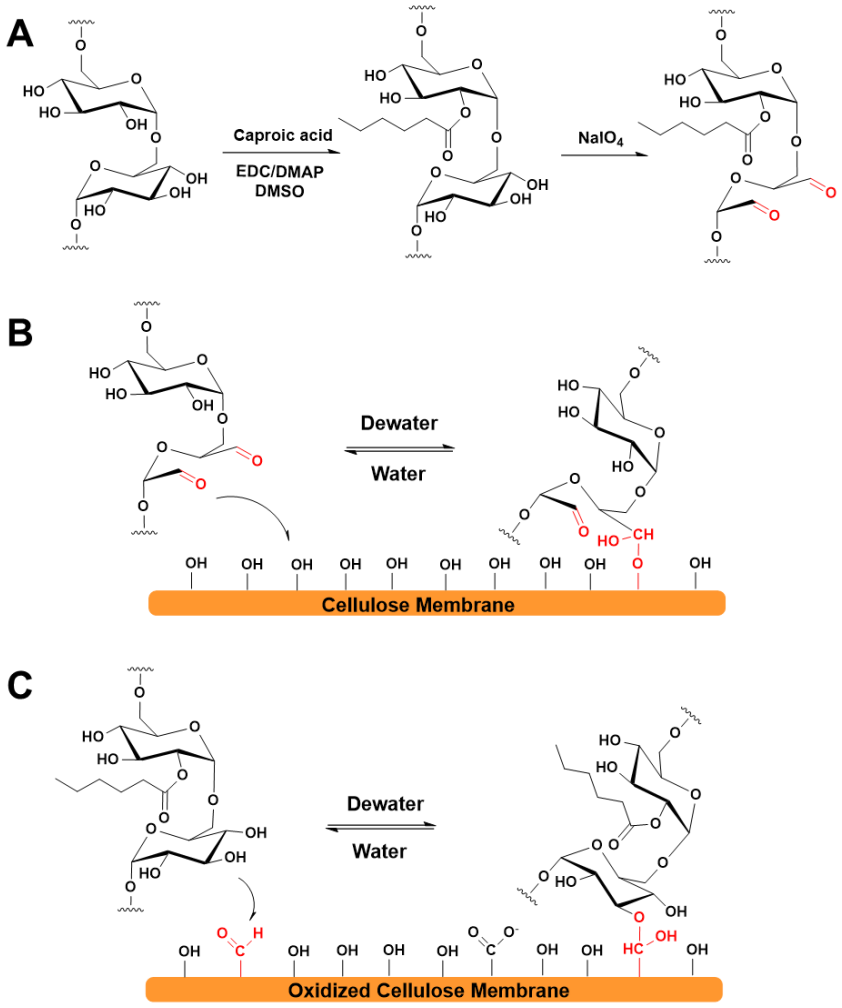

Figure A-1 Schematic diagrams of (A) preparation of oxidized dextran with hydrophobic grafting, (B) reaction between oxidized dextran and cellulose surface, and (C) reaction between hydrophobic dextran and TEMPO oxidized cellulose surface.

Thiol Derivatized Polyacrylic Acid (PAA-thiol). PAA-thiol was prepared by the conjugation of a diamine reagent cystamine with carboxyls on PAA.[14] In a typical reaction, 188 mg PAA sodium salt was dissolved in 50 mL water at room temperature and the pH of solution was adjusted to 4.7. After 30 minutes' stirring, 500 mg EDC was added and 45 mg of cystamine dihydrochloride was added 2 minutes later. The solution was stirred for two hours at room temperature with pH maintaining 4.7. The products were purified by dialysis for one week and then dithiothreitol was added. The final solution was 20 mM dithiothreitol solution with the pH adjusted to 9. The solution was stirred for one hour for the reduction of disulfide bonds. After the further dialysis against water at pH 4 for two days, the purified PAA-thiol solution was adjusted to pH 4 and

stored at 4 °C. The DS of thiol groups (8 mol%) was determined by ^{1}H NMR spectroscopy (Bruker AVANCE 600 MHz, US) with the sample dissolved in D_2O.

Table A-1 Preparation of oxidized dextran with different hydrophobicity. Fatty acids with different chain lengths were used in esterification. Oxidation degree of oxidized dextran is the titratable aldehyde content measured in potentiometric titration.

Esterification						Oxidation	
Hydrophobic dextran	**Dextran (mmol)**	**Fatty acid (mmol)**	**DMAP (mmol)**	**EDC (mmol)**	**DS (mol%)**	**Oxidized dextran**	**Oxidation degree (mmol/g)**
D	-	-	-	-	0	OD	3.6±0.0
D-C6-15	6.17	1.23	0.62	1.23	15.2	OD-C6-15	3.9±0.3
D-C6-7	6.17	0.74	0.37	0.74	7.3	OD-C6-7	4.0±0.1
D-C6-3	6.17	0.37	0.19	0.37	3.1	OD-C6-3	4.3±0.3
D-C8-10	6.17	0.86	0.43	0.86	9.9	OD-C8-10	4.0±0.2
D-C8-6	6.17	0.49	0.25	0.49	5.9	OD-C8-6	4.1±0.1
D-C8-2	6.17	0.25	0.12	0.25	2.1	OD-C8-2	4.3±0.1
D-C12-4	6.17	0.37	0.18	0.37	3.6	OD-C12-4	4.2±0.4
D-C12-1	6.17	0.19	0.09	0.19	1.1	OD-C12-1	4.1±0.3
D-C14-2	6.17	0.19	0.09	0.19	1.8	OD-C14-2	4.3±0.1
D-C14-1	6.17	0.12	0.06	0.12	0.6	OD-C14-1	4.4±0.1

Fluorescence Measurements. Pyrene is a common fluorescent probe to characterize the presence of hydrophobic domains in water soluble polymers. The fluorescent intensity ratio I_1/I_3, is used to evaluate the polarity of the microenvironment.[15, 16] Hydrophobic dextran without oxidation was dissolved in 1 mM NaCl with a pyrene concentration of 6×10^{-7} M. The fluorescence was measured by M1000 Plate Reader (Tecan, US) at 25 °C. The excitation wavelength was 333 nm. The I_1/I_3 ratio of pyrene was determined by the emission intensities at 373 nm (I_1) and 384 nm (I_3). The slit widths were 10 nm for excitation and 5 nm for emission.

Once-dried Wet Adhesion. Regenerated cellulose membranes were cut, pretreated and 2,2,6,6-tetramethylpiperidine-1-yl)oxyl (TEMPO) oxidized as described in Chapter 3. The laminates were prepared by the direct application (Chapter 3). The details of the adhesive solution, including concentration, pH and ionic strength, will be specified in each set of experiment. The laminates were place between two blotter papers and pressed under 2.2 MPa for 30 minutes. The pressing temperature will be specified in each set of experiment.

The once-dried wet adhesion was measured as the wet-peel force by 90-degree wet-peel test, as described in Chapter 3. Before the measurement, all laminates were soaked in 5 mM phosphate buffer at pH 7 and then blotted free of excess water.

Results

In this work, regenerated cellulose was used as the model to simulate the surface chemistry of paper fibers. Polymer solutions were laminated between two wet cellulose membranes, and 90-degree peel test was used to measure the wet adhesion between two cellulose surfaces.

In most of the experiments, regenerated cellulose was used as the substrate, where only hydroxyls were observed on its surface. In some cases, TEMPO oxidized cellulose was used. TEMPO oxidation converted parts of hydroxyls on C6 to aldehydes and carboxyls.[17] As shown in Figure A-2, PAA-thiol provided temporary wet adhesion between oxidized cellulose due to the formation of hemithioacetal bonds between aldehydes and thiols. The hydrolysis of hemithioacetal bonds led to a rapid decrease of cellulose wet adhesion. The same phenomenon was observed with PVA or dextran as the cellulose wet adhesive. The hydroxyls on PVA and dextran crosslinked two oxidized cellulose surfaces by forming hemiacetal bonds with aldehydes (Figure A-1C). The wet adhesion was temporary due to the fast hydrolysis of hemiacetal bonds in water.

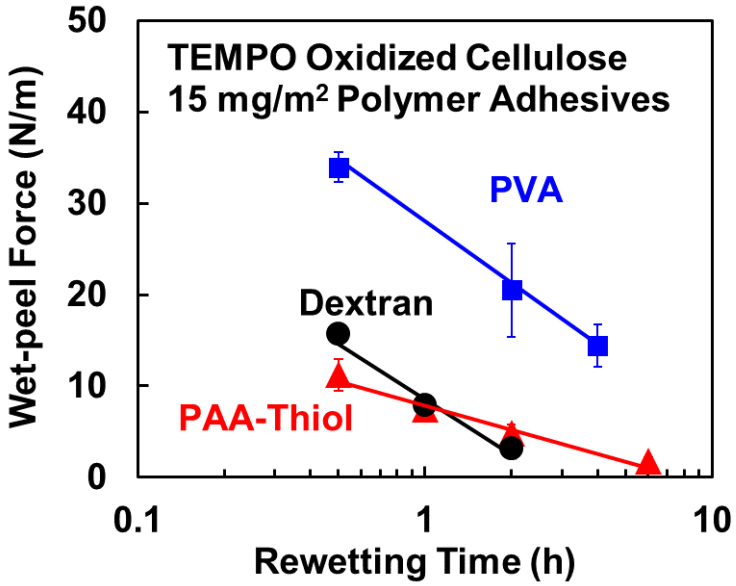

Figure A-2 Temporary wet adhesion of TEMPO-oxidized cellulose. The laminates were prepared with polymer solutions in 1 mM NaCl at pH 7 and pressed at room temperature.

Hemiacetal bonds are commonly found in paper products to provide temporary wet strength.[5] The hydrolysis rate of the hemiacetal determines the decay rate of wet strength. In this study, we synthesized hydrophobic oxidized dextran as cellulose wet adhesives. Periodate oxidation was used to introduce aldehydes to dextran, which can crosslink cellulose surfaces by forming hemiacetal linkages. The hydrophobic grafting of dextran was used to tune the hydrolysis rate of the hemiacetals.

Caproic acid (C6), caprylic acid (C8), lauric acid (C12) and myristic acid (C14) were grafted on dextran via esterification. The hydrophobically modified dextran was characterized by NMR and the DS of grafting was calculated as shown in Figure A-3. D-C8-2 represents the dextran grafted with 2 mol% of C8, in which DS is the number of grafted C8 per glucose unit in dextran. OD-C8-2 is the dextran derivative that is periodate oxidized from D-C8-2. As shown in Figure A-1B, hemiacetal bonds can form between aldehydes of oxidized dextran and hydroxyls of cellulose after drying. The hydrophobicity of the dextran derivatives was tuned by the chain length and the DS of the grafting.

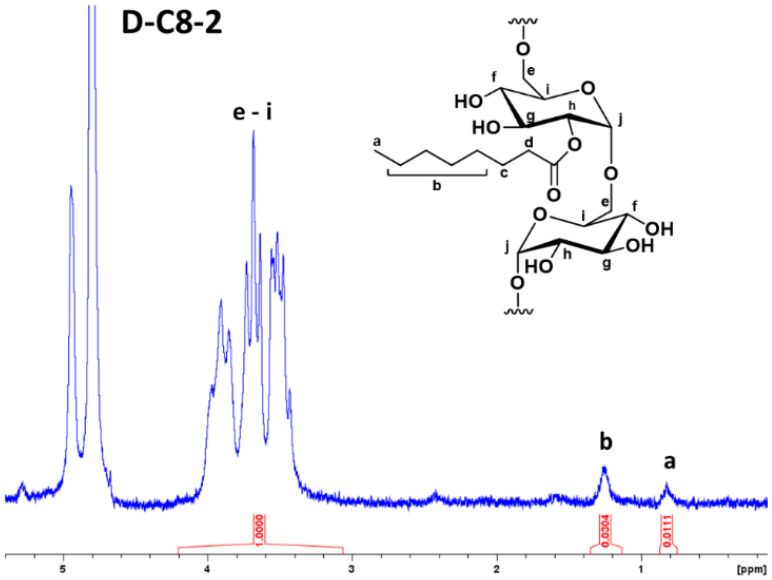

Figure A-3 ^{1}H-NMR spectrum of hydrophobic dextran D-C8-2. Peak at 0.8 ppm represents the methyl group (a) of grafted hydrocarbon chains. Two methylene groups (c) and (d) besides the carbonyl group give broad peaks at 1.5 and 2.3 ppm. The rest of methylene groups (b) of hydrocarbon chains are shown at peak 1.2 ppm.[18] The region of 3.2-3.9 ppm is assigned to non-anomeric protons in sugar rings (e-i).[19]

The water solubility of freeze-dried oxidized dextran is limited at acidic condition due to the presence of intra-/inter-molecular hemiacetals.[20] The same phenomenon was observed in this work. To prepare the oxidized dextran solution at pH 3, 2 g/L oxidized dextran was dissolved in water at neutral pH overnight and then formulated into 1 g/L oxidized dextran solution in phosphate buffer at pH 3. Under this condition, the majority of aldehydes in oxidized dextran are free aldehydes in water solution, while there are still small amounts of enols and hemiacetals.[20, 21] All dextran derivatives for the lamination were fully dissolved and the solutions were transparent.

Oxidized dextran with hydrophobic grafting was laminated between regenerated cellulose as the temporary wet adhesive. The chemistry is illustrated in Figure A-1B. An acidic dextran solution (pH 3) and a high pressing temperature (70 ºC) were used in lamination to increase the initial wet adhesion between cellulose surfaces. In this work, the initial wet adhesion is defined as the once-dried wet adhesion after rewetting < 0.5 h. Figure A-4 showed that the acidic condition and high pressing temperature led to a slower decay rate of wet adhesion, and a higher initial wet adhesion. The formation of hemiacetals can be promoted by acid catalyst and high temperature.[2, 5] Our previous work found that when dextran-aldehydes were used as cellulose wet adhesives the dextran-dextran cohesive bonds can be replaced by dextran-cellulose bonds at pH 3. In other words, cohesive hemiacetal bonds will transform into the more desirable adhesive dextran-cellulose bonds at pH 3.[5]

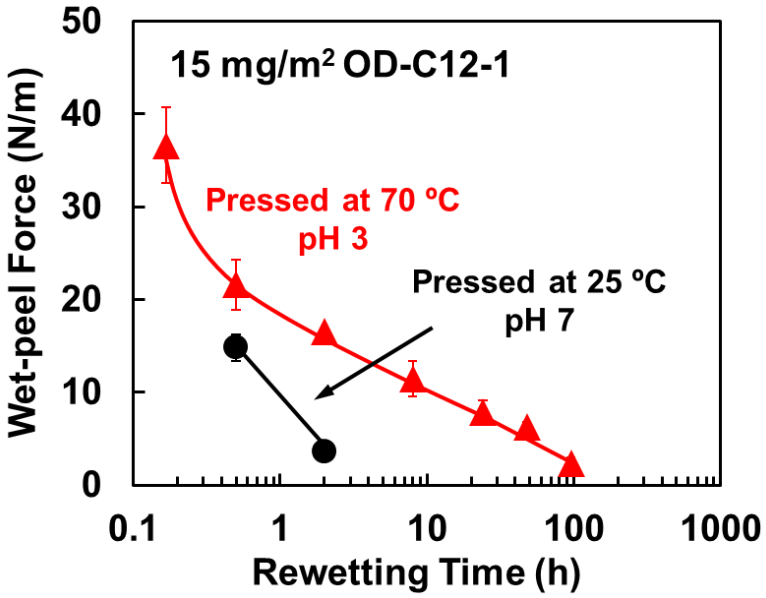

Figure A-4 Influence of polymer solution pHs and curing temperature on the decay rate of cellulose wet adhesion. The laminates were prepared with regenerated cellulose membranes. The pH of the polymer solution used in lamination and the temperature during pressing are shown.

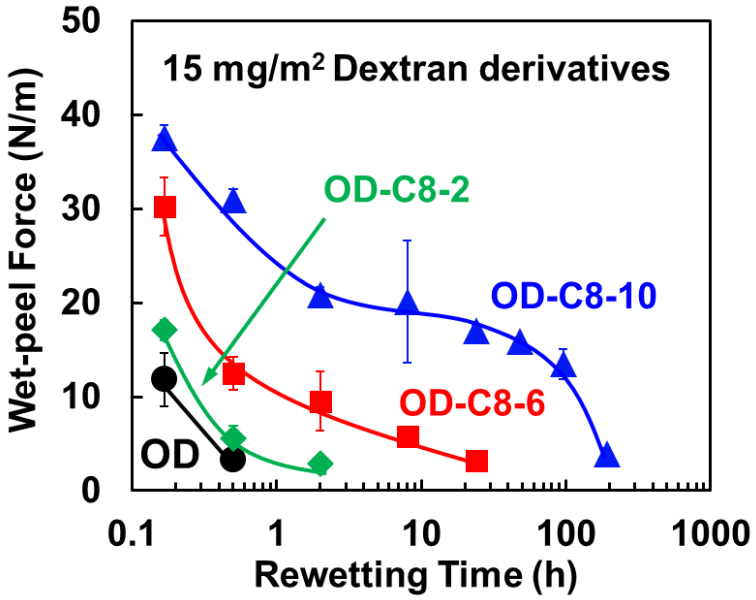

Figure A-5 Degradation of cellulose wet adhesion provided by oxidized dextran with C8 grafting. Regenerated cellulose membranes were laminated with pH 3 dextran solutions and pressed at 70 ºC.

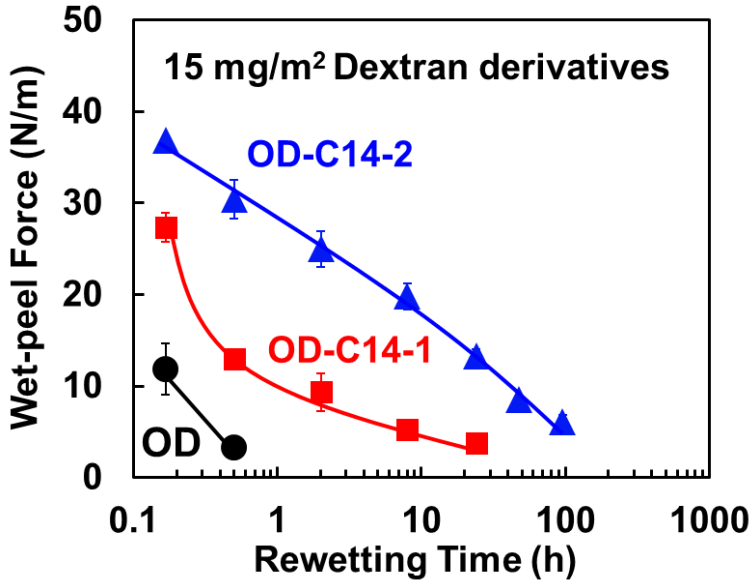

Figure A-6 Degradation of cellulose wet adhesion provided by oxidized dextran with C14 grafting. Regenerated cellulose membranes were laminated with pH 3 dextran solutions and pressed at 70 ºC.

It is interesting to find in both Figure A-5 and Figure A-6 that the initial wet adhesion increased with the DS of hydrophobic grafting on dextran. Also, the wet adhesion of oxidized dextran with a higher density of hydrophobic grafting showed a slower decay rate in water solution. For example, the wet adhesion of OD-C8-2 decreased to 10 N/m in 0.2 hours, whereas OD-C8-10 provided a wet adhesion > 10 N/m for a duration longer than 100 hours.

The chain length of the hydrophobic grafting on oxidized dextran also showed an influence on the decay rate of wet adhesion. For example, OD-C8-2 and OD-C14-2 both had a grafting DS of 2 mol% and an aldehyde contents of ~ 4.3 mmol/g (Table A-1). OD-C14-2 provided a wet adhesion > 10 N/m after rewetting for 50 hours, whose decay rate was much slower than that of OD-C8-2 (0.2 hours).

Why does the hydrophobic grafting on oxidized dextran slow down the decay of cellulose wet adhesion? We found two important reasons: 1) the formation of adhesive hemiacetal linkages between oxidized dextran and cellulose substrate, and 2) the formation of cohesive inter-/intra-molecular hemiacetals within oxidized dextran.

At the beginning, we considered that the hydrophobic grafting on dextran alone can provide hydrophobic micro-environment at cellulose-dextran interfaces, slowing down the hydrolysis of the interfacial hemiacetal. However, Figure A-7 does not support this conclusion.

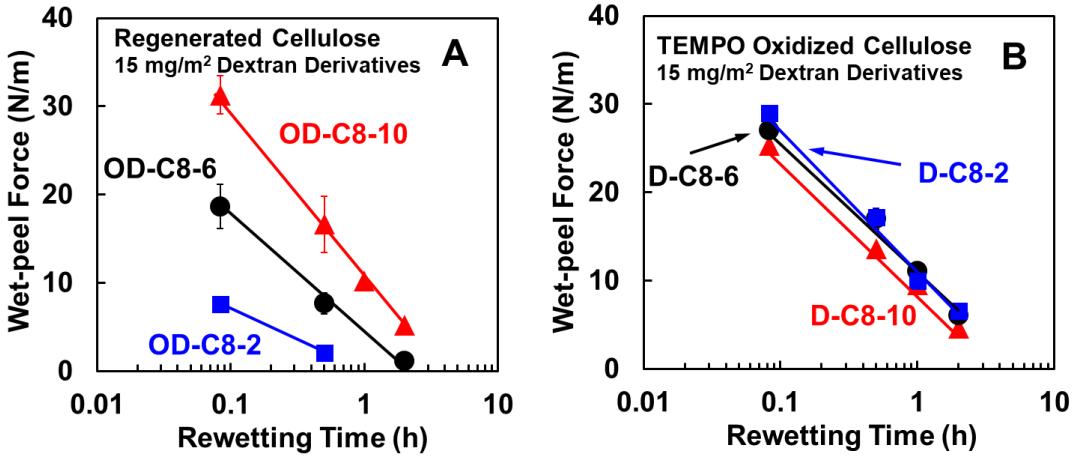

Figure A-7 Degradation of wet adhesion of (A) oxidized dextran with C8 grafting on cellulose substrate and (B) dextran with C8 grafting on oxidized cellulose substrate. Laminates were prepared with pH 7 dextran solutions and pressed at 25 ºC.

In Figure A-7A, regenerated cellulose was laminated with hydrophobic oxidized dextran. The decay rate of wet adhesion decreased with a higher DS of hydrophobic grafting on oxidized dextran. In Figure A-7B, oxidized cellulose membranes were prepared and

laminated with hydrophobic dextran (not oxidized) as the wet adhesive. The hydroxyls of non-oxidized dextran can crosslink with aldehydes on oxidized cellulose surfaces, providing cellulose wet adhesion. However, the decay rate of wet adhesion showed no relation with the hydrophobicity of the dextran adhesive.

In both cases, dextran was grafted with hydrophobic chains and hemiacetals were formed as adhesives bonds at cellulose-dextran interfaces. There was only one difference between these two cases - the oxidized dextran in Figure A-7A can form inter-/intra-molecular hemiacetals as cohesive bonds, but non-oxidized dextran cannot. We believe that the formation of cohesive hemiacetal bonds not only increased the wet adhesion, but also slowed down the degradation rate of wet adhesion. For the oxidized dextran without hydrophobic grafting, the cohesive and adhesive hemiacetals were susceptible to the attack of water molecules, leading to a rapid decay of wet adhesion. With hydrophobic grafting, the hydrolysis of hemiacetals at laminate joints would be slowed down due to the coordination of hydrophobic grafting and cohesive hemiacetal bonds.

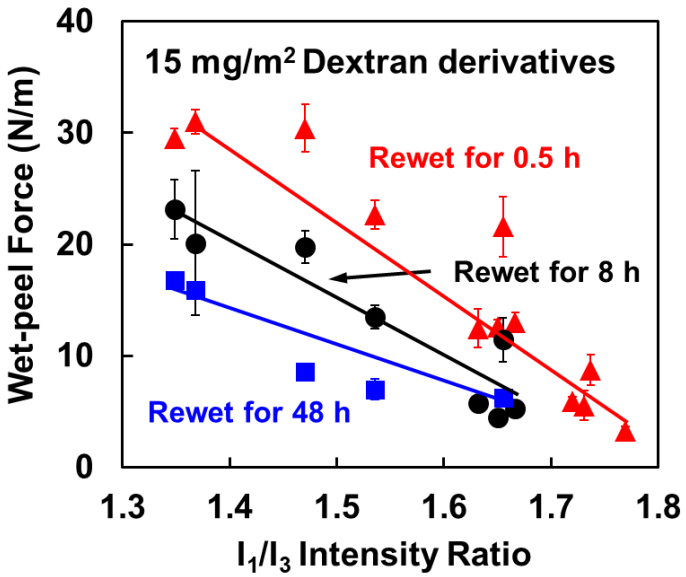

Figure A-8 Relation between cellulose wet adhesion and the hydrophobicity of the corresponding non-oxidized dextran. Oxidized dextran (OD-Cx-y) solution at pH 3 was laminated between regenerated cellulose and pressed at 70 ºC. Corresponding non-oxidized hydrophobic dextran in pyrene solution (D-Cx-y) was used to determine its hydrophobicity (I_1/I_3 intensity ratio). The measurements were made by using dextran derivatives in Table A-1.

The hydrophobicity of dextran derivatives is indicated by I_1/I_3 emission intensity ratio of a fluorescent dye - pyrene.[16] The hydrophobicity was related to both DS and the chain length of hydrophobic grafting. From Figure A-8, we find it is possible to use the hydrophobicity of D-Cx-y to predict the decay rate of cellulose wet adhesion of OD-Cx-

y. For example, after rewetting the laminate for 8 hours in water, the dextran derivative with a higher hydrophobicity (a lower I_1/I_3) provided a higher wet adhesion after the periodate oxidation.

Conclusion

Oxidized dextran with hydrophobic grafting was synthesized as the cellulose wet adhesive that provided a high initial cellulose wet adhesion and a controllable decay rate in water:

1. The decay rate slowed down with a higher hydrophobicity of oxidized dextran, either with a higher DS of the hydrophobic grafting or with a longer grafted hydrophobic chain.
2. The presence of cohesive hemiacetal bonding between oxidized dextran was necessary to control the decay rate of cellulose wet adhesion.

References

(1) Potter, F. S.; Johnson, J. W.; Wright, T. L.; Hagiopol, C. A New Perspective on Tissue Wet Strength Decay: The Real Values. *Tappi* **2013,** *12*, 9-15.

(2) Espy, H. H. The Mechanism of Wet-Strength Development in Paper: A Review. *Tappi Journal* **1995,** *78*, 90-100.

(3) Xu, G. G.; Yang, C. Q.; Deng, Y. Applications of Bifunctional Aldehydes to Improve Paper Wet Strength. *Journal of Applied Polymer Science* **2002,** *83*, 2539-2547.

(4) Xu, G. G.; Yang, C. Q.; Deng, Y. Combination of Bifunctional Aldehydes and Poly(Vinyl Alcohol) as the Crosslinking Systems to Improve Paper Wet Strength. *Journal of Applied Polymer Science* **2004,** *93*, 1673-1680.

(5) Chen, N.; Hu, S.; Pelton, R. Mechanisms of Aldehyde-Containing Paper Wet-Strength Resins. *Industrial & engineering chemistry research* **2002,** *41*, 5366-5371.

(6) Barcus, R. L.; Mohammadi, K. P.; Leimbach, A. M.; Kelly, S. R. Temporary Wet Strength Additives. US Pat. 2010.

(7) Smith, D. J. Temporary Wet Strength Additives. Pat. 1998.

(8) Smith, D. J.; Headlam, M. M. Temporary Wet Strength Polymers from Oxidized Reaction Product of Polyhydroxy Polymer and 1,2-Disubstituted Carboxylic Alkene. Pat. 1997.

(9) Darlington, W. B.; Lanier, W. G. Containing Both Temporary and Permanent Cationic Wet Strength Agents. Pat. 1995.

(10) Bjorkquist, D. W.; Schmidt, W. W. Temporary Wet Strength Resins. Pat. 1986.

(11) Rotureau, E.; Leonard, M.; Dellacherie, E.; Durand, A. Amphiphilic Derivatives of Dextran: Adsorption at Air/Water and Oil/Water Interfaces. *Journal of Colloid and Interface Science* **2004,** *279*, 68-77.

(12) Maia, J.; Carvalho, R. A.; Coelho, J. F. J.; Simões, P. N.; Gil, M. H. Insight on the Periodate Oxidation of Dextran and Its Structural Vicissitudes. *Polymer* **2011,** *52*, 258-265.

(13) Zhao, H.; Heindel, N. Determination of Degree of Substitution of Formyl Groups in Polyaldehyde Dextran by the Hydroxylamine Hydrochloride Method. *Pharm Res* **1991,** *8*, 400-402.

(14) Chen, W.; Pelton, R.; Leung, V. Solution Properties of Polyvinylamine Derivatized with Phenylboronic Acid. *Macromolecules* **2009,** *42*, 1300-1305.

(15) Wang, Y. Hydrophobically Modified Polyvinylamine and Its Influence on Paper Strength. McMaster University, 2004.

(16) Rodrigues, M. R. Hydrophobic Derivatives of Dextran Polysaccharide: Characterization and Properties. *Journal of carbohydrate chemistry* **2005,** *24*, 733-744.

(17) Saito, T.; Isogai, A. Introduction of Aldehyde Groups on Surfaces of Native Cellulose Fibers by Tempo-Mediated Oxidation. *Colloids and Surfaces, A: Physicochemical and Engineering Aspects* **2006,** *289*, 219-225.

(18) Besheer, A.; Hause, G.; Kressler, J.; Mäder, K. Hydrophobically Modified Hydroxyethyl Starch: Synthesis, Characterization, and Aqueous Self-Assembly into Nano-Sized Polymeric Micelles and Vesicles. *Biomacromolecules* **2007,** *8*, 359-367.

(19) Tizzotti, M. J.; Sweedman, M. C.; Tang, D.; Schaefer, C.; Gilbert, R. G. New 1h Nmr Procedure for the Characterization of Native and Modified Food-Grade Starches. *Journal of Agricultural and Food Chemistry* **2011,** *59*, 6913-6919.

(20) Drobchenko, S. N.; Isaeva-Ivanova, L. S.; Kleiner, A. R.; Eneyskaya, E. V. Aldo-Enol Transition in Periodate-Oxidized Dextrans. *Carbohydrate research* **1996,** *280*, 171-176.

(21) Drobchenko, S. N.; Isaeva-Ivanova, L. S.; Kleiner, A. R.; Lomakin, A. V.; Kolker, A. R.; Noskin, V. A. An Investigation of the Structure of Periodate-Oxidised Dextran. *Carbohydrate research* **1993,** *241*, 189-199.

APPENDIX B

Reductant-responsive Wet Adhesives for CMC-modified Cellulose

Paper wet strength is an important property for many paper products, such as coffee filter papers, paper towels, agricultural papers and packaging. For wet strength papers, their recyclability is compromised due to the high wet strength at fiber-fiber joint. In this thesis, we synthesized cellulose wet adhesives that provided wet strength at fiber-fiber joints and were degradable for recycling in response to mild stimuli.

In Appendix B, a layer-by-layer strategy was used to apply wet adhesives at cellulose interfaces. Hydrazide-derivatized carboxymethyl cellulose (CMC) was first applied as a "primer" to modify cellulose surface with carboxyls and hydrazides. Aldehyde-dextran was then laminated between two CMC-modified cellulose. This strategy provided cellulose surfaces both never-dried and once-dried wet adhesion. By introducing labile disulfide bonds to CMC derivatives, a degradable cellulose wet adhesion was achieved. In the discussion part, we compared three strategies to synthesize degradable cellulose wet adhesives that were demonstrated in this thesis, including microgel adhesives (Chapter 4 and 5), polymer adhesives (Chapter 7), and layer-by-layer adhesives (Appendix B).

The data in Appendix B have been collected by me with the assistance of Yang Chen, who worked with me as a summer student. I summarized the data and wrote the draft myself. This part is under preparation for the future publication.

Experimental Section

Materials. Dithiodipropionic acid dihydrazide (DTDH) was a dihydrazide reagent with disulfide bonds. It was synthesized and purified as described in Chapter 4. Oxidized dextran (ODx) was prepared and analyzed as described in Appendix A, in which x mol% is the molar ratio of sodium periodate and dextran (based on glucose unit) in the oxidation. The reaction recipe of dextran sodium periodate oxidation was summarized in Table B-1.

All other chemicals were purchased from Sigma-Aldrich, Canada. CMC used in this study was Mw 250 kDa with DS 0.9. Dextran was from *Leuconostoc* spp. with Mr 450 - 650 kDa. Water type 1 (as per ASTM D1193-6, resistivity 18MΩ/cm) were used in all experiments.

Hydrazide-derivatized CMC. Hydrazide-derivatized CMC was prepared by bioconjugation.[1] Two dihydrazide reagents were employed, including adipic acid dihydrazide (ADH) and the reductant-responsive dihydrazide DTDH. The conjugation recipes are given in Table B-2. ADH-CMC was CMC conjugated with ADH, and DTDH-CMC was conjugated with DTDH. In a typical reaction, 500 mg CMC were dissolved in 100 mL water at room temperature and after thirty minutes stirring, the pH of solution was adjusted to 5. 1-Ethyl-3-(3-dimethylaminopropyl)carbodiimide (EDC) was added and then dihydrazide reagents was added two minutes later. The modification proceeded for two hours at room temperature with pH maintaining 5. The products were purified by dialysis for one week and stored as aqueous solution at 4 °C. The product was characterized by NMR (Figure B-1).

Table B-1 Periodate oxidation of dextran.

Product	Dextran (mg)	$NaIO_4$ (mg)	Water (mL)	Titrated Aldehyde Content (mmol/g)
OD25	400	132	10	1.9±0.1
OD50	400	264	10	4.2±0.2

Table B-2 Preparation of hydrazide-derivatized CMC. Hydrazide DS was calculated from ^{1}H NMR spectra. DS represents the number of hydrazide grafting per glucose ring.

Product	Microgel (mg)	ADH (mg)	DTDH (mg)	EDC (mg)	Hydrazide DS (mol%, glucose ring)
ADH-CMC	500	202	-	187	0.20
DTDH-CMC	500	-	322	260	0.23

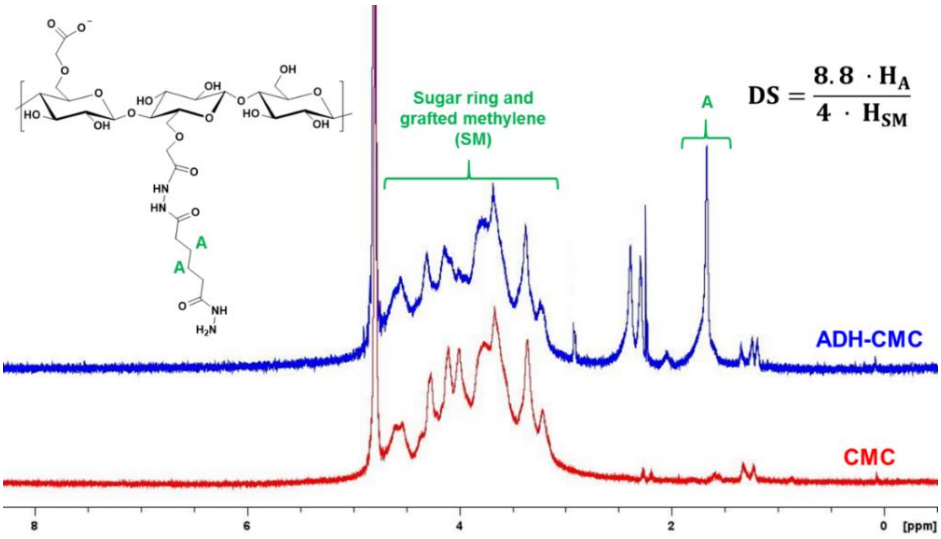

Figure B-1 NMR spectrum of ADH-CMC. 2-3 mg of freeze-dried sample was dissolved in 1 mL D_2O. ^1H NMR was performed using an NMR Spectrometer (Bruker AVANCE 600 MHz, US) at room temperature.

Wet Adhesion Measurement. Cellulose membranes were cut, cleaned and pre-treated by CMC as described in Chapter 2. Dextran adhesives were applied in laminate joints between cellulose membranes by "direct application". The lamination and the wet-peeling measurement were proceeded as described in Chapter 3. For once-dried wet adhesion, laminates were dried for one day and rewetted in aqueous solution for thirty minutes before the wet-peel. The wet-peel force was measured as the once-dried wet adhesion. For never-dried wet adhesion, the wet-peel force of the never-dried wet laminate was measured.

Results

In this study, regenerated cellulose membranes were used as the model to simulate cellulose surfaces. CMC or CMC derivatives were used to modify the surface of cellulose. To enhance cellulose wet adhesion, aldehyde-dextran was laminated between two CMC-modified cellulose surfaces. The wet-peel force to delaminate wet membranes were measured as the wet adhesion. In each laminate, a layer-by-layer adhesive structure formed at the joint, as shown in Figure B-2 – an adhesive layer between two CMC "primed" cellulose surfaces.

Two hydrazide-derivatized CMC were synthesized by bioconjugation, including ADH-CMC and DTDH-CMC. Our previous work showed that hydrazides were very effective groups to provide cellulose wet adhesion.[2] Hydrazide can form hydrazone bonds with aldehydes on oxidized cellulose either with the presence of water or after drying.

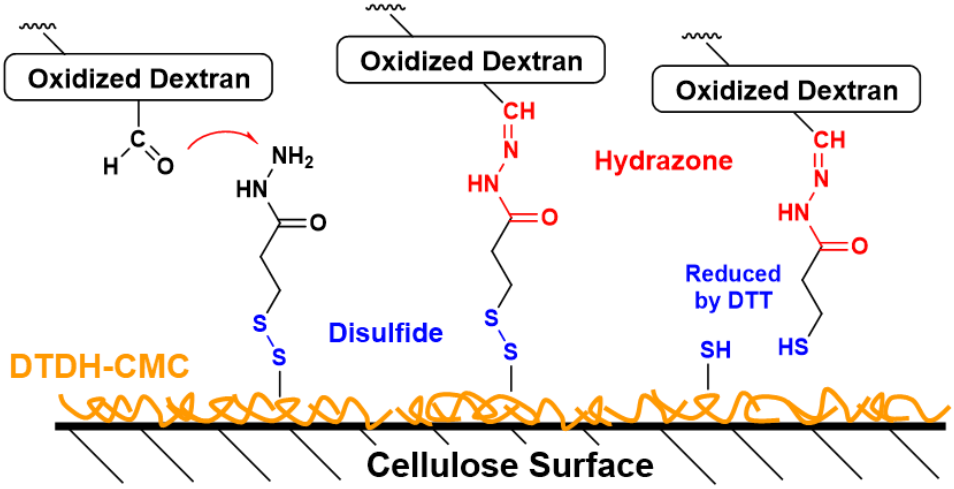

Figure B-2 The reaction between DTDH-CMC modified cellulose and oxidized dextran. The disulfide bonds in DTDH can be degraded into two thiols in response to DTT at basic condition.

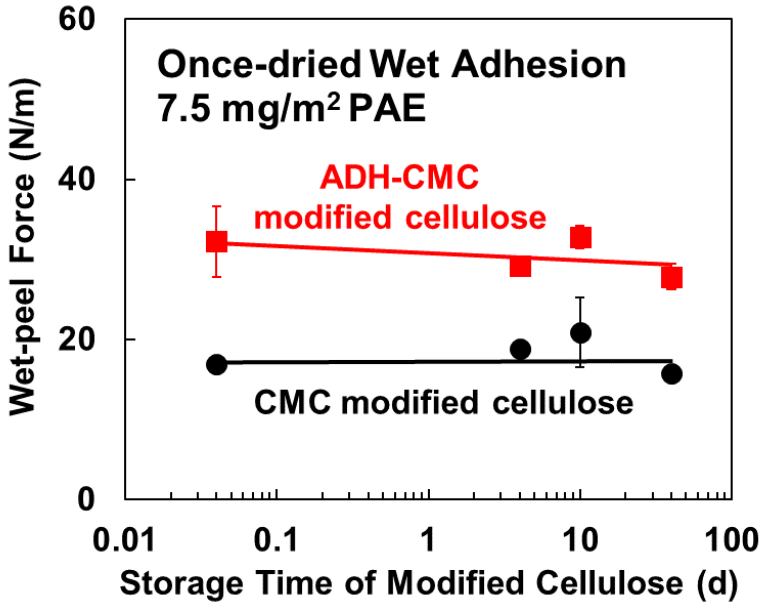

Figure B-3 Stability of CMC or ADH-CMC modified cellulose. The membranes were modified with CMC or its derivatives, rinsed and stored at room temperature from one hour to forty days. PAE was laminated with modified cellulose membranes and dried for one day. Before the wet-peel, laminates were rewetted in 1 mM NaCl, at pH 7 for 30 min.

Hydrazides were grafted on ADH-CMC via stable linkages. The hydrazide DS of ADH-CMC was calculated to be 0.20 by NMR spectra (Figure B-1). By contrast, hydrazides were grafted on DTDH-CMC via labile disulfide linkages with a DS of 0.23. When exposed to reductants, such as dithiothreitol (DTT), at high pHs, adhesive hydrazide groups on DTDH-CMC will leave the CMC backbone due to the reduction of disulfide bonds.

CMC modification is an important technique to modify cellulose surface via irreversible physical adsorption.[3] In a similar process, CMC derivatives were also be used to modify cellulose, according to the previous study.[4] In this work, hydrazide-derivatized CMC was used to modify the surface of regenerated cellulose. As shown in Figure B-3, CMC-modified cellulose was stable in water. No significant loss of CMC or ADH-CMC from cellulose surfaces was observed after stored in neutral, 1 mM NaCl solution at room temperature for over one month.

Dextran was oxidized by sodium periodate as described in the previous study.[5] The degree of oxidation was controlled by changing the molar ratio of sodium periodate and glucose unit in the oxidation. OD25 was the dextran oxidized with an aldehyde content of 1.9 mmol/g, and OD50 was oxidized with an aldehyde content of 4.2 mmol/g. As shown in Table B-3, the wet adhesion performance of dextran derivatives were evaluated. For ADH-CMC modified cellulose, the wet adhesion increased in the order of dextran << OD25 < OD50. The wet adhesion of oxidized dextran was significantly higher, due to the formation of hydrazone linkages between hydrazides and aldehydes. However, a higher density of aldehydes in OD50 did not significantly enhance the cellulose wet adhesion comparing to OD25.

Table B-3 Once-dried wet adhesion of 7.5 mg/m^2 adhesives laminated with CMC-modified cellulose. Before the wet-peel, laminates were rewetted in 1 mM NaCl at pH 7 for 30 min.

Cellulose Modification		**Adhesive**	**Once-dried Wet Adhesion (N/m)**
Top	**Bottom**		
CMC	CMC	-	0.8±0.5
CMC	CMC	ADH-CMC	8.3±1.6
ADH-CMC	CMC	-	4.3±1.0
ADH-CMC	ADH-CMC	-	12.8±2.1
ADH-CMC	ADH-CMC	CMC	7.2±1.0
ADH-CMC	ADH-CMC	ADH-CMC	14.7±2.6
ADH-CMC	ADH-CMC	Dextran	11.8±1.9
ADH-CMC	ADH-CMC	OD25	25.7±1.9
ADH-CMC	ADH-CMC	OD50	28.4±0.1

When 7.5 mg/m^2 of OD25 was applied, the aldehyde density at laminate joint was ~ 14 μmol/m^2. To estimate the hydrazide density, we assume 0.34 mg/m^2 of ADH-CMC was adsorbed on regenerated cellulose.[6] With the DS of 0.23, the estimated hydrazide density was ~ 1 μmol/m^2 at the joint. Aldehyde content of OD25 (14 μmol/m^2) was much higher than hydrazides on cellulose surface (1 μmol/m^2), which explained the reason why the further increase of aldehyde (OD50) did not lead to a significant increase of wet adhesion. For the same reason, the higher coverage of oxidized dextran at laminate joint showed an enhanced wet adhesion in a range of 0 – 7.5 mg/m^2, while reached a plateau after the critical point at 7.5 mg/m^2, as shown in Figure B-4.

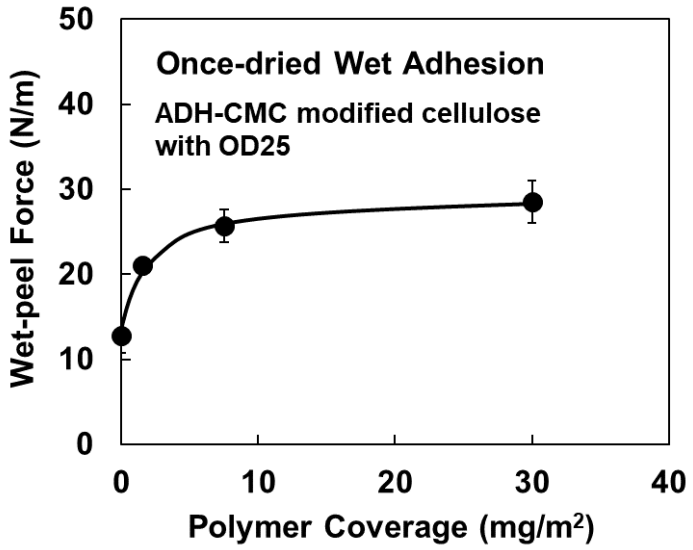

Figure B-4 Once-dried wet adhesion of ADH-CMC modified cellulose laminated with different coverage of oxidized dextran. Before the wet-peel, laminates were rewetted in 1 mM NaCl at pH 7 for 30 min.

Another interesting result was the presence of a medium wet adhesion (13 N/m) between ADH-CMC modified cellulose without any adhesive. Comparing with CMC-modified cellulose membranes, we find the introduction of hydrazides on ADH-CMC modified cellulose increased the wet adhesion from 1 N/m to 13 N/m (Table B-3). From NMR spectra, a small amount of remaining EDC was observed in dialyzed ADH-CMC samples. Thus, the EDC activated carboxyls on the surface of ADH-CMC modified cellulose can bridge the other surface via the formation of ester bonds.

DTDH-CMC was hydrazide-derivatized CMC with labile linkages (Figure B-2). Oxidized dextran provided DTDH-CMC modified cellulose a medium once-dried wet adhesion, due to the formation of hydrazone bonds. The labile disulfide linkages were introduced in DTDH-CMC to provide cellulose a degradable wet adhesion. Disulfide

bonds are reduced to two thiols in response to reductants at basic conditions.[7] In this work, DTT was used as the reductant to "switch off" the cellulose wet adhesion. After rewetting laminates in DTT solution at pH 9, 90% wet adhesion of DTDH-CMC modified cellulose was degraded as the result of the disulfide reduction, as shown in Figure B-5.

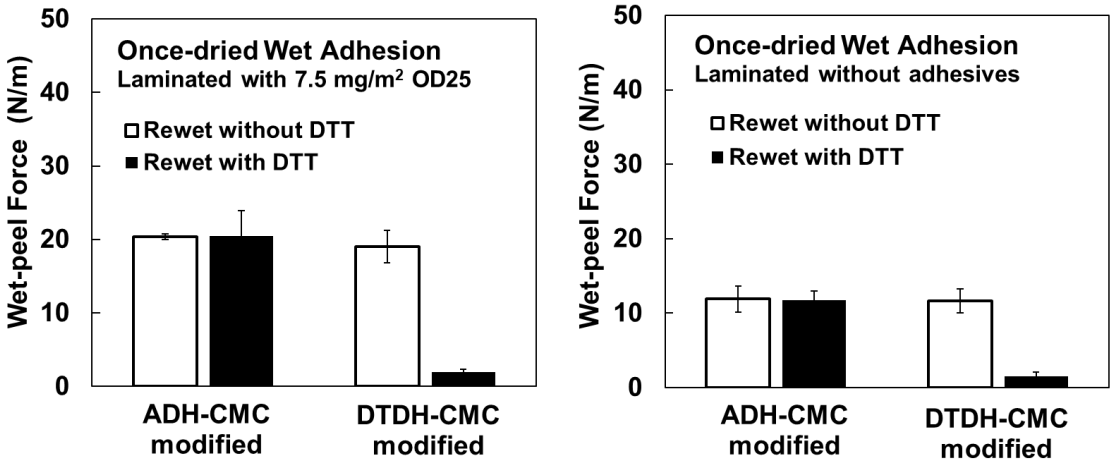

Figure B-5 Once-dried wet adhesion of CMC-modified cellulose laminated with OD25 (left) and without adhesives (right). Before the wet-peel, once-dried laminates were rewetted in 1 mM NaCl, pH 9 solution for 30 min with or without 10 mM DTT.

Our previous work showed hydrazide-derivatized microgels provided never-dried wet adhesion to wet cellulose (Figure B-6).[2] In this work, instead of using microgels, oxidized dextran was applied between CMC "primed" cellulose surfaces to form a layer-by-layer adhesive structure at the laminate joint. As shown in Figure B-7, with the oxidized dextran coverage increasing from 1.5 mg/m^2 to 30 mg/m^2, the never-dried wet adhesion at 55 wt% solids content increased from 9 N/m to 24 N/m. Also, the higher aldehyde content in dextran adhesives led to a higher never-dried wet adhesion.

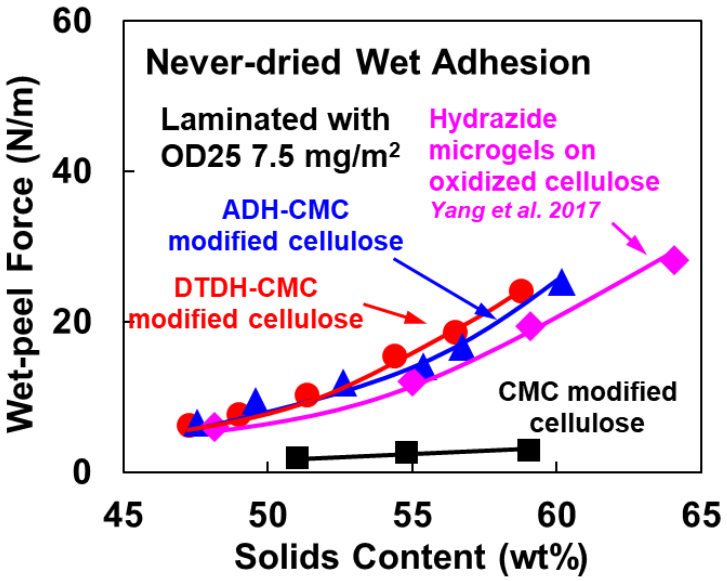

Figure B-6 Never-dried wet adhesion of CMC-modified cellulose laminated with oxidized dextran. Purple curve is the result from Yang *et al.*[2], in which 15 mg/m^2 hydrazide-derivatized microgel adhesives (1 mM NaCl at pH 7) were applied on TEMPO oxidized cellulose.[2]

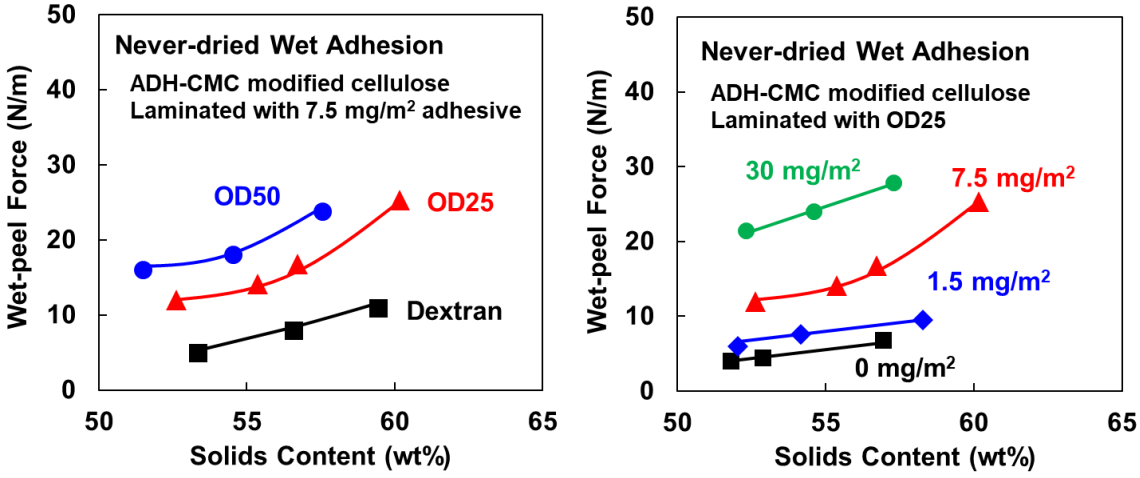

Figure B-7 Never-dried wet adhesion of ADH-CMC modified cellulose laminated with dextran derivatives.

Discussion

In previous chapters, both degradable microgel adhesives and degradable polymer adhesives for wet cellulose materials were demonstrated. Some important properties of these wet adhesives are listed in Table B-4, including their required dosage, wet adhesion performance, the degradability and their responsive properties. For microgel adhesives with labile hydrazides (Chapter 4), the advantages are their high never-dried wet adhesion and their excellent degradability (75 %) in response to reductants.[8] The disadvantages are their high required dosage (30 mg/m^2) and the high content of disulfide bonds and hydrazides.

In Chapter 5, we improved the degradable microgel adhesives by 1> using a commercial wet strength resin polyamide-epichlorohydrin (PAE) to replace the grafted adhesive hydrazides, and 2> using microgel with labile crosslinks to reduce the density of disulfides. However, as the result of these changes, the degradability of wet adhesion was decreased to < 40%. A high lamination temperature (85 ºC) was required to improve the degradability of wet adhesion to approximately 50%.

In Chapter 7, polyvinylamine (PVAm) with controllable cohesive bonds was synthesized. The advantages of cohesive PVAm are their high cellulose wet adhesion (40 N/m) and the low dosage at adhesive joints (10 mg/m^2). However, only < 50% of the wet adhesion was degradable in response of sorbital and pH change.

In this work, CMC with labile hydrazides were used to modify the surface of regenerated cellulose. Oxidized dextran was applied between CMC-modified cellulose to form a layer-by-layer structure in adhesive joints (Figure B-2). There are many advantages of this wet adhesive system. First, no cellulose oxidation is needed to enhance the wet adhesion. Second, the degradability of wet adhesion is excellent - as high as 90%. Compared with microgel adhesives, the dosage of this adhesives is low, and less disulfides or hydrazides are needed in adhesives. In the following study, we will work on further improving the once-dried and never-dried wet adhesion of this layer-by-layer adhesive.

Table B-4 Degradable cellulose wet adhesives. All results listed here are from laminates prepared at room temperature.

	Microgel with labile hydrazides (Chapter 4)	**Degradable microgel-supported PAE (Chapter 5)**	**Cohesive PVAm (Chapter 7)**	**CMC with labile hydrazides (Appendix B)**
Cellulose	Oxidized cellulose	Oxidized cellulose	Oxidized cellulose	Untreated cellulose
Adhesive at laminate joints	2 Adsorbed layers	2 Adsorbed layers	1 + 1 Adsorbed layers	Layer-by-layer
Polymer coverage (mg/m^2)	~ 30	~ 30	~ 10 (PVAm derivatives)	~ 0.7 (CMC derivatives); ~ 5 (Dextran derivatives)
Functional groups (μmol/m^2)	~ 30 Disulfide; ~ 30 Hydrazide	~ 10 Disulfide	~ 20 Boronic acid	~ 1 Disulfide; ~ 1 Hydrazide
Once-dried wet adhesion (N/m)	~ 20	~ 30	~ 40	~ 20
Stimulus	Reductant and pH	Reductant and pH	Sorbitol and pH	Reductant and pH
Degradability (%)	< 75%	< 40%	< 50%	< 90%
Never-dried wet adhesion at 55% solids content (N/m)	12	4	3	13

Conclusion

1. In this study, regenerated cellulose was modified by hydrazide-derivatized CMC, providing cellulose surface both anionic carboxyls and adhesive hydrazides.
2. Aldehyde-dextran were laminated with hydrazide-CMC modified cellulose as wet adhesives. This layer-by-layer adhesive was one of the very few wet adhesives showing both never-dried cellulose wet adhesion and once-dried wet adhesion between non-oxidized cellulose surfaces.
3. Labile disulfide linkages were used to tether adhesive hydrazide groups on CMC, which provided the wet adhesion excellent degradability – 90% of wet adhesion was degraded in response to reductant.
4. Comparing to our previous degradable wet adhesives (Chapter 4, 5 and 7), this layer-by-layer strategy showed many advantages: a) no cellulose oxidation pre-treatment was required; b) adhesives dosage was low; c) less disulfide or hydrazide groups were required.

References

(1) Chen, W.; Pelton, R.; Leung, V. Solution Properties of Polyvinylamine Derivatized with Phenylboronic Acid. *Macromolecules* **2009,** *42*, 1300-1305.

(2) Yang, D.; Gustafsson, E.; Stimpson, T. C.; Esser, A.; Pelton, R. H. Hydrazide-Derivatized Microgels Bond to Wet, Oxidized Cellulose Giving Adhesion without Drying or Curing. *ACS Applied Materials & Interfaces* **2017,** *9*, 21000-21009.

(3) Laine, J.; Lindstrom, T.; Nordmark, G. G.; Risinger, G. Studies on Topochemical Modification of Cellulosic Fibres Part 1. Chemical Conditions for the Attachment of Carboxymethyl Cellulose onto Fibres. *Nordic Pulp & Paper Research Journal* **2000,** *15*, 520-526.

(4) Orelma, H.; Teerinen, T.; Johansson, L.-S.; Holappa, S.; Laine, J. Cmc-Modified Cellulose Biointerface for Antibody Conjugation. *Biomacromolecules* **2012,** *13*, 1051-1058.

(5) Maia, J.; Carvalho, R. A.; Coelho, J. F. J.; Simões, P. N.; Gil, M. H. Insight on the Periodate Oxidation of Dextran and Its Structural Vicissitudes. *Polymer* **2011,** *52*, 258-265.

(6) Liu, Z.; Choi, H.; Gatenholm, P.; Esker, A. R. Quartz Crystal Microbalance with Dissipation Monitoring and Surface Plasmon Resonance Studies of Carboxymethyl Cellulose Adsorption onto Regenerated Cellulose Surfaces. *Langmuir* **2011,** *27*, 8718-8728.

(7) Lukesh, J. C.; Palte, M. J.; Raines, R. T. A Potent, Versatile Disulfide-Reducing Agent from Aspartic Acid. *Journal of the American Chemical Society* **2012,** *134*, 4057-4059.

(8) Yang, D.; Pelton, R. H. Degradable Microgel Wet-Strength Adhesives: A Route to Enhanced Paper Recycling. *ACS Sustainable Chemistry & Engineering* **2017,** *5*, 10544-10550.